CELL ORGANELLE EXPLOITATION BY VIRUSES DURING INFECTION

EDITED BY: Parikshit Bagchi, Indranil Banerjee and
Miguel A. Martín-Acebes

PUBLISHED IN: Frontiers in Microbiology and Frontiers in Plant Science

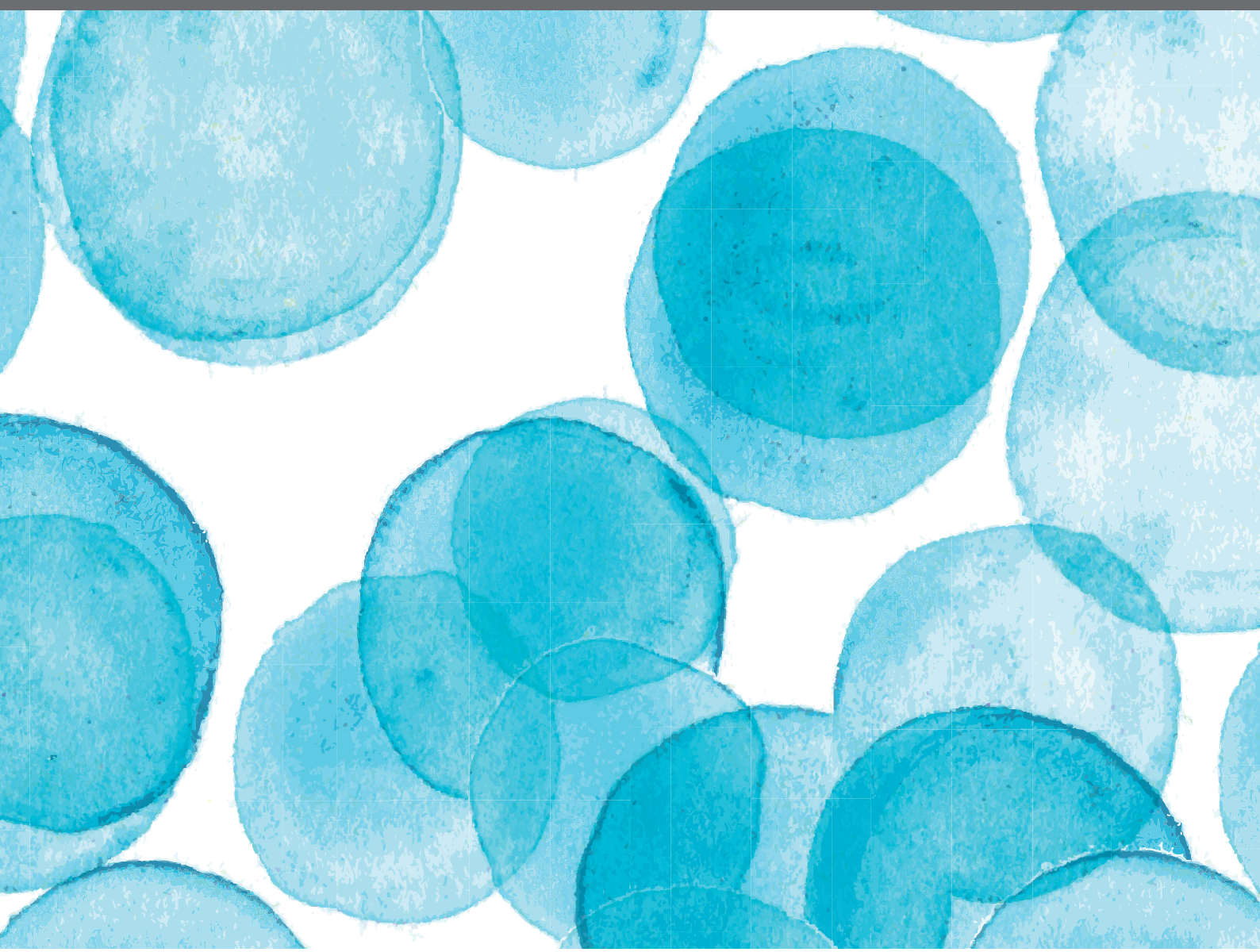

frontiers Research Topics

ISSN 1664-8714
ISBN 978-2-88966-905-9
DOI 10.3389/978-2-88966-905-9

About Frontiers

Frontiers is more than just an open-access publisher of scholarly articles: it is a pioneering approach to the world of academia, radically improving the way scholarly research is managed. The grand vision of Frontiers is a world where all people have an equal opportunity to seek, share and generate knowledge. Frontiers provides immediate and permanent online open access to all its publications, but this alone is not enough to realize our grand goals.

Frontiers Journal Series

The Frontiers Journal Series is a multi-tier and interdisciplinary set of open-access, online journals, promising a paradigm shift from the current review, selection and dissemination processes in academic publishing. All Frontiers journals are driven by researchers for researchers; therefore, they constitute a service to the scholarly community. At the same time, the Frontiers Journal Series operates on a revolutionary invention, the tiered publishing system, initially addressing specific communities of scholars, and gradually climbing up to broader public understanding, thus serving the interests of the lay society, too.

Dedication to Quality

Each Frontiers article is a landmark of the highest quality, thanks to genuinely collaborative interactions between authors and review editors, who include some of the world's best academicians. Research must be certified by peers before entering a stream of knowledge that may eventually reach the public - and shape society; therefore, Frontiers only applies the most rigorous and unbiased reviews.
Frontiers revolutionizes research publishing by freely delivering the most outstanding research, evaluated with no bias from both the academic and social point of view. By applying the most advanced information technologies, Frontiers is catapulting scholarly publishing into a new generation.

What are Frontiers Research Topics?

Frontiers Research Topics are very popular trademarks of the Frontiers Journals Series: they are collections of at least ten articles, all centered on a particular subject. With their unique mix of varied contributions from Original Research to Review Articles, Frontiers Research Topics unify the most influential researchers, the latest key findings and historical advances in a hot research area! Find out more on how to host your own Frontiers Research Topic or contribute to one as an author by contacting the Frontiers Editorial Office: frontiersin.org/about/contact

CELL ORGANELLE EXPLOITATION BY VIRUSES DURING INFECTION

Topic Editors:
Parikshit Bagchi, University of Michigan, United States
Indranil Banerjee, Indian Institute of Science Education and Research Mohali, India
Miguel A. Martín-Acebes, Instituto Nacional de Investigación y Tecnología Agroalimentaria (INIA), Spain

Citation: Bagchi, P., Banerjee, I., Martín-Acebes, M. A., eds. (2021). Cell Organelle Exploitation by Viruses During Infection. Lausanne: Frontiers Media SA. doi: 10.3389/978-2-88966-905-9

Table of Contents

frontiers in Microbiology

EDITORIAL
published: 23 April 2021
doi: 10.3389/fmicb.2021.675152

Editorial: Cell Organelle Exploitation by Viruses During Infection

Parikshit Bagchi[1]*, *Indranil Banerjee*[2]* and *Miguel A. Martín-Acebes*[3]*

[1] Department of Cell and Developmental Biology, University of Michigan Medical School, Ann Arbor, MI, United States, [2] Cellular Virology Lab, Department of Biological Sciences, Indian Institute of Science Education and Research (IISER), Mohali, India, [3] Department of Biotechnology, Instituto Nacional de Investigación y Tecnología Alimentaria (INIA), Madrid, Spain

Keywords: virus, cell, host-virus interaction, cellular organelle, virus replication cycle

Editorial on the Research Topic

Cell Organelle Exploitation by Viruses During Infection

As obligate intracellular pathogens, viruses co-opt numerous cellular processes to gain entry to the host cells and establish successful infection. This research topic highlights how diverse group of viruses utilize host cell organelles at different stages of their replication cycles. Establishing myriad points of contacts with the cellular factors, viruses exploit processes linked to different organelles to deliver their genome into the host cells and turning them into virus-producing units. The articles presented under this topic shed lights on how craftily viruses manipulate the cellular organelles and their associated machineries to facilitate different steps of their life cycle and spread. That viruses are dependent on host cell factors for their entry, replication, and egress, it opens up the possibility of identifying cellular proteins that can be targeted by inhibitors to block viral infections.

The first article of this topic (Liu et al.), focuses on the importance of host long non-coding RNAs (lncRNAs) in viral pathogenesis. By RNA-seq and transcriptomic analyses, the authors show how lncRNAs can be used as efficient tools for studying Porcine delta coronavirus (PDCoV) infection process and designing novel antiviral strategies. As we are currently in the middle of a deadly pandemic caused by SARS-CoV-2, the findings of this study could be applied to gain critical insights into the disease mechanism of this virus and strategizing new therapeutic interventions.

Membrane contact sites or MCS has recently emerged as an exciting field of cell biology research. How different viruses exploit these unique structures of the host cells has drawn the attention of the scientific community. The review article by discusses Lu et al. about how a cellular protein Acyl-coenzyme A binding domain containing 3 (ACBD3) interacts with the viral 3A protein (encoded by members of the *Picornaviridae* family) at the MCS, which are used by diverse viruses to ensure lipid transfer to replication organelles (ROs).

Autophagy is an important catabolic process to maintain cellular homeostasis which involves autophagosome and lysosome, two important cellular organelles. Articles by Huang et al. and Li et al. reveal how autophagy machinery is differentially regulated by two different viruses. While Huang et al. shows how red spotted grouper nervous necrosis virus (RGNNV) induces autophagy and causes cell death by lysosomal vacuolation; Li et al. demonstrates that cellular autophagy is markedly inhibited by Singapore grouper iridovirus (SGIV).

Cellular remodeling is another crucial aspect of virus-host interaction. In this research topic, while the article by shows Otulak-Kozieł et al. how a plant virus alters host cell organelles

Edited by:
Lisa Sedger,
University of Technology Sydney, Australia

Reviewed by:
Mirko Cortese,
Heidelberg University, Germany

Correspondence:
Parikshit Bagchi
pabagchi@med.umich.edu;
pbagchi4@gmail.com
Indranil Banerjee
indranil@iisermohali.ac.in
Miguel A. Martín-Acebes
martin.mangel@inia.es

Specialty section:
This article was submitted to Virology, a section of the journal Frontiers in Microbiology

Received: *02 March 2021*
Accepted: *19 March 2021*
Published: *23 April 2021*

Citation:
Bagchi P, Banerjee I and Martín-Acebes MA (2021) Editorial: Cell Organelle Exploitation by Viruses During Infection. Front. Microbiol. 12:675152. doi: 10.3389/fmicb.2021.675152

and remodels membrane structures by structural analysis of infected plant cells, findings by demonstrates Garcia et al. how Zika virus, a mosquito-borne flavivirus, reorganizes three cellular organelles—promyelocytic leukemia nuclear body (PML-NBs), mitochondria, and lipid droplets, during it course of infection.

For successful infection, viruses exploit almost every important organelle and various cellular functions of the host cell. This important aspect is elaborated by in Banerjee et al. their detailed review on herpes simplex virus or (HSV).

Mitochondria are very important cell organelles that serve as hub of power supply of a cell and involved in cellular respiration and ATP synthesis. It also maintains cellular homeostasis by regulating cellular apoptosis and autophagy. It is also reported that mitochondria play an important role in immune modulation. Given the importance of mitochondria in several critical functions of the cell, they are one of the favorite organelles exploited by many viruses to establish productive infection. Here, the review article by discusses Dutta et al. the interplay between RNA viruses and regulation of mitochondria-induced immune responses.

Finally, the review by focuses Ramdas et al. on how HIV-1 uses various cellular compartments and cellular functions during its replication cycle, starting from its entry to production of progeny virions, and their egress. The authors discuss every step of the virus replication cycle and elaborate how various functions of different cellular compartments are exploited during infection.

The contributions in this special topic highlight current advances in the field of host-virus interactions, and they more precisely elaborate on the importance of cellular organelles in different stages of infection cycle of viruses ranging from plant viruses to human viruses, including both the DNA and RNA viruses. This knowledge could be utilized in further research and to develop novel host-directed antiviral strategies. In fact, host-targeting antiviral approaches have potential benefits such as broad-spectrum activity against related viruses sharing the route of entry or appropriating the same components of cellular machineries. Targeting host factors also provide high genetic barrier against the development of resistant viruses. In summary, the findings presented here could be very useful and relevant not only for boosting our knowledge of virus-host interactions, but also in our preparation to combat the ongoing pandemic and future viral threats.

AUTHOR CONTRIBUTIONS

PB, IB, and MM-A edited the topic and wrote the manuscript. All authors approved the submitted version.

Conflict of Interest: The authors declare that the research was conducted in the absence of any commercial or financial relationships that could be construed as a potential conflict of interest.

frontiers in Microbiology

ORIGINAL RESEARCH
published: 28 January 2020
doi: 10.3389/fmicb.2019.03036

Comprehensive Genomic Characterization Analysis of lncRNAs in Cells With Porcine Delta Coronavirus Infection

Junli Liu[1], Fangfang Wang[1], Liuyang Du[1], Juan Li[1], Tianqi Yu[1], Yulan Jin[2], Yan Yan[2], Jiyong Zhou[2] and Jinyan Gu[1]**

[1] *MOE International Joint Collaborative Research Laboratory for Animal Health and Food Safety, Institute of Immunology, Nanjing Agricultural University, Nanjing, China,* [2] *MOA Key Laboratory of Animal Virology, Department of Veterinary Medicine, Zhejiang University, Hangzhou, China*

OPEN ACCESS

Edited by:
Miguel A. Martín-Acebes, Instituto Nacional de Investigación y Tecnología Agraria y Alimentaria (INIA), Spain

Reviewed by:
Sonia Zuñiga, Centro Nacional de Biotecnología (CNB), Spain
Guangliang Liu, Lanzhou Veterinary Research Institute (CAAS), China

***Correspondence:**
Jinyan Gu
GJY@njau.edu.cn
Jiyong Zhou
jyzhou@zju.edu.cn

Specialty section:
This article was submitted to Virology, a section of the journal Frontiers in Microbiology

Received: *03 September 2019*
Accepted: *17 December 2019*
Published: *28 January 2020*

Citation:
Liu J, Wang F, Du L, Li J, Yu T, Jin Y, Yan Y, Zhou J and Gu J (2020) Comprehensive Genomic Characterization Analysis of lncRNAs in Cells With Porcine Delta Coronavirus Infection. Front. Microbiol. 10:3036. doi: 10.3389/fmicb.2019.03036

Porcine delta coronavirus (PDCoV) is a novel emerging enterocytetropic virus causing diarrhea, vomiting, dehydration, and mortality in suckling piglets. Long non-coding RNAs (lncRNAs) are known to be important regulators during virus infection. Here, we describe a comprehensive transcriptome profile of lncRNA in PDCoV-infected swine testicular (ST) cells. In total, 1,308 annotated and 1,190 novel lncRNA candidate sequences were identified. Gene Ontology (GO) and Kyoto Encyclopedia of Genes and Genomes (KEGG) analysis revealed that these lncRNAs might be involved in numerous biological processes. Clustering analysis of differentially expressed lncRNAs showed that 454 annotated and 376 novel lncRNAs were regulated after PDCoV infection. Furthermore, we constructed a lncRNA-protein-coding gene co-expression interaction network. The KEGG analysis of the co-expressed genes showed that these differentially expressed lncRNAs were enriched in pathways related to metabolism and TNF signaling. Our study provided comprehensive information about lncRNAs that would be a useful resource for studying the pathogenesis of and designing antiviral therapy for PDCoV infection.

Keywords: PDCoV infection, RNA-seq, lncRNA, TNF, metabolic pathway

INTRODUCTION

Long non-coding RNAs (lncRNAs), which are transcripts larger than 200 nt in length that lack protein-coding ability, have previously been described in mammalian cells (Kapranov et al., 2007; Mattick and Rinn, 2015). Most of them have a structure similar to mRNA; they have a 5′ methylguanosine cap and are usually spliced and polyadenylated at their 3′ termini. Notably, lncRNA expression shows significant cell and tissue specificity (Mercer et al., 2008; Derrien et al., 2012). Emerging evidence shows that non-coding RNAs have a regulatory role in multiple cellular processes, such as genomic imprinting, chromatin modification, and alternative splicing of RNA (Mercer et al., 2009). Moreover, some diseases such as cancer and neurological disorders are also related to the dysregulated expression of lncRNA (Qureshi et al., 2010; Tsai et al., 2011). Numerous studies have been conducted to ascertain their functional role during viral infection. For example, NRAV can promote influenza virus replication and virulence through negatively

regulating the initial transcription of varieties of interferon-stimulated genes (ISGs) (Ouyang et al., 2014). lncRNA-ACOD1, named by its neighboring coding gene aconitate decarboxylase 1, significantly reduces virus multiplication by directly interacting with the metabolic enzyme glutamic-oxaloacetic transaminase (Wang et al., 2017). Neat1, one of the lncRNAs induced by HIV-1 infection, is retained in the nucleus and serves as a scaffold for the nuclear paraspeckle substructure. Importantly, Neat1 deficiency enhances HIV-1 replication (Zhang et al., 2013). Although large amounts of data have proved that several lncRNAs are involved in different kinds of virus infection, the mechanisms by which they act are still largely unknown.

Porcine delta coronavirus (PDCoV), a novel emerging pathogenic enterocytetropic virus, was first discovered from the feces of pigs in Hong Kong in 2012. It is an enveloped, single-stranded positive-sense RNA virus. It belongs to the genus *Deltacoronavirus* in the family *Coronaviridae* of the order *Nidovirales* (Woo et al., 2012). The genome length of PDCoV is approximately 25.4 kb. It is similar in structure to other coronaviruses, with shorter non-coding regions (5′-UTR and 3′-UTR) at both terminals. The 3/4 genome from the 5′ end contains two overlapping open reading frames, ORF1a and ORF1b, encoding the pp1a and pp1b, respectively. The downstream of the genome encodes structural protein spike (S), envelope (E), membrane (M), accessory proteins NS6, structural protein nucleocapsid (N), and accessory proteins NS7 and NS7a. A total of 15 non-structural proteins are encoded by the 5′ terminal of the genome (Fang et al., 2017). PDCoV mainly causes acute, watery diarrhea, vomiting, dehydration, and mortality in suckling piglets, including lesions in the stomach and lungs (Ma et al., 2015). The first outbreak of PDCoV infection was reported in the United States in early 2014 and, to date, it has been detected in Canada, South Korea, China, Thailand, and Vietnam, thus posing huge threat to the swine industry and attracting a great deal of attention (Lee and Lee, 2014; Dong et al., 2016; Lorsirigool et al., 2017; Ajayi et al., 2018; Saeng-Chuto et al., 2019).

During infection, the accessory and non-structural proteins of PDCoV usually perform multiple functions to promote replication in infected cells. A previous study showed that NS6 interaction with RIG-I/MDA5 attenuated the binding activity between RIG-I/MDA5 and double-stranded RNA, resulting in a reduced level of IFN-β production (Fang et al., 2018). Also, the non-structural protein nsp5, a 3C-like protease, is an important molecule in suppressing type I IFN signaling (Zhu et al., 2017b). In addition, NEMO, an essential modulator of NF-κB, can also be cleaved by nsp5, causing inhibition of IFN-β production (Zhu et al., 2017a). Though there are many reports of immune evasion by PDCoV, the precise pathogenic mechanism of PDCoV is largely unclear.

Based on the increasing number of reports on host lncRNAs associated with virus infection, we are interested in investigating whether host lncRNAs were involved in PDCoV infection. In this study, genome-wide profiling of lncRNAs in swine testicular (ST) cells infected with PDCoV was performed using RNA-seq. We identified 830 differentially expressed lncRNAs from PDCoV-infected cells. An integrative analysis of lncRNA alterations suggested their putative role in regulating the expression of several key genes in metabolic and TNF signaling pathways during infection. In conclusion, this work supports the role of lncRNAs as important regulators of PDCoV infection.

MATERIALS AND METHODS

Cells and Viruses

Swine testicular cells and porcine jejunum intestinal epithelial cells (IPEC-J2) were grown in DMEM supplemented with 10% (vol/vol) FBS (Gibco, Carlsbad, CA, United States) at 37°C in a humidified 5% CO_2 atmosphere. The PDCoV-CH-HA3-2017 (MK040455) strain, stored in our laboratory, was propagated in ST cells.

Viral Infection and RNA Extraction

For RNA-seq, ST cells were infected with PDCoV at a multiplicity of infection (MOI) of 10; the medium for PDCoV infection was DMEM containing 0.2 ug/ml Trypsin that had been TPCK-treated (Millipore Sigma, St. Louis, MO, United States) for 11 h. Mock-infected cells were placed in the same volume of DMEM, with the same concentration of TPCK-treated Trypsin. Total RNA was isolated from each group using SuPerfecTRI^{TM} Total RNA Isolation Reagent (Pufei, Shanghai, China) according to the manufacturer's instructions. The RNA quality was checked by 1% agarose gel electrophoresis. The purity and concentration of RNA were measured by NanoPhotometer® spectrophotometer (IMPLEN, München, Germany) and Qubit® RNA Assay Kit in Qubit® 2.0 Fluorometer (Life Technologies, Camarillo, CA, United States). RNA integrity was assessed using the RNA Nano6000 Assay Kit of the Bioanalyzer 2100 system (Agilent Technologies, Santa Clara, CA, United States). For quantitative RT-PCR (RT-qPCR), ST and IPEC-J2 cells were infected or mock-infected with PDCoV at an MOI of 10 and harvested at the indicated time. All experiments were conducted in triplicate.

RNA-Seq and Data Analysis

Sequencing libraries were generated using the rRNA-depleted RNA with a NEBNext® Ultra^{TM} Directional RNA Library Prep Kit (New England Biolabs, Ipswich, MA, United States). After determining the quality of the library, RNA-seq was performed using an Illumina HiSeq^{TM} 4000 (Illumina, San Diego, CA, United States) to generate raw reads. After removing poly-N sequences, adapters, and low-quality reads, clean reads were obtained and the paired-end reads were aligned to Ensemble pig genome (Release 76). lncRNAs were identified using TopHat2 (v2.0.9), and reads that were mapped to the pig genome were assembled using Cufflinks v2.1.1 (Trapnell et al., 2010). Cuffdiff (v2.1.1) was used to calculate the FPKMs of both lncRNAs and coding genes in each sample. Gene FPKMs were computed by summing the FPKMs of transcripts in each gene group, and differentially expressed (DE) transcripts were assigned where there was a statistically significant level of expression ($p < 0.05$). RNA-seq and data analysis were completed by Novogene.

GO and KEGG Enrichment Analysis

Gene Ontology (GO) enrichment analysis of differentially expressed genes or lncRNA target genes was conducted with respect to biological process, molecular function, and cellular component with the GOseq R package, in which gene length bias was corrected. Kyoto Encyclopedia of Genes and Genomes (KEGG) was used to perform pathway enrichment analysis[1]. KOBAS software was used to test the level of statistical significance of enrichment of differentially expressed genes and/or lncRNA target genes in KEGG pathways (Mao et al., 2005).

RT-qPCR, RT-PCR, and Statistical Analysis

To determine the reliability of the RNA-seq data, 15 differentially expressed lncRNAs were randomly selected to test the expression by RT-qPCR. Total RNA was extracted from ST and IPEC-J2 cells using SuPerfecTRI^{TM} Total RNA Isolation Reagent (Pufei, Shanghai, China). First-strand cDNA was synthesized with a reverse transcriptase kit (Vazyme, Nanjing, China). RT-qPCR was performed with a SYBR Green master mix (Vazyme, Nanjing, China) on the LightCycler 96 (Roche, Basel, Switzerland). The PDCoV M gene was detected by RT-PCR. All the primers are presented in **Table 1**. Relative expressions were calculated using the $2^{-\Delta\Delta Ct}$ method with *GAPDH* as the internal control. Comparisons between groups were made using two-way ANOVA. The data reported are the mean ± SEM. Differences were considered statistically significant when $p < 0.05$.

[1]http://www.genome.jp/kegg/

TABLE 1 | Primers used for RT-qPCR validation.

Primer	Sequence (5′-3′)	Amplicon
LNC_000034-F	AAGAAAGCGGCAGCCGTGAG	125 bp
LNC_000034-R	TTAATTATTCTCCCTCCGCGTGC	
LNC_000384-F	GCACCCGTCCCCTTCTTTC	166 bp
LNC_000384-R	CCACACGGTCCCCACTTATTC	
LNC_000553-F	TGTGAAGGTCAACTATCTGGGAGC	147 bp
LNC_000553-R	ACACGGGTGAGCTTGGAAATG	
LNC_000597-F	ACAAGCCTTGCCATCATCAAGC	194 bp
LNC_000597-R	CCGAAGTGTCTCTGTATGGAGCTG	
LNC_000625-F	AGTGCCATAGAAGGCGTATTGCAC	180 bp
LNC_000625-R	GTGAATGATGCTGCTTTGAACCTGT	
LNC_000626-F	CACCAAGGCTAAATTCCCAGGTTAC	195 bp
LNC_000626-R	AATACGCCTTCTATGGCACTCACC	
LNC_000660-F	CTCTAAGCATCCGCCACCC	151 bp
LNC_000660-R	TGCCCACCAATCTGTAAGCACTA	
LNC_000819-F	CGCTTGGGTTGCTGTAATGG	114 bp
LNC_000819-R	GGGGAAAGGCGGAGGACTAA	
LNC_000266-F	CAAACGCAGAACACCTGATGTTTG	165 bp
LNC_000266-R	ACGTTTCTAGGGCAGGAGGGAC	
LNC_000676-F	GGGCGGCTGTGGAAGATCAT	101 bp
LNC_000676-R	CCAGAGTCACTGGCTCCAAACAC	
GAPDH-F	TGGTGAAGGTCGGAGTGAAC	225 bp
GAPDH-R	GGAAGATGGTGATGGGATTTC	
PDCoV-M-F	ATGCCACGCGTAATCGTGTGATC	186 bp
PDCoV-M-R	GAGTCATACCAGTACTTGGCCCAGG	

Construction of the lncRNA-Protein-Coding Gene Co-expression Network

For each lncRNA, the Pearson correlation coefficient of its expression value with that of each protein-coding gene was calculated. Under the conditions of an absolute value of the Pearson correlation coefficient >0.998 and $p < 0.00001$, the interaction network of the differentially expressed lncRNAs and protein-coding gene co-expression pairs was then constructed using Cytoscape (v3.5.1) (Shannon et al., 2003).

RESULTS

RNA-Seq and lncRNA Screening in PDCoV-Infected Cells

To identify the lncRNAs in PDCoV-infected cells, we sequenced the transcriptomes of the ST cells with or without PDCoV infection using high-throughput RNA sequencing. Robust and reproducible data were obtained from all samples, and more than 1×10^8 clean reads per sample were retained after removing reads containing adapter or poly-N sequences and reads with low quality. Afterward, all clean reads were aligned onto the pig reference genome (Release 76) using TopHat2 and were compared and assembled with Cuffcompare and Cufflinks, respectively, and coverage analysis was performed on those clean reads on different annotated gene types. The distribution of each type of gene was counted according to the expression level. In total, eight categories of RNA were identified, according to database annotation of those transcripts, in which the protein-coding genes were highly represented (66.54% in PS and 69.10% in ST, respectively) (**Figure 1A**). Next, four software tools, CNCI, CPC, PhyloCSF, and PFAM, were used to calculate the protein-coding potential of assembled-transcripts to screen lncRNAs, then taking the intersection of transcripts with no coding potential in these software products as the novel lncRNA (**Figure 1B**). In total, 1,308 annotated and 1,190 novel lncRNA candidates were identified (**Supplementary Tables S1, S2**).

It has been reported that lncRNAs, in comparison with protein-coding genes, usually share some common genomic features to their sequences. They are generally shorter in length, have fewer but longer exons, and there is lower evolutionary sequence conservation, with only ∼15% of mouse lncRNAs having homologs in humans. lncRNAs also demonstrate low expression levels (the median is ∼10% of that of protein-coding genes) (Heward and Lindsay, 2014). To further determine the characteristics of the lncRNAs identified in the present study, we compared the transcript length, exon number, and degree of conservation between protein-coding genes and lncRNAs. Conservation analysis of exons, introns, and promoters of lncRNAs and protein-coding genes showed that the exons of protein-coding genes were the most conserved and the exons of

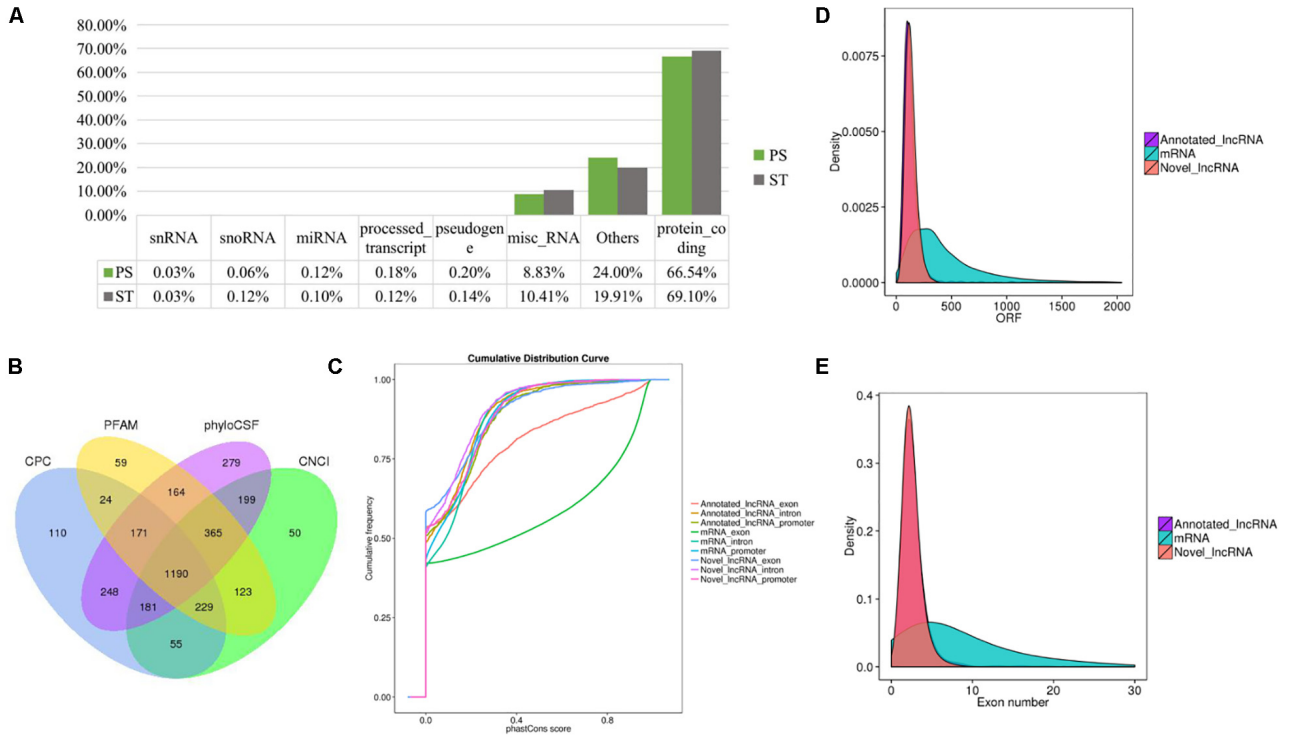

FIGURE 1 | RNA-seq and the characteristics of lncRNAs in PDCoV-infected ST cells. **(A)** RNA categories of quantified genes in RNA-seq. The percentages of each RNA species are shown in infected or mock-infected ST cells. **(B)** Venn diagrams of the identified lncRNAs shared among four software products. CNCI, CPC, PhyloCSF, and PFAM were used to screen novel lncRNAs. The sum of the numbers in each large circle represents the total number of lncRNA candidates of the indicated software, and the overlapping portions of the circles represented the lncRNAs shared between the software products. The 1190 novel lncRNAs were totally identified in ST cells. **(C–E)** Comparison of the conservation **(C)**, exon number **(D)**, and ORF length **(E)** of lncRNAs and protein-coding genes.

lncRNA were far less conserved (**Figure 1C**). Furthermore, fewer exons and shorter ORFs were found in lncRNAs, which was also consistent with the reported lncRNAs (**Figures 1D,E**).

Whole Transcriptome-Wide Functional Prediction of lncRNAs in PDCoV-Infected Cells

Long non-coding RNAs sequences are poorly conserved and do not appear to form large homologous families, so it is difficult to infer their common ancestors by sequence similarity (Ponting et al., 2009). Therefore, it is challenging to predict the functions of a type of lncRNA on the basis of its sequence or structure. There have been reports of using genome-wide association analysis between lncRNAs and the co-expressed and/or co-regulated protein-coding genes to characterize the function of the lncRNA (Huarte et al., 2010). To investigate the putative role of lncRNAs, we first analyzed the whole RNA-seq profiles to identify target protein-coding genes whose location or expression was significantly correlated with the candidate lncRNA. For co-located target gene prediction, we searched coding regions 100 k upstream and downstream of lncRNA. In total, 8,812 pairs of lncRNA-protein-coding genes, containing 2,088 lncRNAs and 3,566 protein-coding genes, were identified (**Supplementary Table S3**). For co-expressed target gene prediction, the expression correlation between lncRNAs and protein-coding genes was evaluated. When the required Pearson correlation coefficient was set above 0.95, 1,048,575 pairs of lncRNA-protein-coding genes, containing 1,730 lncRNAs and 10,581 protein-coding genes, were obtained (**Supplementary Table S4**). We next performed GO and KEGG pathway analysis for the target genes of lncRNAs. The top 20 GO and KEGG pathways with the highest representation of each term are reported (**Figure 2** and **Supplementary Tables S5, S6**). KEGG enrichment analysis revealed that pathways related to the immune system and metabolism were preferentially targeted. The GO-term analysis was divided into three main categories: cellular component, biological process, and molecular function. Significantly, a large number of biological processes, like protein-DNA complex assembly, DNA packaging and transcription, and the cellular macromolecule metabolic process, were enriched. Furthermore, protein binding and nucleic acid binding and the nucleosome and organelles, belonging to molecular function and cellular component, respectively, were also enriched. GO and KEGG pathway enrichment analysis of target genes revealed that lncRNAs may act in *cis* or *trans* to participate in the regulation of expression of multiple important genes in different processes including protein binding, DNA transcription, metabolism, and immune response.

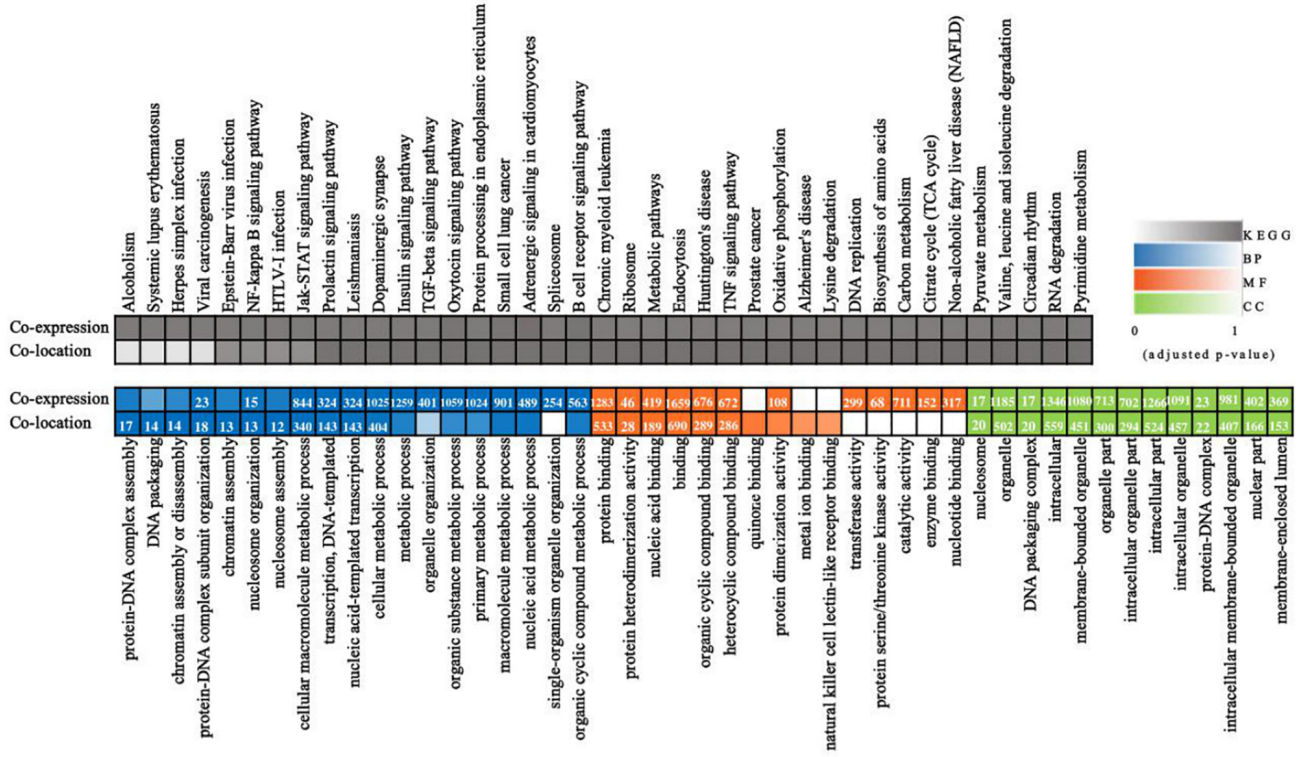

FIGURE 2 | Whole transcriptome-wide functional prediction of lncRNA identified in ST cells. Representative overrepresented KEGG (top) and GO (bottom) terms of gene-expression clusters. The number of genes within each cluster is shown for significantly enriched terms ($p < 0.05$). BP, biological process; MF, molecular function; CC, cellular component.

Clustering Analysis Identified Differentially Expressed lncRNAs in PDCoV-Infected Cells

To identify the PDCoV-associated lncRNAs, Cuffdiff software was used to investigate the differentially expressed (DE) lncRNAs in PDCoV-infected cells. The hierarchical clustering heat map in **Figure 3A** shows the DE lncRNA expression profiling data. Out of the 1,308 annotated and 1,190 novel lncRNAs, we obtained 454 annotated DE lncRNAs (225 up-regulated and 229 down-regulated) and 376 novel DE lncRNAs (252 up-regulated and 124 down-regulated) after PDCoV infection ($p < 0.05$; **Supplementary Table S7**). Importantly, we observed 20 lncRNAs whose expression levels were decreased to FPKM = 0 after PDCoV infection, while the FPKMs of another 12 lncRNAs, all novel lncRNAs, were 0 before PDCoV infection (**Supplementary Table S7**). This suggests that these 32 lncRNAs, though they have very low expression levels, might be strongly associated with the viral infection. Furthermore, to evaluate the reliability of RNA-seq data analysis, 15 lncRNAs were selected for RT-qPCR analysis in PDCoV-infected cells. As shown in **Figure 3B**, the expression levels of the 15 selected lncRNAs, though exhibiting no significant differences at 4 h post-infection (hpi), were all significantly changed at 11 hpi in ST cells. Also, different expression patterns of lncRNAs were detected in IPEC-J2 cells. As shown in **Figure 3C**, 11 out of the 15 selected RNA were significantly altered at 11 hpi, and all of them were differently expressed at 24 hpi. For both ST and IPEC-J2 cells, they had a strong expression pattern consistent with the RNA-seq results (**Table 2**).

Co-location Analysis of DE lncRNAs Revealed Their Potential Regulation of Their Neighboring Protein-Coding Genes

The lncRNA in the genome is not randomly distributed, so locus classification will be an effective first step in analyzing its regulatory functions at the genome level (Luo et al., 2016). In general, lncRNAs function either in *cis* or in *trans* to affect the transcription of genes within or far from the same genomic locus (Clark and Blackshaw, 2014). To understand the potential functional association between lncRNAs and cognate genes, we investigated their genomic distribution pattern relative to protein-coding loci and classified all DE lncRNAs to ascertain their potential biological roles. All DE lncRNAs were classified into six categories comprising sense-upstream lncRNA, sense-downstream lncRNA, sense-overlapping lncRNA, antisense-upstream lncRNA, antisense-downstream lncRNA and antisense-overlapping lncRNA. As shown in **Figure 4A**, 26% of DE lncRNAs were located in the same strand but upstream of protein-coding genes and 24% were located downstream, while antisense-upstream and antisense-overlapping comprised

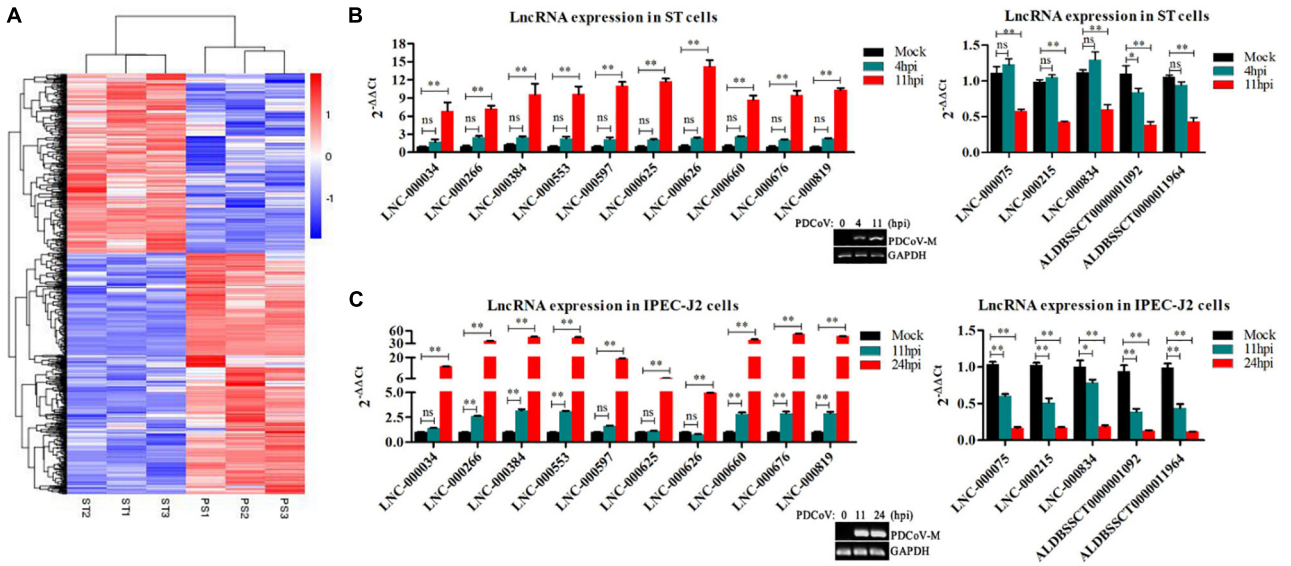

FIGURE 3 | Identification of differentially expressed lncRNAs during PDCoV infection. **(A)** Hierarchic clustering analyses of 830 lncRNAs that were differentially expressed in the PDCoV-infected ST cells (PS) compared with the mock-infected ST cells (ST) ($p < 0.05$). **(B,C)** Validation of 10 up-regulated (left) and five down-regulated (right) lncRNAs from RNA-Seq in ST **(B)** and IPEC-J2 cells **(C)** were performed by RT-qPCR. The PDCoV M gene was confirmed by RT-PCR. Data are shown as mean ± SEM, $n = 3$. $^{*}p < 0.05$, $^{**}p < 0.01$.

27 and 1%, respectively, and the remaining 22% were antisense-downstream lncRNAs. Next, in order to define the lncRNA functions more precisely, GO enrichment analysis of the co-located genes of up- and down-regulated lncRNAs were analyzed independently. The results showed that protein-coding genes associated with DE lncRNAs were mainly enriched in terms of molecular function and cellular component, primarily under the category of nucleic acid binding and intracellular membrane-bounded organelle (**Figure 4B**). Notably, by analyzing the relative expression level, we found that antisense lncRNA and protein-coding genes were specifically co-expressed, in which two pairs showed a positive and three pairs showed a negative correlation in their expression patterns (**Figure 4C** and **Supplementary Table S8**). We speculated that these antisense lncRNAs act in *cis* to modulate the expression of their cognate genes.

Correlation Analysis Provided a Resource to Functionally Identify PDCoV Driver Metabolism- and Immunity-Related lncRNAs

The functional association between regulatory lncRNA and protein-coding gene transcripts can be determined by performing expression correlation analysis coupled with ascertaining their putative role in related physiological processes. To further investigate the potential mechanism of action of the PDCoV-associated lncRNAs, the DE lncRNAs and their predicted target DE protein-coding genes were investigated by delineating lncRNA-protein-coding gene functional interactions. Here we identified 1,048,575 pairs of DE lncRNA-DE protein-coding genes, containing 821 lncRNAs and 8,799 protein-coding genes ($p < 0.01$). Next, KEGG pathway analysis was repeated once again (**Figure 5A**), and we found that metabolic and TNF signaling pathways were significantly enriched.

The interaction network involving the metabolic and TNF signaling pathways was then constructed. Several key genes in metabolism were positively or negatively regulated by lncRNAs (**Figure 5B**). Of the significantly enriched genes, ATP5L and ATP5F1, two of the mitochondrial membrane ATP synthase subunits, were regulated by LNC-000625, LNC-001104, ALDBSSCT0000008902, and ALDBSSCT0000006348.

TABLE 2 | Expression level of 15 selected lncRNAs in RNA-seq.

Transcript_id	PS_FPKM	ST_FPKM	Log2 (fold change)	*P* value
LNC_000034	686.329	0	inf	5.00E−05
LNC_000266	2.36983	0.0858038	4.7876	0.00615
LNC_000384	1.31737	0	inf	5.00E−05
LNC_000553	1.39484	0	inf	5.00E−05
LNC_000597	1.38574	0.0480706	4.84936	0.0001
LNC_000625	6.10358	0.199175	4.93754	5.00E−05
LNC_000626	10.5832	0.256783	5.36509	5.00E−05
LNC_000660	3.55981	0.024732	7.16928	0.01105
LNC_000676	0.925249	0.0338341	4.77329	0.005
LNC_000819	1.44203	0	inf	5.00E−05
ALDBSSCT0000001092	0.442178	3.44013	−2.95976	5.00E−05
ALDBSSCT0000011964	0.0812138	0.613515	−2.9173	5.00E−05
LNC_000075	0.221325	1.10022	−2.31355	0.00015
LNC_000215	0.194968	1.04174	−2.41769	5.00E−05
LNC_000834	0.126095	1.51747	−3.58908	0.00145

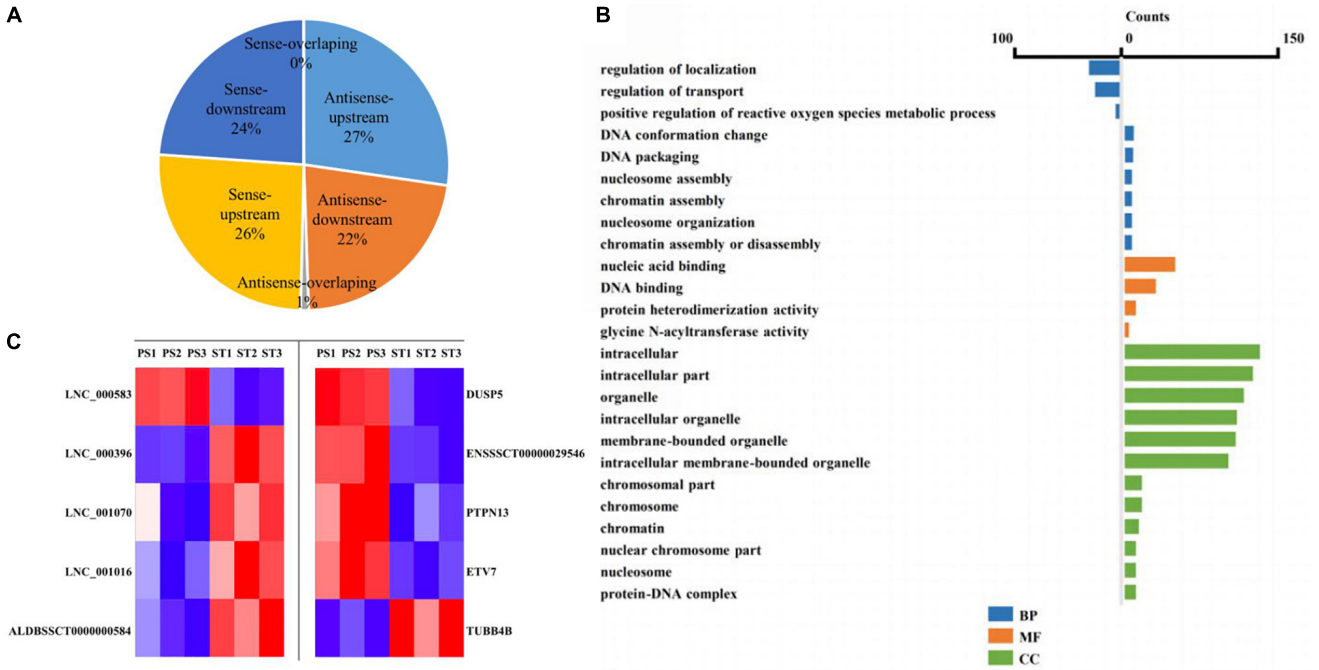

FIGURE 4 | Co-location analysis revealed the potential regulation ability of lncRNAs on their neighboring protein-coding genes. **(A)** Pie chart showing the percentage of each class of lncRNA classified by their location. **(B)** Over-represented GO terms of up-regulated (left) and down-regulated (right) co-located genes ($p < 0.05$). BP, biological process; MF, molecular function; CC, cellular component. **(C)** Heatmap showing the expression correlation of selected antisense lncRNA-protein-coding gene pairs.

In addition, three lncRNAs, LNC-000459, LNC-000258, and ALDBSSCT0000005568, might regulate acyl-coenzyme A thioesterase four expression. These results suggest that these lncRNAs might be involved in the regulation of metabolic processes particularly involving energy and lipid metabolism. Meanwhile, an inducible program of inflammatory gene expression is central to antiviral defense. Many of them, i.e., CCL5, CCL20, CXCL2, CXCL10, MAP3K8, NF-κB1, and interleukin 6 (IL-6), were protein-coding genes known to have roles in the inflammatory response. In the network (**Figure 5C**), eight lncRNAs have putative regulatory roles in IL-6 expression. Six of them, LNC-000173, LNC-000269, LNC-000242, LNC-000657, ALDBSSCT0000009132, and ALDBSSCT0000001339, might exert positive regulation, while LNC-001173 and ALDBSSCT0000010894 showed the opposite effect. This suggests that these lncRNAs might act as the regulatory module of the circuit that is involved in the inflammatory response.

DISCUSSION

Numerous studies have shown that lncRNAs play a key role during viral infection. The lncRNAs THRIL, NeST, NEAT, and lincRNA-Cox2 can participate in immune responses against viral infection mainly through regulating the expression of TNF-α, IFN-γ, IL8, and inflammatory response, respectively (Carpenter et al., 2013; Gomez et al., 2013; Imamura et al., 2014; Li et al., 2014). PDCoV is an important enteric virus mainly causing diarrhea in suckling pigs. Infection with PDCoV causes changes in the expression levels of several host cell proteins of host innate immune response, but little is known about the critical roles of lncRNAs in these processes.

Here, we performed RNA-seq to identify the lncRNAs involved in PDCoV infection. The results of comparing clean reads to the genome showed that more than 60% of reads are protein-coding genes, and no lncRNA classifications were identified due to the limited lncRNA database annotation in pig. In our results, 1,190 novel lncRNAs were identified. Further analysis showed that the basic characteristics of these novel lncRNAs are consistent with the known ones. Our RNA-seq results further enrich the pig lncRNA database.

In total, we found 454 annotated and 376 novel lncRNAs that were differentially expressed during PDCoV infection. These lncRNAs were classified as sense-upstream lncRNA, sense-downstream lncRNA, sense-overlapping lncRNA, antisense-upstream lncRNA, antisense-downstream lncRNA, and antisense-overlapping lncRNA. Many antisense-overlapping lncRNAs have inverse expression patterns with their sense transcript counterparts. This suggests that these antisense-overlapping lncRNAs may have a negative regulatory effect on them. In contrast, many lncRNAs that do not contain overlapping sequences display expression patterns correlated with their neighboring protein-coding gene transcripts. In the present study, two out of five antisense overlapping lncRNAs were found to have high consistency in their expression (**Figure 4**). Similarly, the lncRNA *Evx1as*, which initiates

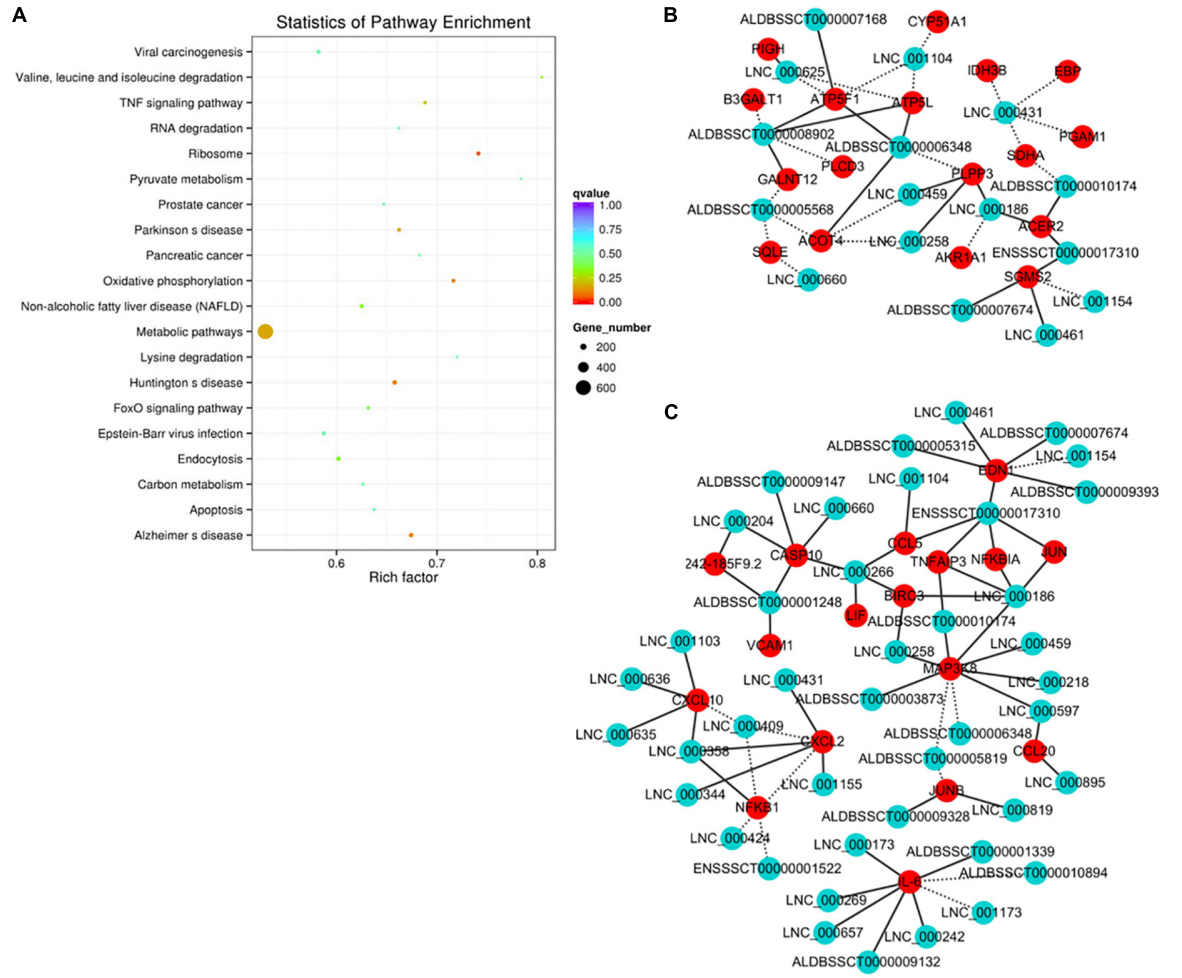

FIGURE 5 | Correlation analysis provides a resource to functionally identify PDCoV driver metabolism- and immunity-related lncRNAs. **(A)** The top 20 overrepresented KEGG pathways of co-expressed genes. **(B,C)** The network of co-expressed lncRNA-protein-coding gene pairs based on a threshold of a Pearson's correlation coefficient of 0.998. The network of lncRNAs with metabolic- **(B)** or immunity-related genes **(C)** is presented ($p < 0.00001$). The solid line represents a positive correlation, while the dotted line represents a negative correlation.

within the first exon of the gene *EVX1*, has an overlap of eight nucleotides with the EVX1 mRNA and promotes transcription of its neighbor gene by increasing the binding affinity of histone H3 lysine 4 tri-methylation (H3K4me3) and histone H3 lysine 4 acetylation (H3K27ac) at the promoter region. Considering that most lncRNAs might function through their secondary structure rather than the primary one, this suggests that the regulation of antisense transcripts by antisense-overlapping lncRNA may not be mediated through base-complementary pairing.

Correlation analysis of DE lncRNA and protein-coding genes identified a number of DE lncRNA-DE protein-coding gene pairs. The main enriched KEGG pathways of these protein-coding genes were in metabolism and oxidative phosphorylation. In a recent report, 5-day-old neonatal pigs were infected with PDCoV, and transcriptome profile and KEGG pathway enrichment analysis were performed at different stages of infection (Wu et al., 2019). In our study, we found that the lncRNA targeted genes enriched in those pathways that were perturbed during the late stage of infection. In addition, the expression level of transglutaminase 3 (TGM3) and apolipoprotein A-2 (APOA2) in a Wu et al. (2019) study were significantly changed. Similarly, we also found that TGM1 was up-regulated, and APOA1, APOA4, and APOA5 were down-regulated during PDCoV infection (data not shown). Moreover, our data show that many cytokines and chemokines, which elicit an inflammatory response, were differentially expressed in the infected cells compared to mock cells. The inflammation causes injury to the intestinal tissues, resulting in diarrhea or even death. Raised CCL and CXCL10 levels were associated with the severity of virus infection (Betakova et al., 2017; Masood et al., 2018). Here, we identified a number of lncRNAs that may regulate the expression of these inflammatory molecules.

To the best of our knowledge, this is the first study focusing on the expression profile of cellular lncRNAs after PDCoV infection. Our data show the expression landscape of lncRNAs, with special emphasis on the lncRNA-protein modules

operating in response to PDCoV infection. Moreover, this study provides a comprehensive genome-wide resource for exploring the molecular and cellular regulatory functions of lncRNAs. This study will also be useful for identifying lncRNAs as potential biomarkers for the diagnosis of PDCoV infection and designing better prophylactic and therapeutic tools against virus infection.

CONCLUSION

In the present study, the expression profiles of lncRNAs were determined in PDCoV-infected ST cells. In total, 1,190 novel lncRNAs were identified. A total of 830 lncRNAs were differentially expressed between PDCoV-infected or mocked-infected ST cells. KEGG pathway analysis of DE lncRNA co-expressed genes revealed that they might be primarily involved in regulating metabolism and TNF signaling pathways. Our study systematically characterizes lncRNA expression during PDCoV infection and provides a useful resource for identifying and functionally characterizing the cognate gene products of those lncRNAs. This study will also be useful for assigning lncRNAs as potential biomarkers of PDCoV infection and designing better preventive and therapeutic measures against the virus infection, which would be economically beneficial for the pig farming community.

DATA AVAILABILITY STATEMENT

The raw data supporting the conclusions of this article will be made available by the authors, without undue reservation, to any qualified researcher.

AUTHOR CONTRIBUTIONS

JLL, JG, and JZ conceived and designed the experiments. FW, LD, and JL performed the experiments. JLL, YY, YJ, and TY analyzed the data. JLL drafted the manuscript. All authors read and approved the final manuscript.

FUNDING

This work was supported by the National Key Research & Development Program of China (2016YFD0500102).

SUPPLEMENTARY MATERIAL

The Supplementary Material for this article can be found online at: https://www.frontiersin.org/articles/10.3389/fmicb.2019.03036/full#supplementary-material

REFERENCES

Ajayi, T., Dara, R., Misener, M., Pasma, T., Moser, L., and Poljak, Z. (2018). Herd-level prevalence and incidence of porcine epidemic diarrhoea virus (PEDV) and porcine deltacoronavirus (PDCoV) in swine herds in Ontario, Canada. *Transbound. Emerg. Dis.* 65, 1197–1207. doi: 10.1111/tbed.12858

Betakova, T., Kostrabova, A., Lachova, V., and Turianova, L. (2017). Cytokines induced during influenza virus infection. *Curr. Pharm. Des.* 23, 2616–2622. doi: 10.2174/1381612823666170316123736

Carpenter, S., Aiello, D., Atianand, M. K., Ricci, E. P., Gandhi, P., Hall, L. L., et al. (2013). A long noncoding RNA mediates both activation and repression of immune response genes. *Science* 341, 789–792. doi: 10.1126/science.1240925

Clark, B. S., and Blackshaw, S. (2014). Long non-coding RNA-dependent transcriptional regulation in neuronal development and disease. *Front. Genet.* 5:164. doi: 10.3389/fgene.2014.00164

Derrien, T., Johnson, R., Bussotti, G., Tanzer, A., Djebali, S., Tilgner, H., et al. (2012). The GENCODE v7 catalog of human long noncoding RNAs: analysis of their gene structure, evolution, and expression. *Genom. Res.* 22, 1775–1789. doi: 10.1101/gr.132159.111

Dong, N., Fang, L., Yang, H., Liu, H., Du, T., Fang, P., et al. (2016). Isolation, genomic characterization, and pathogenicity of a Chinese porcine deltacoronavirus strain CHN-HN-2014. *Vet. Microbiol.* 196, 98–106. doi: 10.1016/j.vetmic.2016.10.022

Fang, P., Fang, L., Hong, Y., Liu, X., Dong, N., Ma, P., et al. (2017). Discovery of a novel accessory protein NS7a encoded by porcine deltacoronavirus. *J. Gen. Virol.* 98, 173–178. doi: 10.1099/jgv.0.000690

Fang, P., Fang, L., Ren, J., Hong, Y., Liu, X., Zhao, Y., et al. (2018). Porcine deltacoronavirus accessory protein NS6 antagonizes interferon beta production by interfering with the binding of RIG-I/MDA5 to double-stranded RNA. *J. Virol.* 92:e00712-18. doi: 10.1128/JVI.00712-18

Gomez, J. A., Wapinski, O. L., Yang, Y. W., Bureau, J. F., Gopinath, S., Monack, D. M., et al. (2013). The NeST long ncRNA controls microbial susceptibility and epigenetic activation of the interferon-gamma locus. *Cell* 152, 743–754. doi: 10.1016/j.cell.2013.01.015

Heward, J. A., and Lindsay, M. A. (2014). Long non-coding RNAs in the regulation of the immune response. *Trends Immunol.* 35, 408–419. doi: 10.1016/j.it.2014.07.005

Huarte, M., Guttman, M., Feldser, D., Garber, M., Koziol, M. J., Kenzelmann-Broz, D., et al. (2010). A large intergenic noncoding RNA induced by p53 mediates global gene repression in the p53 response. *Cell* 142, 409–419. doi: 10.1016/j.cell.2010.06.040

Imamura, K., Imamachi, N., Akizuki, G., Kumakura, M., Kawaguchi, A., Nagata, K., et al. (2014). Long noncoding RNA NEAT1-dependent SFPQ relocation from promoter region to paraspeckle mediates IL8 expression upon immune stimuli. *Mol. Cell* 53, 393–406. doi: 10.1016/j.molcel.2014.01.009

Kapranov, P., Cheng, J., Dike, S., Nix, D. A., Duttagupta, R., Willingham, A. T., et al. (2007). RNA maps reveal new RNA classes and a possible function for pervasive transcription. *Science* 316, 1484–1488. doi: 10.1126/science.1138341

Lee, S., and Lee, C. (2014). Complete genome characterization of korean porcine deltacoronavirus strain KOR/KNU14-04/2014. *Genom. Announc.* 2:e01191-14. doi: 10.1128/genomeA.01191-14

Li, Z., Chao, T. C., Chang, K. Y., Lin, N., Patil, V. S., Shimizu, C., et al. (2014). The long noncoding RNA THRIL regulates TNFalpha expression through its interaction with hnRNPL. *Proc. Natl. Acad. Sci. U.S.A.* 111, 1002–1007. doi: 10.1073/pnas.1313768111

Lorsirigool, A., Saeng-Chuto, K., Madapong, A., Temeeyasen, G., Tripipat, T., Kaewprommal, P., et al. (2017). The genetic diversity and complete genome analysis of two novel porcine *Deltacoronavirus* isolates in Thailand in 2015. *Virus Genes* 53, 240–248. doi: 10.1007/s11262-016-1413-z

Luo, S., Lu, J. Y., Liu, L., Yin, Y., Chen, C., Han, X., et al. (2016). Divergent lncRNAs regulate gene expression and lineage differentiation in pluripotent cells. *Cell Stem Cell* 18, 637–652. doi: 10.1016/j.stem.2016.01.024

Ma, Y., Zhang, Y., Liang, X., Lou, F., Oglesbee, M., Krakowka, S., et al. (2015). Origin, evolution, and virulence of porcine deltacoronaviruses in the United States. *mBio* 6:e00064. doi: 10.1128/mBio.00064-15

Mao, X., Cai, T., Olyarchuk, J. G., and Wei, L. (2005). Automated genome annotation and pathway identification using the KEGG Orthology (KO) as a controlled vocabulary. *Bioinformatics* 21, 3787–3793. doi: 10.1093/bioinformatics/bti430

Masood, K. I., Jamil, B., Rahim, M., Islam, M., Farhan, M., and Hasan, Z. (2018). Role of TNF alpha, IL-6 and CXCL10 in Dengue disease severity. *Iran J. Microbiol.* 10, 202–207.

Mattick, J. S., and Rinn, J. L. (2015). Discovery and annotation of long noncoding RNAs. *Nat. Struct. Mol. Biol.* 22, 5–7. doi: 10.1038/nsmb.2942

Mercer, T. R., Dinger, M. E., and Mattick, J. S. (2009). Long non-coding RNAs: insights into functions. *Nat. Rev. Genet.* 10, 155–159. doi: 10.1038/nrg2521

Mercer, T. R., Dinger, M. E., Sunkin, S. M., Mehler, M. F., and Mattick, J. S. (2008). Specific expression of long noncoding RNAs in the mouse brain. *Proc. Natl. Acad. Sci. U.S.A.* 105, 716–721. doi: 10.1073/pnas.0706729105

Ouyang, J., Zhu, X., Chen, Y., Wei, H., Chen, Q., Chi, X., et al. (2014). NRAV, a long noncoding RNA, modulates antiviral responses through suppression of interferon-stimulated gene transcription. *Cell Host Microb.* 16, 616–626. doi: 10.1016/j.chom.2014.10.001

Ponting, C. P., Oliver, P. L., and Reik, W. (2009). Evolution and functions of long noncoding RNAs. *Cell* 136, 629–641. doi: 10.1016/j.cell.2009.02.006

Qureshi, I. A., Mattick, J. S., and Mehler, M. F. (2010). Long non-coding RNAs in nervous system function and disease. *Brain Res.* 1338, 20–35. doi: 10.1016/j.brainres.2010.03.110

Saeng-Chuto, K., Jermsutjarit, P., Stott, C. J., Vui, D. T., Tantituvanont, A., and Nilubol, D. (2019). Retrospective study, full-length genome characterization and evaluation of viral infectivity and pathogenicity of chimeric porcine deltacoronavirus detected in Vietnam. *Transbound. Emerg. Dis.* doi: 10.1111/tbed.13339 [Epub ahead of print].

Shannon, P., Markiel, A., Ozier, O., Baliga, N. S., Wang, J. T., Ramage, D., et al. (2003). Cytoscape: a software environment for integrated models of biomolecular interaction networks. *Genom. Res.* 13, 2498–2504. doi: 10.1101/gr.1239303

Trapnell, C., Williams, B. A., Pertea, G., Mortazavi, A., Kwan, G., van Baren, M. J., et al. (2010). Transcript assembly and quantification by RNA-Seq reveals unannotated transcripts and isoform switching during cell differentiation. *Nat. Biotechnol.* 28, 511–515. doi: 10.1038/nbt.1621

Tsai, M. C., Spitale, R. C., and Chang, H. Y. (2011). Long intergenic noncoding RNAs: new links in cancer progression. *Cancer Res.* 71, 3–7. doi: 10.1158/0008-5472.CAN-10-2483

Wang, P., Xu, J., Wang, Y., and Cao, X. (2017). An interferon-independent lncRNA promotes viral replication by modulating cellular metabolism. *Science* 358, 1051–1055. doi: 10.1126/science.aao0409

Woo, P. C., Lau, S. K., Lam, C. S., Lau, C. C., Tsang, A. K., Lau, J. H., et al. (2012). Discovery of seven novel Mammalian and avian *Coronaviruses* in the genus *Deltacoronavirus* supports bat *Coronaviruses* as the gene source of *Alphacoronavirus* and *Betacoronavirus* and avian *Coronaviruses* as the gene source of *Gammacoronavirus* and *Deltacoronavirus*. *J. Virol.* 86, 3995–4008. doi: 10.1128/JVI.06540-11

Wu, J. L., Mai, K. J., Li, D., Wu, R. T., Wu, Z. X., Tang, X. Y., et al. (2019). Expression profile analysis of 5-day-old neonatal piglets infected with porcine *Deltacoronavirus*. *BMC Vet. Res.* 15:117. doi: 10.1186/s12917-019-1848-2

Zhang, Q., Chen, C. Y., Yedavalli, V. S., and Jeang, K. T. (2013). NEAT1 long noncoding RNA and paraspeckle bodies modulate HIV-1 posttranscriptional expression. *mBio* 4:e596-12. doi: 10.1128/mBio.00596-12

Zhu, X., Fang, L., Wang, D., Yang, Y., Chen, J., Ye, X., et al. (2017a). Porcine *Deltacoronavirus* nsp5 inhibits interferon-beta production through the cleavage of NEMO. *Virology* 502, 33–38. doi: 10.1016/j.virol.2016.12.005

Zhu, X., Wang, D., Zhou, J., Pan, T., Chen, J., Yang, Y., et al. (2017b). Porcine *Deltacoronavirus* nsp5 antagonizes type I interferon signaling by cleaving STAT2. *J. Virol.* 91:e00003-17. doi: 10.1128/JVI.00003-17

Conflict of Interest: The authors declare that the research was conducted in the absence of any commercial or financial relationships that could be construed as a potential conflict of interest.

frontiers in Microbiology

MINI REVIEW
published: 08 April 2020
doi: 10.3389/fmicb.2020.00608

Emerging Role for Acyl-CoA Binding Domain Containing 3 at Membrane Contact Sites During Viral Infection

Yue Lu[1,2†], *Siqi Song*[2,3†] *and Leiliang Zhang*[2*]

[1] School of Medicine and Life Sciences, University of Jinan-Shandong Academy of Medical Sciences, Jinan, China, [2] Institute of Basic Medicine, The First Affiliated Hospital of Shandong First Medical University, Jinan, China, [3] School of Basic Medicine, Qingdao University, Qingdao, China

Acyl-coenzyme A binding domain containing 3 (ACBD3) is a multifunctional protein residing in the Golgi apparatus and is involved in several signaling pathways. The current knowledge on ACBD3 has been extended to virology. ACBD3 has recently emerged as a key factor subverted by viruses, including kobuvirus, enterovirus, and hepatitis C virus. The ACBD3-PI4KB complex is critical for the role of ACBD3 in viral replication. In most cases, ACBD3 plays a positive role in viral infection. ACBD3 associates with viral 3A proteins from a variety of *Picornaviridae* family members at membrane contact sites (MCSs), which are used by diverse viruses to ensure lipid transfer to replication organelles (ROs). In this review, we discuss the mechanisms underlying the involvement of ACBD3 in viral infection at MCSs. Our review will highlight the current research and reveal potential avenues for future research.

Keywords: ACBD3, PI4KB, membrane contact sites, replication organelles, picornavirus

OPEN ACCESS

Edited by:
Miguel A. Martín-Acebes, Instituto Nacional de Investigación y Tecnología Agraria y Alimentaria (INIA), Spain

Reviewed by:
Minetaro Arita, National Institute of Infectious Diseases (NIID), Japan
Evzen Boura, Institute of Organic Chemistry and Biochemistry (ASCR), Czechia

***Correspondence:**
Leiliang Zhang
armzhang@hotmail.com

†These authors share first authorship

Specialty section:
This article was submitted to Virology, a section of the journal Frontiers in Microbiology

Received: *18 December 2019*
Accepted: *19 March 2020*
Published: *08 April 2020*

Citation:
Lu Y, Song S and Zhang L (2020) Emerging Role for Acyl-CoA Binding Domain Containing 3 at Membrane Contact Sites During Viral Infection. Front. Microbiol. 11:608. doi: 10.3389/fmicb.2020.00608

INTRODUCTION

Ten years ago, PI4KB (for enterovirus) and PI4KA (for hepatitis C virus, HCV) were identified as host factors to produce phosphatidylinositol-4-phosphate (PI4P) for virus replication (Hsu et al., 2010; Reiss et al., 2011). Subsequently, PI4KB was discovered as the target of a group of potent antiviral candidates (major enviroxime-like compounds) with unknown target for about 30 years (Arita et al., 2011; Delang et al., 2012), which confirmed the importance of PI4KB in enterovirus replication and in antiviral development.

Acyl-coenzyme A binding domain containing 3 (ACBD3), is a multifunctional protein that resides in the Golgi apparatus and is mainly involved in the maintenance of the Golgi apparatus structure and the regulation of intracellular transport between the endoplasmic reticulum (ER) and the Golgi apparatus (Sohda et al., 2001). ACBD3 also regulates the synthesis of fatty acyl-coenzyme A (Chen et al., 2012). ACBD3 contains several functional domains, including an acyl-coenzyme A binding (ACB) domain, a coiled-coiled domain, a glutamine-rich domain (Q-domain), and a Golgi dynamic domain (GOLD domain) (Klima et al., 2016). Three groups independently identified ACBD3 as a binding partner of viral 3A proteins by mammalian two-hybrid screening (Sasaki et al., 2012), yeast two-hybrid screening (Teoule et al., 2013), or affinity purification coupled with mass spectrometry (AP-MS) (Greninger et al., 2012). Identification of ACBD3 attracted intense attention for its importance as a potential hub between PI4KB and viral proteins in viral replication. However, the following studies did not necessarily consistent with this original concept of the role of ACBD3, and currently the role of ACBD3 is rather ambiguous.

The concept of membrane contact sites (MCSs) in virus infection was established by the discovery of oxysterol-binding protein (OSBP) as the target of minor enviroxime-like compounds (Arita et al., 2013), and as the effector of PI4KB (Arita, 2014) or of PI4KA (Wang et al., 2014) in virus replication. MCSs are regions where the membranes of two organelles come into close proximity to facilitate communication of the organelles with each other. To integrate compartmentalized cellular functions, MCSs promote non-vesicular exchange of lipids and ions. Many viruses remodel host membranes into specialized membranous replication organelles (ROs) to facilitate viral replication. Virus-induced MCSs (vMCSs) generate ROs by supporting the synthesis and redistribution of lipids, which requires a number of proteins at MCSs, such as OSBP, PI4KB, and ACBD3.

It has been found that ACBD3 recruits PI4KB to the Golgi and trans-Golgi network (TGN) membranes and increases PI4KB enzymatic activity to produce PI4P locally (Baumlova et al., 2014; Boura and Nencka, 2015). PI4P regulates the docking of OSBP to the Golgi, which in turn delivers cholesterol from the ER to the Golgi. In the last decade, researchers have discovered that PI4P is necessary for viral replication in many viruses (Graham and Burd, 2011). Those viruses hijack the ACBD3 protein to recruit PI4KB to the viral ROs to produce PI4P (Hsu et al., 2010; Ronnberg et al., 2012; Nchoutmboube et al., 2013). The aim of this mini-review is to summarize the role of ACBD3 at MCSs during viral infection. By describing the interaction between viral proteins and ACBD3, we will reveal the diversity of the interplay between ACBD3 and viruses, offering a broad perspective on this emerging host–virus interaction.

ACBD3 IN KOBUVIRUS INFECTION

Aichi virus (AiV), a member of the kobuvirus genus in the *Picornaviridae* family, is one of the pathogenic factors of gastroenteritis. Researchers demonstrated that the non-structural proteins 2B, 2BC, 2C, 3A, and 3AB from Aichi virus interacted with ACBD3 and PI4KB to form a protein complex at ROs to promote PI4P synthesis (Greninger et al., 2012; Sasaki et al., 2012; Klima et al., 2017; McPhail et al., 2017; Chalupska et al., 2019). Silencing of ACBD3 or PI4KB inhibited viral replication by about 70% (ACBD3) or 99% (PI4KB). Expression of the viral proteins 2B, 2BC, 2C, 3A, and 3AB alone could promote PI4P synthesis (Ishikawa-Sasaki et al., 2014). In cells that are not infected with AiV, the C-terminal sequence of ACBD3 binds to the cytoplasmic region of the giantin C-terminal, and giantin is anchored to the Golgi membrane through the C-terminal anchor domain. PI4KB localizes to the Golgi apparatus by interacting with ACBD3. In cells infected by AiV, the viral proteins 2B, 2BC, 2C, 3A, and 3AB compete with Golgi giantin to bind to ACBD3, causing viral protein/ACBD3/PI4KB formation, and the colocalization of giantin and ACBD3 disappears (Greninger et al., 2012; Sasaki et al., 2012; Klima et al., 2017; McPhail et al., 2017; Chalupska et al., 2019).

Researchers have shown that the AiV non-structural protein 3A plays an important role in membrane rearrangement and inhibition of the host cell ER-to-Golgi transport pathway (Greninger et al., 2012). When it binds to the GOLD domain of ACBD3, the intrinsically disordered protein AiV 3A adopts a highly ordered structure and is targeted to the membrane (Klima et al., 2017; McPhail et al., 2017). Then, 3A recruits and activates PI4KB, resulting in the production of PI4P (Chalupska et al., 2019). Researchers have analyzed the conformation of the ACBD3 protein and viral 3A protein in solution by using small angle X-ray scattering (SAXS) and computer simulation (Rozycki and Boura, 2014; Peti et al., 2018). Both the ACBD3 protein and the 3A:ACBD3 protein complex exhibit extended and flexible conformations in solution (Chalupska et al., 2019).

Interestingly, cholesterol accumulates on the AiV ROs via protein-protein interactions of VAP/OSBP/SAC1 with the AiV proteins and with ACBD3 (Ishikawa-Sasaki et al., 2018). OSBP, VAP-A/B, SAC1, and PITPNB are well-known components of the cholesterol transport pathway. Silencing of these proteins reduced AiV replication, indicating the involvement of the cholesterol transport pathway in AiV RNA replication (Ishikawa-Sasaki et al., 2018). Based on the interactions between ACBD3 and the component proteins of the cholesterol transport pathway, ACBD3 is defined as a novel component of this pathway.

ACBD3 IN ENTEROVIRUS INFECTION

Enterovirus A71 (EV-A71)

Enterovirus A71 (EV-A71), a member of the EV-A species of the *Picornaviridae* family, is one of the causative agents of hand, foot, and mouth disease (HFMD) and induces neurological complications such as aseptic meningitis and brainstem and cerebellar encephalitis (Solomon et al., 2010; Xing et al., 2014). EV-A71-induced PI4P production is dependent on PI4KB and ACBD3 (Xiao et al., 2017). EV-A71 3A associates with the GOLD domain of ACBD3. Silencing of ACBD3 by siRNA or knockout of ACBD3 inhibited the replication of EV-A71 by 70% (siRNA) or nearly 100% (knockout) in RD cells, suggesting that ACBD3 is critical for EV-A71 replication (Lei et al., 2017). Silencing of PI4KB by siRNA or knockout of PI4KB suppressed the replication of EV-A71 by about 80% or by about 95%, indicating the key role for PI4KB in EV-A71 replication (Xiao et al., 2017). EV-A71 3A promotes the formation of a stable ACBD3-PI4KB complex (Lei et al., 2017). I44A or H54Y substitution in EV-A71 3A interrupted the interaction between 3A and ACBD3 (Lei et al., 2017). Moreover, I44 and H54 are important for stabilizing the ACBD3-PI4KB complex and are critical for EV-A71 replication (Xiao et al., 2017). Surprisingly, a recent study on trans-rescue of EV-A71 pseudovirus replication with PI4KB deletion mutants suggested that ACBD3-binding site of PI4KB is not essential for EV-A71 replication (Arita, 2019). The role of ACBD3-PI4KB interaction involved in EV-A71 infection need to be further investigated.

Coxsackievirus (CV)

Coxsackievirus (CV), a member of the EV-B species of the *Picornaviridae* family, infects the human body through the respiratory tract and digestive tract. After infection,

people exhibit cold symptoms such as fever, sneezing and coughing. Infection during pregnancy can cause non-paralytic poliomyelitis, intrauterine infection and teratogenicity of the fetus. CV is divided into groups A and B. Early studies have suggested that the recruitment of PI4KB to the CVB3 RO has nothing to do with GBF1/ARF1 and ACBD3 (White and Aitken, 1989; van der Schaar et al., 2012; Dorobantu et al., 2014). The GOLD domain of ACBD3 directly interacts with CVB3 3A (Greninger et al., 2012; Dorobantu et al., 2014). Silencing of ACBD3 did not affect the recruitment of PI4KB to the RO by 3A (van der Schaar et al., 2012; Klima et al., 2017). Recent studies showed that CVB3 enhanced the recruitment of PI4KB through binding to GBF1/ARF1 and interaction with ACBD3 (Klima et al., 2017). A previous study did not observe an effect on ACBD3 replication caused by CVB3 in HeLa cells with more than 90% knockdown (Dorobantu et al., 2014, 2015). However, 100% knockdown by CRISPR reduced CVB3 replication by more than 90% in HeLa cells (Lyoo et al., 2019). Overall, the current opinion is that ACBD3 promotes CVB3 replication.

Poliovirus (PV)

Poliovirus (PV), a member of the EV-C species of the *Picornaviridae* family, invades the central nervous system, damages motor nerve cells in the anterior horn of the spinal cord, and causes limb relaxation paralysis, which is often observed in children. PV proteins modulate PI4KB activity and thus provide PI4P for recruitment of OSBP to accumulate with unesterified cholesterol in ROs (Arita, 2014). The PV protein 3A interacts with ACBD3, and silencing of ACBD3 reduced PV replication in HeLa cells (Greninger et al., 2012). Subsequent experiments showed that ACBD3 inhibited PVS2 PV and PVS2 recombinant virus expressing the CV-A17 virus 3A in HEK-293T, IMR5, and HeLa cells (Teoule et al., 2013). Recently, researchers investigated the role of ACBD3 in PV replication by the CRISPR-Cas9 technique in HeLa cells (Lyoo et al., 2019). They demonstrated that ACBD3 promoted PV replication by more than 10-fold (Lyoo et al., 2019). A recent study on trans-rescue of PV1 pseudovirus replication with PI4KB deletion mutants showed that ACBD3-binding site of PI4KB is not essential for PV1 pseudovirus replication (Arita, 2019). Whether the interaction of ACBD3-PI4KB is involved in *bona fide* PV1 infection need more studies to clarify.

Enterovirus D68 (EV-D68)

Enterovirus D68 (EV-D68), a member of the EV-D species of the *Picornaviridae* family, is an emerging respiratory pathogen. EV-D68 3A associated with ACBD3 and enhanced the ACBD3-PI4KB interaction. Silencing of ACBD3 by siRNA or knockout of ACBD3 suppressed EV-D68 replication by about 60% (siRNA) or about 90% (knockout) in RD cells, suggesting that ACBD3 is critical for EV-D68 replication (Lei et al., 2017). Knockout of PI4KB suppressed the replication of EV-D68 by about 95%, indicating the key role for PI4KB in EV-D68 replication (Xiao et al., 2017).

The crystal structure of the complex of the ACBD3 GOLD domain and EV-D68 3A indicated that the GOLD-3A interaction was mediated through multiple hydrophobic interactions and hydrogen bonds (Horova et al., 2019). The alpha helices P19-V29 in 3A ($\alpha1^{3A}$) and Q32-K41 in 3A ($\alpha2^{3A}$) interacted with a shallow cavity of the GOLD domain formed by antiparallel beta strands of ACBD3. The beta strand V53-I58 in 3A ($\beta2^{3A}$) associated with the strand V402-P408 in ACBD3, while the beta strand I44-I46 in 3A ($\beta1^{3A}$) interacted with the strand K518-R528 in ACBD3 (Horova et al., 2019). Because no direct interaction between PI4KB and the enterovirus 3A proteins has been identified, the ACBD3-PI4KB interaction stimulated by 3A and the subsequent enhancement of the membrane-targeting of PI4KB in infected cells depend on the ACBD3-3A association.

Rhinovirus (RV)

Rhinoviruses (RVs), belonging to the enterovirus genus of the *Picornaviridae* family, are the causative agents for common cold. Over 150 types of RVs are classified into three species: RV-A, RV-B, and RV-C. Studies have shown that the 3A proteins from

TABLE 1 | Summary of the role of ACBD3 in viral replication.

Virus	Family (Genus)	Effect on viral replication	Proposed mechanism	References
Aiv	*Picornaviridae (kobuvirus)*	Promotion	AiV virus protein binds to ACBD3 protein and recruits PI4KB to form virus protein/ACBD3/PI4KB complex to synthesize PI4P for replication.	Sasaki et al., 2012; McPhail et al., 2017
EV-A71	*Picornaviridae (enterovirus)*	Promotion	EV-A71 3A associates with ACBD3. EV-A71 3A promotes the formation of a stable ACBD3-PI4KB complex. ACBD3 is critical for EV-A71 replication.	Xiao et al., 2017
CV	*Picornaviridae (enterovirus)*	Promotion	CVB3 3A interacts with ACBD3. ACBD3 promotes CVB3 replication. CVB3 enhanced the recruitment of PI4KB through interaction with ACBD3.	Lyoo et al., 2019
PV	*Picornaviridae (enterovirus)*	Promotion	Poliovirus protein 3A interacts with ACBD3 and ACBD3 knockout reduces poliovirus replication.	Lyoo et al., 2019
EV-D68	*Picornaviridae (enterovirus)*	Promotion	EV-D68 3A associated with ACBD3 and increased ACBD3-PI4KB interaction. ACBD3 is critical for EV-D68 replication.	Xiao et al., 2017
RVA2, RVB14	*Picornaviridae (enterovirus)*	Promotion	3A proteins from RVA2 and RVB14 interact with ACBD3. ACBD3 is critical for the replication of RVA2 and RVB14.	Lyoo et al., 2019
RVA16	*Picornaviridae (enterovirus)*	Inhibition	3A proteins from RVA16 interact with ACBD3. ACBD3 inhibited RVA16 replication.	Xiao et al., 2017
HCV	*Flaviridae (hepacivirus)*	Inhibition	ACBD3 inhibits HCV replication. NS5A from different GTs of HCV compete with PI4KB to bind ACBD3.	Hong et al., 2014

rhinovirus A2 (RVA2), rhinovirus A16 (RVA16), and rhinovirus B14 (RVB14) (Greninger et al., 2012) interact with ACBD3. Previous studies suggested that silencing of ACBD3 had no effect on RVA2 and RVB14 replication (Dorobantu et al., 2014, 2015). Recently, this conclusion was corrected by a more careful study. ACBD3 knockout inhibits replication of RVA2 and RVB14 by more than 90% in HeLa and HAP1 cells (Lyoo et al., 2019). ACBD3 is important for proper localization of 3A of RVA2 and RVB14. Interestingly, silencing of ACBD3 by siRNA or knockout of ACBD3 increased the replication of HRV16 by about 50% in HeLa cells, suggesting that ACBD3 inhibited RVA16 replication (Xiao et al., 2017).

ACBD3 IN INFECTIONS CAUSED BY OTHER VIRUSES

HCV

HCV belongs to the *Flaviridae* family and causes chronic liver diseases, liver cirrhosis and even liver cancer. Studies have shown that PI4P and PI4KA play an important role in HCV infection. HCV NS5A (Tai et al., 2009; Reiss et al., 2011) protein can hijack ARFGAP1 to maintain the PI4P concentration required for replication (Li et al., 2014). However, the role of PI4KB in HCV replication is genotype (GT)-dependent.

ACBD3 knockdown in the OR6 HCV replicon system increased HCV replication by around 70%, while ACBD3 overexpression reduced HCV replication by about 40%, indicating that ACBD3 could inhibit HCV replication (Hong et al., 2014). Further study revealed an interaction between NS5A and ACBD3. It was found that there was a GT-dependent association between NS5A and ACBD3. The binding ability of 1b NS5A to ACBD3 was stronger than that of other subtypes. NS5A associates with the same region of ACBD3 as PI4KB, that is, the amino acid sequence 116–327 of ACBD3. Therefore, NS5A and PI4KB competitively interacted with ACBD3. NS5A could hijack ACBD3 from the PI4KB/ACBD3 complex to form the NS5A/ACBD3 complex and release PI4KB to produce PI4P, which is beneficial for HCV infection (Hong et al., 2014).

African Swine Fever Virus (ASFV)

African swine fever virus (ASFV) is an acute, febrile and highly contagious virus that causes hemorrhagic fever in wild and

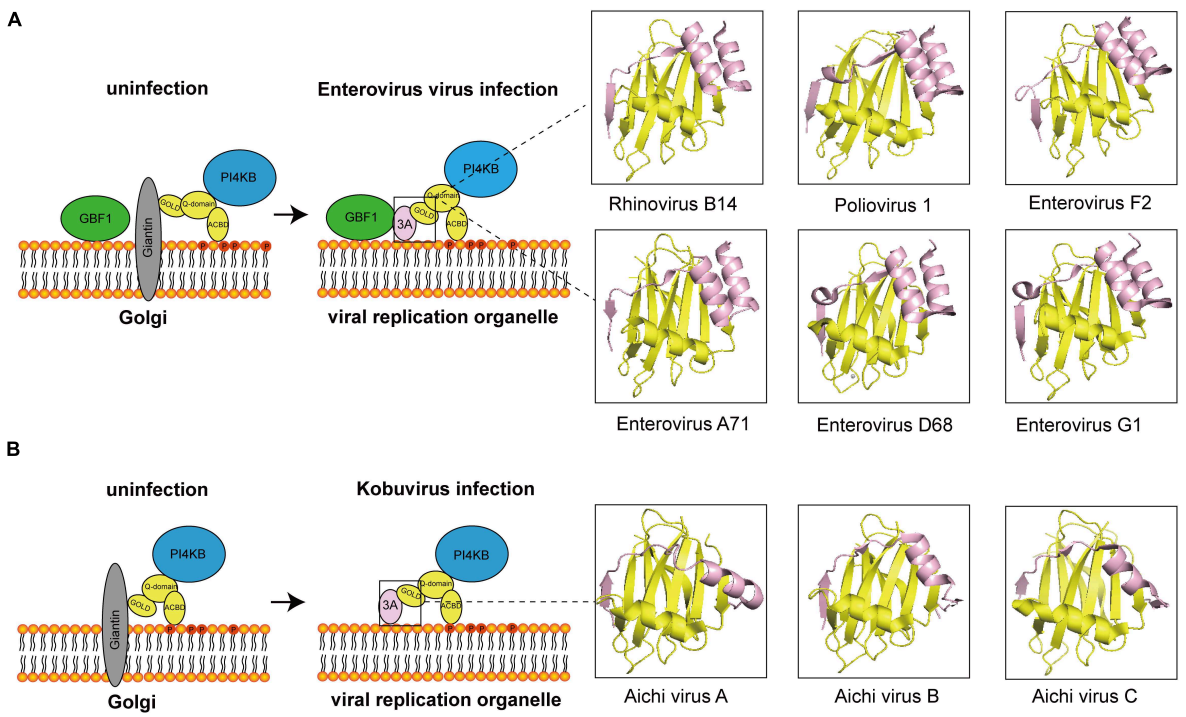

FIGURE 1 | The diagram of how 3A proteins from enterovirus and kobuvirus hijack ACBD3. **(A)** In uninfected cells, the GOLD domain of ACBD3 binds to giantin that is anchored to the Golgi membrane. GBF1 is localized in membrane. PI4KB is localized to the Golgi through interaction with the Q-domain of ACBD3. In enterovirus-infected cells, viral proteins 3A compete with giantin for binding to ACBD3. 3A also interacts with GBF1. The 3C/ACBD3/PI4KB complex is formed in viral ROs. The crystal structures of ACBD3 GOLD domain in complex with 3A protein from human Rhinovirus B14 (Protein Data Bank ID: 6HLT), human Poliovirus 1 (Protein Data Bank ID: 6HLV), bovine human Enterovirus F2 (Protein Data Bank ID: 6Q68), human Enterovirus A71 (Protein Data Bank ID: 6HLW), human Enterovirus D68 (Protein Data Bank ID: 6HLN), and porcine Enterovirus G1 (Protein Data Bank ID: 6Q69) were shown in the right. **(B)** In uninfected cells, the GOLD domain of ACBD3 binds to giantin that is anchored to the Golgi membrane. PI4KB is localized to the Golgi through interaction with the Q-domain of ACBD3. In Kobuvirus-infected cells, viral proteins 3A compete with giantin for binding to ACBD3. The 3C/ACBD3/PI4KB complex is formed in viral ROs. The crystal structures of ACBD3 GOLD domain in complex with 3A protein from human Aichi virus A (Protein Data Bank ID: 5LZ3), human Aichi virus B (Protein Data Bank ID: 5LZ6), porcine Aichi virus C (Protein Data Bank ID: 6Q67) were shown in the right.

domestic pigs with high mortality. It is an enveloped double-stranded DNA virus in the *Asfarviridae* family (Alonso et al., 2018). The length of the ASFV genome is 170–190 kb, which encodes a 151–167 open reading frame (ORF) (Chapman et al., 2008; de Villiers et al., 2010).

ASFV generates viral ROs to amplify its genome, and lipid exchange is the basis for the formation of ROs. ASFV replication requires cholesterol transport mediated by OSBP. Itraconazole (ITZ) targets OSBP and OSBP-related protein 4 (ORP4) to reduce sterol synthesis. 25-Hydroxycholesterol (25-HC) inhibits cholesterol transport by binding OSBP. ITZ at 100 μM reached 65% inhibition of ASFV replication, while 25-HC at 50 μM reduced ASFV replication by about 70% (Galindo et al., 2019). Upon ASFV infection, a number of proteins at MCSs, such as OSBP, PI4KB, and ACBD3, are recruited to ROs, confirming that cholesterol shuttling is required for ASFV RO formation (Galindo et al., 2019). However, whether ACBD3 plays an important role for ASFV replication remains to be investigated.

DISCUSSION

With the accumulating investigations of the role of ACBD3 in viruses, the mechanisms by which ACBD3 is involved in viral infection are gradually being elucidated. ACBD3 interacts with many 3A proteins from *Picornaviridae* family to affect viral replication (**Table 1**). Studies have confirmed that ACBD3 has the following effects on viral replication: (1) to promote the infection caused by viruses such as AiV; (2) to inhibit the infection caused by viruses such as HCV.

The results of different studies on the role of ACBD3 in the replication of CV, RV, and PV are not completely consistent. ACBD3 has been recognized as an important but not always essential protein for the replication of enteroviruses. One key reason is the different interference approaches used for knockout and knockdown. In previous studies, researchers applied siRNA technology. It is not possible to completely knock out ACBD3; thus, the remaining small amount of ACBD3 could also support viral replication. With the technical improvements that came with CRISPR method, it is possible to assess the role of ACBD3 in viral replication in the knockout setting. It has become obvious that ACBD3 is an essential factor for these enteroviruses.

At present, most of the viruses that interact with ACBD3 are from the *Picornaviridae* family and are PI4P-dependent viruses. In most of viruses, ACBD3 plays a central role in recruiting 3A and PI4KB to produce PI4P. The structures of how 3A proteins from enterovirus and kobuvirus hijack ACBD3 have been elucidated, which is illustrated in **Figure 1**. How does viral-induced PI4P facilitate viral replication? The original hypothesis is that PI4P recruits the viral RNA-dependent RNA polymerase (RdRP) $3D^{pol}$ (Hsu et al., 2010). However, a recent study indicated that negative charge and the membrane-tethered 3B protein worked together to recruit $3D^{pol}$ (Dubankova et al., 2017). Interestingly, researchers found that PI4P recruited OSBP to accumulate cholesterol on viral ROs (Arita, 2014; Roulin et al., 2014). Recent studies on PI4KB-resistant enteroviruses suggest that cleavage of viral 3AB protein and development of viral ROs are the targets of PI4KB/OSBP pathway in enterovirus replication (Arita, 2016; Melia et al., 2017; Arita and Bigay, 2019). In addition to $3D^{pol}$-recruitment models, these observations provide a fair view on the understanding of PI4KB/OSBP pathway. In summary, ACBD3 could be a scaffold responsible for viral ROs formation, representing a new direction for future research.

The role of ACBD3 in the replication of other viruses such as the African swine virus is less well-described. ACBD3 has been identified as a binding partner for other viruses. Yeast two-hybrid screening revealed an interaction between ACBD3 and NS3 from duck Tembusu virus (DTMUV) (Wang et al., 2019). ACBD3 associates with the Hantavirus non-structural protein (Ronnberg et al., 2012). Further research is needed to explore whether ACBD3 plays a role in additional viruses.

AUTHOR CONTRIBUTIONS

LZ conceived the work. YL, SS, and LZ wrote the manuscript and approved the final version for publication.

FUNDING

This work was supported by grants from National Natural Science Foundation of China (81871663 and 81672035), the Innovation Project of Shandong Academy of Medical Sciences, and Academic promotion programme of Shandong First Medical University (2019LJ001).

ACKNOWLEDGMENTS

We thank the reviewers for constructive comments.

REFERENCES

Alonso, C., Borca, M., Dixon, L., Revilla, Y., Rodriguez, F., Escribano, J. M., et al. (2018). ICTV virus taxonomy profile: asfarviridae. *J. Gen. Virol.* 99, 613–614. doi: 10.1099/jgv.0.001049

Arita, M. (2014). Phosphatidylinositol-4 kinase III beta and oxysterol-binding protein accumulate unesterified cholesterol on poliovirus-induced membrane structure. *Microbiol. Immunol.* 58, 239–256. doi: 10.1111/1348-0421.12144

Arita, M. (2016). Mechanism of poliovirus resistance to host phosphatidylinositol-4 kinase III beta inhibitor. *ACS Infect. Dis.* 2, 140–148. doi: 10.1021/acsinfecdis.5b00122

Arita, M. (2019). Essential domains of phosphatidylinositol-4 kinase III beta required for enterovirus replication. *Microbiol. Immunol.* 63, 285–288. doi: 10.1111/1348-0421.12718

Arita, M., and Bigay, J. (2019). Poliovirus evolution toward independence from the phosphatidylinositol-4 Kinase III beta/oxysterol-binding protein family I pathway. *ACS Infect. Dis.* 5, 962–973. doi: 10.1021/acsinfecdis.9b00038

Arita, M., Kojima, H., Nagano, T., Okabe, T., Wakita, T., and Shimizu, H. (2011). Phosphatidylinositol 4-kinase III beta is a target of enviroxime-like compounds for antipoliovirus activity. *J. Virol.* 85, 2364–2372. doi: 10.1128/jvi.02249-10

Arita, M., Kojima, H., Nagano, T., Okabe, T., Wakita, T., and Shimizu, H. (2013). Oxysterol-binding protein family I is the target of minor

enviroxime-like compounds. *J. Virol.* 87, 4252–4260. doi: 10.1128/jvi.03556-12

Baumlova, A., Chalupska, D., Rozycki, B., Jovic, M., Wisniewski, E., Klima, M., et al. (2014). The crystal structure of the phosphatidylinositol 4-kinase IIalpha. *EMBO Rep.* 15, 1085–1092. doi: 10.15252/embr.201438841

Boura, E., and Nencka, R. (2015). Phosphatidylinositol 4-kinases: function, structure, and inhibition. *Exp. Cell Res.* 337, 136–145. doi: 10.1016/j.yexcr.2015.03.028

Chalupska, D., Rozycki, B., Klima, M., and Boura, E. (2019). Structural insights into acyl-coenzyme A binding domain containing 3 (ACBD3) protein hijacking by picornaviruses. *Protein Sci.* 28, 2073–2079. doi: 10.1002/pro.3738

Chapman, D. A., Tcherepanov, V., Upton, C., and Dixon, L. K. (2008). Comparison of the genome sequences of non-pathogenic and pathogenic African swine fever virus isolates. *J. Gen. Virol.* 89(Pt 2), 397–408. doi: 10.1099/vir.0.83343-0

Chen, Y., Patel, V., Bang, S., Cohen, N., Millar, J., and Kim, S. F. (2012). Maturation and activity of sterol regulatory element binding protein 1 is inhibited by acyl-CoA binding domain containing 3. *PLoS ONE* 7:e49906. doi: 10.1371/journal.pone.0049906

de Villiers, E. P., Gallardo, C., Arias, M., da Silva, M., Upton, C., Martin, R., et al. (2010). Phylogenomic analysis of 11 complete African swine fever virus genome sequences. *Virology* 400, 128–136. doi: 10.1016/j.virol.2010.01.019

Delang, L., Paeshuyse, J., and Neyts, J. (2012). The role of phosphatidylinositol 4-kinases and phosphatidylinositol 4-phosphate during viral replication. *Biochem. Pharmacol.* 84, 1400–1408. doi: 10.1016/j.bcp.2012.07.034

Dorobantu, C. M., Ford-Siltz, L. A., Sittig, S. P., Lanke, K. H., Belov, G. A., van Kuppeveld, F. J., et al. (2015). GBF1- and ACBD3-independent recruitment of PI4KIIIbeta to replication sites by rhinovirus 3A proteins. *J. Virol.* 89, 1913–1918. doi: 10.1128/JVI.02830-14

Dorobantu, C. M., van der Schaar, H. M., Ford, L. A., Strating, J. R., Ulferts, R., Fang, Y., et al. (2014). Recruitment of PI4KIIIbeta to coxsackievirus B3 replication organelles is independent of ACBD3, GBF1, and Arf1. *J. Virol.* 88, 2725–2736. doi: 10.1128/JVI.03650-13

Dubankova, A., Humpolickova, J., Klima, M., and Boura, E. (2017). Negative charge and membrane-tethered viral 3B cooperate to recruit viral RNA dependent RNA polymerase 3D (pol). *Sci. Rep.* 7:17309. doi: 10.1038/s41598-017-17621-6

Galindo, I., Cuesta-Geijo, M. A., Del Puerto, A., Soriano, E., and Alonso, C. (2019). Lipid exchange factors at membrane contact sites in african swine fever virus infection. *Viruses* 11:199. doi: 10.3390/v11030199

Graham, T. R., and Burd, C. G. (2011). Coordination of golgi functions by phosphatidylinositol 4-kinases. *Trends Cell Biol.* 21, 113–121. doi: 10.1016/j.tcb.2010.10.002

Greninger, A. L., Knudsen, G. M., Betegon, M., Burlingame, A. L., and Derisi, J. L. (2012). The 3A protein from multiple picornaviruses utilizes the golgi adaptor protein ACBD3 to recruit PI4KIIIbeta. *J. Virol.* 86, 3605–3616. doi: 10.1128/JVI.06778-11

Hong, Z., Yang, X., Yang, G., and Zhang, L. (2014). Hepatitis C virus NS5A competes with PI4KB for binding to ACBD3 in a genotype-dependent manner. *Antiv. Res.* 107, 50–55. doi: 10.1016/j.antiviral.2014.04.012

Horova, V., Lyoo, H., Rozycki, B., Chalupska, D., Smola, M., Humpolickova, J., et al. (2019). Convergent evolution in the mechanisms of ACBD3 recruitment to picornavirus replication sites. *PLoS Pathog.* 15:e1007962. doi: 10.1371/journal.ppat.1007962

Hsu, N. Y., Ilnytska, O., Belov, G., Santiana, M., Chen, Y. H., Takvorian, P. M., et al. (2010). Viral reorganization of the secretory pathway generates distinct organelles for RNA replication. *Cell* 141, 799–811. doi: 10.1016/j.cell.2010.03.050

Ishikawa-Sasaki, K., Nagashima, S., Taniguchi, K., and Sasaki, J. (2018). Model of OSBP-mediated cholesterol supply to aichi virus RNA replication sites involving protein-protein interactions among viral proteins, ACBD3, OSBP, VAP-A/B, and SAC1. *J. Virol.* 92:e1952-17. doi: 10.1128/JVI.01952-17

Ishikawa-Sasaki, K., Sasaki, J., and Taniguchi, K. (2014). A complex comprising phosphatidylinositol 4-kinase IIIbeta, ACBD3, and Aichi virus proteins enhances phosphatidylinositol 4-phosphate synthesis and is critical for formation of the viral replication complex. *J. Virol.* 88, 6586–6598. doi: 10.1128/JVI.00208-14

Klima, M., Chalupska, D., Rozycki, B., Humpolickova, J., Rezabkova, L., Silhan, J., et al. (2017). Kobuviral non-structural 3A proteins act as molecular harnesses to hijack the host ACBD3 protein. *Structure* 25, 219–230. doi: 10.1016/j.str.2016.11.021

Klima, M., Toth, D. J., Hexnerova, R., Baumlova, A., Chalupska, D., Tykvart, J., et al. (2016). Structural insights and in vitro reconstitution of membrane targeting and activation of human PI4KB by the ACBD3 protein. *Sci. Rep.* 6:23641. doi: 10.1038/srep23641

Lei, X., Xiao, X., Zhang, Z., Ma, Y., Qi, J., Wu, C., et al. (2017). The Golgi protein ACBD3 facilitates Enterovirus 71 replication by interacting with 3A. *Sci. Rep.* 7:44592. doi: 10.1038/srep44592

Li, H., Yang, X., Yang, G., Hong, Z., Zhou, L., Yin, P., et al. (2014). Hepatitis C virus NS5A hijacks ARFGAP1 to maintain a phosphatidylinositol 4-phosphate-enriched microenvironment. *J. Virol.* 88, 5956–5966. doi: 10.1128/JVI.03738-13

Lyoo, H., van der Schaar, H. M., Dorobantu, C. M., Rabouw, H. H., Strating, J., and van Kuppeveld, F. J. M. (2019). ACBD3 is an essential pan-enterovirus host factor that mediates the interaction between viral 3A protein and cellular protein PI4KB. *MBio* 10:e02742-18. doi: 10.1128/mBio.02742-18

McPhail, J. A., Ottosen, E. H., Jenkins, M. L., and Burke, J. E. (2017). The molecular basis of aichi virus 3A protein activation of phosphatidylinositol 4 kinase IIIbeta, PI4KB, through ACBD3. *Structure* 25, 121–131. doi: 10.1016/j.str.2016.11.016

Melia, C. E., van der Schaar, H. M., Lyoo, H., Limpens, R., Feng, Q., Wahedi, M., et al. (2017). Escaping host factor PI4KB inhibition: enterovirus genomic RNA replication in the absence of replication organelles. *Cell Rep.* 21, 587–599. doi: 10.1016/j.celrep.2017.09.068

Nchoutmboube, J. A., Viktorova, E. G., Scott, A. J., Ford, L. A., Pei, Z., Watkins, P. A., et al. (2013). Increased long chain acyl-Coa synthetase activity and fatty acid import is linked to membrane synthesis for development of picornavirus replication organelles. *PLoS Pathog.* 9:e1003401. doi: 10.1371/journal.ppat.1003401

Peti, W., Page, R., Boura, E., and Rozycki, B. (2018). Structures of dynamic protein complexes: hybrid techniques to study MAP kinase complexes and the ESCRT system. *Methods Mol. Biol.* 1688, 375–389. doi: 10.1007/978-1-4939-7386-6_17

Reiss, S., Rebhan, I., Backes, P., Romero-Brey, I., Erfle, H., Matula, P., et al. (2011). Recruitment and activation of a lipid kinase by hepatitis C virus NS5A is essential for integrity of the membranous replication compartment. *Cell Host Microbe.* 9, 32–45. doi: 10.1016/j.chom.2010.12.002

Ronnberg, T., Jaaskelainen, K., Blot, G., Parviainen, V., Vaheri, A., Renkonen, R., et al. (2012). Searching for cellular partners of hantaviral nonstructural protein NSs: Y2H screening of mouse cDNA library and analysis of cellular interactome. *PLoS ONE* 7:e34307. doi: 10.1371/journal.pone.0034307

Roulin, P. S., Lotzerich, M., Torta, F., Tanner, L. B., van Kuppeveld, F. J., Wenk, M. R., et al. (2014). Rhinovirus uses a phosphatidylinositol 4-phosphate/cholesterol counter-current for the formation of replication compartments at the ER-Golgi interface. *Cell Host Microbe* 16, 677–690. doi: 10.1016/j.chom.2014.10.003

Rozycki, B., and Boura, E. (2014). Large, dynamic, multi-protein complexes: a challenge for structural biology. *J. Phys. Condens. Matter* 26:463103. doi: 10.1088/0953-8984/26/46/463103

Sasaki, J., Ishikawa, K., Arita, M., and Taniguchi, K. (2012). ACBD3-mediated recruitment of PI4KB to picornavirus RNA replication sites. *EMBO J.* 31, 754–766. doi: 10.1038/emboj.2011.429

Sohda, M., Misumi, Y., Yamamoto, A., Yano, A., Nakamura, N., and Ikehara, Y. (2001). Identification and characterization of a novel Golgi protein, GCP60, that interacts with the integral membrane protein giantin. *J. Biol. Chem.* 276, 45298–45306. doi: 10.1074/jbc.M108961200

Solomon, T., Lewthwaite, P., Perera, D., Cardosa, M. J., McMinn, P., and Ooi, M. H. (2010). Virology, epidemiology, pathogenesis, and control of enterovirus 71. *Lancet Infect. Dis.* 10, 778–790. doi: 10.1016/S1473-3099(10)70194-8

Tai, A. W., Benita, Y., Peng, L. F., Kim, S. S., Sakamoto, N., Xavier, R. J., et al. (2009). A functional genomic screen identifies cellular cofactors of hepatitis C virus replication. *Cell Host Microbe* 5, 298–307. doi: 10.1016/j.chom.2009.02.001

Teoule, F., Brisac, C., Pelletier, I., Vidalain, P. O., Jegouic, S., Mirabelli, C., et al. (2013). The Golgi protein ACBD3, an interactor for poliovirus protein 3A, modulates poliovirus replication. *J. Virol.* 87, 11031–11046. doi: 10.1128/JVI.00304-13

van der Schaar, H. M., van der Linden, L., Lanke, K. H., Strating, J. R., Purstinger, G., de Vries, E., et al. (2012). Coxsackievirus mutants that can bypass host factor

PI4KIIIbeta and the need for high levels of PI4P lipids for replication. *Cell Res.* 22, 1576–1592. doi: 10.1038/cr.2012.129

Wang, H., Perry, J. W., Lauring, A. S., Neddermann, P., De Francesco, R., and Tai, A. W. (2014). Oxysterol-binding protein is a phosphatidylinositol 4-kinase effector required for HCV replication membrane integrity and cholesterol trafficking. *Gastroenterology* 146, 1373–1385.e1-11. doi: 10.1053/j.gastro.2014.02.002

Wang, Y., Zhang, S., Tang, Y., and Diao, Y. (2019). Screening of duck tembusu virus NS3 interacting host proteins and identification of its specific interplay domains. *Viruses* 11:740. doi: 10.3390/v11080740

White, D. R., and Aitken, R. J. (1989). Influence of epididymal maturation on cyclic AMP levels in hamster spermatozoa. *Int. J. Androl.* 12, 29–43. doi: 10.1111/j.1365-2605.1989.tb01283.x

Xiao, X., Lei, X., Zhang, Z., Ma, Y., Qi, J., Wu, C., et al. (2017). Enterovirus 3A facilitates viral replication by promoting phosphatidylinositol 4-kinase IIIBETA-ACBD3 interaction. *J. Virol.* 91:e791-17. doi: 10.1128/JVI.00791-17

Xing, W., Liao, Q., Viboud, C., Zhang, J., Sun, J., Wu, J. T., et al. (2014). Hand, foot, and mouth disease in China, 2008-12: an epidemiological study. *Lancet Infect. Dis.* 14, 308–318. doi: 10.1016/s1473-3099(13)70342-6

Conflict of Interest: The authors declare that the research was conducted in the absence of any commercial or financial relationships that could be construed as a potential conflict of interest.

frontiers in Plant Science

ORIGINAL RESEARCH
published: 28 April 2020
doi: 10.3389/fpls.2020.00491

Ultrastructural Analysis of Cells From Bell Pepper (*Capsicum annuum*) Infected With Bell Pepper Endornavirus

Katarzyna Otulak-Kozieł[1], Edmund Kozieł[1]*, Cesar Escalante[2] and Rodrigo A. Valverde[2]*

[1] Institute of Biology, Department of Botany, Warsaw University of Life Sciences—SGGW, Warsaw, Poland, [2] Department of Plant Pathology and Crop Physiology, Louisiana State University Agricultural Center, Baton Rouge, LA, United States

OPEN ACCESS

Edited by:
Miguel A. Martín-Acebes, Instituto Nacional de Investigación y Tecnología Agraria y Alimentaria (INIA), Spain

Reviewed by:
Marilyn Roossinck, Pennsylvania State University (PSU), United States
Won Kyong Cho, Seoul National University, South Korea

***Correspondence:**
Katarzyna Otulak-Kozieł
katarzyna_otulak@sggw.edu.pl
Edmund Kozieł
edmund_koziel@sggw.edu.pl

Specialty section:
This article was submitted to Virology, a section of the journal Frontiers in Plant Science

Received: *31 January 2020*
Accepted: *01 April 2020*
Published: *28 April 2020*

Citation:
Otulak-Kozieł K, Kozieł E, Escalante C and Valverde RA (2020) Ultrastructural Analysis of Cells From Bell Pepper (Capsicum annuum) Infected With Bell Pepper Endornavirus. Front. Plant Sci. 11:491. doi: 10.3389/fpls.2020.00491

Endornaviruses include viruses that infect fungi, oomycetes, and plants. The genome of plant endornaviruses consists of linear ssRNA ranging in size from approximately 13-18 kb and lacking capsid protein and cell-to-cell movement capability. Although, plant endornaviruses have not been shown to cause detectable changes in the plant phenotype, they have been associated with alterations of the host physiology. Except for the association of cytoplasmic vesicles with infections by *Vicia faba* endornavirus, effects on the plant cell ultrastructure caused by endornaviruses have not been reported. Bell pepper endornavirus (BPEV) has been identified in several pepper (*Capsicum* spp.) species. We conducted ultrastructural analyses of cells from two near-isogenic lines of the bell pepper (*C. annuum*) cv. Marengo, one infected with BPEV and the other BPEV-free, and found cellular alterations associated with BPEV-infections. Some cells of plants infected with BPEV exhibited alterations of organelles and other cell components. Affected cells were located mainly in the mesophyll and phloem tissues. Altered organelles included mitochondrion, chloroplast, and nucleus. The mitochondria from BPEV-infected plants exhibited low number of cristae and electron-lucent regions. Chloroplasts contained plastoglobules and small vesicles in the surrounding cytoplasm. Translucent regions in thylakoids were observed, as well as hypertrophy of the chloroplast structure. Many membranous vesicles were observed in the stroma along the envelope. The nuclei revealed a dilation of the nuclear envelope with vesicles and perinuclear areas. The organelle changes were accompanied by membranous structure rearrangements, such as paramural bodies and multivesicular bodies. These alterations were not observed in cells from plants of the BPEV-free line. Overall, the observed ultrastructural cell alterations associated with BPEV are similar to those caused by plant viruses and viroids and suggest some degree of parasitic interaction between BPEV and the plant host.

Keywords: plant virus, *Endornaviridae*, electron microscopy, symptomless plants, plant organelle alterations, near isogenic lines, persistent virus

INTRODUCTION

Peppers (Capsicum species in the family Solanaceae) are native plants from the Americas and are cultivated worldwide as food crops (DeWitt and Bosland, 1996; Pickersgill, 1997). Although there are five domesticated Capsicum species (*C. annuum, C. baccatum, C. chinense, C. frutescens,* and *C. pubescens*), *C. annuum* is the most commonly cultivated (Bosland et al., 1996; DeWitt and Bosland, 1996; Pickersgill, 1997). Several *C. annuum* horticultural types have been identified, including bell, cayenne, jalapeño, ancho, serrano, poblano, and others (Smith et al., 1987).

Based on host symptom expression, plant viruses can be divided into two categories: acute and persistent (Roossinck, 2010). Acute viruses are transmitted horizontally and, in some cases, vertically. Their genome encodes for a cell-to-cell movement protein (MP), which in combination with other proteins gives them the ability to spread from the point of initial infection (Rojas et al., 2016). In contrast, persistent viruses do not cause morphological symptoms; they lack MP and are transmitted only vertically via gametes (Roossinck, 2010; Fukuhara, 2019). Persistent plant viruses include members of the families *Amalgaviridae, Chrysoviridae, Endornaviridae, Nardaviridae, Partitiviridae,* and *Totiviridae* (Roossinck, 2010; Nibert et al., 2018; Fukuhara, 2019; Takahashi et al., 2019). Persistent viruses have been reported to infect economically important crops such as alfalfa, avocado, corn, sugar beet, common bean, rice, pepper, melon, radish, and tomato (Boccardo et al., 1987; Fukuhara et al., 1993; Pfeiffer, 1998; Okada et al., 2011; Villanueva et al., 2012; Li et al., 2013; Sabanadzovic et al., 2016; Akinyemi et al., 2018). However, due to the lack of symptom induction and the lack of transmission by conventional methods, persistent viruses have been poorly studied. Interactions of persistent viruses with the host, acute viruses, and other biotic and abiotic agents have not been investigated.

Viruses in the family *Endornaviridae* infect fungi, oomycetes, and plants (Fukuhara, 2019; Valverde et al., 2019). The genome of plant endornaviruses consist of linear positive sense ssRNA ranging in size from approximately 13–18 k and lacking capsid protein (CP) and MP (Roossinck et al., 2011; Dolja and Koonin, 2018; Valverde et al., 2019). Indirect evidence suggests they are present in all tissues of the infected plant (Valverde et al., 2019). Like other persistent plant viruses, they have not been shown to cause visible phenotypic changes in the host (Khankhum and Valverde, 2018; Escalante and Valverde, 2019; Fukuhara, 2019). Nevertheless, plant endornaviruses have been associated with alterations of the host physiology such as seed germination, cytoplasmic male sterility, and chlorophyll content (Grill and Garger, 1981; Khankhum and Valverde, 2018; Escalante and Valverde, 2019).

Bell pepper endornavirus (BPEV) has been identified in many *C. annum* cultivars but particularly in the bell pepper horticultural type (Valverde et al., 1990; Okada et al., 2011; Safari and Roossinck, 2018). Moreover, a closely related virus, Capsicum frutescens endornaviurus 1 (CFEV 1), has been reported infecting several domesticated *Capsicum* species (Safari and Roossinck, 2018). Safari and Roossinck showed that BPEV occur only in *C. annuum*. In contrast, CFEV 1 was detected in *C. frutescens, C. chinense, and C. baccatum*. These results suggest that endornaviruses of *Capsicum* are not species-specific.

In a comparative study using near-isogenic lines (NILs) of bell pepper cv. Marengo, one BPEV-infected and the other BPEV-free, Escalante and Valverde (2019) determined that BPEV was not associated with changes in the host phenotype. However, the plant height, number of fruits, and total fruit weight was higher in plants of the BPEV-free line than in plants of the BPEV-infected line. However, in most experiments, the differences were not statistically significant. Escalante and Valverde (2019) concluded that BPEV appears to have a weak parasitic relationship with the host.

Except for the association of cytoplasmic vesicles in *Vicia faba* with infections by Vicia faba endornavirus (VfEV) (Dulieu et al., 1988), studies on the effects on the plant cell ultrastructure by endornaviruses have not been reported. One factor contributing to the lack of studies is that plant endornaviruses are not transmitted by conventional virus-inoculation methods; therefore, results from comparative studies using different plant genotypes are not reliable. The availability of BPEV-infected and BPEV-free near-isogenic lines provided us with material to conduct a comparative study to determine if ultrastructural changes in bell pepper are associated with BPEV infections. In this investigation, we conducted an ultrastructural analysis of leaf tissues of two near-isogenic lines of the bell pepper cultivar Marengo, one infected with BPEV and the other BPEV-free, and report the association of ultrastructural cytopathology with BPEV infections.

MATERIALS AND METHODS

Plant Material

Seeds from two NILs of *C. annuum* cv. Marengo, one infected with BPEV and the other BPEV-free, developed in previous investigations (Escalante and Valverde, 2019) were planted and grown in a phytotron growth chamber at 20°C and 16 h light with an intensity of 400 μmol m-2 s-1 PAR (photosynthetically active radiation). The plant phenotype of both lines was visually examined (daily) throughout their life cycle. The presence or absence of BPEV in experimental plants was tested by analysis of viral replicative form dsRNA by gel electrophoresis and reverse transcription PCR (RT-PCR) as described in previous investigations (Okada et al., 2011; Khankhum et al., 2017). Furthermore, plants were tested for the presence of pepper mild mottle virus by RT-PCR (Jarret et al., 2008). Total RNA extracted from healthy tobacco (*Nicotiana tabaccum*) plants with the Spectrum Plant Total RNA Kit (Sigma-Aldrich, St. Louis, MO) was used as negative control in RT-PCR reactions.

Tissue Preparation for Light Microscopy and Transmission Electron Microscopy (TEM) Examinations

Leaves from two-month-old plants of both NILs at similar developmental stage were selected for transmission electron microscope examinations. Thirty-five sections (2 mm^2) were

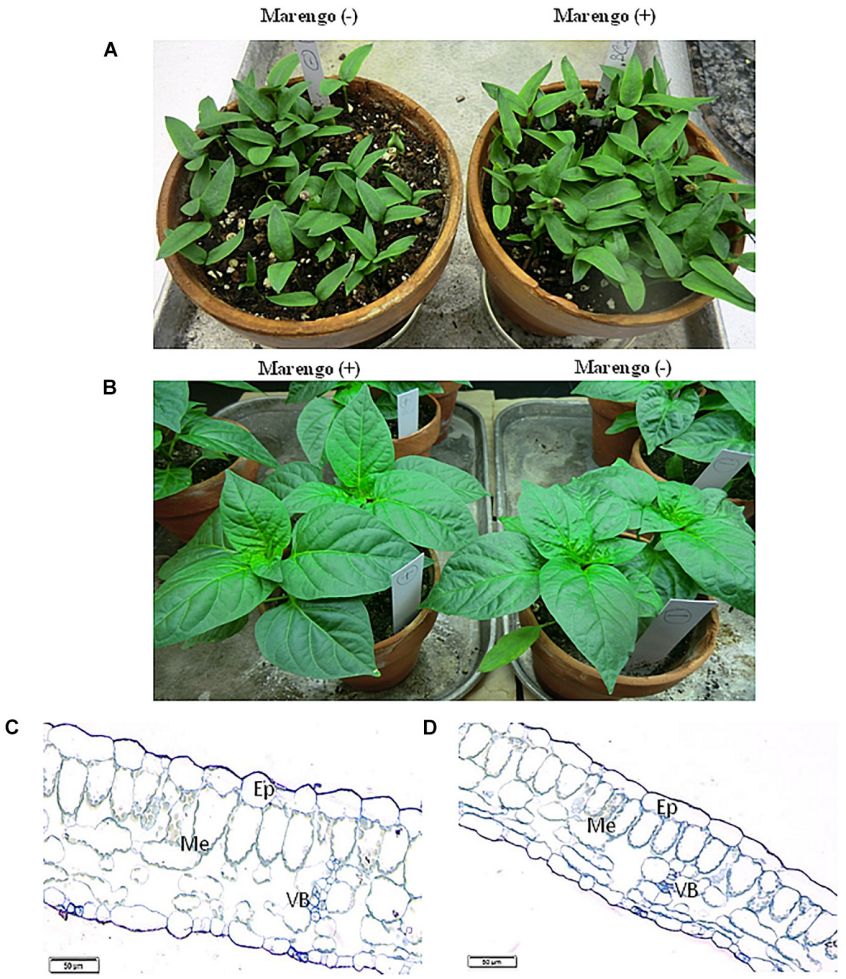

FIGURE 1 | Morphology and anatomy of two near-isogenic lines of bell pepper cv. Marengo, one infected with BPEV [Marengo (+)] and the other BPEV-free [Marengo (–)]. **(A)** Seedlings, **(B)** Two- month-old plants. **(C,D)** Light microscopy of cross sections of tissues from two-month-old plants showing epidermis (Ep), Mesophyll (Me), and vascular bundles (VB). Bar 50 μm.

excised from each NIL and fixed as reported previously (Otulak-Kozieł et al., 2018, 2019). Briefly, tissues were initially fixed as described by Karnovsky (1965) and in 2% (w/v) osmium tetroxide solution in 0.05 M cacodylate buffer for 2 h at 4°C. Samples were dehydrated in ethanol series and embedded in Epoxy resin (Epon812, Sigma) with polymerization for 24 h at 60°C. For the examination of the anatomy, glass slides with macro-sections were stained with crystal violet solution (Otulak and Garbaczewska, 2010) and examined with a AX70 PROVIS light microscope with an Olympus UP90 High Definition camera (Olympus, Warsaw, Poland) using Olympus Cell Sense Standard Software (Olympus, Center Valley, PA, United States, version 1.18). Ultrathin sections (70–80 nm) were obtained using an UCT ultramicrotome (Leica Microsystems) and collected on formvar-coated copper grids. Grids were stained with 1.2% uranyl acetate and 2.5% lead citrate. Analyses of ultrathin sections from leaves of both NILs were performed using a transmission electron microscope (268D Morgagni TEM (FEI) at 80 kV) as previously described (Otulak-Kozieł et al., 2018, 2019). Images were captured with a Morada digital camera (Olympus SIS). All foliar sections were examined without knowledge of whether they were BPEV-infected or BPEV-free.

RESULTS

Gel electrophoresis and RT-PCR testing of plants of the two lines used for the ultrastructural analysis confirmed the presence of BPEV in BPEV-infected plants and absence of BPEV in BPEV-free plants (**Supplementary Figures S1A,B**). Moreover, pepper mild mottle virus was not detected in any of the experimental plants.

Morphology and Anatomy of Near-Isogenic Lines (NILs)

As reported in previous investigations (Okada et al., 2011; Escalante and Valverde, 2019), we did not observe phenotypical differences between the BPEV-infected and the BPEV-free

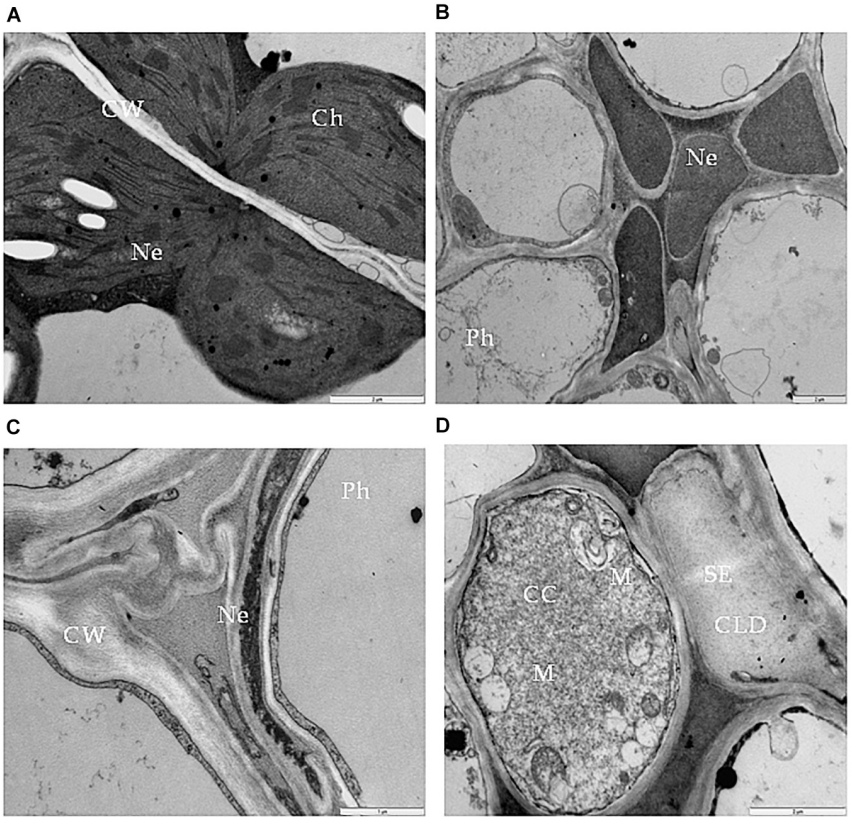

FIGURE 2 | Necrosis in bell pepper tissues infected with BPEV. **(A)** Necrosis (Ne) of palisade mesophyll cells. Bar 2 μm. **(B)** Necrosis (Ne) in phloem (Ph) elements. Bar 2 μm. **(C)** Collapsed sieve element and necrosis of companion cell (CC). Bar 2 μm. **(D)** Sieve element (SE) filled with callose like deposition and companion cell (CC) with expanded mitochondria (M). Bar 2 μm.

bell pepper NILs (**Figures 1A,B**). Moreover, light microscopy examinations of cross sections of foliar tissues from both lines did not show visible differences on their anatomy (**Figures 1C,D**).

Cellular Ultrastructural Changes Associated With Bell Pepper Endornavirus Infection

Electron microscopy examinations of foliar tissues of the two lines did not yield any evidence of virus-like particles or viral inclusion bodies.

Ultrastructural alterations of cell organelles and other components were observed in bell pepper tissues infected with BPEV. Some or all of these alterations were consistently observed in some cells of all 35 analyzed leaf sections. The altered cells were located mainly in the mesophyll and phloem tissues.

One type of alteration consisted of necrosis of palisade mesophyll cells, which contained electron-dense cytoplasm (**Figure 2A**). Necrosis of some phloem elements was also observed (**Figure 2B**). The necrosis of the phloem cells was associated with collapsing of the sieve tubes and cell wall invaginations (**Figure 2C**). The altered ultrastructure of the sieve tubes was associated with abnormal companion cells. When compared with similar cells of the BPEV-free line (**Figure 3**), cells of the BPEV-infected line showed a decreased number of mitochondria and contained some mitochondria without crista (**Figure 2D**). In addition, these cells exhibited electron-dense regions along the cell wall, whereas, sieve tubes were filled with callose-like material (**Figure 2D**). Further analyses of phloem tissue cells revealed alterations of the cell wall. The spectrum of cell wall changes ranged from loss of cell wall structure, often near plasmodesmata (**Figure 4A**) to irregular cell wall invaginations associated with membranous paramural bodies (**Figures 4B–E**). Paramural bodies were observed associated with the cell wall of some phloem parenchyma, epidermis, and mesophyll cells. These paramular bodies were often located near the tonoplast of vacuoles, suggesting movement from the apoplast to the vacuoles. Membrane bound structures associated with the symplast region, such as multivesicular bodies were commonly observed in some cells from tissues of the BPEV-infected line. These multivesicular bodies varied in shape and occurred in the cytoplasm and vacuoles of mesophyll, phloem, and sometimes xylem parenchyma cells (**Figures 5A–D**). Numerous granular structures were frequently present inside the multivesicular bodies.

Further analysis of cells from the BPEV-infected line revealed ultrastructural changes in some cell organelles. The mitochondria exhibited a variety of structural alterations, which

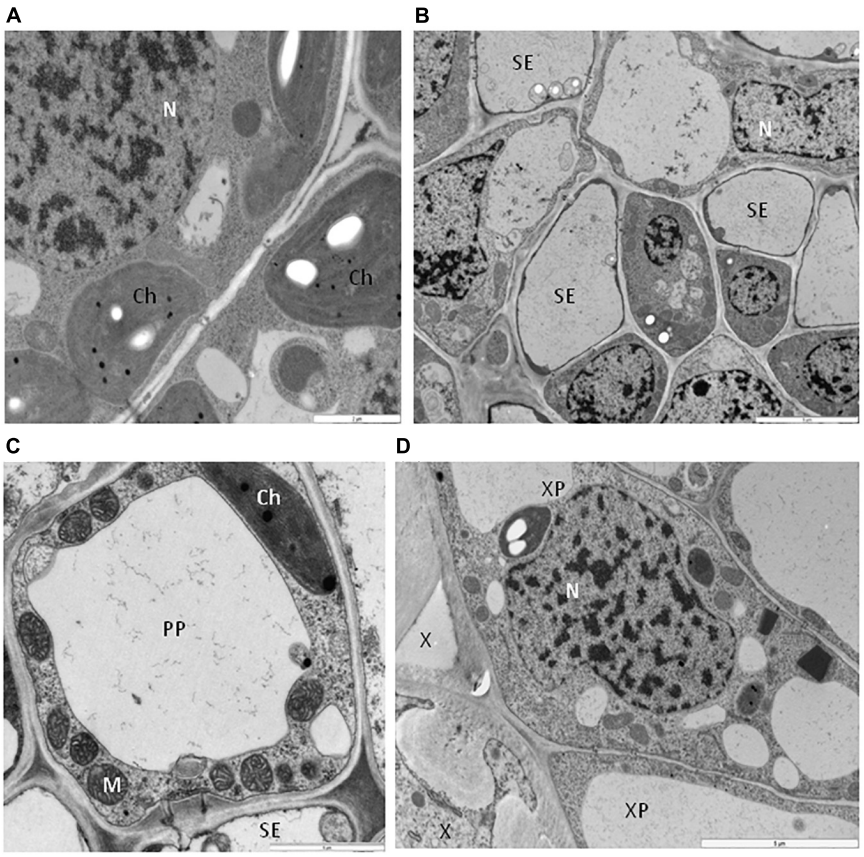

FIGURE 3 | Cells of bell pepper tissues free of BPEV. **(A)** Spongy mesophyll cells. Ch-chloroplast, N-nucleus. Bar 2 μm. **(B)** Phloem cells. N-nucleus, SE-sieve element. Bar 5 μm. **(C)** Sieve element (SE) with companion cell (CC). Ch-chloroplast, M-mitochondria. Bar 5 μm. **(D)** Xylem cells. N-nucleus, X-xylem tracheary elements, XP-xylem parenchyma. Bar 5 μm.

included a decrease number of crista and electron-lucent regions (**Figures 6A,B**). Mitochondria with electron-lucent areas formed an expanded exosome like vesicles (**Figures 6C,D**). None of these changes were observed in mitochondria of cells of the BPEV-free line (**Figure 6E**).

When compared with chloroplast from cells of the BPEV-free line (**Figure 7A**), alterations of the chloroplast structure was observed in cells of the BPEV-infected line. The structure of the chloroplast thylakoids was altered (**Figure 7B**). Changes of the normal chloroplast shape and presence of small vesicles inside stroma were observed in some BPEV-infected cells (**Figure 7C**). Plastoglobules and small vesicles were often observed outside the chloroplast envelope (**Figures 7C,D**). Hypertrophy of the chloroplast structure included translucent regions in thylakoids and the presence of numerous membranous vesicles in stroma along envelope (**Figures 7E,F**).

Some phloem parenchyma cells from the BPEV-infected line contained nuclei with dilation of the nuclear envelope and vesicles and perinuclear areas (**Figure 8A**). Whereas, in the mesophyll cells, lobed nucleus with translucent regions containing small vesicles were often observed (**Figures 8B,C**), including strong chromatin condensation (**Figure 8D**). None of the changes in cell organelles and other cell components described above were observed in cells of BPEV-free line (**Figure 8E**).

The alterations described above were not observed in all cells of the BPEV-infected line. Many cells of the BPEV-infected line contained unaltered organelles and other cell components which were undistinguishable from the organelles and cell components of the BPEV-free line.

DISCUSSION

Previous studies have reported that plants infected with endornaviruses are symptomless (Khankhum and Valverde, 2018; Escalante and Valverde, 2019; Fukuhara, 2019). The genomes of these viruses do not code for a CP, and therefore, it is not surprising that virions have not been reported in endornavirus-infected cells (Valverde et al., 1990; Zabalgogeazcoa and Gildow, 1992; Fukuhara, 1999). Limited studies on the cellular location of the RNA of plant endornaviruses suggest that they are concentrated in the cytoplasm (Lefebvre et al., 1990; Valverde et al., 1990; Okada et al., 2013; Liu et al., 2018). The replicative form of the genomic RNA (dsRNA) of VfEV-infected *V. faba* has been found to be associated with cytoplasmic vesicles and viral

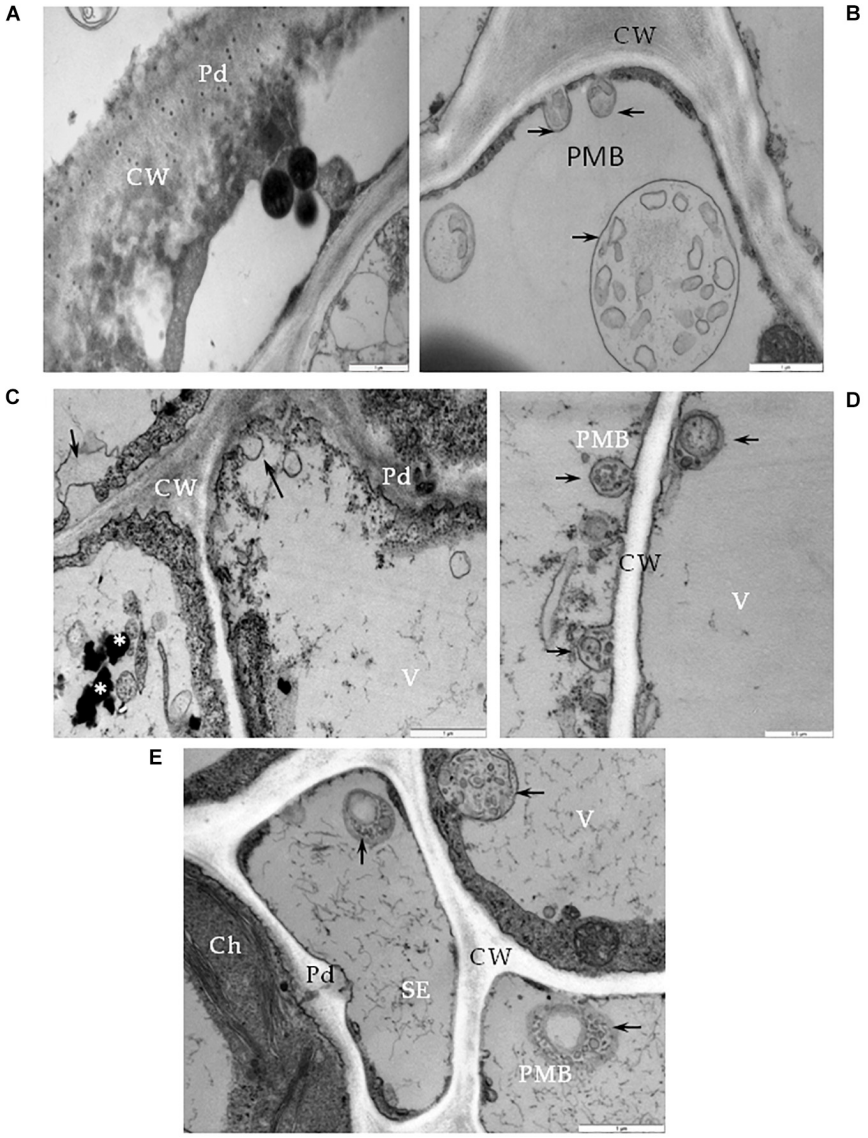

FIGURE 4 | Cell wall alterations in cells of BPEV-infected tissues. **(A)** Phloem parenchyma (PP) cell wall (CW) loosening in the area near the plasmodesmata (Pd). Bar 1 μm. **(B)** Paramular bodies (PMB) formation (arrows) in epidermis cell. CW-cell wall. Bar 1 μm. **(C)** Changed cell wall (CW) structure with the formation of paramular bodies (arrows) in phloem parenchyma cells. Vesicular structures around phenolic compounds in vacuole (*). Pd-plasmodesmata. Bar 1 μm. **(D)** Paramular bodies (arrows, PMB) between cell wall (CW) and vacuole (V) in mesophyll cells. Bar 0.5 μm. **(E)** Paramular bodies (arrows, PMB) in sieve elements (SE) and companion phloem cells. Ch-chloroplast, Pd-plasmodesmata. Bar 1 μm.

dsRNA isolated from purified vescicles (Lefebvre et al., 1990). As mentioned earlier in this paper, at the present time, other than the vesicles in VfEV-infected cells, no cytopathic effects have been reported as associated with endornaviruses, and there is no information on the effect of endornaviruses to cell organelles or other cell components.

The formation of cytoplasmic vesicles is one of the most common cellular responses to infection of plants by viruses (Francki, 1987). In this investigation, we observed cytoplasmic vesicles and multivesicular bodies in BPEV-infected cells which were similar to those reported in plants infected with acute viruses. In plant cells, single-stranded positive-sense RNA viruses generate cytoplasmic membranous vesicles, where viral replication takes place (Wei and Wang, 2008). These vesicles contain viral ssRNA, replicative dsRNA, and proteins involved in virus replication (Lefebvre et al., 1990; Cotton et al., 2009; Cabanillas et al., 2018). Vesicles can be developed from membranes of various cell organelles such as chloroplasts, mitochondria, peroxisomes, endoplasmic reticulum, or tonoplast (Hatta and Ushiyama, 1973; Hatta and Francki, 1980; Martelli et al., 1984; Laliberté and Zheng, 2014). Multivesicular bodies have been reported in cells infected with tomato bunchy top virus (Martelli et al., 1984). Cytoplasmic vesicles apparently formed by invaginations of the plasma membrane have been

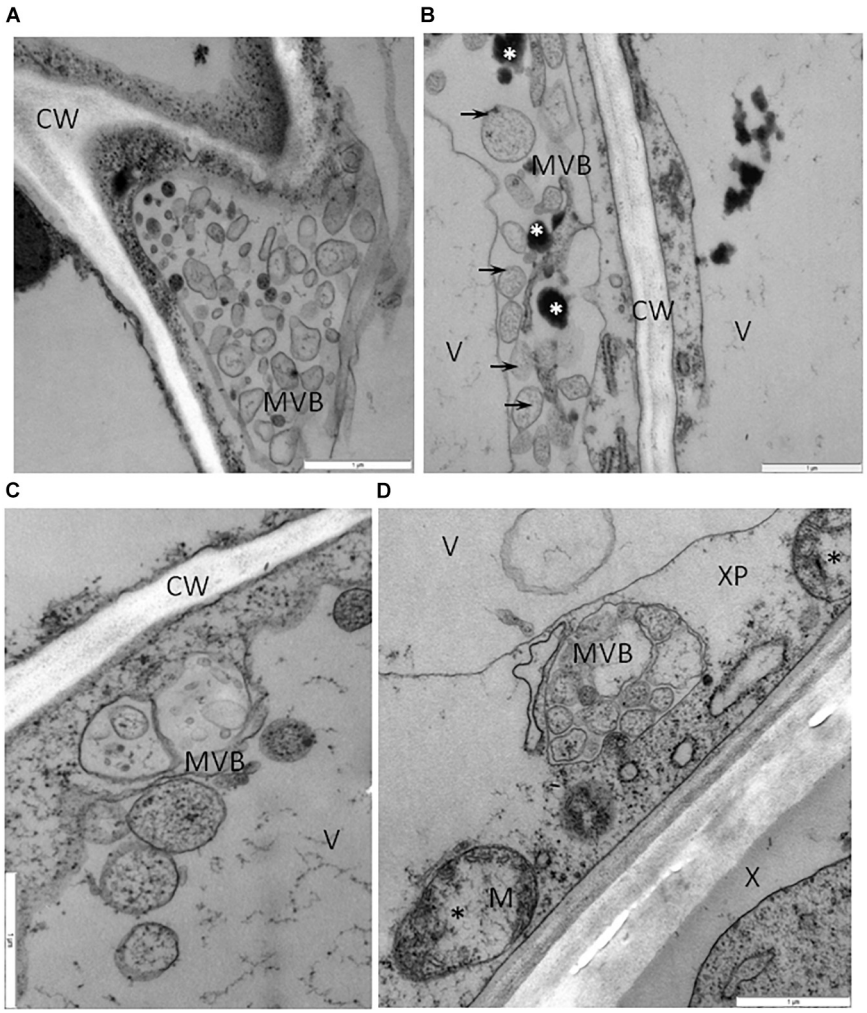

FIGURE 5 | Vesicles and multivesicular structures in cells of BPEV-infected tissues. **(A)** Multivesicular structures (MVB) in vacuole of phloem parenchyma cell. CW-cell wall. Bar 1 μm. **(B)** Multivesicular structures (arrows, MVB) and phenolic compounds (white *) in cytoplasm of mesophyll cell. CW-cell wall, V-vacuole. Bar 1 μm. **(C)** Vesicles and multivesicular structures (MVB) in vacuole (V) of mesophyll cell. CW-cell wall bar 1 μm. **(D)** Multivesicular structures (MVB) in cytoplasm of xylem parenchyma (XP) cell. Mitochondria (M) with electron-lucent area (black *). X-xylem tracheary elements. Bar 1 μm.

reported in tomato plants infected with potato spindle tuber viroid. Membrane-bound vesicles (50-90 nm in diameter) have been observed in fungi infected with hypoviruses (Newhouse et al., 1990; Khalifa and Pearson, 2014). Moreover, the presence of a large number multivesicular bodies has been associated with viral genome replication (Laliberté and Sanfaçon, 2010; Laliberté and Zheng, 2014). Multivesicular bodies have also been associated with cell wall-associated defense response in barley leaves infected with the pathogen that causes powdery mildew (An et al., 2006a,b). Cytoplasmic vesicles and multivesicular bodies generated in BPEV-infected cells suggest involvement of these structures in the virus replication as reported for brome mosaic virus (Bamunusinghe et al., 2011). Paramural bodies observed in cells infected with BPEV are similar to paramular bodies observed in the potato virus Y (PVY)-resistant potato cultivar Sárpo Mira when infected with PVY (Otulak-Kozieł et al., 2018). Paramural bodies and membrane alterations have also been reported in cells infected with potato spindle tuber viroid (Hari, 1980).

Plant viruses have been shown to target photosynthesis and negatively affect the chloroplast function, including host chlorophyll content (Zhao et al., 2016). Morphological changes of the chloroplast have been reported to be associated with plant virus or viroid infections (Hari, 1980; Lin and Langenberg, 1984). It has been shown that the chloroplasts of potato spindle tuber viroid-infected cells exhibit reduced grana and loosely arranged thylakoids (Hari, 1980). Lin and Langenberg (1984) reported that barley stripe mosaic virus caused alterations of the wheat chloroplast membranes, characterized by the clustering of outer membrane-invaginated spherules in inner membrane-derived packets. They also observed diverse morphologies of cytoplasmic invaginations with spherules at the periphery and different sized openings connecting the cytoplasmic invaginations with the cytoplasm (Lin and Langenberg, 1984).

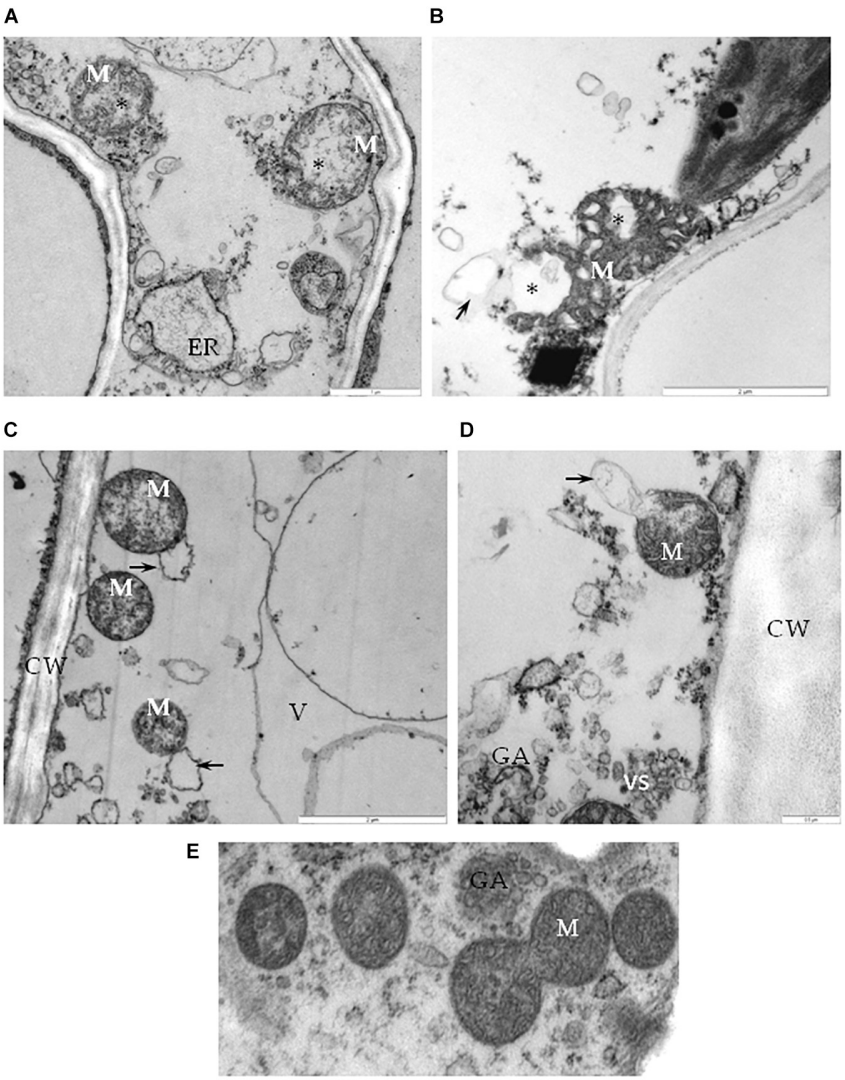

FIGURE 6 | Alterations of mitochondria in cells of BPEV-infected tissues. **(A)** Mitochondria (M) with electron-lucent area (*) and expanded endoplasmatic reticulum (ER) in phloem parenchyma cell. Bar 1 μm. **(B)** Mitochondria (M) with an electron-lucent area (*) forming a vesicle-like structure (arrow) in mesophyll cell. Bar 2 μm. **(C)** Mitochondria (M) forming exosome like vesicles (arrows) in phloem parenchyma cell. CW-cell wall, V- vacuole. Bar 2 μm. **(D)** Mitochondria (M) with exosome like structure (arrow) in phloem companion cell. GA- trans Golgi network, vs-vesicles. Bar 0.5 μm. **(E)** Mitochondria (M) of a BPEV-free mesophyll cell. GA- trans Golgi network Bar 0.5 μm.

We observed similar changes of the chloroplast and cytoplasm in cells of the BPEV-infected line. In a comparative study of endornavirus-infected and endornavirus-free common bean (*Phaseolus vulgaris),* Khankhum and Valverde (2018) reported statistically significantly lower chlorophyll content of the endornavirus-infected line. Although in the case of bell pepper and BPEV, Escalante and Valverde (2019) did not find statistically significant differences on the amount of chlorophyll content between infected and healthy lines.

The mitochondria in BPEV-infected cells exhibited a variety of structural alterations which included electron-lucent areas and expanded exosome like vesicles. In turnip, infections by turnip mosaic virus causes vesicularization of the outer mitochondrial membranes (Blake et al., 2007; Otulak and Garbaczewska, 2013; Otulak et al., 2015). Electron microscopic observations of thin sections of cells from tissues infected with cucumber green mottle mosaic virus revealed the formation of small vesicles in the mitochondria (Hatta and Ushiyama, 1973). Gómez-Aix et al. (2015) reported that melon necrotic spot virus replication occurs in association with altered mitochondria. Cytoplasmic vesicles that develop from modified mitochondria have been shown to be associated with infections by tombusviruses (Di Franco et al., 1984). Park et al. (2006) reported smaller and fewer mitochondria in the fungus *Chalara elegans* infected with a mitovirus. Mitoviruses are small RNA viruses that infect plants and fungi and replicate in the mitochondria (Nibert et al., 2018).

Many of the cellular alterations reported in this investigation resemble effects caused by biotic and abiotic stresses in plants.

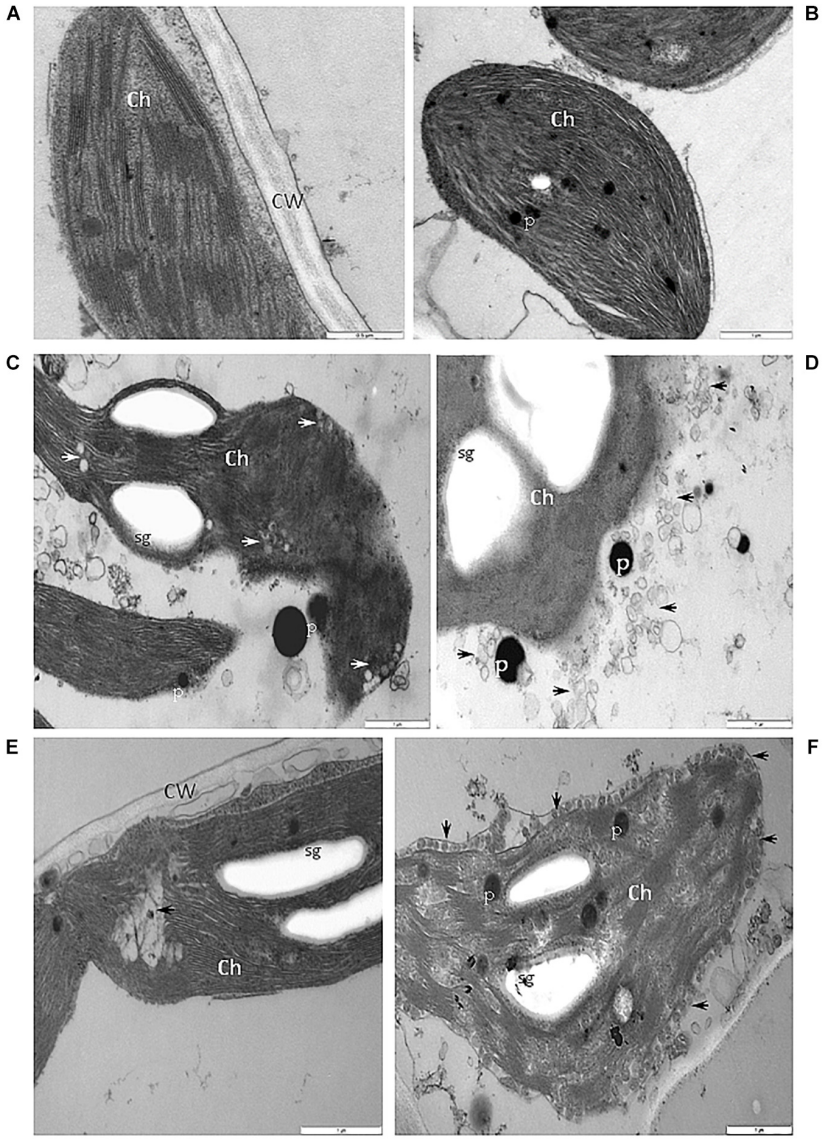

FIGURE 7 | Alterations of the structure of chloroplasts in cells of BPEV-infected tissues. **(A)** Chloroplast (Ch) of a BPEV-free mesophyll cell. CW-cell wall. Bar 0.5 μm. **(B)** Abnormal structure of thylakoids. Ch-chloroplast, P-plastoglobules. Bar 1 μm. **(C)** Alteration of the chloroplast (Ch) morphology and small vesicles inside stroma (arrows). P-plastoglobules, sg-starch grains. Bar 1 μm. **(D)** Small vesicles (arrows) and plastoglobules (P) between the chloroplast (Ch) and the chloroplast membrane. sg-starch grains. Bar 1 μm. **(E)** Electron lucent area (arrow) inside chloroplast (Ch). CW-cell wall, sg-starch grains. Bar 1 μm. **(F)** Small vesicles (arrows) of stroma fragmentation and altered chloroplast (Ch) envelope. P-plastoglobules, sg-starch grains. Bar 1 μm.

Although infected bell pepper plants containing the described cell alterations did not appear diseased, these alterations should negatively affect the normal plant physiology. In spite of the presence of clusters of necrotic cells, we did not observe tissue necrosis. It is possible that the number of necrotic cells was below the threshold to cause visible necrosis. The observed cellular alterations may explain the lower seed germination, plant height, number of fruits, and total fruit weight of BPEV-infected plants than plants of the BPEV-free line reported by Escalante and Valverde (2019).

While conducting investigations on the coevolution of *Capsicum* endornaviruses and the host, Safari and Roossinck (2018) generated data to support the idea that the ancestor of CFEV 1, may have evolved as BPEV in *C. annuum*. In the United States, BPEV has been detected in all tested bell pepper (*C. annuum*) cultivars (Okada et al., 2011; Escalante and Valverde, 2019). This suggests that bell pepper breeders have selected only BPEV-infected lines to develop commercial cultivars and therefore BPEV may provide an unknown beneficial effect to the plant. Similarly, most melon cultivars tested for Cucumis melo endornavirus have been found infected (Sabanadzovic et al., 2016). Nevertheless, it is possible that the beneficial effects may be effective only under certain environmental conditions. Common bean (*Phaseolus vulgaris*)

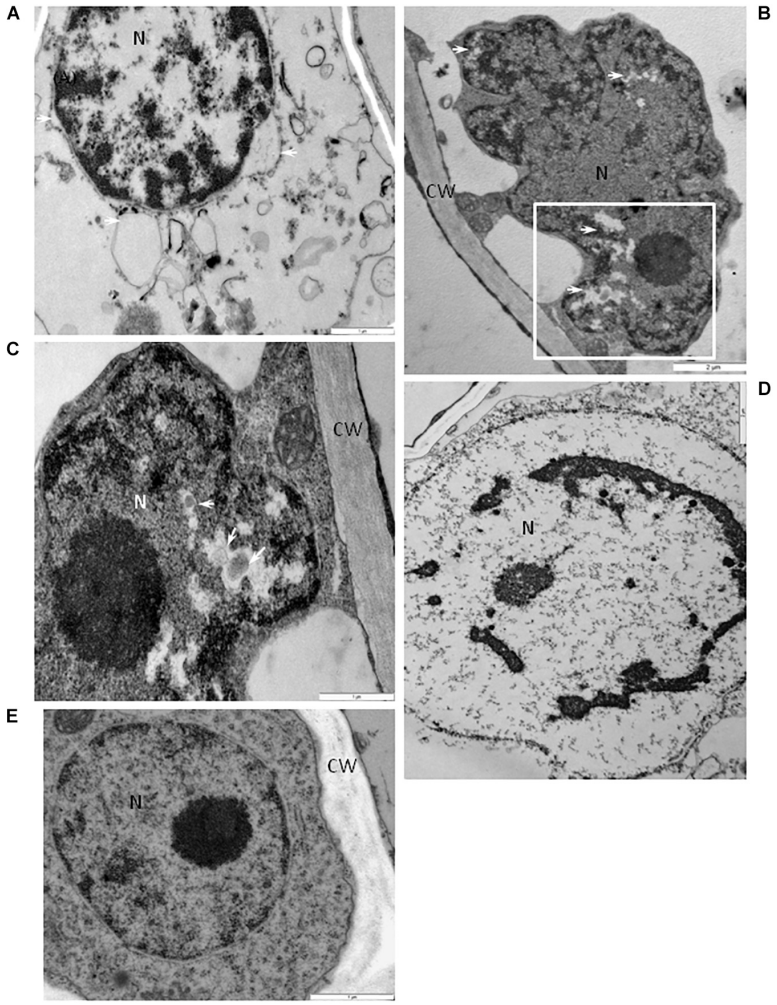

FIGURE 8 | Alterations of the nuclear structure in cells of BPEV-infected tissues. **(A)** Dilatation of the nuclear envelope (arrows) with vesicles in the perinuclear areas. N-nucleus. Bar 1 μm. **(B)** Nucleus (N) with electron-lucent areas (arrows) in a mesophyll cell. CW-cell wall. Framed area enlarged in **(C)**. Bar 2 μm. **(C)** Enlargement from the framed area of figure **(B)**. Small vesicles (arrows) in electron-lucent area. CW-cell wall, N-nucleus. Bar 1 μm. **(D)** Chromatin condensation in nucleus (N). Bar 1 μm. **(E)** Nucleus (N) of a BPEV-free phloem parenchyma cell. CW-cell wall. Bar 1 μm. CC, companion cell; Ch, chloroplast; CLD, callose like deposition; CW, cell wall; ER, endoplasmic reticulum; Ep, epidermis; GA, trans Golgi network; M, mitochondria; Me, mesophyll; MVB, multivesicular bodies; N, nucleus; Ne, necrosis; P, plastoglobules; Ph, phloem; PMB, paramular bodies; SE, sieve element; sg, starch grain; vs, vesicles; V, vacuole; VB, vascular bundle; X, xylem tracheary element; XP, xylem parenchyma.

cultivars of Mesoamerican origin have been reported to be double-infected by two endornaviruses, Phaseolus vulgaris endornavirus 1 (PvEV1) and Phaseolus vulgaris endornavirus 2 (PvEV2), whereas most genotypes of Andean origin were endornavirus-free (Okada et al., 2013; Khankhum et al., 2015). This differential occurrence according to the crop origin suggests that like BPEV, PvEV1 and PvEV2 may provide unidentified beneficial effects to common bean grown in Mesoamerica but not to that grown in the Andean region. A differential infection pattern has also been reported for Oryza sativa endornavirus in Indica and Japonica rice (Fukuhara et al., 1993).

Only limited studies on the association of endornaviruses with changes in the host biology have been conducted (Grill and Garger, 1981; Khankhum and Valverde, 2018; Escalante and Valverde, 2019). Endornaviruses of common bean and bell pepper have been associated with statistically significant variations in seed germination rates (Khankhum and Valverde, 2018; Escalante and Valverde, 2019). There is evidence that suggests that endornaviruses activate the plant host gene silencing system and therefore play an active role in the physiology of the infected plant (Urayama et al., 2010; Sela et al., 2012). The lack of symptom induction suggests that endornaviruses are able to evade the silencing mechanism of the host, possibly by using a unique suppressor of silencing or other unknown mechanism. Fukuhara (2019) has suggested that the host regulates endornavirus copy

number and propagation and that unknown host factors, which could be proteins involved in RNA silencing, control virus replication. Nevertheless, in the case of bell pepper, alterations of the ultrastructure of some host cells were associated with BPEV infections without causing visible external symptoms. Although not yet experimentally confirmed, it is assumed that endornaviruses are present in all cells of an infected plant; we do not have an explanation for the presence of cells with altered and non-altered organelles and other cell components in BPEV-infected plants. It is possible that alterations occur only in cells lacking host control on endornavirus replication.

DATA AVAILABILITY STATEMENT

All datasets generated for this study are included in the article/**Supplementary Material**.

AUTHOR CONTRIBUTIONS

KO-K and EK conducted the light and electron microscopy experiments, data analyses, and participated in writing the manuscript. CE conducted dsRNA extractions and RT-PCR testing. RV developed bell pepper near-isogenic lines and participated in writing the manuscript.

FUNDING

This investigation was partly financed by the Statutory research fund of the Institute of Biology, Department of Botany (Warsaw University of Life Sciences-SGGW). Partial support for this investigation was also provided by the National Institute of Food and Agriculture, USDA, United States.

ACKNOWLEDGMENTS

We would like to express sincere thanks to EZ for her excellent ultramicrotome work and to M. J. Roossinck, Penn State University, United States for kindly providing the original endornavirus-free line of Marengo bell used to develop the near-isogenic lines used in this study. We also thank A. Hebert, Middleton Library, Louisiana State University, for editing the manuscript.

SUPPLEMENTARY MATERIAL

The Supplementary Material for this article can be found online at: https://www.frontiersin.org/articles/10.3389/fpls.2020.00491/full#supplementary-material

REFERENCES

Akinyemi, I. A., Wang, F., Chang, Z. X., and Wu, K. (2018). Genome characterization of the newly identified maize-associated totivirus Anhui. *Arch. Virol.* 163:2929. doi: 10.1007/s00705-018-3929-0

An, Q., Hückelhoven, R., Kogel, K. H., and van Bel, A. J. E. (2006a). Multivesicular bodies participate in a cell wall-associated defence response in barley leaves attacked by the pathogenic powdery mildew fungus. *Cell. Microbiol.* 8, 1009–1019. doi: 10.1111/j.1462-5822.2006.00683.x

An, Q., Ehlers, K., Kogel, K. H., van Bel, A. J. E., and Hückelhoven, R. (2006b). Multivesicular compartments proliferate in susceptible and resistant MLA12-barley leaves in response to infection by the biotrophic powdery mildew fungus. *New Phytol.* 172, 563–576. doi: 10.1111/j.1469-8137.2006.01844.x

Bamunusinghe, D., Seo, J. K., and Rao, A. L. (2011). Subcellular localization and rearrangement of endoplasmic reticulum by Brome mosaic virus capsid protein. *J. Virol.* 85, 2953–2963. doi: 10.1128/JVI.02020-10

Blake, J. A., Kit, W., Lee, K. W., Morris, T. J., and Elton, T. E. (2007). Effects of turnip crinkle virus infection on the structure and function of mitochondria and expression of stress proteins in turnips. *Physiol. Plant.* 129, 698–706. doi: 10.1111/j.1399-3054.2006.00852.x

Boccardo, G., Lisa, V., Luisoni, E., and Milne, R. G. (1987). Cryptic plant viruses. *Adv. Virus Res.* 32, 171–214. doi: 10.1016/s0065-3527(08)60477-7

Bosland, P. W., Bailey, A. L., and Iglesias-Olivas, J. (1996). *Capsicum Pepper Varieties and Classification*. New Mexico: State University Cooperative Extension Service.

Cabanillas, D. G., Jiang, J., Movahed, N., Germain, H., Yamaji, Y., Zheng, H., et al. (2018). Turnip mosaic virus uses the SNARE protein VTI11 in an unconventional route for replication vesicle trafficking. *Plant Cell* 30, 2594–2615. doi: 10.1105/tpc.18.00281

Cotton, S., Grangeon, R., Thivierge, K., Mathieu, I., Ide, C., Wei, T., et al. (2009). Turnip mosaic virus RNA replication complex vesicles are mobile, align with microfilaments, and are each derived from a single viral genome. *J. Virol.* 83, 10460–10471. doi: 10.1128/jvi.00819-09

DeWitt, D., and Bosland, P. D. (1996). *Peppers of the World: An Identification Guide*. Berkeley, CA: Ten Speed Press.

Di Franco, A., Russo, M., and Martelli, G. P. (1984). Ultrastructure and origin of cytoplasmic multivesicular bodies induced by carnation Italian ringspot virus. *J. Gen. Virol.* 65, 1233–1237. doi: 10.1099/0022-1317-65-7-1233

Dolja, V. V., and Koonin, E. V. (2018). Metagenomics reshapes the concepts of RNA virus evolution by revealing extensive horizontal virus transfer. *Virus Res.* 244, 36–52. doi: 10.1016/j.virusres.2017.10.020

Dulieu, P., Penin, P., Dulieu, H., and Gautheron, D. C. (1988). Purification of virus-like particles from *Vicia faba* and detection by ELISA in crude leaf extracts. *Plant Sci.* 56, 9–14. doi: 10.1016/0168-9452(88)90178-1

Escalante, C., and Valverde, R. A. (2019). Morphological and physiological characteristics of endornavirus-infected and endornavirus-free near-isogenic lines of bell pepper (*Capsicum annuum*). *Sci. Hort.* 250, 104–112.

Francki, R. I. B. (1987). "Responses of plant cells to virus infection with special reference to the sites of RNA replication," in *Positive Strand RNA Viruses*, eds M. A. Brinton and R. R. Rueckert (New York, NY: Alan R Liss Inc), 423.

Fukuhara, T. (1999). Double-stranded RNA in rice. *J. Plant Pathol.* 112, 131–138.

Fukuhara, T. (2019). Endornaviruses: persistent dsRNA viruses with symbiotic properties in diverse eukaryotes. *Virus Genes* 55, 165–173. doi: 10.1007/s11262-019-01635-5

Fukuhara, T., Moriyama, H., Pak, J. Y., Hyakutake, H., and Nita, T. (1993). Enigmatic double-stranded RNA in Japonica rice. *Plant Mol. Biol.* 1993, 1121–1130. doi: 10.1007/bf00023608

Gómez-Aix, C., García-García, M., Aranda, M. A., and Sánchez-Pina, M. A. (2015). Melon necrotic spot virus replication occurs in association with altered mitochondria. *Mol. Plant Microbe Interat.* 28, 387–397. doi: 10.1094/mpmi-09-14-0274-r

Grill, L. K., and Garger, S. J. (1981). Identification and characterization of double-stranded RNA associated with cytoplasmic male sterility in *Vicia faba*. *Proc. Natl. Acad. Sci. U.S.A.* 78, 7043–7046. doi: 10.1073/pnas.78.11.7043

Hari, V. (1980). Ultrastructure of potato spindle tuber viroid-infected tomato leaf tissue. *Phytopathology* 70, 385–387.

Hatta, T., and Francki, R. I. B. (1980). Cytopathic structures associated with tonoplasts of plant cells Infected with cucumber mosaic and tomato aspermy viruses. *J. Gen. Virol.* 53, 343–346. doi: 10.1099/0022-1317-53-2-343

Hatta, T., and Ushiyama, R. (1973). Mitochondrial vesiculation associated with cucumber green mottle mosaic virus-infected plants. *J. Gen. Virol.* 2I, 9–17. doi: 10.1099/0022-1317-21-1-9

Jarret, R. L., Gillaspie, A. G., Barkley, N. A., and Pinnow, D. L. (2008). The occurrence and control of pepper mild mottle virus (PMMoV) in the USDA/ARS *Capsicum* germplasm collection. *Seed Technol.* 30, 26–36.

Karnovsky, M. J. (1965). A formaldehyde-glutaraldehyde fixative of high osmolality for use in electron-microscopy. *J. Cell Biol.* 27, 137–138.

Khalifa, M. E., and Pearson, M. N. (2014). Characterisation of a novel hypovirus from *Sclerotinia sclerotiorum* potentially representing a new genus within the *Hypoviridae*. *Virology* 464-465, 441–449. doi: 10.1016/j.virol.2014.07.005

Khankhum, S., Escalante, C., Rodrigues de Souto, E., and Valverde, R. A. (2017). Extraction and electrophoretic analysis of large dsRNAs from desiccated plant tissues infected with plant viruses and biotrophic fungi. *Eur. J. Plant. Pathol.* 147, 431–441. doi: 10.1007/s10658-016-1014-7

Khankhum, S., and Valverde, R. A. (2018). Physiological traits of endornavirus-infected and endornavirus-free common bean (*Phaseolus vulgaris*) cv Black Turtle Soup. *Arch. Virol.* 163, 1051–1056. doi: 10.1007/s00705-018-3702-4

Khankhum, S., Valverde, R. A., Pastor-Corrales, M., Osorno, J. M., and Sabanadzovic, S. (2015). Two endornaviruses show differential infection patterns between gene pools of *Phaseolus vulgaris*. *Arch.Virol.* 160, 1131–1137. doi: 10.1007/s00705-015-2335-0

Laliberté, J. F., and Sanfaçon, H. (2010). Cellular remodeling during plant virus infection. *Annu. Rev. Phytopathol.* 48, 69–91. doi: 10.1146/annurev-phyto-073009-114239

Laliberté, J. F., and Zheng, H. (2014). Viral manipulation of plant host membranes. *Annu. Rev. Virol.* 1, 237–259. doi: 10.1146/annurev-virology-031413-085532

Lefebvre, A., Scalla, R., and Pfeiffer, P. (1990). The double-stranded RNA associated with the '447' cytoplasmic male sterility in *Vicia faba* is packaged together with its replicase in cytoplasmic membranous vesicles. *Plant Mol. Biol.* 14, 477–490. doi: 10.1007/bf00027494

Li, L., Liu, J., Xu, A., Wang, T., Chen, J., and Zhu, X. (2013). Molecular characterization of a trisegmented chrysovirus isolated from the radish *Raphanus sativus*. *Virus Res.* 176, 169–178. doi: 10.1016/j.virusres.2013.06.004

Lin, N.-S., and Langenberg, W. G. (1984). Chronology of appearance of barley stripe mosaic virus protein in infected wheat cells. *J. Ultrastruct. Res.* 89, 309–323. doi: 10.1016/s0022-5320(84)80047-7

Liu, W., Xin, M., Cao, M., Qin, M., Liu, H., Zhao, S., et al. (2018). Identification, characterization and full-length sequence analysis of a novel endornavirus in common sunflower (*Helianthus annuus*). *J. Integra. Agric.* 17, 60345–60347.

Martelli, G. P., Di Franco, A., and Russo, M. (1984). The origin of multivesicular bodies in tomato bushy stunt virus-Infected *Gomphrena globosa* plants. *J. Ultrastruct. Res.* 88, 275–281. doi: 10.1016/s0022-5320(84)90125-4

Newhouse, J. R., MacDonald, W. L., and Hoch, H. C. (1990). Virus-like particles in hyphae and conidia of European hypovirulent (dsRNA-containing) strains of Crypho-nectria parasitica. *Can. J. Bot.* 68, 90–101. doi: 10.1139/b90-013

Nibert, M. L., Vong, M., Karen, K., Fugate, K. K., and Debat, H. J. (2018). Evidence for contemporary plant mitoviruses. *Virology* 518, 14–24. doi: 10.1016/j.virol.2018.02.005

Okada, R., Kiyota, E., Sabanadzovic, S., Moriyama, H., Fukuhara, T., Saha, P., et al. (2011). Bell pepper endornavirus: molecular and biological properties and occurrence in the genus *Capsicum*. *J. Gen. Virol.* 92, 2664–2673.

Okada, R., Yong, C. K., Valverde, R. A., Sabanadzovic, S., Aoki, N., Hotate, S., et al. (2013). Molecular characterization of two evolutionarily distinct endornaviruses co-infecting common bean (*Phaseolus vulgaris*). *J. Gen. Virol.* 94, 220–229. doi: 10.1099/vir.0.044487-0

Otulak, K., Chouda, M., Bujarski, J., and Garbaczewska, G. (2015). The evidence of Tobacco rattle virus impact on host plant organelles ultrastructure. *Micron* 70, 7–20. doi: 10.1016/j.micron.2010.11

Otulak, K., and Garbaczewska, G. (2010). Ultrastructural events during hypersensitive response of potato cv. Rywal infected with necrotic strains of potato virus Y. *Acta Physiol. Plant.* 32, 635–644.

Otulak, K., and Garbaczewska, G. (2013). The participation of plant cell organelles in compatible and incompatible Potato virus Y-tobacco and-potato plant interaction. *Acta Physiol. Plant.* 36, 85–99. doi: 10.1007/s11738-013-1389-4

Otulak-Kozieł, K., Kozieł, E., and Lockhart, B. E. L. (2018). Plant cell wall dynamics in compatible and incompatible potato response to infection caused by potato virus Y (PVYNTN). *Int. J. Mol. Sci.* 19:862. doi: 10.3390/ijms19030862

Otulak-Kozieł, K., Kozieł, E., and Valverde, R. A. (2019). The respiratory burst oxidase homolog D (RbohD) cell and tissue distribution in potato–potato virus Y (PVYNTN) hypersensitive and susceptible reactions. *Int. J. Mol. Sci.* 20:2741. doi: 10.3390/ijms20112741

Park, Y., Chen, X., and Punja, Z. K. (2006). Molecular and biological characterization of a mitovirus in *Chalara elegans* (*Thielaviopsis basicola*). *Phytopathology* 96, 468–479. doi: 10.1094/phyto-96-0468

Pfeiffer, P. (1998). Nucleotide sequence, genetic organization and expression strategy of the double-stranded RNA associated with the '447' cytoplasmic male sterility in *Vicia faba*. *J. Gen. Virol.* 79, 2349–2358. doi: 10.1099/0022-1317-79-10-2349

Pickersgill, B. (1997). Genetic resources and breeding of *Capsicum* spp. *Euphytica* 96, 129–133.

Rojas, M. R., Maliano, M. R., de Souza, J. O., Vasquez-Mayorga, M., de Macedo, M. A., Ham, B.-K., et al. (2016). "Cell-to-cell movement of plant viruses: a diversity of mechanisms and strategies," in *Current Research Topics in Plant Virology*, eds A. Wang and X. Zhou (Cham: Springer), doi: 10.1007/978-3-319-32919-2_5

Roossinck, M. J. (2010). Lifestyles of plant viruses. *Philos. Trans. R. Soc. Lond. B Biol. Sci.* 365, 1899–1905. doi: 10.1098/rstb.2010.0057

Roossinck, M. J., Sabanadzovic, S., Ryo Okada, R., and Valverde, R. A. (2011). The remarkable evolutionary history of endornaviruses. *J. Gen. Virol.* 92, 2674–2678. doi: 10.1099/vir.0.034702-0

Sabanadzovic, S., Wintermantel, W. M., Valverde, R. A., McCreight, J. D., and Aboughanem-Sabanadzovic, N. (2016). *Cucumis melo* endornavirus: genome organization, host range and co-divergence with the host. *Virus Res.* 214, 49–58. doi: 10.1016/j.virusres.2016.01.001

Safari, M., and Roossinck, M. J. (2018). Coevolution of a persistent plant virus and its pepper hosts. *Mol. Plant Microb. Interact.* 31, 766–776. doi: 10.1094/mpmi-12-17-0312-r

Sela, N., Luria, N., and Dombrovsky, A. (2012). Genome assembly of bell pepper endornavirus from small RNA. *J. Virol.* 86:7721. doi: 10.1128/jvi.00983-12

Smith, P. G., Villalon, B., and Villa, P. L. (1987). Horticultural classification of peppers grown in the United States. *HortScience* 22, 11–13.

Takahashi, H., Fukuhara, T., Kitazawa, H., and Kormelink, R. (2019). Virus Latency and the impact on plants. *Front. Microbiol.* 10:2764. doi: 10.3389/fmicb.2019.02764

Urayama, S., Moriyama, H., Aoki, N., Nakazawa, Y., Okada, R., Kiyota, E., et al. (2010). Knock-down of OsDCL2 in rice negatively affects maintenance of the endogenous dsRNA virus, *Oryza sativa* endornavirus. *Plant Cell Physiol.* 51, 58–67. doi: 10.1093/pcp/pcp167

Valverde, R. A., Khalifa, M. E., Okada, R., Fukuhara, T., and Sabanadzovic, S. (2019). ICTV Virus taxonomy profile: *Endornaviridae*. *J. Gen. Virol.* 100, 1204–1205. doi: 10.1099/jgv.0.001277

Valverde, R. A., Nameth, S., Abdalla, O., Al-Musa, O., Desjardins, P. R., and Dodds, J. A. (1990). Indigenous double-stranded RNA from pepper (*Capsicum annum*). *Plant Sci.* 67, 195–201. doi: 10.1016/0168-9452(90)90243-h

Villanueva, F., Sabanadzovic, S., Valverde, R. A., and Navas-Castillo, J. (2012). Complete genome sequence of a double-stranded RNA virus from avocado. *J. Virol.* 86, 1282–1283. doi: 10.1128/jvi.06572-11

Wei, T., and Wang, A. (2008). Biogenesis of cytoplasmic membranous vesicles for plant potyvirus replication occurs at the endoplasmic reticulum exit sites in a COPI- and COPII-dependent manner. *J. Virol.* 82, 12252–12264. doi: 10.1128/jvi.01329-08

Zabalgogeazcoa, I. A., and Gildow, F. E. (1992). Double-stranded ribonucleic acid in 'Barsoy' Barley. *Plant Sci.* 83, 187–194. doi: 10.1016/0168-9452(92)90078-z

Zhao, J., Zhang, X., Hong, Y., and Liu, Y. (2016). Chloroplast in plant–virus interaction. *Front. Microbiol.* 7:1565. doi: 10.3389/fmicb.2019.01565

Conflict of Interest: The authors declare that the research was conducted in the absence of any commercial or financial relationships that could be construed as a potential conflict of interest.

frontiers in Microbiology

ORIGINAL RESEARCH
published: 30 April 2020
doi: 10.3389/fmicb.2020.00790

Autophagy Participates in Lysosomal Vacuolation-Mediated Cell Death in RGNNV-Infected Cells

Youhua Huang[1,2], Ya Zhang[1], Zetian Liu[1], Chuanhe Liu[3], Jiaying Zheng[1], Qiwei Qin[1,2,4] and Xiaohong Huang[1,2]**

[1] College of Marine Sciences, South China Agricultural University, Guangzhou, China, [2] Guangdong Laboratory for Lingnan Modern Agriculture, Guangzhou, China, [3] Instrumental Analysis & Research Center, South China Agricultural University, Guangzhou, China, [4] Laboratory for Marine Biology and Biotechnology, Qingdao National Laboratory for Marine Science and Technology, Qingdao, China

OPEN ACCESS

Edited by:
Miguel A. Martín-Acebes, Instituto Nacional de Investigación y Tecnología Agraria y Alimentaria (INIA), Spain

Reviewed by:
Kim Dawn Thompson, Moredun Research Institute, United Kingdom
Isabel Bandín, University of Santiago de Compostela, Spain

***Correspondence:**
Qiwei Qin
qinqw@scau.edu.cn
Xiaohong Huang
huangxh@scau.edu.cn

Specialty section:
This article was submitted to Virology, a section of the journal Frontiers in Microbiology

Received: *11 January 2020*
Accepted: *02 April 2020*
Published: *30 April 2020*

Citation:
Huang Y, Zhang Y, Liu Z, Liu C, Zheng J, Qin Q and Huang X (2020) Autophagy Participates in Lysosomal Vacuolation-Mediated Cell Death in RGNNV-Infected Cells. Front. Microbiol. 11:790. doi: 10.3389/fmicb.2020.00790

Nervous necrosis virus (NNV) is the etiological agent of viral nervous necrosis (VNN), also known as viral encephalopathy and retinopathy (VER), which results in heavy economic losses to the aquaculture industry worldwide. Dramatic cytoplasmic vacuoles were observed during NNV infection both *in vitro* and *in vivo*; however, the origin and mechanism of cytoplasmic vacuolization remains unknown. In this report, we found that the cytoplasmic vacuole morphology became fused and enlarged during infection with red spotted grouper nervous necrosis virus (RGNNV), which was accompanied by increased cell death. Notably, Lyso-Tracker, but not Mito-Tracker or ER-Tracker, was accumulated in the vacuoles, and abnormal lysosome swelling was observed in RGNNV-infected cells, suggesting that the cytoplasmic vacuoles originated from lysosomal organelles. Cytoplasmic vacuolization and cell death in RGNNV-infected cells was completely blocked by the vacuolar H^+-ATPase inhibitor (bafilomycin A1), and was significantly weakened by chloroquine (CQ), a lysosomotropic agent that induces the acidification of the lysosomes. This suggests that lysosome acidification was essential for vacuole formation. Significant inhibitory effects on vacuolization and cell death were also observed in the RGNNV-infected cells following treatment with nigericin and monensin (ionophores that uncouple the proton gradient present in lysosomes). This indicated that lysosome function was tightly associated with RGNNV infection-induced cell death. In addition, vacuoles were found to be partially co-localized with GFP-LC3II punctate dots during RGNNV infection. Moreover, the severity of vacuolization and cell death were both significantly decreased after treatment with the autophagy inhibitor, 3-MA, suggesting that autophagy was involved in lysosomal vacuolization and cell death evoked by RGNNV infection. Thus, our results demonstrate that autophagy participates in lysosomal vacuolation-mediated cell death during RGNNV infection, and provides new insight into our understanding of the potential mechanisms underlying nodavirus pathogenesis *in vitro*.

Keywords: RGNNV, vacuolization, lysosome, autophagy, cell death

INTRODUCTION

Viral nervous necrosis (VNN), otherwise termed viral encephalopathy and retinopathy (VER), caused by nervous necrosis virus (NNV) (genus *Betanodavirus*, family *Nodaviridae*) is a highly infective neuropathological disease that can be detected in more than 177 marine species worldwide (Costa and Thompson, 2016; Doan et al., 2017; Bandín and Souto, 2020). Moreover, NNV infection causes more than 90% mortality in several marine cultured fish species at the larval and juvenile stages (Parameswaran et al., 2007). Currently, betanodaviruses are classified into four genotypes based on the RNA2 sequence: (1) red-spotted grouper NNV (RGNNV); (2) barfin flounder NNV (BFNNV); (3) tiger puffer NNV (TPNNV); and (4) striped jack NNV (SJNNV) (Nishizawa et al., 1997) with a proposed fifth, turbot NNV (TNNV) (Johansen et al., 2004), and three other known unclassified viruses (Sahul Hameed et al., 2019). Strains belonging to the RGNNV genotype cause a high mortality in the grouper industry in many countries (Hegde et al., 2002), and evoke mass cytoplasmic vacuolization in the retina and brain of infected fish (Chi et al., 1997). Moreover, the numerous cytoplasmic vacuoles are also observed in RGNNV-infected cells (Huang et al., 2011); however, the origin and potential mechanism of vacuolization during NNV infection remains poorly understood.

Cytoplasmic vacuolization, commonly termed vacuolation, is an acknowledged morphological phenomenon observed in mammalian cells both *in vivo* and *in vitro* during exposure to bacterial or viral pathogens, as well as to various drugs and other substances (Aki et al., 2012; Shubin et al., 2016). To date, the vacuolization effects caused by viral infection have been investigated in members of 15 viral families, including hepatitis A virus (HAV), hepatitis C virus (HCV), bovine virus diarrhea virus (BVDV), murine leukemia virus (MuLV), Zika virus, hepatitis B virus (HBV), and polyomaviruses (Shubin et al., 2016; Monel et al., 2017). Viral products (e.g., enveloped or capsid proteins) have been shown to act as vacuolization inducers (Shubin et al., 2015; Luo et al., 2016), and the mechanisms underlying the vacuolization effects differ. For example, 3C protease of hepatitis A virus (3Cpro) has induced numerous non-acidic cytoplasmic vacuoles, which were originated from the endosome and lysosome compartments (Shubin et al., 2015). Moreover, simian virus 40 (SV40) induces substantial cytoplasmic vacuoles at the late productive infection stage, and the binding of viral major capsid protein VP1 to the cell surface ganglioside, GM1, triggers the formation of cytoplasmic vacuoles (Murata et al., 2008; Luo et al., 2016).

Vacuolization evoked by an exogenous stimulus has been demonstrated to be derived from different membrane organelles, including mitochondria, endoplasmic reticulum (ER), lysosome, Golgi apparatus, and autolysosomes (Aki et al., 2012). Moreover, vacuolization usually accompanies different types of cell death, such as paraptosis-like cell death, necroptosis, and autophagy-associated cell death (Shubin et al., 2015; Monel et al., 2017). Therefore, an investigation of the vacuole origin and properties will contribute to elucidating the mechanisms of the pathomorphological effects of vacuolization inducers. For example, the MuLV envelope protein (Env)-induced cytoplasmic vacuoles were derived from the ER, and partially formed from fused endosomal/lysosomal organelles and autophagosomes (Whatley et al., 2008). During HBV infection, the large HBV surface antigen (L-HBsAg) was also found to trigger ER vacuolization (Foo et al., 2002), whereas the vacuolating effect of L-HBsAg appears to be the cause of cell death (Xu et al., 1997). In addition, BVDV infection induces vacuolization of acidic endosomal/lysosomal organelles, and the formation of vacuoles and cell death is autophagy-independent (Birk et al., 2008).

In the present study, we investigated the origin of the vacuoles triggered by an infection with RGNNV in grouper cells. Furthermore, the critical factors and events involved in vacuole formation and cell death were clarified. Together, our data will both shed important light on the characteristics of RGNNV-induced vacuolization and cell death, as well as contribute to our understanding of the mechanisms of nodavirus pathogenesis.

MATERIALS AND METHODS

Cell Culture, Virus, and Reagents

Grouper spleen (GS) cells were established and maintained in our lab (Huang et al., 2009). GS cells were grown in Leibovitz's L15 medium containing 10% fetal bovine serum (Gibco) at 28°C. The RGNNV used in the study was prepared as described previously (Huang et al., 2011). For RGNNV infection, the GS cells were infected with RGNNV at a multiplicity of infection (MOI) of 2.

Monensin sodium salt (an ionophore that mediates Na+/H+ exchange) and nigericin sodium salt (a K+/H+ ionophore) were purchased from MedChemExpress (MCE). z-FA-FMK (inhibitor of cysteine proteases, including cathepsins B, S, and L) was purchased from Selleck. Chloroquine (CQ), bafilomycin A1 (Baf), E64D (L-trans-epoxysuccinyl (OEt)-leu-3-methylbutylamide-ethyl ester, pan-cysteine cathepsin inhibitor), and CA-074 (L-trans-epoxysuccinyl-Ile-Pro-OH propylamide, an inhibitor of cathepsin B) were purchased from Sigma-Aldrich. All reagents were dissolved in DMSO. 3-Methyladenine (3-MA) was purchased from Selleck and dissolved in sterile water. Lyso-Tracker (Red DND-99), Image-it dead green viability stain, Mito-Tracker (Red CMXRos), and ER-Tracker (Red) were obtained from Invitrogen. In addition, the plasmids, pEGFP-N3 (control vector), pEGFP-LC3 (GFP-tagged LC3 plasmid, a versatile marker of autophagy), pEGFP-Rab5 (marker for the early endosome), and pEGFP-Rab7 (marker for the late endosome), used in this study were stored in our lab as previously described (Wang et al., 2014).

Virus Infection

GS cells were grown in either 24- or 6-well plates pretreated with DMSO, water, or different reagents (the optimal concentration used in this study was determined using a cell viability assay) for 2 h. The GS cells were infected with RGNNV at a MOI of 2 and cultured at 28°C. At 24 h post-infection (p.i.), the cytopathic effect (CPE) of the cells was observed under microscopy (Zeiss).

Cell Viability Assay

To evaluate cell viability, cells treated with DMSO- or different reagents (Z-FA-FMK, CA-074, Baf, CQ, Monensin, Nigericin or 3-MA) were incubated with Image-It Dead green viability stain for 15 min, and the cells were imaged under a fluorescence microscope.

The percentage of cell death was also determined by trypan blue exclusion (Mullick et al., 2013). Briefly, the cells were collected by trypsinization and stained with trypan blue. Cell mortality (%) was presented as the percentage of dead cells out of the total number of cells.

Evaluation of Autophagy

The effects of 3-MA on RGNNV-induced autophagy was determined using a Cyto-ID Autophagy detection kit (Enzo life sciences) as described previously (Huang et al., 2015). Briefly, the cells were seeded into 24-well plates at ∼80% confluence. Following treatment with 2 or 5 mM 3-MA, the cells were infected with RGNNV for 24 h, washed once in fresh medium, and subsequently stained with Cyto-ID green detection reagent for 30 min. Finally, the expression of bright green fluorescence in the vesicles was observed under a fluorescence microscope (Zeiss).

Electron Microscopy

Mock- and RGNNV-infected cells were harvested at 24 h p.i. and 48 h p.i., and were washed with PBS. The cell pellets were fixed in 2.5% glutaraldehyde overnight. Sample preparation was performed as previously described (Huang et al., 2009). Briefly, after washing with PBS, the cells were post-fixed in 1% osmium tetroxide (OsO4) for 1 h, and then dehydrated in graded ethanol. Then cells were embedded in Epon resin. Sections were double stained with uranyl acetate and lead citrate. The grids containing ultrathin sections were examined using a Talos L120C electron microscope (Thermo Fisher Scientific) at 120 KV and micrographics were obtained using a CDD camera.

Cell Transfection

Transfection was performed using Lipofectamine 2000 (Invitrogen) according to the manufacturer's instruction as previously described (Huang et al., 2009). Briefly, GS cells were seeded into 24-well plates for 18 h, after which the cells were transfected with a mixture of Lipofectamine 2000 and pEGFP-N3, pEGFP-LC3, pEGFP-Rab7, or pEGFP-Rab5, respectively. After 24 h from the time of transfection, cells were infected with RGNNV for another 24 h, and then fixed in 4% paraformaldehyde for 1 h at 4°C. Finally, cells were stained with 1 μg/mL of 6-diamidino-2-phenyl-indole (DAPI, Sigma), and then observed under fluorescence microscopy (Zeiss).

Immunofluorescence Assay

To evaluate protein synthesis during RGNNV infection, CP protein expression was detected using an immunofluorescence assay as described previously (Zheng et al., 2019). In brief, GS cells were grown in a 24-well plate overnight. The cells were pretreated with various reagents (CQ, Baf, Monensin or Nigericin), and infected with RGNNV in the presence of these reagents for an additional 24 h. Both mock- and RGNNV-infected treated cells were fixed in 4% paraformaldehyde at room temperature for 1 h, and then permeabilized with 0.2% triton X-100 for 15 min. After blocking with 2% bovine serum albumin (BSA), cells were incubated with rabbit anti-CP serum (1:300) (prepared in our lab) for 2 h, followed by the second antibody anti-rabbit IgG Fab2 Alexa Fluor 488 (1:200; Molecular probe). Finally, the cells were stained with DAPI and observed under a fluorescence microscope.

RNA Extraction, cDNA Synthesis, and Quantitative PCR (qPCR)

To determine the effects of different reagents on RGNNV replication, the transcript of CP (fragment from 391–621 nn) was detected by qPCR. In brief, mock- or RGNNV-infected cells were collected, and the total RNA was extracted using an SV total RNA isolation system (Promega) according to the manufacturer's instructions. The RNA was reverse transcribed using a ReverTra Ace qPCR RT Kit (TOYOBO). Amplification was examined using a SYBR Green I Reaction Mix (Toyobo) in an Applied Biosystems QuantStudio 5 Real Time Detection System (Thermofisher, United States). Each assay was carried out under the following cycling conditions: 95°C for 1 min for activation, followed by 40 cycles at 95°C for 15 s, 60°C, for 15 s, and 72°C for 45 s. The primers used in the experiment were those that were described previously (Zhang et al., 2019). The level of target gene expression normalized to β-actin was calculated using the $2^{-\Delta\Delta CT}$ method. The data are representative of one representative experiment carried out in triplicate.

Statistical Analysis

The results are presented as the mean ± standard deviation (SD). Statistical comparisons were performed using a Student's *t*-test, and the statistical differences between groups were considered to be significant (*) if the p-value < 0.05.

RESULTS

Cytoplasmic Vacuolation Is a Typical Cytopathic Effect Induced by RGNNV Infection

We first performed a detailed investigation of the characteristics of vacuolization evoked by RGNNV infection. As shown in **Figure 1A**, a large number of vacuoles were observed in RGNNV-infected GS cells at 24 h p.i. At 48 h p.i., the cell detachment of round cells led to the formation of large gaps throughout the monolayer, and enlarged vacuoles were observed in the infected cells. Furthermore, the dynamics of vacuolation induced by RGNNV were observed under phase microscopy. Small vacuoles could be observed in RGNNV-infected cells at 3 h p.i. The number of vacuoles was increased in the infected cells (from 3 h to 10 h p.i.), and small vacuoles were fused into large ones (from 6 h to 9 h p.i.) as the infection progressed (**Figure 1B**).

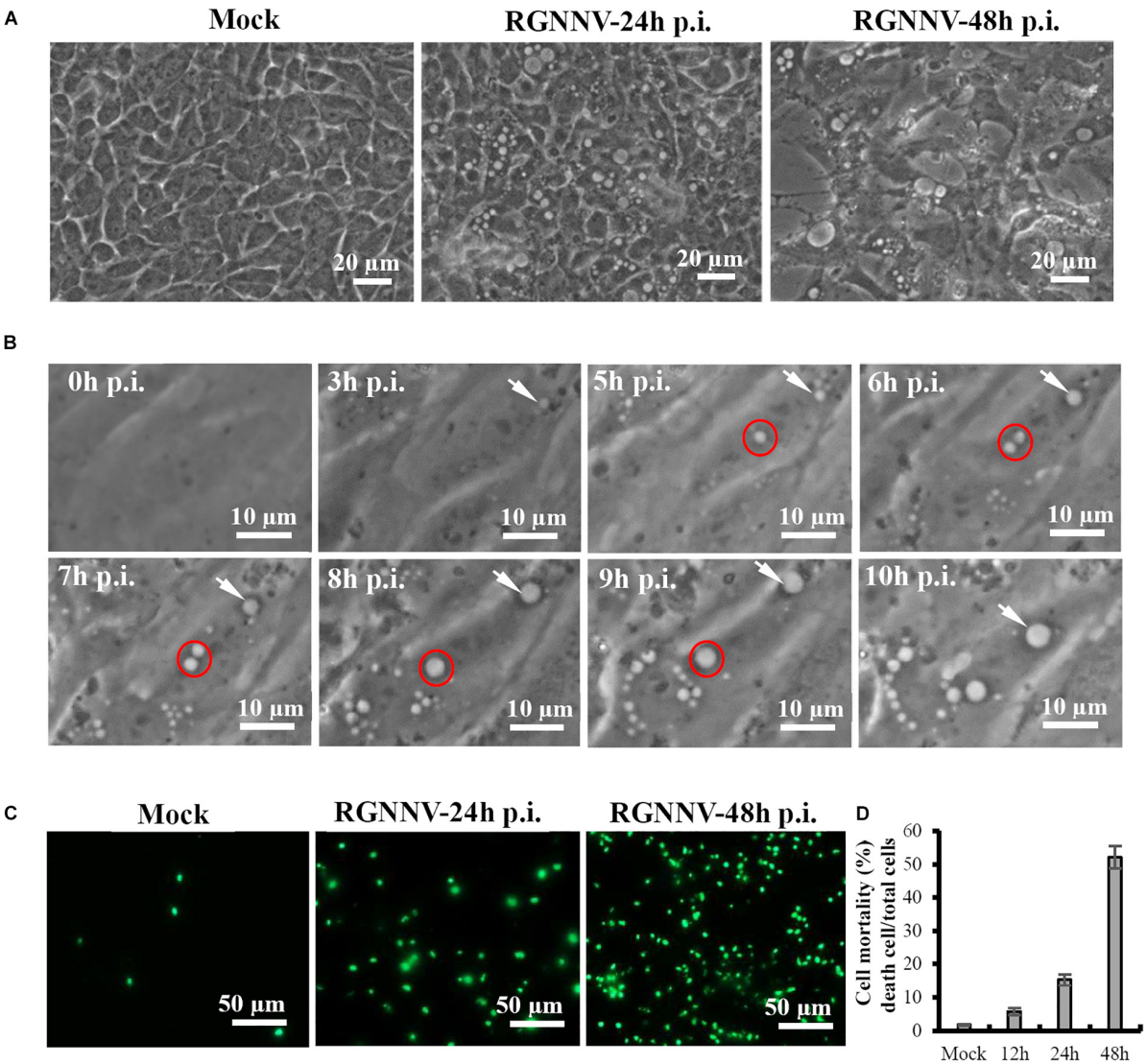

FIGURE 1 | RGNNV induced massive cytoplasmic vacuoles in grouper cells. **(A)** RGNNV induced massive cytoplasmic vacuoles in GS cells. **(B)** Time-course observation of vacuoles from 3 to 10 h during RGNNV infection. The arrows indicate enlargement of vacuoles. The circles show the fusion of the vacuoles. **(C)** Cell death induced by RGNNV infection was determined by Image-It Dead green viability staining. **(D)** The percentage of the dead cells were quantified using a trypan blue assay.

Interestingly, the number of the dead cells stained by Image-It Dead green were significantly increased with the increase in infection time (**Figure 1C**). The cell mortality induced by RGNNV was approximately 15 and 52% at 24 h p.i. and 48 h p.i., respectively (**Figure 1D**).

To visualize the ultrastructure of cytoplasmic vacuoles, cells infected with RGNNV at 24 h were immediately fixed and observed using electron microscopy. As shown in **Figure 2**, an increased number of cytoplasmic vacuoles with various sizes were observed in RGNNV-infected GS cells. While few cytoplasmic vacuoles were observed in the mock-infected cells (**Figures 2A–C**). Interestingly, monolayer-membrane structures which contain numerous virus particles (viral replication compartments, VRCs) were observed in RGNNV-infected cells (**Figures 2B,C**). Viral particles approximately 30 nm in diameter were observed in some cytoplasmic vacuoles in addition to cell debris. The viral particles were primarily closed to the inner membrane of the vacuoles (**Figures 2D–G**). In addition, vacuoles with double- and single-membrane structures containing viruses were observed in the RGNNV-infected cells (**Figures 2H–K**).

RGNNV Induced Cytoplasmic Vacuoles Derived From Lysosomes

To clarify the origin and composition of the vacuole, RGNNV-infected cells were stained with several organelle markers, including Mito-Tracker, Lyso-Tracker, and ER-Tracker. As

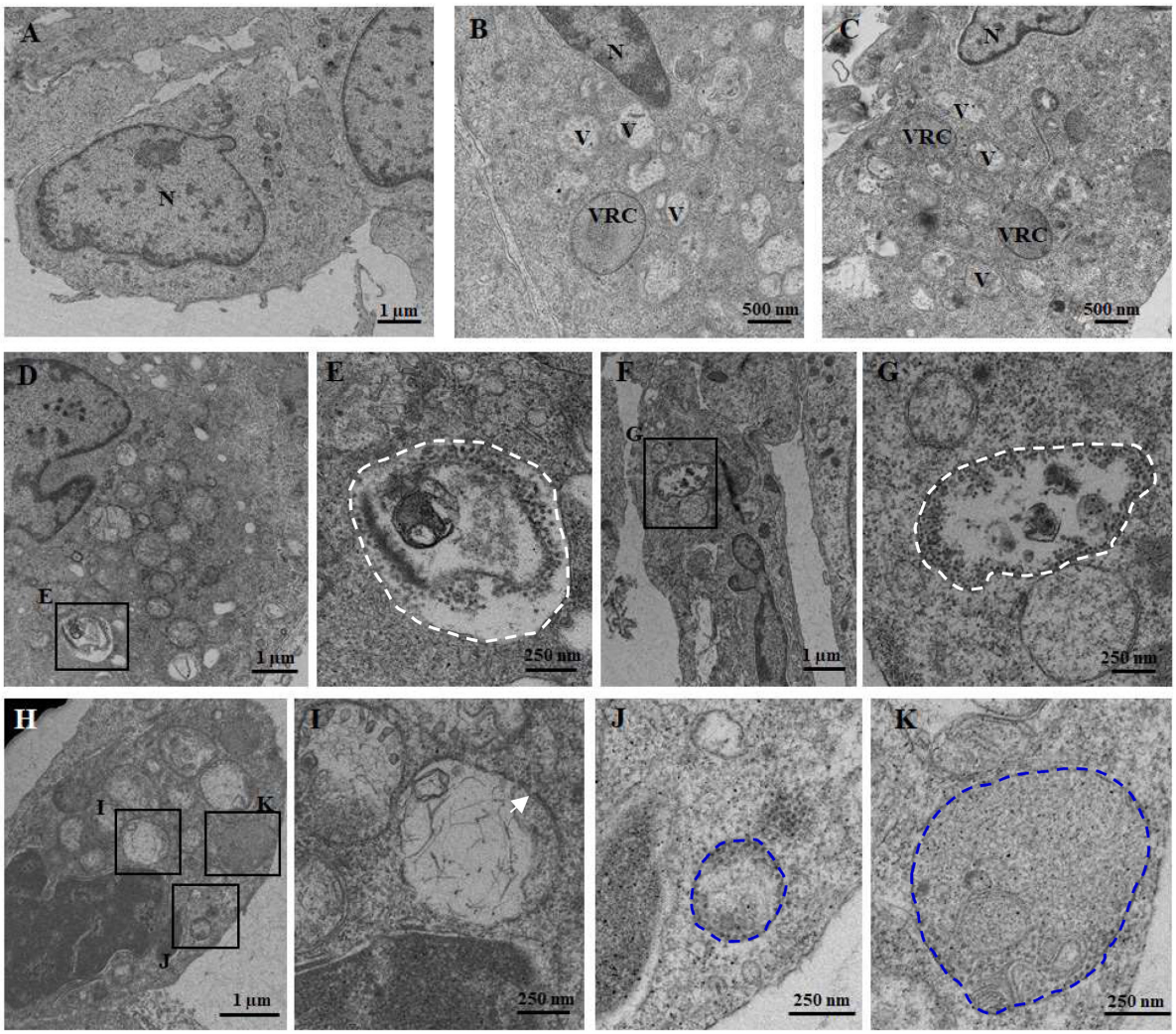

FIGURE 2 | The ultrastructure of the vacuoles in mock **(A)** and RGNNV-infected cells **(B–K)**. **(A)** A normal nucleus, but not vacuoles, were observed in the mock-infected cells. **(B, C)** A condensed nucleus and numerous vacuoles were observed in the RGNNV-infected cells. "V" indicates vacuoles and "VRC" shows the virus replication center. **(D–G)** The white dotted circles show the vacuoles containing cell debris and viral particles. **(H–K)** The blue dotted circles show the monolayer membrane structures containing viruses, and the white arrows show the vacuoles with double-membrane structures.

shown in **Figure 3A**, the mitochondria in mock-infected cells exhibited a filamentous, elongated morphology, and the ER was evenly distributed throughout the cytoplasm. In contrast, the Lyso-Tracker-labeled vesicles were scattered throughout the cytoplasm. Following RGNNV infection, Mito-Tracker and ER-Tracker were excluded from the vacuoles and were not colocalized with the vacuoles, whereas Lyso-Tracker accumulated in the vacuoles. Thus, the results suggested that the vacuoles in the RGNNV-infected cells might be associated with the lysosomal compartments. To ascertain whether the endosome was associated with vacuolar membranes in RGNNV-infected cells, GS cells were transfected with pEGFP-Rab5 or pEGFP-Rab7, and subsequently infected with RGNNV. As shown in **Supplementary Figure 1**, the green fluorescence omitted from GFP-Rab5- or GFP-Rab7-transfected cells primarily resided on the vacuole membrane, which indicated that endosomal/lysosomal compartment organelles were involved in RGNNV infection-induced vacuole formation.

To detect the details of the lysosome dynamics during RGNNV infection, cells were infected with RGNNV at the indicated time points (2, 12, 24 h p.i.), stained with Lyso-Tracker, and observed under fluorescence microscopy. No obvious changes were observed in the lysosome morphology after RGNNV infection for 2 h compared to the control cells. From 12 to 24 h p.i., the fluorescence aggregates were enlarged and gathered in cytoplasmic vacuoles in RGNNV-infected cells. Accompanied by the severity of the vacuolation, the fluorescence aggregates were extremely enlarged and the majority had acuminated into the vacuoles (**Figure 3B**). This indicated that RGNNV infection significantly altered lysosome morphology, characterized by lysosome swelling. In combining the ultrastructure of the vacuoles during RGNNV infection, we

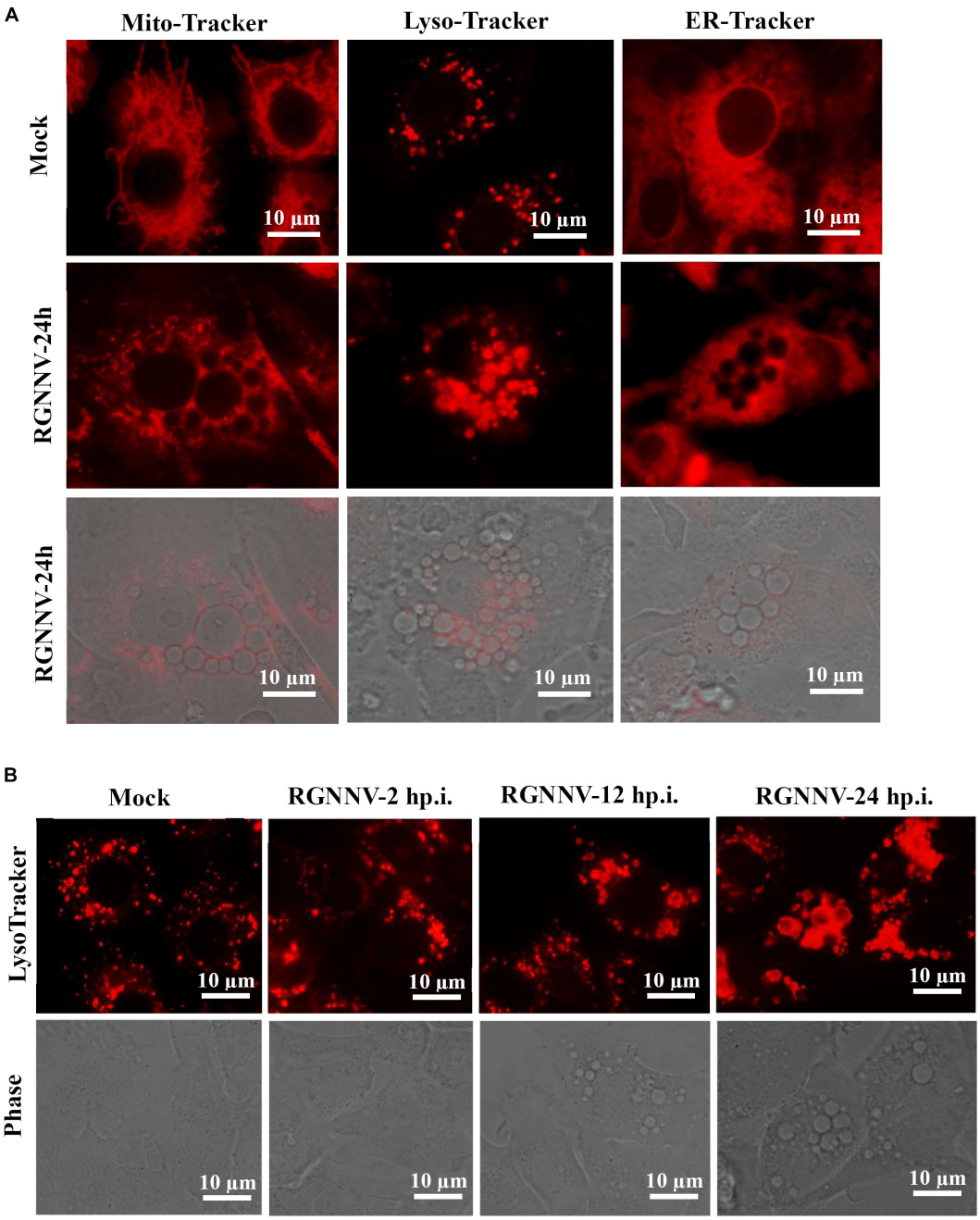

FIGURE 3 | The RGNNV infection-induced cytoplasmic vacuoles were derived from endosome/lysosome organelles. **(A)** The status of the lysosome, endoplasmic reticulum (ER), and mitochondria in vacuolated cells. Mock- or RGNNV-infected cells were stained with Mito-Tracker, Lyso-Tracker, or ER-Tracker, respectively, and then observed under an immunofluorescence microscope. **(B)** The morphology of the lysosome and vacuoles at different time points during RGNNV infection.

speculate that the cytoplasmic vacuoles induced by RGNNV infection were derived from the lysosome.

Cathepsin Activity Is Not Required for Vacuolization During RGNNV Infection

To clarify whether lysosomal cathepsins were involved in vacuolization and cell death induced by RGNNV infection, different cathepsin inhibitors were employed in this study, including Z-FA-FMK, CA-074, and E64D. As shown in **Figure 4A**, cells pretreated with Z-FA-FMK, CA-074, and E64D did not exhibit obvious effects on the formation of vacuoles induced by RGNNV infection. Consistent with this finding, RGNNV-induced cell death was not affected in the presence of Z-FA-FMK (**Figure 4B**). A quantitative analysis also showed that none of these inhibitors affected cell viability (**Figure 4C**).

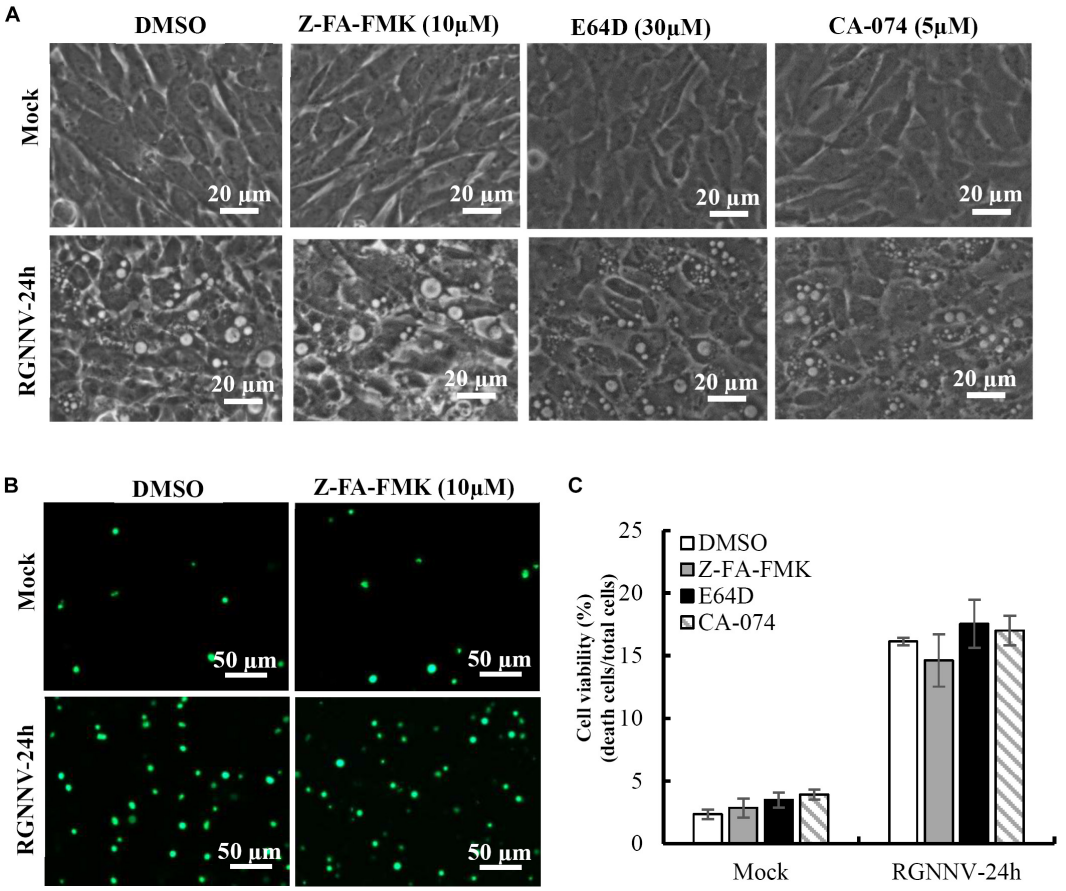

FIGURE 4 | The effects of cathepsin inhibitors on vacuole formation during RGNNV infection. **(A)** The effects of different inhibitors on RGNNV infection-induced vacuolization. **(B)** The effect of Z-FA-FMK on cell death induced by RGNNV. **(C)** The percentage of cell death during RGNNV infection upon treatment with different inhibitors.

Thus, our results indicate that cathepsin activation was not essential for vacuole formation and the cell death induced by RGNNV infection.

Lysosomal Acidification Is Required for RGNNV-Induced Vacuolization and Cell Death

To further verify whether the RGNNV-evoked vacuole formation was dependent on lysosomal acidification, bafilomycin A1 and chloroquine (CQ) were used to destroy lysosomal acidification. The effects of these inhibitors on vacuole formation were then subsequently determined. Bafilomycin A1, an inhibitor of vacuolar-type H^+-ATPase, prevents the trafficking from early to late endosomes. Chloroquine is a lysosomotropic agent that prevents endosomal acidification. As expected, treatment with Bafilomycin A1 reduced Lyso-Tracker Red staining, which indicated that the lysosome structure was destroyed by Bafilomycin A1. Vacuolization induced by RGNNV was almost completely blocked by pretreatment with bafilomycin A1 compared with the DMSO-treated cells (**Figure 5A**). Interestingly, chloroquine treatment significantly inhibited vacuole fusion during RGNNV infection. Both bafilomycin A1 and chloroquine displayed a noticeable decrease in the cell death induced by RGNNV infection (**Figures 5B,C**). In addition, expression and transcription of the coat protein (CP) were also significantly inhibited in the presence of bafilomycin A1 or chloroquine in a dose-dependent manner (**Figures 5D,E**).

Na^+ and K^+ Ionophore Exerts a Critical Role in Vacuole Formation

To clarify the potential role of the proton gradient in the lysosomes during RGNNV infection, the effects of several ionophores on cytoplasmic vacuole formation and cell death were assessed. Nigericin and monensin, ionophores that uncouple the proton gradient present in lysosomes, were used in this study. As shown in **Figure 6A**, both monensin and nigericin were able to block the formation of cytoplasmic vacuoles induced by RGNNV. Moreover, treatment with monensin and nigericin significantly decreased the cell death induced by RGNNV compared to that of the DMSO-treated cells (**Figures 6B,C**). In addition, the transcription and protein synthesis of RGNNV CP both significantly weakened monensin or nigericin-treated infected

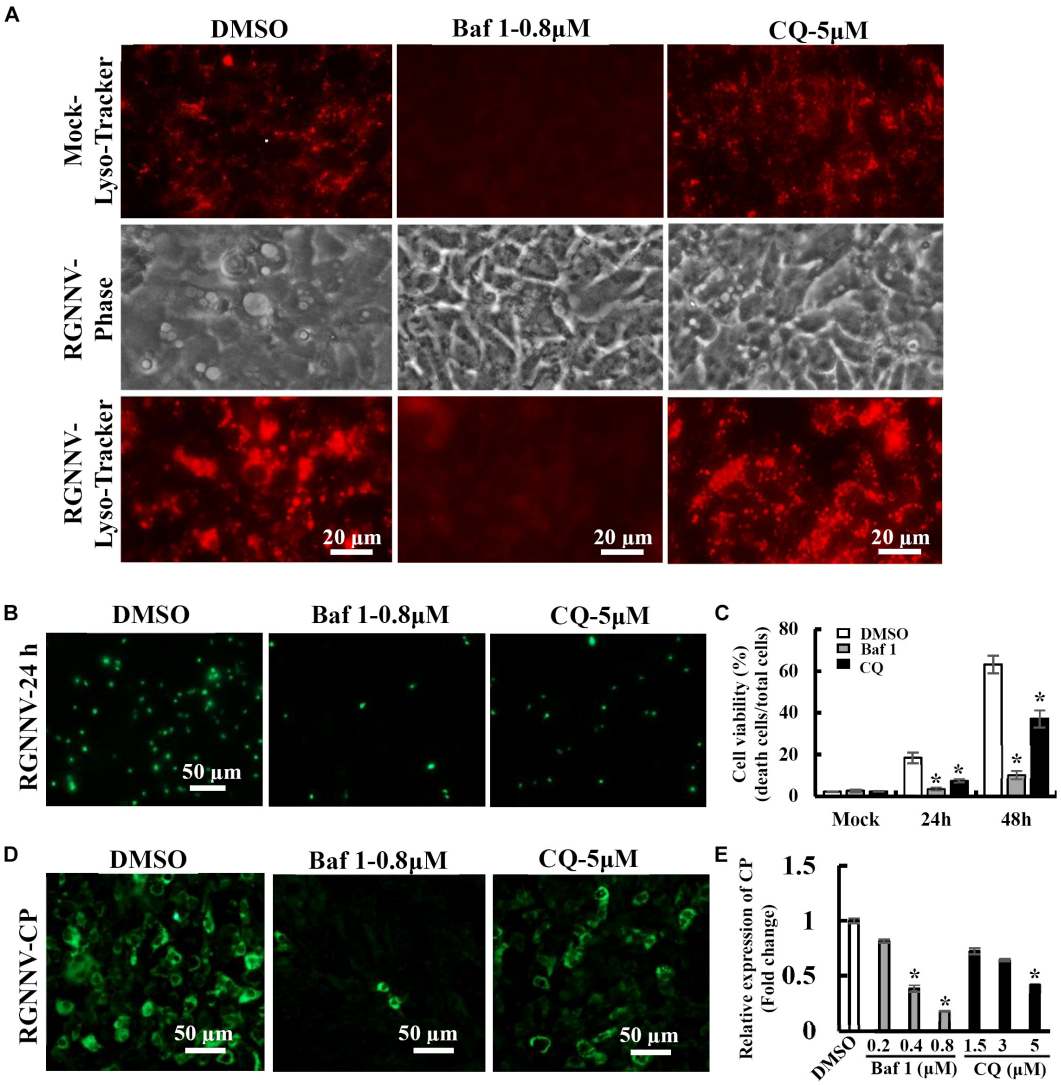

FIGURE 5 | Vacuole formation and viral replication during RGNNV infection were dependent on lysosomal acidification. **(A)** The effects of bafilomycin A1 and CQ on lysosome morphology and vacuole formation. **(B)** The effect of bafilomycin A1 and CQ on RGNNV infection-induced cell death. **(C)** The percentage of cell death in RGNNV-infected cells following treatment with bafilomycin A1 or CQ. **(D)** Treatment with bafilomycin A1 or CQ significantly inhibited viral protein synthesis. **(E)** Quantitative analysis of RGNNV CP viral transcription.

cells compared to the DMSO-treated cells (**Figures 6D,E**). Thus, these data indicate that the Na^+ and K^+ imbalance play a vital role in the vacuolization and cell death evoked by an RGNNV infection.

To further verify whether monensin and nigericin affected the lysosome structure that subsequently blocked vacuole formation, the lysosome morphology in the monensin- and nigericin-treated cells were observed under fluorescence microscopy. Compared with DMSO treatment, monensin treatment resulted in an observed decrease in the number of lysosomal-labeled dots in the mock-infected cells, and the labeled lysosomes were clustered together in the cytoplasm. In contrast, nigericin treatment did not show an obvious effect on lysosome morphology compared to DMSO treatment (**Figure 7A**). In addition, the effects of monensin and nigericin treatment on the cellular ultrastructure was further assessed by electron microscopy. As shown in **Figure 7B**, dense granules surrounded by a monolayer, as well as small vacuoles about 100–150 nm in diameter, were observed in the monensin treated mock-infected cells. It is proposed that the dense granules induced by monensin treatment might be lysosome aggregates. Following RGNNV infection, cytoplasmic vacuoles were observed in the DMSO-treated infected cells, as well as VRCs, which contained numerous viral particles (**Figure 7B**). However, VRCs and scattered virions were not observed in the monensin- or nigericin-treated infected cells. This finding was consistent with the finding that both monensin and nigericin significantly inhibited viral CP expression. Although no obvious abnormal structures

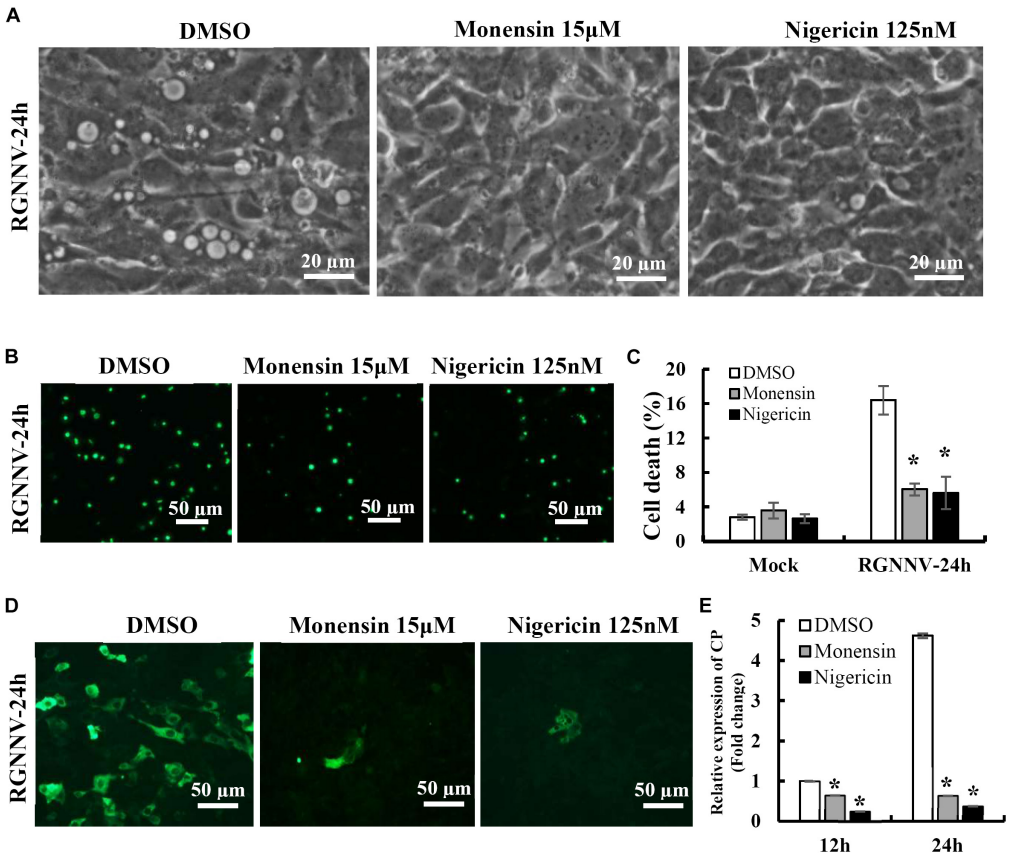

FIGURE 6 | The Na+ and K+ ionophore exerted a vital role on vacuole formation. **(A)** The effects of nigericin and monensin treatment on vacuole formation during RGNNV infection. **(B)** The effect of nigericin and monensin on RGNNV infection-induced cell death. **(C)** The percentage of cell death in RGNNV-infected cells following treatment with nigericin and monensin. **(D)** Nigericin and monensin treatment significantly inhibited viral protein synthesis. **(E)** Quantitative analysis of the viral transcription of RGNNV CP.

were present in the nigericin-treated cells, double-membraned organelles were observed in the cytoplasm in the RGNNV-infected nigericin-treated cells. However, whether these double membrane organelles were involved in affecting the formation of cytoplasmic vacuoles was uncertain.

Autophagy Participates in RGNNV-Induced Vacuolization and Cell Death

To determine whether autophagy was involved in RGNNV-induced lysosomal vacuolation, we investigated the roles of autophagosomes during RGNNV-induced vacuolization. When autophagy is stimulated, cytosolic form of LC3 is conjugated to phosphatidylethanolamine to form LC3-phosphatidylethanolamine conjugate, which is recruited to autophagosomal membranes. In pEGFP-LC3 transfected cells, the punctate fluorescence signals (which primarily represent autophagosomes) can be observed under fluorescence microscope. As shown in **Figure 8A**, the pEGFP-LC3 fluorescence signals redistributed from a diffuse pattern in mock infected cells to a punctate cytoplasmic pattern in RGNNV-infected cells. Moreover, fluorescence spots were partially localized in the vacuolar lumen during RGNNV infection (**Figure 8A**). This suggested that autophagosomes might be involved in the vacuole formation induced by RGNNV. Next, 3-Methyladenine (3-MA), a drug which inhibits autophagy by blocking autophagosome formation via the inhibition of type III Phosphatidylinositol 3-kinases (PI-3K) was used in this study to further examine the role of autophagy during vacuole formation. As shown in **Figure 8B**, treatment with 3-MA decreased the number of fluorescently labeled cells during RGNNV infection. Of note, both the severity of the vacuolization and cell death induced by RGNNV were significantly weakened in the 3-MA-treated cells (**Figures 8C,D**). Collectively, these results suggest that autophagy participates in RGNNV-induced vacuolization and cell death.

DISCUSSION

As a major aquaculture pathogen of larval and juvenile marine finfish worldwide, NNV was found to induce the vacuolation and necrosis of the central nervous system

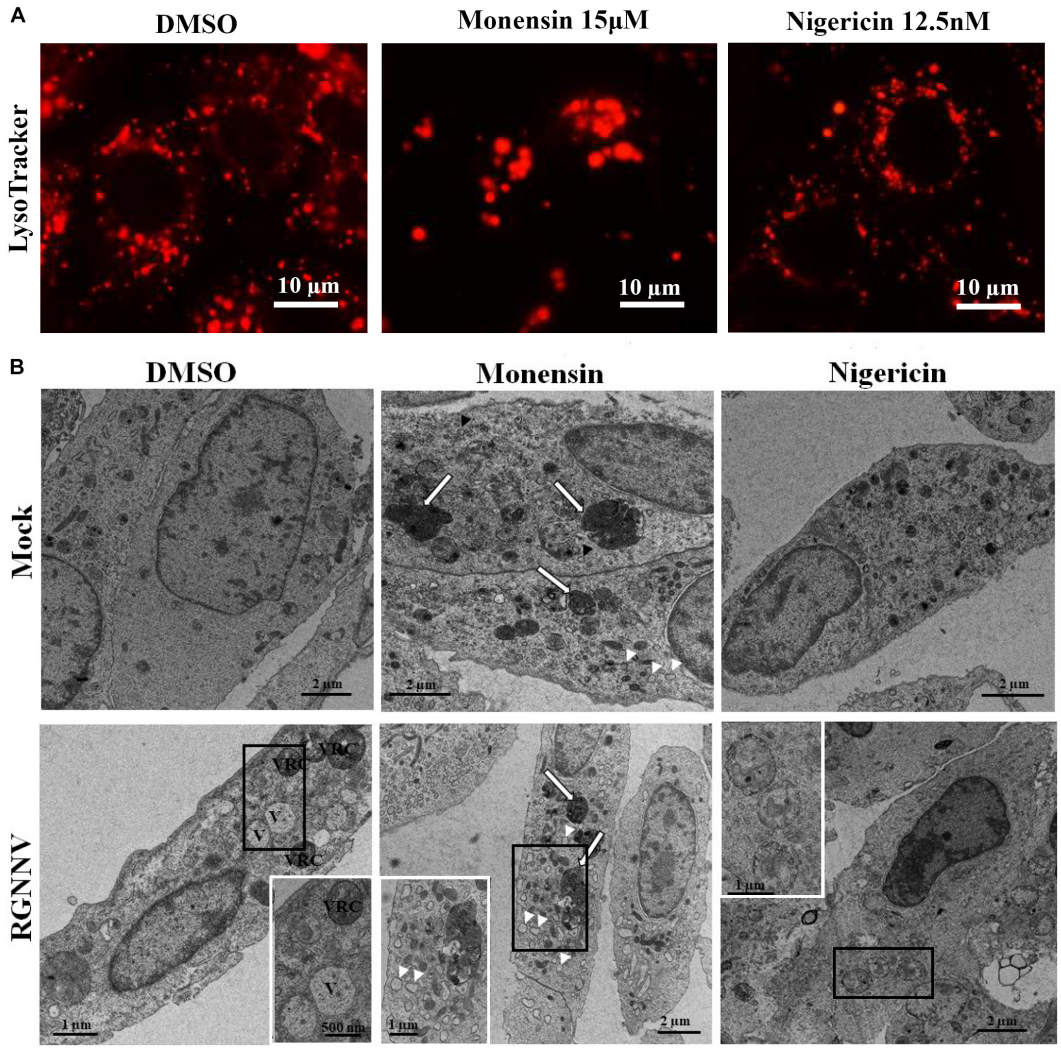

FIGURE 7 | The effect of nigericin and monensin on the lysosome structure during RGNNV infection. **(A)** The lysosome structure upon nigericin and monensin treatment using fluorescence microscopy. **(B)** The lysosome ultrastructure in RGNNV-infected cells under electron microscopy.

(Ransangan and Manin, 2010; Doan et al., 2017; Yong et al., 2017). An *in vitro* NNV infection was found to evoke typical cytoplasmic vacuolization in a variety of cells, including grouper spleen (GS) and brain (GB) cells (Qin et al., 2006; Huang et al., 2011), striped snakehead fish cells (SSN-1) (Iwamoto et al., 2000), and European sea bass brain cells (DLB-1) (Chaves-Pozo et al., 2019). This indicates that cytoplasmic vacuolization caused by RGNNV was independent of the cell type. To our knowledge, the origin of the vacuoles evoked by RGNNV and the critical events during vacuolization remain poorly understood.

Increased evidence has found that numerous viruses can trigger cytoplasmic vacuolization (Shubin et al., 2016). Viral proteins (e.g., envelope or capsid proteins) typically act as inducers to trigger vacuole formation (Shubin et al., 2015; Luo et al., 2016). Although the origin of virus-induced vacuoles has not been fully characterized, several reports have demonstrated that the vacuoles evoked by different viruses may originate from different membrane organelles (e.g., ER and lysosomal organelles) (Shubin et al., 2016). In this report, double-membrane structures in the cytoplasmic vacuoles induced by RGNNV were observed under electron microscopy. The temporal analysis indicated that small cytoplasmic vacuoles were present during the early stages of RGNNV infection, some of which fused into one large cell as the infection progressed. Further analysis showed that both Mito-Tracker and ER-Tracker were excluded from vacuoles, whereas Lyso-Tracker had accumulated in the vacuoles of the RGNNV-infected cells, and the vacuolar membranes simultaneously labeled the endosome markers, Rab5 and Rab7. Moreover, the increase in lysosome volume was observed to be accompanied by the occurrence of cytoplasmic vacuoles. Thus, we speculated that RGNNV-induced vacuoles might originate from the endosomal/lysosomal compartments, rather than the mitochondria and ER. Bovine viral diarrhea virus

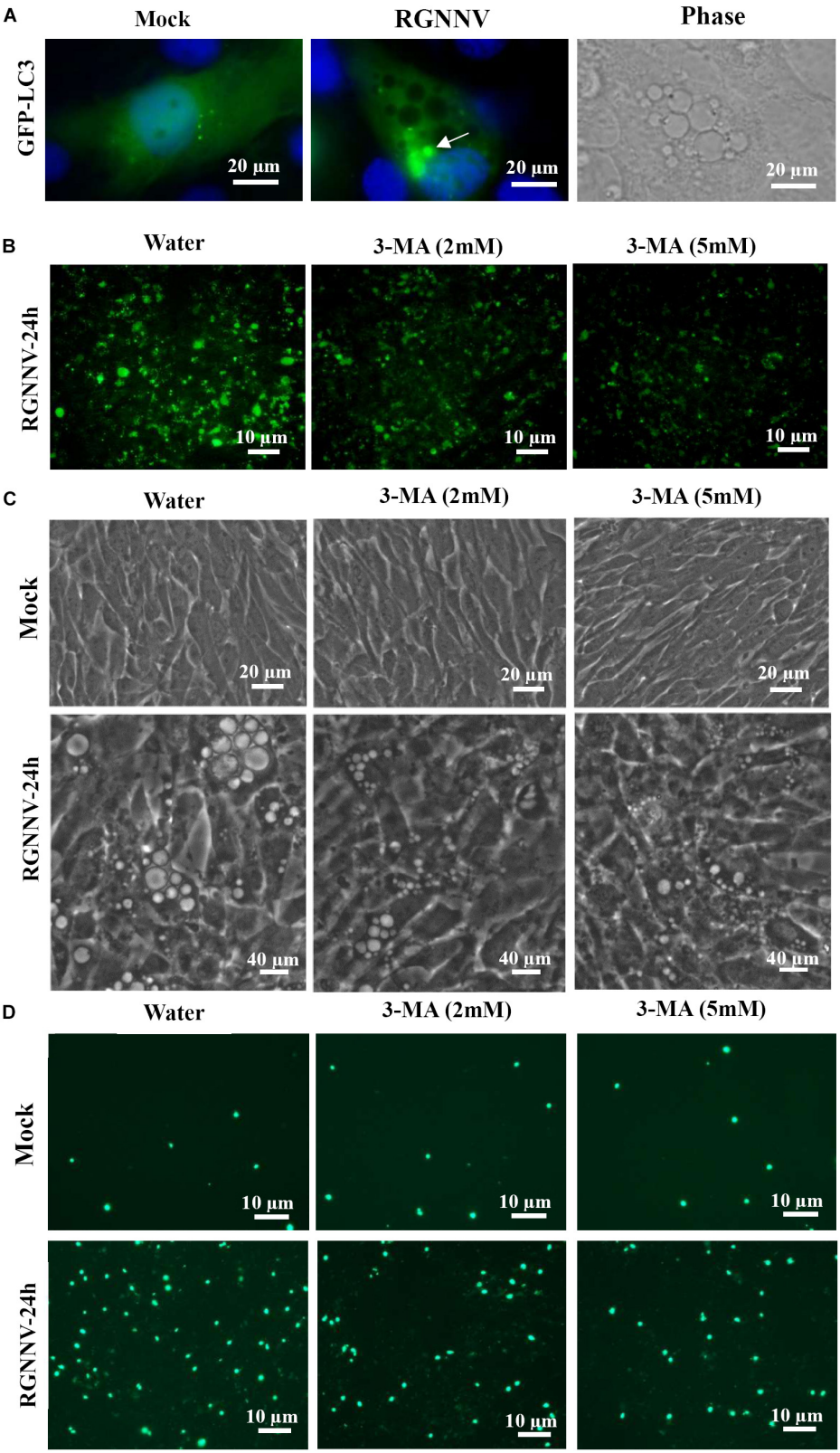

FIGURE 8 | The role of autophagy in vacuole formation during RGNNV infection. **(A)** The localization patterns of LC3 during RGNNV infection-induced vacuolization. Arrow indicates the LC3 fluorescent puncta. **(B)** Detection of autophagy in RGNNV-infected cells under treatment with 3-MA. **(C)** The effects of 3-MA on RGNNV infection-induced vacuolization. **(D)** The effects of 3-MA on RGNNV infection-induced cell death.

and SV40 also induced the vacuolization of acidic endosomal-lysosomal organelles in infected cells (Birk et al., 2008; Luo et al., 2016). In addition, vacuolization of different intracellular compartments always indicates the pathological status and accompanies different types of cell death (Shubin et al., 2015; Monel et al., 2017). Our results also show that the proportion of cell death at different time points was consistent with the severity of vacuolization, suggesting that RGNNV-triggered vacuolization of lysosomal/endosomal organelles was accompanied by cell death during viral infection.

As an important cellular organelle, lysosomes maintain an acidic luminal pH for the purpose of degrading internalized macromolecules and lysosomal proteases (e.g., cathepsins exert a crucial role in maintaining cell metabolism homeostasis and participate in different types of cell death (Repnik et al., 2012; Mauvezin et al., 2015). The V-ATPase inhibitor bafilomycin A was able to completely block vacuolization in RGNNV-infected cells, indicating that RGNNV-induced vacuoles also required V-ATPase activity. Moreover, chloroquine, a lysosomotropic agent that prevents endosomal acidification, also significantly inhibited the fusion of the vacuole formation during RGNNV infection. Thus, we speculated that the maintenance of lysosome acidification is required for RGNNV-induced vacuolization and cell death. To clarify the role of cathepsins in RGNNV-induced vacuolization, different cathepsin inhibitors, including Z-FA-FMK, CA-074, and E64D, were used in this study. Interestingly, none of these selected inhibitors showed obvious effects on RGNNV-triggered vacuolization and cell death. This suggests that multiple cathepsins (i.e., cathepsins B, L, and K) were not involved in this process.

Cytoplasmic vacuolization always accompanies different types of cell death, including autophagy, paraptosis-like cell death, and necroptosis (Kar et al., 2009; Huang et al., 2011; Singha et al., 2013). When autophagy occurs, LC3 becomes conjugated to phosphatidylethanolamine at autophagosome-forming sites, and redistributes from a diffuse pattern to a punctate cytoplasmic pattern (Kabeya et al., 2000; Tanida et al., 2008). Given that our previous studies indicated that RGNNV infection could induce autophagy (Huang et al., 2015), we raised the question of whether autophagy was involved in lysosomal vacuolization during RGNNV infection. To address this issue, we first examined whether autophagosome-like vesicles and the altered distribution for LC3 proteins occurred in vacuolization. The results showed that the autophagic vacuoles containing intact cytoplasmic material and viral particles, and the small amount of LC3 proteins, were observed in the lumen of RGNNV-induced cytoplasmic vacuoles, suggesting that autophagosomes were involved in RGNNV infection. Secondly, we found that 3-MA treatment had remarkable inhibitory effects on RGNNV-induced vacuolation and cell death. In addition, the Bafilomycin A1-mediated inhibition on the number and volume of vacuoles might provide further evidence of the involvement of autophagy in vacuolization. This is because Bafilomycin A1 can also function as an inhibitor of late phase of autophagy by preventing the fusion

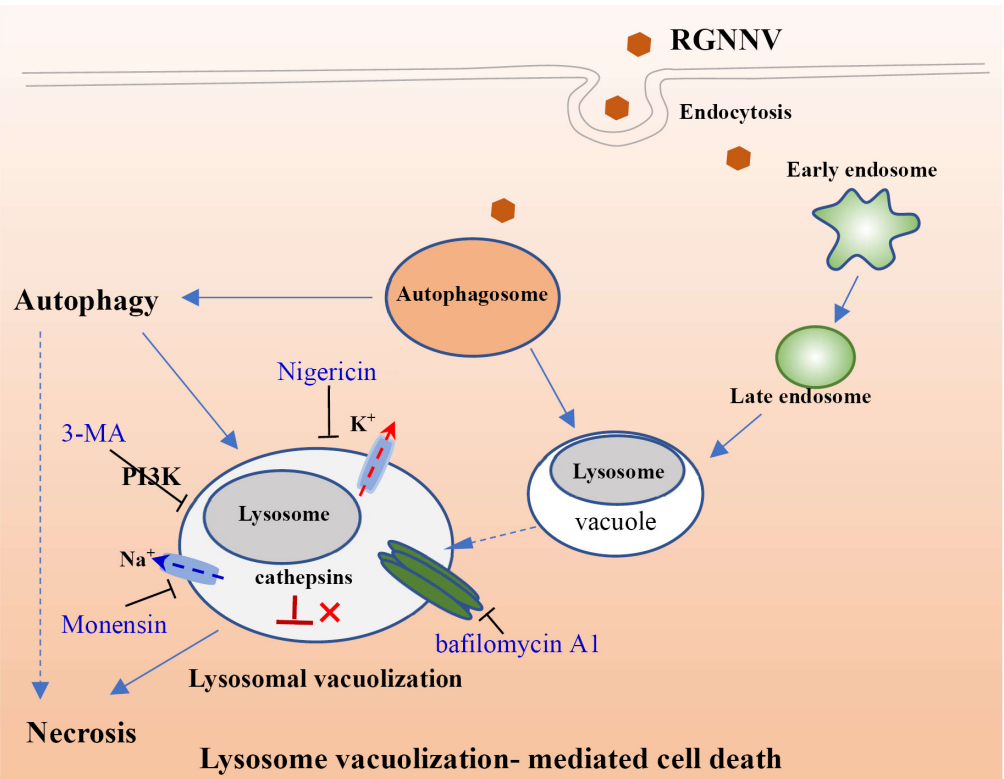

FIGURE 9 | Proposed model of lysosomal vacuolization-mediated cell death during RGNNV infection.

between autophagosomes and lysosomes, as well as lysosomal degradation (Kissing et al., 2015; Mauvezin et al., 2015). Based on these findings, we speculate that autophagy participates in RGNNV-induced lysosomal vacuolization.

In addition to V-ATPase activity, the proton-selective ionophore, monensin (Na^+/H^+), as well as nigericin (K^+/H^+), have been demonstrated to raise the pH of the acidified compartments, and inhibit autophagosome-lysosome fusion (Lim et al., 2012; Yoon et al., 2013). In this study, we elucidated an important role of intracellular ionophores in the lysosomal vacuolization induced by RGNNV infection. Our data show that treatment with both monensin and nigericin have observable effects on cytoplasmic vacuolization in RGNNV-infected cells. Combined with the inhibitory effect of Bafilomycin A1, our results further demonstrated that the maintenance of lysosome acidic was required for RGNNV infection-induced vacuolization and cell death (**Figure 9**). Moreover, alterations in the lysosome structure (e.g., lysosome swelling) were also observed in monensin-treated cells. Thus, we presumed that in the process of RGNNV infection, acidic lysosomes were first fused with late endosomes to form cytoplasmic vacuoles, which was followed by lysosome swelling. The results from electron microscopy also showed that viral particles were present in some cytoplasmic vacuoles in conjunction with cell debris. Given the critical role of lysosomes in acidic degradation, we speculated that the cytoplasmic vacuoles derived from endosomal/lysosomal organelles might be an important host defense strategy for the degradation of viral proteins or virion clearance.

In conclusion, the findings of this study suggest that RGNNV-induced vacuoles originate from endosomal/lysosomal organelles and evoke an alteration of the lysosomal structure. Moreover, V-ATPase activity and the balance of the intracellular ionophore, but not cathepsin activation are essential for RGNNV infection-induced lysosomal vacuolization and cell death. In addition, autophagy might exert a critical role on vacuole formation and cell death during RGNNV infection (**Figure 9**). Taken together, we propose that autophagy participates in RGNNV infection-induced lysosomal vacuolization and cell death. Thus, our data will provide novel insight into our understanding of the molecular mechanisms of nodavirus pathogenesis.

DATA AVAILABILITY STATEMENT

All datasets generated for this study are included in the article/**Supplementary Material**.

AUTHOR CONTRIBUTIONS

XH and YH carried out the main experiments, analyzed the data, and drafted the manuscript. YZ and ZL participated in the qPCR experiments and trypan blue staining. JZ participated in the immunofluorescence experiment. CL prepared the ultrathin sections. XH and QQ designed the experiments and reviewed the manuscript. All authors read and approved the final manuscript.

FUNDING

This work was supported by grants from the National Key R&D Program of China (2018YFD0900500) and China Agriculture Research System (CARS-47-G16). Electron microscopy sections were carried out at the Instrumental Analysis & Research Center at South China Agricultural University.

SUPPLEMENTARY MATERIAL

The Supplementary Material for this article can be found online at: https://www.frontiersin.org/articles/10.3389/fmicb.2020.00790/full#supplementary-material

FIGURE S1 | Rab5 and Rab7 localization during RGNNV infection. GS cells were transfected with pEGFP-Rab5 or pEGFP-Rab7, and subsequently infected with RGNNV. At 24 h p.i., the cells were stained with DAPI and the fluorescence was observed via fluorescence microscopy.

REFERENCES

Aki, T., Nara, A., and Uemura, K. (2012). Cytoplasmic vacuolization during exposure to drugs and other substances. *Cell. Biol. Toxicol.* 28, 125–131. doi: 10.1007/s10565-012-9212-3

Bandín, I., and Souto, S. (2020). Betanodavirus and VER disease: a 30-year research review. *Pathogens* 9:106. doi: 10.3390/pathogens9020106

Birk, A. V., Dubovi, E. J., Cohen-Gould, L., Donis, R., and Szeto, H. H. (2008). Cytoplasmic vacuolization responses to cytopathic bovine viral diarrhoea virus. *Virus. Res.* 132, 76–85. doi: 10.1016/j.virusres.2007.10.017

Chaves-Pozo, E., Bandín, I., Olveira, J. G., Esteve-Codina, A., Gómez-Garrido, J., Dabad, M., et al. (2019). European sea bass brain DLB-1?cell line is susceptible to nodavirus: a transcriptomic study. *Fish. Shellfish. Immunol.* 86, 14–24. doi: 10.1016/j.fsi.2018.11.024

Chi, S. C., Lo, C. F., Kou, G. H., Chang, P. S., Peng, S. E., and Chen, S. N. (1997). Mass mortalities associated with viral nervous necrosis (VNN) disease in two species of hatchery-reared grouper, Epinephelus fuscogutatus and Epinephelus akaara (Temminck & Schlegel). *J. Fish. Dis.* 20, 185–193. doi: 10.1046/j.1365-2761.1997.00291.x

Costa, J. Z., and Thompson, K. D. (2016). Understanding the interaction between Betanodavirus and its host for the development of prophylactic measures for viral encephalopathy and retinopathy. *Fish. Shellfish. Immunol.* 53, 35–49. doi: 10.1016/j.fsi.2016.03.033

Doan, Q. K., Vandeputte, M., Chatain, B., Morin, T., and Allal, F. (2017). Viral encephalopathy and retinopathy in aquaculture: a review. *J. Fish. Dis.* 40, 717–742. doi: 10.1111/jfd.12541

Foo, N. C., Ahn, B. Y., Ma, X., Hyun, W., and Yen, T. S. (2002). Cellular vacuolization and apoptosis induced by hepatitis B virus large surface protein. *Hepatology* 36, 1400–1407. doi: 10.1002/hep.1840360616

Hegde, A., Chen, C. L., Qin, Q. W., Lam, T. J., and Sin, Y. M. (2002). Characterization, pathogenicity and neutralization studies of a nervous necrosis virus isolated from grouper. Epinephelus tauvina, in Singapore. *Aquaculture* 213, 55–72. doi: 10.1016/s0044-8486(02)00092-3

Huang, X. H., Huang, Y. H., Ouyang, Z. L., and Qin, Q. W. (2011). Establishment of a cell line from the brain of grouper (*Epinephelus akaara*) for cytotoxicity testing and virus pathogenesis. *Aquaculture* 311, 65–73. doi: 10.1016/j.aquaculture.2010.11.037

Huang, X. H., Huang, Y. H., Sun, J. J., Han, X., and Qin, Q. W. (2009). Characterization of two grouper Epinephelus akaara cell lines: application to

studies of Singapore grouper iridovirus (SGIV) propagation and virus-host interaction. *Aquaculture* 292, 172–179. doi: 10.1016/j.aquaculture.2009.04.019

Huang, Y., Huang, X., Yang, Y., Wang, W., Yu, Y., and Qin, Q. (2015). Involvement of fish signal transducer and activator of transcription 3 (STAT3) in nodavirus infection induced cell death. *Fish. Shellfish. Immunol.* 43, 241–248. doi: 10.1016/j.fsi.2014.12.031

Iwamoto, T., Nakai, T., Mori, K., Arimoto, M., and Furusawa, I. (2000). Cloning of the fish cell line SSN-1 for piscine nodaviruses. *Dis. Aquat. Organ.* 43, 81–89. doi: 10.3354/dao043081

Johansen, R., Sommerset, I., Tørud, B., Korsnes, K., Hjortaas, M. J., Nilsen, F., et al. (2004). Characterization of nodavirus and viral encephalopathy and retinopathy in farmed turbot. *Scophthalmus maximus* (L.). J. Fish. Dis. 27, 591–601. doi: 10.1111/j.1365-2761.2004.00581.x

Kabeya, Y., Mizushima, N., Ueno, T., Yamamoto, A., Kirisako, T., Noda, T., et al. (2000). LC3, a mammalian homologue of yeast Apg8p, is localized in autophagosome membranes after processing. *EMBO J.* 19, 5720–5728. doi: 10.1093/emboj/19.21.5720

Kar, R., Singha, P. K., Venkatachalam, M. A., and Saikumar, P. (2009). A novel role for MAP1 LC3 in nonautophagic cytoplasmic vacuolation death of cancer cells. *Oncogene* 28, 2556–2568. doi: 10.1038/onc.2009.118

Kissing, S., Hermsen, C., Repnik, U., Nesset, C. K., von Bargen, K., Griffiths, G., et al. (2015). Vacuolar ATPase in phagosome-lysosome fusion. *J. Biol. Chem.* 290, 14166–14180. doi: 10.1074/jbc.M114.628891

Lim, J., Lee, Y., Kim, H. W., Rhyu, I. J., Oh, M. S., Youdim, M. B., et al. (2012). Nigericin-induced impairment of autophagic flux in neuronal cells is inhibited by overexpression of Bak. *J. Biol. Chem.* 287, 23271–23282. doi: 10.1074/jbc.M112.364281

Luo, Y., Motamedi, N., Magaldi, T. G., Gee, G. V., Atwood, W. J., and DiMaio, D. (2016). Interaction between Simian Virus 40 Major Capsid Protein VP1 and Cell Surface Ganglioside GM1 Triggers Vacuole Formation. *MBio* 7:e00297. doi: 10.1128/mBio.00297-16

Mauvezin, C., Nagy, P., Juhász, G., and Neufeld, T. P. (2015). Autophagosome-lysosome fusion is independent of V-ATPase-mediated acidification. *Nat. Commun.* 6:7007. doi: 10.1038/ncomms8007

Monel, B., Compton, A. A., Bruel, T., Amraoui, S., Burlaud-Gaillard, J., Roy, N., et al. (2017). Zika virus induces massive cytoplasmic vacuolization and paraptosis-like death in infected cells. *EMBO. J.* 36, 1653–1668. doi: 10.15252/embj.201695597

Mullick, C. S., Lalwani, G., Zhang, K., Yang, J. K., Neville, K., and Sitharaman, B. (2013). Cell specific cytotoxicity and uptake of graphene nanoribbons. *Biomaterials* 34, 283–293. doi: 10.1016/j.biomaterials.2012.09.057

Murata, H., Peden, K., and Lewis, A. M. Jr. (2008). Identification of a mutation in the SV40 capsid protein VP1 that influences plaque morphology, vacuolization, and receptor usage. *Virology* 370, 343–351. doi: 10.1016/j.virol.2007.08.040

Nishizawa, T., Furuhashi, M., Nagai, T., Nakai, T., and Muroga, K. (1997). Genomic classification of fish nodaviruses by molecular phylogenetic analysis of the coat protein gene. *Appl. Environ. Microbiol.* 63, 1633–1636. doi: 10.1128/aem.63.4.1633-1636.1997

Parameswaran, V., Kumar Rajesh, S., Ishaq Ahmed, V. P., and Sahul Hameed, A. S. (2007). A fish nodavirus associated with mass mortality in hatchery-reared Asian Sea bass. *Lates calcarifer*. Aquaculture 275, 366–369. doi: 10.1016/j.aquaculture.2008.01.023

Qin, Q. W., Wu, T. H., Jia, T. L., Hegde, A., and Zhang, R. Q. (2006). Development and characterization of a new tropical marine fish cell line from grouper, Epinephelus coioides susceptible to iridovirus and nodavirus. *J. Virol. Methods* 131, 58–64. doi: 10.1016/j.jviromet.2005.07.009

Ransangan, J., and Manin, B. O. (2010). Mass mortality of hatchery-produced larvae of Asian seabass, Lates calcarifer (Bloch), associated with viral nervous necrosis in Sabah, Malaysia. *Vet. Microbiol.* 145, 153–157. doi: 10.1016/j.vetmic.2010.03.016

Repnik, U., Stoka, V., Turk, V., and Turk, B. (2012). Lysosomes and lysosomal cathepsins in cell death. *Biochim. Biophys. Acta* 1824, 22–33. doi: 10.1016/j.bbapap.2011.08.016

Sahul Hameed, A. S., Ninawe, A. S., Nakai, T., Chi, S. C., and Johnson, K. L. (2019). Ictv report consortium. *ICTV* Virus Taxonomy Profile: Nodaviridae. *J. Gen. Virol.* 100, 3–4. doi: 10.1099/jgv.0.001170

Shubin, A. V., Demidyuk, I. V., Komissarov, A. A., Rafieva, L. M., and Kostrov, S. V. (2016). Cytoplasmic vacuolization in cell death and survival. *Oncotarget* 7, 55863–55889. doi: 10.18632/oncotarget.10150

Shubin, A. V., Demidyuk, I. V., Lunina, N. A., Komissarov, A. A., Roschina, M. P., Leonova, O. G., et al. (2015). Protease 3C of hepatitis A virus induces vacuolization of lysosomal/endosomal organellesand caspase-independent cell death. *BMC. Cell. Biol.* 16:4. doi: 10.1186/s12860-015-0050-z

Singha, P. K., Pandeswara, S., Venkatachalam, M. A., and Saikumar, P. (2013). Manumycin A inhibits triple-negative breast cancer growth through LC3-mediated cytoplasmic vacuolation death. *Cell. Death. Dis.* 4:e457. doi: 10.1038/cddis.2012.192

Tanida, I., Ueno, T., and Kominami, E. (2008). LC3 and Autophagy. *Methods Mol. Biol.* 445, 77–88. doi: 10.1007/978-1-59745-157-4_4

Wang, S., Huang, X., Huang, Y., Hao, X., Xu, H., Cai, M., et al. (2014). Entry of a novel marine DNA virus, Singapore grouper iridovirus, into host cells occurs via clathrin-mediated endocytosis and macropinocytosis in a pH-dependent manner. *J. Virol.* 88, 13047–13063. doi: 10.1128/JVI.01744-14

Whatley, B. R., Li, L., and Chin, L. S. (2008). The ubiquitin-proteasome system in spongiform degenerative disorders. *Biochim. Biophys. Acta* 1782, 700–712. doi: 10.1016/j.bbadis.2008.08.006

Xu, Z., Jensen, G., and Yen, T. S. (1997). Activation of hepatitis B virus S promoter by the viral large surface protein via induction of stress in the endoplasmic reticulum. *J. Virol.* 71, 7387–7392. doi: 10.1128/jvi.71.10.7387-7392.1997

Yong, C. Y., Yeap, S. K., Omar, A. R., and Tan, W. S. (2017). Advances in the study of nodavirus. *Peer. J.* 5: e3841. doi: 10.7717/peerj.3841

Yoon, M. J., Kang, Y. J., Kim, I. Y., Kim, E. H., Lee, J. A., Lim, J. H., et al. (2013). Monensin, a polyether ionophore antibiotic, overcomes TRAIL resistance in glioma cells via endoplasmic reticulum stress, DR5 upregulation and c-FLIP downregulation. *Carcinogenesis* 34, 1918–1928. doi: 10.1093/carcin/bgt137

Zhang, Y., Wang, L., Huang, X., Wang, S., Huang, Y., and Qin, Q. (2019). Fish cholesterol 25-Hydroxylase inhibits virus replication via regulating interferon immune response or affecting virus entry. *Front. Immunol.* 10:322. doi: 10.3389/fimmu.2019.00322

Zheng, J., Zhang, Y., Zhi, L. Y., Lv, S. Y., Xiao, L., Huang, X. H., et al. (2019). The novel gene TRIM44L from orange-spotted grouper negatively regulates the interferon response. *Fish Shellfish Immunol.* 92, 746–755. doi: 10.1016/j.fsi.2019.06.062

Conflict of Interest: The authors declare that the research was conducted in the absence of any commercial or financial relationships that could be construed as a potential conflict of interest.

frontiers in Microbiology

REVIEW
published: 07 May 2020
doi: 10.3389/fmicb.2020.00733

Herpes Simplex Virus: The Hostile Guest That Takes Over Your Home

*Anwesha Banerjee, Smita Kulkarni and Anupam Mukherjee**

Division of Virology, Indian Council of Medical Research-National AIDS Research Institute, Pune, India

Alpha (α)-herpesviruses (HSV-1 and HSV-2), like other viruses, are obligate intracellular parasites. They hijack the cellular machinery to survive and replicate through evading the defensive responses by the host. The viral genome of herpes simplex viruses (HSVs) contains viral genes, the products of which are destined to exploit the host apparatus for their own existence. Cellular modulations begin from the entry point itself. The two main gateways that the virus has to penetrate are the cell membrane and the nuclear membrane. Changes in the cell membrane are triggered when the glycoproteins of HSV interact with the surface receptors of the host cell, and from here, the components of the cytoskeleton take over. The rearrangement in the cytoskeleton components help the virus to enter as well as transport to the nucleus and back to the cell membrane to spread out to the other cells. The entire carriage process is also mediated by the motor proteins of the kinesin and dynein superfamily and is directed by the viral tegument proteins. Also, the virus captures the cell's most efficient cargo carrying system, the endoplasmic reticulum (ER)–Golgi vesicular transport machinery for egress to the cell membrane. For these reasons, the host cell has its own checkpoints where the normal functions are halted once a danger is sensed. However, a cell may be prepared for the adversities from an invading virus, and it is simply commendable that the virus has the antidote to these cellular strategies as well. The HSV viral proteins are capable of limiting the use of the transcriptional and translational tools for the cell itself, so that its own transcription and translation pathways remain unhindered. HSV prefers to constrain any self-destruction process of the cell—be it autophagy in the lysosome or apoptosis by the mitochondria, so that it can continue to parasitize the cell for its own survival. This review gives a detailed account of the significance of compartmentalization during HSV pathogenesis. It also highlights the undiscovered areas in the HSV cell biology research which demand attention for devising improved therapeutics against the infection.

Keywords: herpes, organelles, autophagy, apoptosis, encephalitis, therapeutics

OPEN ACCESS

Edited by:
Parikshit Bagchi,
University of Michigan, United States

Reviewed by:
Deepak Shukla,
The University of Illinois at Chicago, United States
Yu-Jie Chen,
University of Michigan, United States

****Correspondence:***
Anupam Mukherjee
amukherjee@nariindia.org;
mukherjee.a@icmr.gov.in

Specialty section:
This article was submitted to Virology, a section of the journal Frontiers in Microbiology

Received: *13 February 2020*
Accepted: *30 March 2020*
Published: *07 May 2020*

Citation:
Banerjee A, Kulkarni S and Mukherjee A (2020) Herpes Simplex Virus: The Hostile Guest That Takes Over Your Home. Front. Microbiol. 11:733. doi: 10.3389/fmicb.2020.00733

INTRODUCTION

Alpha (α)-herpesviruses are DNA viruses belonging to the family *Herpesviridae; herpein* meaning "to creep." Their members belong to one of the genera: *Iltovirus, Mardivirus, Scutavirus, Simplexvirus, and Varicellovirus*. The virions of α-herpesviruses are encased within a lipid bilayer envelope and capable of productive lysis as well as establishing a latent infection that is reactivable. The human α-herpesviruses, consisting of herpes simplex virus (HSV-1 and HSV-2) and varicella

zoster virus (VZV), have a wide range of vertebrate and invertebrate hosts to infect (Pellett and Roizman, 2013). Infection from HSV-1 causes corneal keratitis and/or cold sores at the orolabial region, whereas HSV-2 infection is mainly accountable for lesions at the genitalia (Shukla and Spear, 2001). In some exceptional cases, HSV-1 can cause genital herpes and HSV-2 could be responsible for oral herpes as well. HSV, although asymptomatic in many cases, causes viral shedding when the viral load is high and direct contact with infected patients through mucus and other body fluids results in the acquisition of infection (Fatahzadeh and Schwartz, 2007). Therefore, HSV-2 could be transmitted from mother to newborn during child birth *via* an infected birth canal (Anzivino et al., 2009). Most severe manifestations of HSV are encephalitis, meningitis, and blindness (Connolly et al., 2011). In developed countries, HSV-1 is marked as the major cause of corneal blindness and encephalitis through viruses (Herpetic Eye Disease Study Group, 1998; Shoji et al., 2002). Infection *via* HSV can cause direct destruction of the cell *via* lysis or can hide itself from the attacks of the host immune system by establishing latency (Whitley and Roizman, 2001) in a cell type-specific manner. HSV-1 and HSV-2 cause latency in the sensory neurons and the ganglia. By the establishment of latency, HSV can avoid encountering the antiviral drugs such as acyclovir and its analogs (James and Prichard, 2014).

Herpes simplex viruses are enveloped double-stranded DNA viruses. The outer envelope consists of 16 membrane proteins, out of which 12 are glycoproteins (Campadelli-Fiume et al., 2000; Mettenleiter, 2004; Diefenbach et al., 2008). These glycoproteins (gB, gC, gD, gE, gG, gH, gI, gJ, gK, gL, gM, and gN) mainly assist the entry of the virus into host cells. Below the envelope is the tegument which contains about 22 viral proteins (VPs). Beneath the tegument lies the icosahedral capsid encapsulating the HSV genome. The capsid has 162 capsomeres and six VPs on its surface (Diefenbach et al., 2008). The innermost core of the virus particle is the HSV genome of about 152 kB, from where at least 74 genes are encoded (McGeoch et al., 2006). From the beginning of the encounter of the virus with the host cell, HSV is ready with a strategized plan to divert the components of the host cell toward its pathogenesis to establish a productive infection. At present, our knowledge of understanding toward organelle dynamics during HSV infections is still at its infancy. In this review, we briefly summarize those mechanistic processes of HSV toward the various cellular organelles that lead to an extensive host cellular reorganization for prosperous establishment of the viral life cycle. This review will serve as a connection between the two most important sections, HSV virology and host cellular biology, which lead toward the development of new research avenues. The review goes about the events that take place at the cell organelles during an HSV infection.

THE CELL MEMBRANE

The "Main Gateway" to Herpes Simplex Virus Entry

The membrane of a cell acts as the fence of the cell, giving it the characteristic shape. It also acts as the "doorway" for entry as well as exit of substances from the cell. The cell membrane of the target cells of HSV, like any other animal cell, is semipermeable that is selective to the contents moving in and out of the cell. HSV is capable of targeting such cells because it has adapted itself to do so in the course of evolution (Karasneh and Shukla, 2011). HSV is an enveloped virus, and its envelop is derived from the cell membrane of the host cell it infects during the process of "budding out." Although membrane fusion for entry is a speciality of the enveloped viruses due to the presence of a lipid bilayer around them, HSV is capable of exploiting other routes of entry as well (Wittels and Spear, 1991; Clement et al., 2006) (**Figure 1**). It is capable of introducing membrane disruptions by forming pores or fragmentations in the membrane to induce endocytosis (Wittels and Spear, 1991). The route of entry is cell-specific. The virus enters the epithelial cells *via* the endocytic pathway and the neuronal cells *via* the membrane fusion pathway (Nicola et al., 2005; Miranda-Saksena et al., 2018) (**Figure 1**). The factors that direct the virus to choose the entry route in a cell are unclear. However, this choice is highly dependent on the replication cycle of the virus. HSV uses the epithelial cells to establish its lytic phase and the neuronal cells to establish a lysogenic phase. However, HSV replication has been observed in neuronal cells as well. Increased viral replication (such as during reactivation) in neurons may lead to critical manifestations such as encephalitis (Kennedy and Steiner, 2013). There are three events occurring at the cell membrane of the target host cell, namely, attachment, penetration and release (**Figure 1**). All of these processes involve the crucial participation of viral glycoproteins.

Attachment

An attachment process involving a receptor–ligand interaction is a common phenomenon for an HSV particle entering the cell, irrespective of the route of entry. The glycoproteins present on the surface of the HSV act as the ligands to the receptors present on the host cell surface to initiate the attachment process. There are 15 membrane proteins on the lipid envelope of HSV-1, of which 12 are glycosylated (Karasneh and Shukla, 2011). Of all glycosylated proteins or the glycoproteins (g), only four (gD, gH, gL, and gB) are essential for the entry process (Turner et al., 1998; Heldwein and Krummenacher, 2008). Glycoprotein B (gB), along with gC (a non-essential glycoprotein), is required for the attachment of the HSV to the heparan sulfate (HS) proteoglycans (HSPGs) on the cell surface (Heldwein and Krummenacher, 2008). After the attachment of gB to its receptor, gD binds to any one of its receptors, nectin-1 or herpes virus entry mediator (HVEM) or HS modified by the 3-OST family (3-OS-HS), to bring about a conformational change in itself (Agelidis and Shukla, 2015). Nectin-1 and nectin-2 are members of the immunoglobulin superfamily. Whereas HSV-2 entry can be mediated with both, nectin-2-mediated wild-type HSV-1 entry has not been observed yet (Krummenacher et al., 2004). HVEM is one of the members of tumor necrosis factor (TNF)-receptor superfamily that is mainly involved in facilitating the entry of HSV in T cells and some of the ocular epithelial cells. Although both nectin-1 and HVEM are receptors of gD, they have their

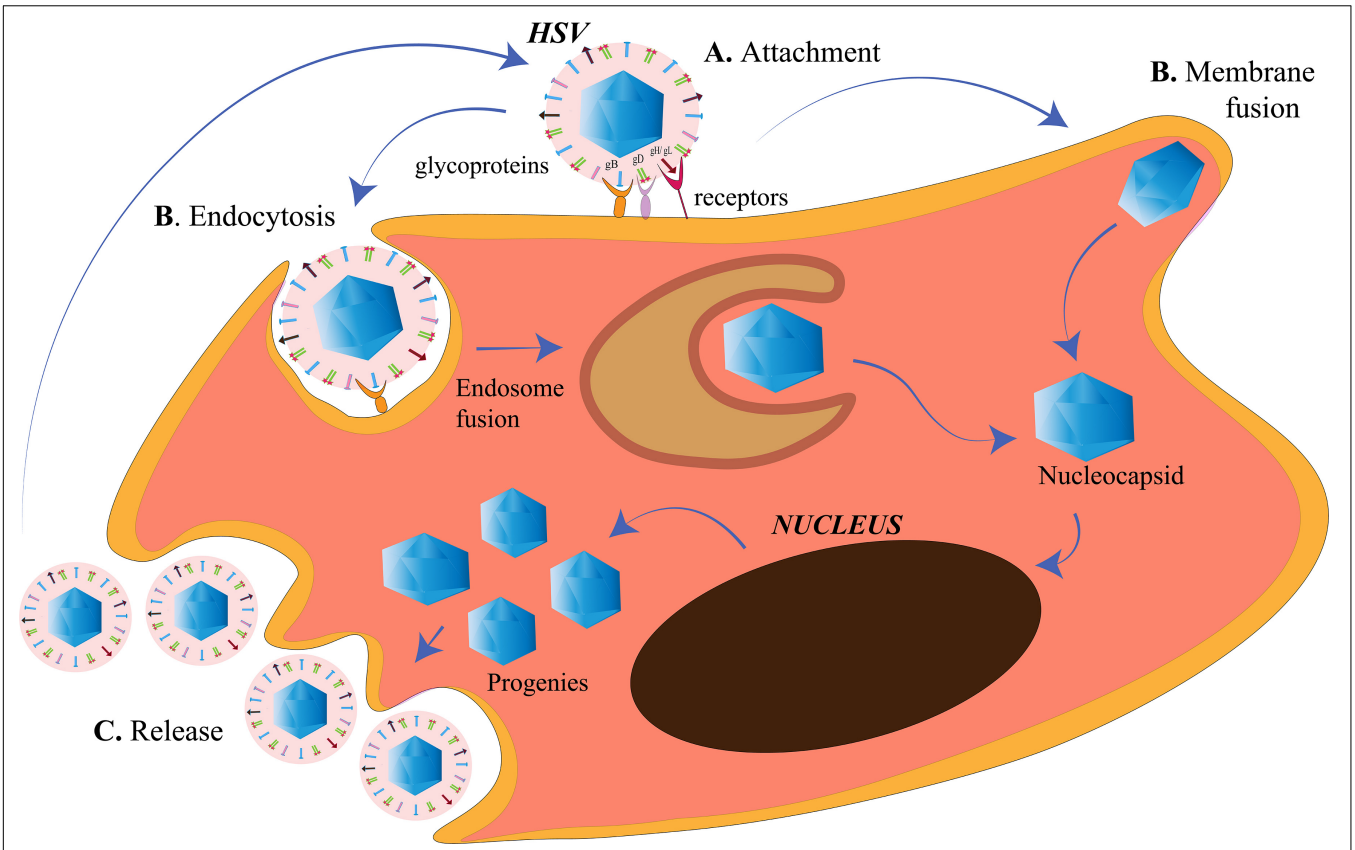

FIGURE 1 | Herpes simplex virus (HSV) entry and release at the cell membrane. **(A)** *Attachment*. The HSV envelope glycoproteins gB, gD, and gH/gL interact with the receptors on the cell membrane. **(B)** *Penetration*. Entry of HSV into the cell takes place either by membrane fusion, where the membrane of the virus and the cell fuse for the cellular uptake of the nucleocapsid only or, by endocytosis, where the enveloped virus is engulfed in an endosome followed by endosome fusion to release the nucleocapsids. The nucleocapsids enter into the nucleus for viral replication. **(C)** *Release*. The HSV progenies are released into the cytoplasm, acquire the membrane from the host cell in a process called *budding*.

own distinct pathways of HSV entry and block the entry of the virus through the other (Zhang et al., 2011). 3-OS-HS is the major receptor for HSV in the corneal fibroblasts where nectin-1 and HVEM have diminished expressions (Tiwari et al., 2006). The change in the conformation of gD is the displacement of the C-terminus after which the fusion-activating domain of gD is exposed (Gallagher et al., 2013). The changed gD conformation allows it to bind to a heterodimer of gH/gL (Fan et al., 2014). The gD/gH/gL complex then activates the fusogenic domain of gB to initiate the penetration process. The gD/gH/gL complex along with the gB is referred to as the core receptor-binding apparatus of the HSV (Atanasiu et al., 2013). It is also laudable the extent up to which the virus controls cell receptors, such that these proteins prioritize their role in the viral pathogenesis rather than their normal duty toward the host cell. gD of HSV is known to bind to the homodimerization interface of the nectin-1 so that nectin-1 is unable to function as a cell adhesion molecule (Zhang et al., 2011). Heparan sulfate (HS) and gB are also required for HSV surfing. HSV surfing is the phenomenon by which HSV-1 virions are known to transport to the cell bodies. This phenomenon is aided by the actin filaments of the cytoskeleton, whereas small Rho GTPase, Cdc42, is one of the regulators for the same (Oh et al., 2010). Once HSV has exploited the receptors for its entry, it is ready to penetrate the cell to establish an infection.

Penetration

After the attachment of HSV on the host cell, the membrane of the virus and the host cell need to be fused. Fusogens are specialized glycoproteins on the viral surface that mediate the fusion of the two membranes by introducing conformational changes in the membranes. The fusogen is generally spring-loaded and is triggered when the virus lands on the correct target cell or the intracellular compartment such as the endosome. The activation of the fusogen is either receptor-dependent or dependent on the pH of the compartment (Mas and Melero, 2013). HSV-1 gB is a fusogen that mediates the membrane fusion to facilitate the penetration of the HSV into the host cell (Atanasiu et al., 2013).

HSV-1 and HSV-2 has been known to use the endocytic pathway to enter the host cells. Clement et al. (2006) demonstrated a new phagocytosis-like mechanism for HSV endocytosis. While approaching the epithelial cells, HSV-1 interacted with the membrane protrusions and was then

engulfed by epithelium. The phagocytosis mechanism involved rearrangement of the cytoskeleton by the activation of Rho GTPases, followed by en-routing the virus in phagosome-like vesicles. The endocytosis was not clathrin-mediated because Eps15-deleted mutants were not affected for HSV-1 entry. Nectin or HVEM clustering in the phagosomes were also observed in HSV-1-infected cells, suggesting the contact between the envelope of the virus and that of the phagosomal membrane. Phagocytosis-mediated HSV uptake had since been a novel mechanism for HSV entry in epithelial cells (non-professional phagocytes). Efficient replication of HSV prepares the progenies and the cell for the release into the extracellular environment to spread and infect the neighborhood cells.

Release

As in the case of the viral entry, the release of HSV-1 from the infected cells requires certain glycoproteins. The virus is willing to leave the hijacked cell in order to spread to the other uninfected cells to further increase its number of progeny viruses. For example, the gp heterodimer, gE/gI, redistributes itself to the cell junctions to facilitate viral spread to the other cells (Farnsworth and Johnson, 2006). In neuronal cells, the gE/gI helps the transport of the capsids from the cell body through the axons by bringing them close to the kinesin motor proteins for anterograde transport (Howard et al., 2012). Thus, gE/gI may also use the same mechanism for reactivation from latency by facilitating the spread of HSV from the cell body of the neurons to the epithelial cells (Howard et al., 2014). Also, gK was discovered to be responsible for the spread of HSV from the corneal epithelium to the neurons, suggesting that gK is important for the establishment of latency as corneal infection with HSV-1 that had a mutation in the N-terminus of gK, failed to infect the trigeminal ganglia in mice (David et al., 2008, 2012; Saied et al., 2014). Heparanase is an endoglycosidase that can degrade HS by catalyzing the cleavage of the β-(1,4)-glycosidic bond between the glucuronic acid and glucosamine residues of HS (Agelidis et al., 2017). HSV requires heparanase-1 (HPSE) to be released from the infected cells (Hadigal et al., 2015). HPSE loosens the binding between the virus and the receptor HS to be free from the cell. It is simply wondrous that HSV controls the cell in such a manner that the HPSE levels increase gradually after infection. This eventual increment in the HPSE levels is a preplanned strategy to shift the cell from the viral attachment to the HSV viral detachment state, so that the release of HSV is smooth. The released HSV progenies are capable of reinitiating the entry process in the nearby cells. The cytoskeleton takes over after the virus has entered the cells.

CYTOSKELETON

The "Highways" for Herpes Simplex Virus Trafficking Within the Cell

The cytoskeleton is the backbone of the cell. It is an intracellular network of microfilaments, intermediate filaments, and microtubules and is capable of interacting with HSV (Feierbach et al., 2006). During HSV infection, the virus utilizes this network to enter and travel across the cell to the nucleus. In the nucleus, the viral replication is assisted by the microfilaments and assemble with a capsid before egress. The changes in the cytoskeleton structure either help in pathogenesis of HSV or counteract them. These cytoskeletal transformations in the cells can render them cancerous (Zheng et al., 2007).

Herpes Simplex Virus Exploits the Microfilaments and the Microtubules for Retrograde/Anterograde Transport

Prior to HSV penetration in the cell, the virus comes across the actin filaments lying toward the cytosolic side of the cell membrane and those which are bound to the surface receptors. When HSV-1 gD interacts with the nectin-1 on the cell surface, the Rho GTPase signaling is activated, which further causes the rearrangement of the actin connected to them (Hoppe et al., 2006). Even during the HSV egress process, the interaction of non-muscle myosin IIA (NMIIA) with VP22, which is an HSV tegument protein, is vital for the virions that leave the cell to enter into the extracellular milieu (Conti and Adelstein, 2008; Wang et al., 2017). After successful entry into the cells, the microfilaments, along with the motor protein dynein, assist the HSV from the membrane to the nucleus. As reviewed by Wu et al. (2019), when HSV needs to spread itself to the other host cells, it utilizes the US3 protein kinase to phosphorylate RhoA to rearrange the actin microfilaments and promote the breakdown of the actin stress fibers (contractile bundles composed of actin microfilament and NMIIA).

Herpes simplex viruse relies on the host transport machinery for its transport to the nucleus. Microtubules, one of the components of the cytoskeleton, play an important role in HSV transport from the plasma membrane to the nucleus (Dohner et al., 2005). This transport is driven by the motor proteins, kinesin and dynein (Lyman and Enquist, 2009). HSV is capable of employing a plus end-tracking protein (+ TIP) complex to begin a retrograde transport toward the nucleus (**Figure 2**). This complex is made up of end-binding protein 1 (EB1), a cytoplasmic linker protein 170 (CLIP-170), and the dynactin-1 (DCTN1) (Jovasevic et al., 2015). HSV retrogradely transports along the minus end of the microtubules toward the microtubule organizing center (MTOC), located beside the nucleus (Dammermann et al., 2003). The recruitment of the motor proteins, dynein, dynactin, kinesin-1, and kinesin-2, is done by the pUS3, pUL36, pUL37, ICP0, pUL14, pUL16, and pUL21, the capsid proteins exposed to the cytoplasm post-HSV entry. Different proteins on the HSV interact with different motor proteins to facilitate the transport process. VP26 is an outer capsid protein of HSV which interacts with RP3 and Tctex1, the dynein light chains (Douglas et al., 2004). Also, UL34 protein [a component of the HSV nuclear egress complex (NEC)] binds to the dynein intermediate chain (Reynolds et al., 2002). The transport of the virus capsids from the nucleus to the periphery of the cell takes place in an anterograde fashion, along the plus-end of the microtubules (Lee et al., 2006) (**Figure 2**). The capsid protein pUL37 recruits dystonin (BPAG1), which helps in this trafficking (McElwee et al., 2013; Pasdeloup et al., 2013). In tumor

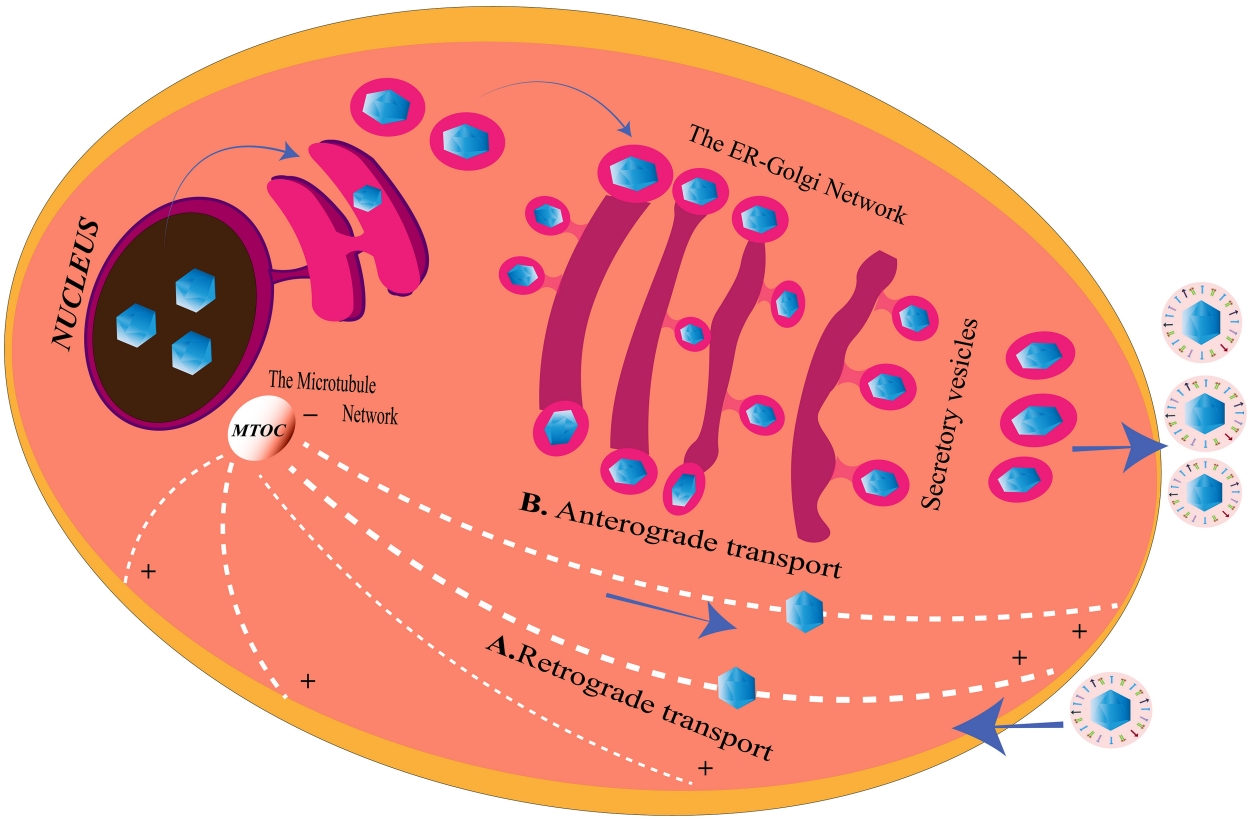

FIGURE 2 | Herpes simplex virus (HSV) transport system inside the cell. **(A)** *Retrograde transport*. After entering the cell, microtubules with the help of the motor proteins transport the virus along the minus end toward the microtubule organizing center (MTOC), from where they enter into the nucleus for genome replication. HSV may also use the endoplasmic reticulum (ER)–Golgi network to travel from the cell membrane to the nucleus for the same since ER shares a continuous membrane connecting the perinuclear space (PNS) and the Golgi apparatus. **(B)** *Anterograde transport*. After replication, the viruses are transported from the nucleus to the MTOC, from the minus end to the plus end of the microtubules to reach the cell membrane from where they are released. The progeny viruses may also travel through the PNS into the ER. The nucleocapsids enclosed in ER membranes are transported on the GA where it is transported along the *trans*-Golgi network into vesicles and released at the cell membrane, a process similar to the release of the secretory proteins of the cell.

cells arising from oncolytic HSV-1 (oHSV) infection, histone deacetylase 6 (HDAC6) could promote the spread of oHSVs by modulating the trafficking of the oncolytic virus particles (OVs) through acetylation of the microtubule (Nakashima et al., 2015). Other than the microtubule network, HSV is capable of exploiting the endoplasmic reticulum (ER)–Golgi network for its transport within the cell.

THE ENDOPLASMIC RETICULUM AND THE GOLGI APPARATUS

Herpes Simplex Virus Strategies for Overcoming Endoplasmic Reticulum Stress

It is also extremely appreciable that HSV is powerful enough to exploit the imperative organelle of the cell for its benefit. The largest cellular organelle, the ER, is a complex network extending throughout the cytoplasm of the cell. It is the site for protein synthesis [rough ER (RER)], modification, and transport of membrane, as well as secretory proteins. As a major organelle for protein folding (essential, as folding provides protein functionality), dysregulation in the ER is capable of changing the entire biology of the cell and drive the cell toward death. ER has a threshold to this folding, and too much protein load forces the ER to cause misfolding of the proteins triggering the unfolded protein response (UPR) pathway. Thus, ER possesses stress-sensing molecules, which regulate the amount of protein taken up for folding. This is because UPR delays the protein folding process, until the protein folding capabilities of the ER would be replenished (Harding et al., 2002). The activation of the UPR pathway may lead to response from either of the two branches. The IRE1/ATF-6 branch directly regulates the ER folding by expressing genes that hold forth the ability of the ER to correctly fold the proteins. The other branch is represented by the kinases which cause a temporary halt in the translation process by phosphorylating and thereby inactivating the translation initiation factor, eIF2α. The two branches of the UPR converge to maintain homeostasis; a counterattack to any stress forced upon the ER (Harding et al., 2002). One of these stresses is virus infection. Viruses require eIF-2 for the production of its own

proteins (Liu et al., 2004). However, the phosphorylation of eIF-2 at the α subunit prevents the conversion between guanosine triphosphate (GTP) and guanosine diphosphate (GDP). This further inhibits the recycling process to maintain the production of active eIF-2 for the recruitment of tRNA to the 40S ribosome (Mohr, 2006). Being dependent on the host cell machinery for its life processes, viruses rely on the ER for their protein folding. This creates a stressful condition within the ER where the ER is loaded with a lot of proteins for proper folding, the cellular plus the viral proteins, thus leading to the activation of UPR (Harding et al., 2002). Protein kinase R (PKR) is a component of the UPR that phosphorylates eIF2α. In the early infection stage, HSV-1 shuts off the host gene expression, limiting the load of cellular proteins entering the ER for folding (Harding et al., 2002). Also, products of viral genes Us11 and $\gamma_1$34.5 are able to alleviate the phosphorylation on eIF2α to continue the production of proteins (He et al., 1997; Novoa et al., 2001). It is important to note that Us11 and $\gamma_1$34.5 mutants of HSV-1 can resist acute ER stress, shedding light on the possibility of other mechanisms for blocking the UPR (Mulvey et al., 2006). Thus, the importance of PERK (PKR-like endoplasmic reticulum kinase) in the resistance of UPR was established (Mulvey et al., 2007). HSV-1 uses its gB to accumulate viral polypeptides inside the host cell. The glycoprotein gB of HSV-1 was found to interact with the luminal domain of PERK, the domain that is responsible for recognizing ER stress. A possible mechanism suggested by Mulvey et al. (2007) for the interaction of gB with PERK is similar to the interaction of gB with the MHC-II to disrupt the processing of proteins in the infected cells. The luminal domains in IRE1 and PERK are alike, and both sense the unfolded proteins by the formation of oligomers in these domains (Harding et al., 1999; Bertolotti et al., 2000). These oligomers in PERK create a groove which resembles the peptide binding groove of the major histocompatibility complex (MHC) (Credle et al., 2005). Since gB has an affinity for such a groove in the MHC-II, which it uses to disable the protein processing pathway (Sievers et al., 2002; Neumann et al., 2003), it is possible that gB interacts with the luminal side of PERK in the same way and blocks the ability of PERK to perceive ER stress. PERK remains inactive during HSV-1 infection (Mulvey et al., 2007).

Herpes Simplex Virus Remodels the Endoplasmic Reticulum–Golgi Structure for Its Survival

Viruses are capable of modifying the membranes of the cellular organelles in the host (Suhy et al., 2000; Tolonen et al., 2001; Egger et al., 2002). There are mainly two reasons for them to remodel the host cellular organelle membrane. Firstly, viruses that replicate in the cytoplasm of the cell require these modified membranes to make compartments. These compartments are called *replication factories* that assist the synchronized gathering of the viral and cellular components for proficient virus replication and assembly. Secondly, the viruses alter the membranes to create a barrier in order to hide from the cellular immune responses (Suhy et al., 2000; Tolonen et al., 2001; Egger et al., 2002). Although not much is known about the membrane remodeling by HSV-1, the Golgi apparatus (GA) and the *trans*-Golgi network (TGN) have been discovered to be dispersed throughout the cytoplasm in the HSV-1-infected cells (Campadelli et al., 1993). ER is not only involved in protein synthesis but also imparts functionality to the protein by folding it in a correct conformation. It is then the ER which provides the virus with the final products of its genes, the proteins that help the virus establish pathogenesis (Romero-Brey and Bartenschlager, 2016). HSV-1 uses its viral protein UL34 to intensely alter the global ER edifice in order to enter the nucleus for replication (Maeda et al., 2017). The entire ER architecture, along with viral factor UL34 and host membrane protein CD98 heavy chain (CD98hc), was found compressed around the nuclear membrane (NM). UL34 is a component of the HSV–egress complex which is involved in the egress mechanism known as the vesicle-mediated nucleocytoplasmic transport (Roller et al., 2000; Reynolds et al., 2001; Mettenleiter et al., 2013). According to this proposed mechanism, HSV acquires a primary envelopment during egress from the inner NM (INM), de-envelops at the outer NM (ONM), which is fusion with the ONM, to expose into the cytoplasm (Johnson and Baines, 2011; Mettenleiter et al., 2013). UL34 along with UL31 helps in the envelopment process and the compression of the ER around the NM. CD98hc is a cell surface glycoprotein that serves as an amino acid transporter by associating with one of the light chains (Verrey et al., 2004). It associates with integrin β1 and β3 to regulate integrin signaling and hence cell adhesion and migration (Fenczik et al., 1997; Feral et al., 2005; Prager et al., 2007). CD98hc, like UL34 in HSV, is involved in the fusion process of other enveloped viruses such as the Newcastle disease virus, parainfluenza virus type-2, and HIV (Ito et al., 1992; Ohgimoto et al., 1995; Okamoto et al., 1997). Despite being a membrane glycoprotein, CD98hc retention at the plasma membrane (PM) is inhibited by HSV components, causing the accumulation of CD98hc in the ER. UL34 induces the compression of ER around the NM, bringing the CD98hc along with it (Maeda et al., 2017). It can be inferred that the remodeling of the ER by the virus is done to build up an environment of fusion molecules around the NM for efficient egress of HSV. Since the ER–Golgi network is continuous, the GA is also transformed post-HSV infection.

The GA works hand in hand with the ER to modify the proteins to be secreted outside the cells (**Figure 2**). Therefore, the membrane of GA is an extension of the ER membrane for efficient transport of proteins from the GA to the periphery of the cells (Bauerfeind and Huttner, 1993). As mentioned above, HSV-1, apart from remodeling the ER for its own needs, also disturbs the Golgi integrity (Campadelli et al., 1993). Martin et al. (2017) observed that two players in GA integrity, Src tyrosine kinase and dynamin 2 (Dyn2) GTPase, mediate the disturbance of GA structure post-HSV-1 infection in primary neuronal cells. HSV-1-infected primary neuronal cells depicted activated Src kinase and subsequent phosphorylation of its substrate dynactin 2 to reveal perturbation in the GA structural integrity. This distortion in the organelle structure could be an evidence for the HSV neuropathogenesis through the destruction of the secretory system. Src (pronounced as "sarc" for the

short form of sarcoma) protein kinases are non-receptor kinases involved in oncogenesis. They play major roles in cell growth, division, migration, and survival pathways (Roskoski, 2015). Src tyrosine kinases are themselves activated by phosphorylation at Y424 residue and phosphorylates its substrate Dyn2 at the residues Y231 and Y597 (Weller et al., 2010). Phosphorylation of Dyn2 activates its GTPase activity (Cao et al., 2010). The GTPase activity of Dyn2 controls the fragmentation of GA and the TGN during the secretory processes (Ishida et al., 2011). Continued activation of Src kinase and Dyn 2 have been known to disturb the integrity of GA in other cell types as well (Weller et al., 2010). Martin et al. (2017) demonstrated that the viral tegument protein VP11/12 of HSV-1 is not crucial but a partial contributor to the activation of Dyn2 through Src kinases, leading to degradation of the GA during HSV-1 multiplication in the primary neurons.

There are two possible propositions to the mechanism of Src activation in the HSV-1-infected neurons. One possibility is activation through direct HSV interaction with the cellular receptors. As known with other herpesviruses, gH/gL gps initiate the entry process by interacting with αvβ8 integrin and require activated Dyn2 for the same (Gianni et al., 2010). Dyn2 physically interacts with focal adhesion kinase (FAK) to be recruited to the focal adhesion sites. Here, Dyn2 is activated by Src and promotes the induction of endocytosis of the integrins, thus, easing the invasion of the cells (Wang et al., 2011). Another possible mechanism for Src activation is the interaction of the viral proteins with Src, after the entry of HSV. The SH2 domain of the Src is bound by the VP11/12 tyrosine motifs to stimulate the phosphoinositide 3-kinase (PI3K)/AKT pathway in the T cells (Strunk et al., 2016). Therefore, VP11/12 may activate Src kinases post-virus entry in neuronal cells as well, although Src activation through other mechanisms is possible.

The Endoplasmic Reticulum–Golgi Network as the Carriage for the Transport of Herpes Simplex Virus

Different courses of nuclear egress have been proposed through the years. According to one of those proposed routes, fusion at the ONM is quite a popular one. Fusion at the ONM is supported by the evidences of primary envelopment at the INM, succeeded by de-envelopment or fusion at the ONM. This fusion or the de-envelopment process, where the primary envelop fuses with the ONM, requires gH/gL of the HSV. However, enveloped virions were observed in the cytoplasm as well as the extracellular space in gH/gL deleted mutants, suggesting that there are other departure routes of the HSV from the cell. Wild et al. (2018) remarked that HSV exploits the ER–Golgi transport system of the cell for egress from the NM to the PM and out of the cell. In natural circumstances, the freight is transported from the ER to the GA *via* vesicles budding out of the ER exit positions (Bonifacino and Glick, 2004) or through an ER–Golgi intermediate compartment (EGIC) (Hauri and Schweizer, 1992; Klumperman, 2000; Saraste et al., 2009). In the cisternae of the GA, the freight is parceled in granules to be released outside the cell (Palade, 1975) (**Figure 2**). The packaging process results in a loss of the GA membrane, but the GA has multiple ways of replenishing it (Orci et al., 1981). After HSV replication and capsid assembly in the host nucleus, the capsids are sent to the GA for the acquisition of the tegument and envelope. The enveloped virion is then covered into a transport vacuole. This enclosing procedure is known as *wrapping* (Roizman et al., 2014). When HSV-1-infected cells were observed between 8 and 16 h post-infection (hpi), the membranes of the GA, ER, and ONM were connected to establish a continuum between the perinuclear space (PNS) and the Golgi cisternae (**Figure 2**). The number of virions in the ER was increased to almost four times by the end of 24 hpi after which the GA was degraded (Wild et al., 2015). Therefore, GA integrity is important for the transport of virions out of the ER. The path of HSV transport is similar to the transport of secretory proteins out of the cell, which is through vesicle formation or EGIC (Klumperman, 2000). Also, the intraluminally transported virions are coated with a dense proteinaceous layer. The layer may be used as a protection against the fusion of the viral membrane with the transport organelle membranes, thus strengthening the possibility of an alternative route for HSV egress. The translation of HSV proteins is an important step before the packaging of viral particles. Ribosomes, being a part of the RER and site of viral translation, are also manipulated by HSV for its pathogenesis.

RIBOSOMES

The Role of the Ribosomal and Viral Proteins in Herpes Simplex Virus Translation

Ribosome is the cellular factory for the production of proteins; a process known as "translation" in the central dogma. It contains ribosomal RNAs (rRNAs) that catalyze the peptide bond formation between the amino acids and ribosomal proteins (RPs) to regulate the translation process. The formation of ribosomes in eukaryotes (80S) takes place in the nucleolus. The eukaryotic 80S ribosome is composed of a small subunit (40S) and a large subunit (60S). The 40S subunit, known for decoding the mRNA for the incorporation of the appropriate amino acid, is made up of the 18S rRNA and 33 RPs. The 5S, 5.8S, and the 28S rRNA along with around 47 RPs assemble into the 60S subunit that catalyzes the peptide bond formation. Therefore, the eukaryotic ribosome is composed of four rRNAs and about 80 RPs (Wilson and Doudna Cate, 2012). RPs, such large in numbers, function as chaperones to stabilize and facilitate the correct folding of the rRNAs for ribosomal assembly (Fromont-Racine et al., 2003). The RPs are also important in the regulation of cell proliferation, cell cycle, apoptosis, tumorigenesis, development, and genome integrity (Chen and Ioannou, 1999; Bhavsar et al., 2010; De Las Heras-Rubio et al., 2014; Xu et al., 2016). During some viral infections, such as those with herpesviruses, the translation of cellular mRNA transcripts may be halted or remarkably decreased, whereas that of RP mRNAs are increased and persisted late to sustain the propagation of virus (Greco et al., 1997;

Simonin et al., 1997). L22, an RP, has been known to interact with infected cell protein 4 (ICP4). The ICP4 protein of HSV-1 is an immediate early protein and a transcription regulator of many of the early and the late HSV-1 genes required for the synthesis of viral DNA and increasing pathogenesis in the host (Leopardi and Roizman, 1996; Li, 2019).

Initiation of translation of the mRNA transcripts to proteins requires the recruitment of the cap binding complex eukaryotic initiation factor 4F (eIF4F), which is composed of eIF4E, eIF4G, eIF4A, eIF4B, and eIF4H, to the 5′m7G-cap of the mRNA. eIF4G in the bound state staffs the assembly of the 43S preinitiation complex. The pre-initiation complex which mainly constitutes the 40S ribosomal subunit moves over the 5′ untranslated region (UTR) to trace the start codon. The joining of the 60S ribosomal subunit to the pre-initiation complex creates a functionally active 80S ribosome, ready for translation (Jackson et al., 2010). Like other biological processes, HSV is dependent on the translation machinery of the host for the translation of around 70 encoded proteins. Therefore, it would always try and make the translation process more efficient and unhindered through a number of strategies (Smith et al., 2008; Walsh and Mohr, 2011). One such strategy is the enhancement of the translation initiation by increased assembly of the cap binding complex. The ICP6, ICP27, and the HSV Ser/Thr kinase US3 are the three proteins responsible for the improved assembly of the cap binding complex (Walsh and Mohr, 2004; Hargett et al., 2005; Walsh and Mohr, 2006; Chuluunbaatar et al., 2010). For efficient translation of its own proteins, HSV may paralyze the host cellular gene expression such that more of its mRNA transcripts gain access to the translation machinery. HSV encodes the virion host shutoff (vhs) protein which acts as an endonuclease and is an mRNA-specific destructor. Vhs is essential for the translation of late mRNAs of HSV-1 (Dauber et al., 2014) (**Figure 3**). It is encoded by the UL41 gene and is a tegument protein. Vhs destabilizes the cellular mRNAs by associating with helicase and helicase cofactors (Doepker et al., 2004; Feng et al., 2005; Page and Read, 2010; Read, 2013; Shiflett and Read, 2013). The mRNA degradation is assisted by the cellular RNase, XrnI (Gaglia et al., 2012). Vhs-mediated mRNA destruction achieves two goals for the virus at the same time. Firstly, it reduces the competition among the mRNA transcripts to be translated by the host translation machinery and, secondly, cripples the antiviral immune response of the host (Paladino and Mossman, 2009). Although it might seem odd, vhs destabilizes viral mRNAs as well (Read, 2013). Such destabilizations are vital for the shifts between the immediate early, early, leaky late, and true-late HSV gene expression, so that the competition for the accessibility toward the translation apparatus is further reduced. Nevertheless, the translation of the true-late mRNA transcripts, US11, UL47, and gC, was impaired in vhs-deficient HSV-1-infected Hela cells. The levels of US11 could be restored if the US11 late-mRNA transcripts are present before the ribosomes and the factors required for translation become limiting. These results suggest that in the absence of vhs, the translation machinery is overwhelmed with mRNAs of both the host and HSV and will not translate the mRNAs that have entered later that is the mRNAs of late-viral genes (Dauber et al., 2014). Our cell, however, has its own mechanism of "self-clearance" of these viral proteins, which is housed by the lysosomes of the cell.

LYSOSOMES

Importance of "Self-Clearance" in Cytoprotection

Lysosomes are intracellular membrane-bound compartments that contain digestive enzymes for the degradation of unwanted contents in the cytoplasm such as toxic, defective, or excess proteins, bacteria, and viruses. This degradation process is called *autophagy* and is triggered in response to a pathogen attack, starvation, stress, and hypoxia, with more than 35 proteins (ATG) directing the process. This way, autophagy by lysosomes is a mechanism of cleansing of the cell to increase its longevity. The steps in autophagy can be chronologically stated as: (1) phagophore initiation; (2) elongation of the membrane; (3) formation of the autophagosome; (4) fusion of the autophagosome with the hydrolytic enzymes in the lysosome (Mizushima et al., 2011). The targets of autophagy are selected depending upon the selective receptors expressed on the phagophore. These receptors have ubiquitin binding domain (UBD) to interact with the ubiquitin tags on the targets and LC3-interacting region (LIR) motif that interacts with the LC3 proteins (Stolz et al., 2014). Tank-binding kinase 1 (TBK1) is a regulator of autophagy and is instrumental in the destruction of pathogens by the lysosome (Wild et al., 2011; Pilli et al., 2012; Sparrer et al., 2017). In case of a viral attack, the process of autophagy could be modulated by the virus for its own survival or can be simply evaded by the expression of specific proteins by the virus. The virus needs to avoid the autophagic process when autophagy is protective to the cell in various ways. The cytoprotective strategies of autophagy are: targeting pathogens for destruction, promoting and/or regulating inflammation, promoting antigen presentation, and spreading protection *via* autophagy to the neighboring cells (Levine, 2005; Levine et al., 2011; Jackson, 2015; Paul and Münz, 2016). HSV-1 is such a virus that inhibits the protective effects of autophagy. Primary neuronal cells in mice choose autophagy over interferon-mediated antiviral effects to eliminate the virus (Yordy et al., 2012). HSV-1 inhibits autophagy by the action of US11 and ICP34.5 proteins (**Figure 4**). US11 dephosphorylates PKR and inhibits the phosphorylation of eIF2α; phosphorylated eIF2α being the inducer of autophagy (Lussignol et al., 2013). ICP34.5 interacts with beclin-1 and inhibits autophagy (Orvedahl et al., 2007).

Autophagy can allow the cell to survive for longer periods of time by obstructing pathogenesis. Mouse mutant cells having high basal autophagy levels restricted HSV-1 replication (Le Sage and Banfield, 2012). Moreover, evidence shows that drugs that induce autophagy are capable of reducing viral loads. MG132 is one such inducer that can decrease the HSV-1 titers in human corneal epithelial cells (Yakoub and Shukla, 2015). Similarly, rapamycin could restrict the pathogenesis of HSV-1 in human fibroblast cells and promote the survival of the

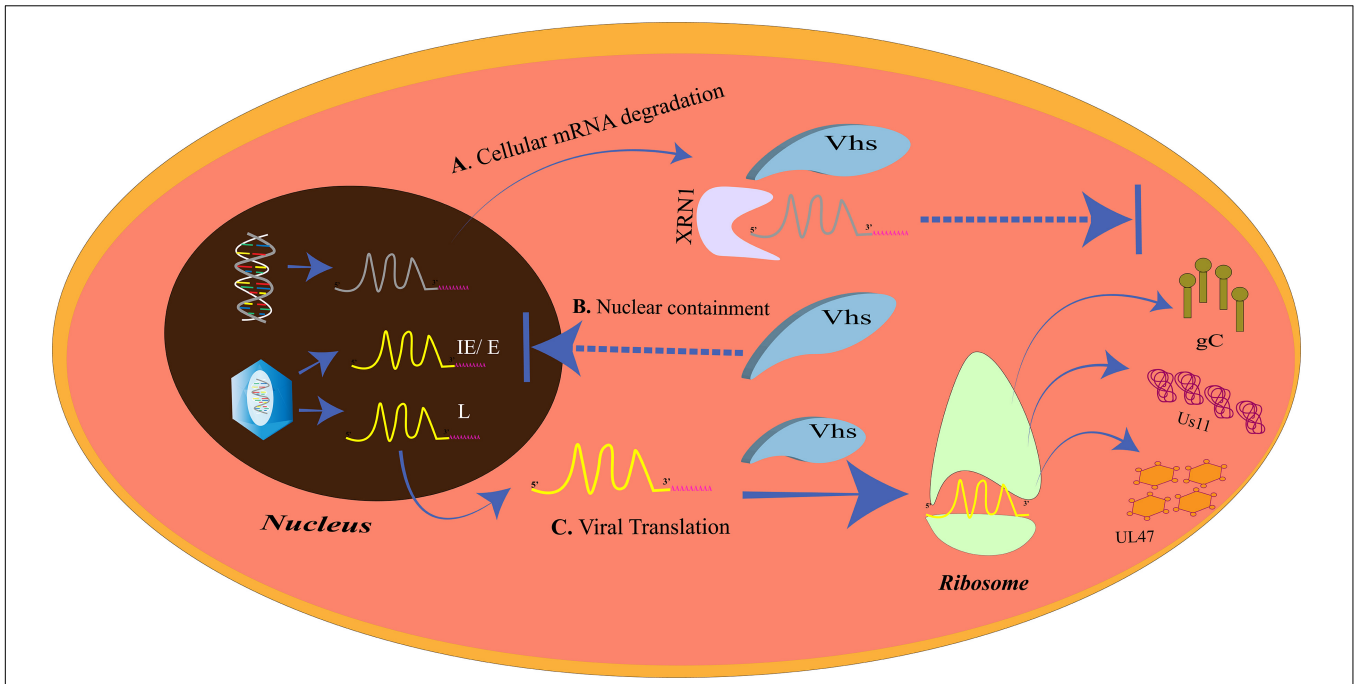

FIGURE 3 | The virion host shutoff (vhs)-mediated translational regulation. **(A)** *Cellular mRNA degradation*. The vhs protein triggers the degradation of the cellular mRNAs by XRN1. **(B)** *Nuclear containment*. Vhs also prevents the mRNA overloading at the ribosomes at the time of late gene expression by restricting the IE/E viral mRNAs in the nucleus. **(C)** *Viral translation*. Cellular mRNA degradation and nuclear containment of other IE/E mRNAs allows only the late viral mRNAs to exit the nucleus and be translated at the ribosomes. The late gene proteins, gC, Us11, and UL47, inhibit the host immune complement system, prevent autophagy, and promote nuclear egress, respectively.

cells (Ahmad et al., 2019). The protective autophagic effect in the cells with HSV-1 infection has been attributed to TBK-1. TBK-1 is a cellular kinase that phosphorylates and activates the selective receptors on the phagophore for the selective targeting of the cargo to be carried to the lysosome for destruction by the hydrolytic enzymes (Ahmad et al., 2019). Antiviral responses such as those from interferon (IFN)γ are significantly reduced when the MHC-II antigen presentation is reduced. Autophagy can allow HSV-1 antigens to be cross-presented to MHC-I. Studies have shown that the HSV-1 gB could be cross-presented on MHC-I of the BMA3.1A7 macrophage in an autophagy-dependent fashion (English et al., 2009; Radtke et al., 2013). Also, cells infected with HSV-1 could be induced to show autophagic effects *via* TBK-1-mediated paracrine signaling. The paracrine-mediated autophagy occurs early in the HSV-1 infection and protects the infected cell from dying (Ahmad et al., 2019). Another mechanism of viral clearance is the programmed death of the cell to destroy itself and the pathogen within it to restrict the viral spread.

MITOCHONDRIA

Herpes Simplex Virus Manipulates the "Power House" of the Cell

Another cellular organelle that may share a common membrane with the ER is mitochondria. Mitochondria, known as "*the power house of the cell*" as they are the main compartments for the production of ATPs, are dispersed throughout the cytoplasm of the cell. Mitochondrion has its own genome, replication equipment, and transcription/translation machinery but is also dependent on the nuclear genes, without the expression of which it cannot function actively. Also, if the mitochondria fail, the cell cannot survive. This is because apart from energy synthesis, mitochondria are involved in a number of cell processes such as apoptosis and regulation of calcium levels, which affect the survival of the cell. Hence, the mitochondrial changes induced by a viral attack are critical for the cell (Murata et al., 2000).

Maintenance and Exploitation of Mitochondria Until Mid-Herpes Simplex Virus Infection, Followed by Its Degradation at the Later Stages

Herpes simplex viruse infection of the cell has been known to degrade the mitochondrial DNA (mtDNA) rapidly and completely by an HSV nuclease, UL12 gene product (Saffran et al., 2007). This is in compliance with the early findings where the production of mitochondrial proteins decreased by 60% in HSV-infected cells when compared to the uninfected cells (Lund and Ziola, 1986; Latchman, 1988). In another study, the mitochondrial damage has been associated with encephalitis caused by HSV infection. Neuronal cells have confirmed the severe destruction of mitochondrial mRNA transcripts and mtDNA through the pUL12.5 or US3 viral proteins of HSV

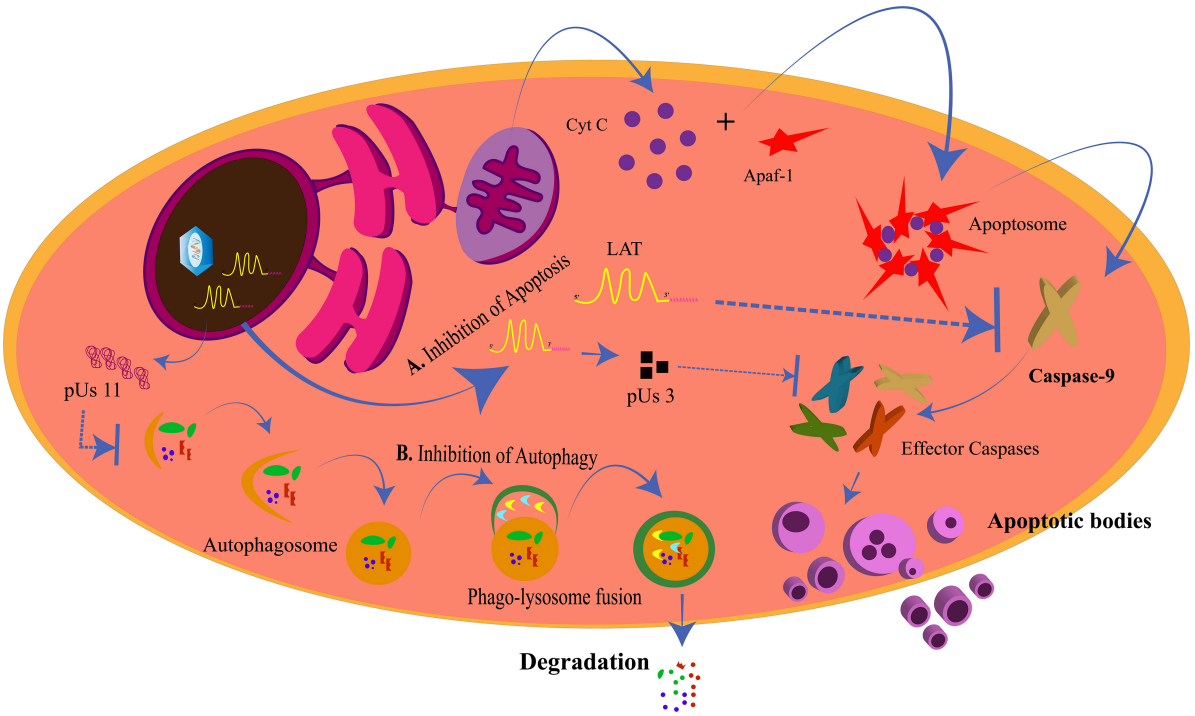

FIGURE 4 | Inhibition of apoptosis and autophagy by herpes simplex virus (HSV). **(A)** *Inhibition of Apoptosis*. The intrinsic apoptotic pathway for the programmed death of a cell is generated from the mitochondria when cytochrome C is released and forms the apoptosome along with Apaf-1 and other proteins. This allows for the activation of caspase-9 and the other effector caspases to generate the apoptotic bodies. LAT and pUs 3 block the activation of caspase-9 and the effector caspases, respectively, to prevent the cell from dying for its own survival. **(B)** *Inhibition of Autophagy*. pUs 11 inhibits the process of autophagy through which the enzymes from the lysosomes degrade the viral proteins, hence inhibiting viral clearance from the cell.

(Wnêk et al., 2016). The cytochrome C oxidase (CO), the last enzyme in the electron transport chain, was markedly decreased in astrocytes at 24 hpi (Wnêk et al., 2016). Murata et al. (2000) found that the mitochondria gathered around the nucleus along with the tegument proteins UL41 and UL46, post-HSV infection. HSP60, a protein responsive to stress, was found elevated in such conditions. ATP and lactate levels in the cells were maintained up to 6 hpi but decreased later on, which indicates that mitochondria are responsive to HSV infection. They migrate with the tegument proteins to the PNS, forming a ring-like structure around one side of the nucleus, functioning optimally until the mid-infection stage after which the mitochondrial integrity decreases. The presence of mitochondria in its condensed state around the nucleus, where the mitochondria are highly active for respiration, is essential when the HSV morphogenesis is under process, so that the morphogenesis process is provided with an ample supply of energy *via* ATP (Murata et al., 2000).

Modulation of Apoptosis by Herpes Simplex Virus

Mitochondria are involved in the process of apoptosis. Programmed cell death or apoptosis is critical for the cell as it decides the fate of the cell. The process is well-defined and causes the destruction of cells to promote development or inhibit the spread of an infection or growth of a cancerous tissue. Cells undergoing apoptosis are distinguished by shrinkage, formation of apoptotic bodies, and nuclear fragmentation (Wyllie, 1997). The two pathways of apoptosis, the intrinsic and the extrinsic pathways, converge at the activation of cysteine-specific aspartate protease (caspase) enzymatic pathway causing proteolysis and ultimately death of the cell (Galluzzi et al., 2012). The *intrinsic pathway* is so called due to the involvement of the cell's own component, the mitochondria. The mitochondrial pathway is initiated with the triggering of the mitochondrial outer membrane permeabilization (MOMP). This allows the exit of the cytochrome C from the inner mitochondrial membrane to the cytoplasm through the pores in the mitochondrial membrane. The apoptotic pathway is regulated by the members of the Bcl-2 protein family. Cytochrome C binds to Apaf-1 to initiate the apoptosome assembly. The apoptosome recruits procaspase-9. Procaspase-9 is cleaved to generate the active caspase-9. Thus, the caspase cascade is triggered with the subsequent activation of the other caspases for complete destruction of the cell (Yuan and Akey, 2013; Yuan et al., 2013; Jiang, 2014). PERK, which is an ER stress responsive protein, is also a contributor to the intrinsic apoptotic pathway (Verma and Datta, 2012). Apoptosis of virus-infected cells restricts replication and transmission of the viruses. Hence, HSV tries to inhibit apoptosis in the infected cells (**Figure 4**). The anti-apoptotic proteins of HSV are US3, gJ, and latency-associated transcript (LAT). The LAT is transcribed and spliced during HSV latency and is an inhibitor of apoptosis

in the infected cells (Wagner et al., 1988; Jones, 2013). It inhibits caspase 8/9-mediated apoptosis (Henderson et al., 2002) by the maintenance of phosphorylated levels of AKT, which in turn phosphorylates to inactivate the pro-apoptotic proteins (Bad, Bax, caspase 9) (Liu and Cohen, 2015). The LAT gene is 8.3 kb of which the initial 1.5 kb transcribes into two small RNAs of 62 and 36 nucleotides, those that are responsible for the anti-apoptotic effects of LAT (Shen et al., 2009). On one hand, where LAT is capable of preventing apoptosis even when the other HSV-1 genes are absent (Carpenter et al., 2007), ICP22 is not a very strong anti-apoptotic protein. ICP22 is a regulator of the expression of the anti-apoptotic genes of HSV-1 and does not directly interfere with the apoptotic signaling (Aubert et al., 2008). ICP22 inhibits the pro-apoptotic functions of p53 by alleviating the inhibitions on Bax (Pietsch et al., 2008). The C-terminus of ICP27 is also an indirect inducer of anti-apoptotic effects, increasing the anti-apoptotic gene expressions (Fontaine-Rodriguez and Knipe, 2008) and also promoting the activation of nuclear factor (NF)κB, encouraging cell survival (Hargett et al., 2006). US3 protein kinase is another direct inhibitor of procaspase 3, impeding the mitochondria-mediated apoptotic pathway (Benetti and Roizman, 2007). The viral protein US3 is also involved in the egress of HSV from the nucleus. The nucleus being the "brain of the cell" is one of the major target organelles for the virus.

NUCLEUS

Temporal Retention of the Herpes Simplex Virus Genes to Avoid Load on the Host Machinery

Nucleus is the compartment for cellular and viral genome replication as well as the transcription of mRNA from the genetic information. Since the genetic code for all life processes is contained in the nucleus, the nucleus is also known as the "information center" of the cell. The mRNA transcripts leave the nucleus when they are needed to be translated into proteins. Vhs, the HSV host shutoff protein responsible for cellular mRNA degradation, is also responsible for the retention of viral mRNAs in the nucleus (Elliott et al., 2018). Vhs causes the retention of the IE and the E mRNA transcripts in the nucleus but allows the late transcripts to translocate to the cytoplasm. This occurs at the beginning of the late gene transcription. As a regulator of vhs, VP22 is able to release the vhs-induced nuclear retention on the late transcripts, to permit their translocation to the cytoplasm, so that the late proteins could be translated from them. HSV-1 checks the load of transcripts entering the translation machinery for the efficient progression of infection by not only restricting the cellular mRNAs but also its own mRNAs (Pheasant et al., 2018).

The Nuclear Envelope Disruption Model for Herpes Simplex Virus Egress

The nuclear envelope (NE) serves as a barrier for the viruses; the second gateway for the HSV to pass through (**Figure 5**). The NE of the nucleus is divided into three regions: the ONM, the PNS, and the INM. The gap between the ONM and the INM is the PNS with a diameter of 20–50 nm and is continuous with the ER. The PNS is spanned by the nuclear pore complexes (NPCs) connecting the nucleus to the cytoplasm (Stewart et al., 2007). Assembly of the HSV-1 capsids takes place in the nucleus. After assembly, it is either transported to the PNS and buds off at the ONM or impairs the nuclear pore (protein channels) to create distortions in the NE to exit the nucleus (Leuzinger et al., 2005; Wild et al., 2005). Beneath the INM, toward the nucleoplasm, is the nuclear lamina. The function of the nuclear lamina is to provide structural sustenance to the NE, hence, it is made up of an assembly of lamin A/C/B along with the membrane proteins. The HSV nucleocapsids, being larger in size (120–130 nm in diameter) than the lamin network (with spacing of about 15 nm) or nuclear pores (with a diameter of about 38 nm), need a different mechanism to modify the lamina and the NE to exit from the nucleus (Alber et al., 2007; Goldberg et al., 2008; Lee and Chen, 2010). One such mechanism is the interaction of the nuclear HSV egress complex (pUL31 and pUL34) with lamin to disrupt the further associations between the lamins (Reynolds et al., 2004). Another mechanism is the hyperphosphorylation of emerin, a membrane protein. PKC-δ and US3 hyperphosphorylate the emerin to disturb its interaction with the lamins (Leach et al., 2007; Morris et al., 2007). Although PKC-α, but not PKC-ζ, is also recruited to the NE after HSV-1 infection, PKC-α is not uniquely required for replication of HSV-1 (Leach and Roller, 2010). The US3 kinase is also involved in the alterations of the nuclear pore for virus egress. Wild et al. (2019) demonstrated the role of US3 in nuclear pore impairment post-HSV infection. Confocal super resolution microscopy and cryo-field emission showed significant loss of nuclear pores in HSV-infected cells, and this extreme decrement was not observed in US3-deleted variants of HSV. Moreover, the maximum numbers of capsids were retained in the nucleus in US3-deleted mutants and very minimum were observed in the cytosol, whereas the opposite scenario was observed in the wild-type HSV-1 infection. Thus, it was concluded that US3 is vital in damaging the nuclear pore of the host nucleus for the egress of HSV (Wild et al., 2019).

The Nuclear Membrane Fusion Model for Herpes Simplex Virus Egress

According to an alternative route for nuclear egress, HSV leaves the nucleus *via* the membrane fusion mechanism (**Figure 5**). There are two steps according to the fusion model:

(1) *Primary envelopment*, where the newly formed nucleocapsids bud from the INM. During this process, they acquire the membrane components of the INM and become enveloped. After budding, the enveloped HSV particles are present in the PNS. The NEC comprising the HSV protein products of the gene UL31 and UL34 assists the primary envelopment. Without the NEC, the nucleocapsids are retained in the nucleus (Reynolds et al., 2001). Other proteins encoded by the HSV may be recruited by the NEC to help them in the primary envelopment. HSV-1 encodes UL41 and ICP22 that were found to be co-localized with the NEC at the INM to assist the NEC by interacting with the proteins involved in HSV-1 nuclear

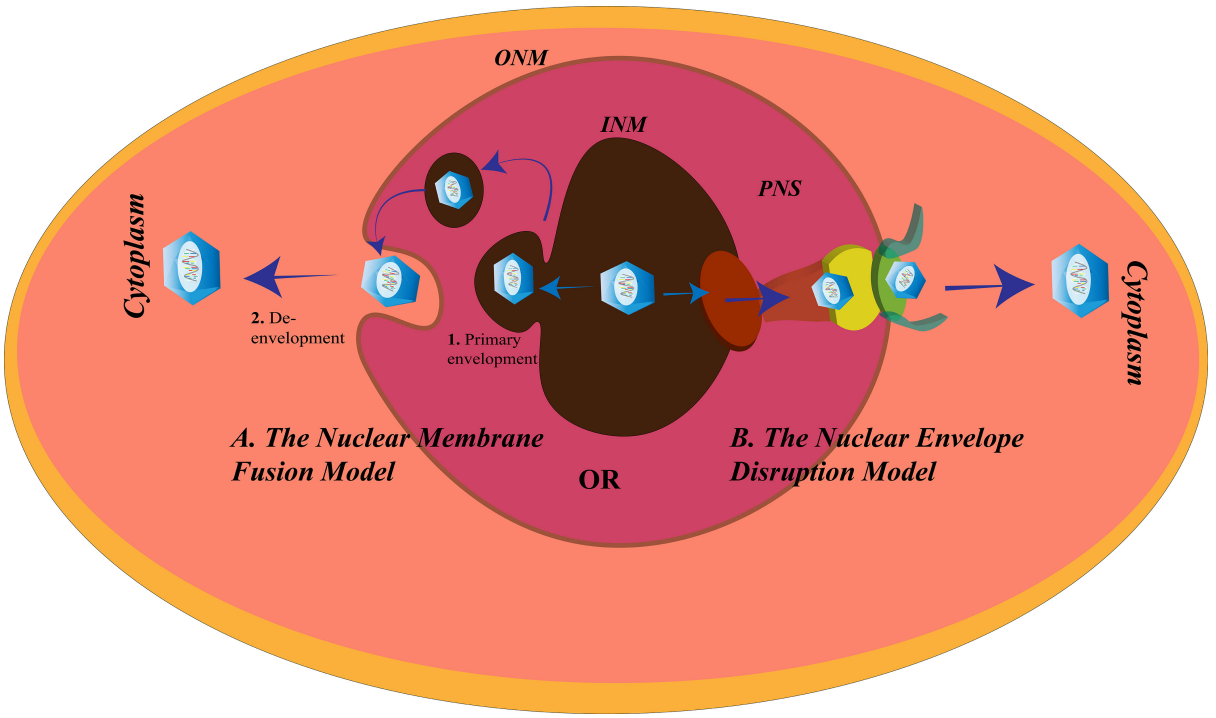

FIGURE 5 | Herpes simplex virus (HSV) nuclear egress. There are two proposed mechanisms for the exit of HSV from the nucleus of the cells. **(A)** *The nuclear membrane fusion model* in which the HSV nucleocapsid acquires the inner nuclear membrane (INM) envelope (1. Primary envelopment) and is released into the perinuclear space (PNS), followed by fusion of this acquired envelope with the outer NM (ONM) to allow the exit of the nucleocapsid from the nucleus and enter the cytoplasm (2. De- envelopment), and **(B)** *the nuclear envelope disruption model* in which the lamins underlying the INM are modified and the nuclear pore disrupted to make way for the exit of the HSV nucleocapsid into the cytoplasm.

egress (Liu et al., 2014; Maruzuru et al., 2014). UL16 and UL21 of HSV-2 are known to contribute to its primary envelopment (Le Sage et al., 2013; Gao et al., 2017).

(2) *De-envelopment*, where the HSV envelope fuses with the ONM to release the nucleocapsids into the cytoplasm. Like the fusion at the cell membrane, the fusion between the primary virions and ONM, involves glycoproteins. In the absence of gB and gH, HSV-1 fails to exit from the NE (Farnsworth et al., 2007). pUS3 mediated phosphorylation of pUL31, and gB is essential for the fusion process (Mou et al., 2009; Wisner et al., 2009). Also, recruitment of CD98hc, p32, and incorporation of β1 integrin to the membrane of the nucleus after HSV-1 infection is supportive of the fusion model (Hirohata et al., 2015; Liu et al., 2015). Failure to recruit any of these proteins causes accumulation of the virions in the PNS or vesicles derived from INM.

CONCLUSION

The entry of the virus into the host cells can be considered as the most important step in the HSV-1 infection cycle. This is because HSV-1 needs to enter the cell in order to begin its replicative cycle. Hence, small molecules, peptides, or nanoparticles that can block the HSV-1 entry into the cells might prove to be strong antiviral candidates. One such small molecule is epigallocatechin gallate that competitively inhibits the binding of HS to HSV-1 (Colpitts and Schang, 2014). Certain small, cationic peptides have been recognized as HSV-1 attachment inhibitors and block HSV-1 entry (Tiwari et al., 2011; Jose et al., 2013; Jaishankar et al., 2015). BX795, a TBK-1 inhibitor, lowers ocular HSV-1 infection by inhibiting the Akt pathway, ultimately blocking the HSV-1 protein synthesis. This kinase inhibitor is being considered at par with trifluorothymidine (TFT), which is the currently prescribed therapeutic for ocular herpes (Jaishankar et al., 2018). Yadavalli et al. (2019) have found activated carbon particles to be efficient acyclovir (ACV)-drug delivery systems that trapped the virions within themselves. Zinc oxide micro-nanoparticles and nanowires can inhibit HSV-1 entry as well (Antoine et al., 2012; Trigilio et al., 2012). Such nanowires can block HSV-1 cell-to-cell spread. With respect to the cytoskeleton remodeling by HSV-1, there have been inhibitors of the microtubule, such as nocodazole (Naranatt et al., 2005), but they have not proven to be much successful antivirals. It may also be brought to our attention that the complete trafficking process which leads to cancer has not yet been elucidated. High-resolution imaging such as atomic force microscopy (AFM) can reveal the ultrastructure of the tumors caused by HSV infection (Deng et al., 2018). This might shed some more light on the formation of tumors by the manipulation of the cytoskeleton by viruses. Autophagy in HSV-infected cells may impart protection to certain cell types by restricting the HSV load in these cells and allowing the cells to survive. Therefore,

HSV tries to inhibit autophagy. In neuronal cells, where HSV prefers to hide itself from the immune cell attacks from the host, autophagy-enhancing agents can be selected as the appropriate therapeutics for decreasing the HSV infection (Yakoub and Shukla, 2015; Ahmad et al., 2019). Similarly, HSV does not allow the cell to die through apoptosis, or else its only life support system would be destroyed. Hence, HSV puts in a lot of effort to inhibit apoptosis of the target cells. Inhibiting apoptosis is a very effective mechanism while establishing a latent infection (Jones, 2013). Therefore, a clarification of these anti-apoptotic effects of HSV can lead to the development of drugs that can promote cell death of the infected cells at the early stage of the infection, exposing HSV to the host immune attacks. Also, the cellular morphology is affected in post-HSV infection. Membrane-bound organelles such as ER and mitochondria are compressed around the nucleus for the proper recruitment and accessibility to the factors required for HSV egress. Thus, this review gives an idea about HSV–host cell interaction and how the knowledge of these interactions would help bridge the gaps in HSV research. It is evident that HSV, being a virus that has co-evolved with humans, is capable of exploiting the cellular organelles for increasing its pathogenesis. Whether it be the rearrangement of the organelle's membrane (cell membrane, ER–Golgi, mitochondria, nucleus) or inhibiting the counterattacks from the organelles (autophagy, apoptosis, ER stress), HSV successfully overpowers the host cell. Further investigations in unraveling these mechanisms deeper at the molecular level would open up new avenues in the discovery of drugs or vaccines against HSV that would be more effective than the present ones.

AUTHOR CONTRIBUTIONS

AB and AM conceptualized the review. AB wrote the article and made the figures. SK was involved in revision. AM edited and supervised the manuscript.

FUNDING

This work was supported by the Indian Council of Medical Research (ICMR), the Department of Biotechnology (DBT/JRF/15/AL/224), and the RAMANUJAN research grant (SB/S2/RJN-065/2015 SERB-DST, India) and the facilities provided by ICMR-National AIDS Research Institute.

REFERENCES

Agelidis, A. M., Hadigal, S. R., Jaishankar, D., and Shukla, D. (2017). Viral activation of heparanase drives pathogenesis of herpes simplex virus-1. *Cell Rep.* 20, 439–450. doi: 10.1016/j.celrep.2017.06.041

Agelidis, A. M., and Shukla, D. (2015). Cell entry mechanisms of HSV: What we have learned in recent years. *Future Virol.* 10, 1145–1154. doi: 10.2217/fvl.15.85

Ahmad, L., Mashbat, B., Leung, C., Brookes, C., Hamad, S., Krokowski, S., et al. (2019). Human TANK binding kinase 1 is required for early autophagy induction upon herpes simplex virus 1 infection. *J. Allergy Clin. Immunol.* 143, 765–769.e7. doi: 10.1016/j.jaci.2018.09.013

Alber, F., Dokudovskaya, S., Veenhoff, L. M., Zhang, W., Kipper, J., Devos, D., et al. (2007). The molecular architecture of the nuclear pore complex. *Nature* 450, 695–701.

Antoine, T. E., Mishra, Y. K., Trigilio, J., Tiwari, V., Adelung, R., and Shukla, D. (2012). Prophylactic, therapeutic and neutralizing effects of zinc oxide tetrapod structures against HSV type-2 infection. *Antiviral Res.* 96, 363–375. doi: 10.1016/j.antiviral.2012.09.020

Anzivino, E., Fioriti, D., Mischitelli, M., Bellizzi, A., Barucca, V., Chiarini, F., et al. (2009). HSV infection in pregnancy and in neonate: status of art of epidemiology, diagnosis, therapy and prevention. *Virol. J.* 6:40. doi: 10.1186/1743-422X-6-40

Atanasiu, D., Cairns, T. M., Whitbeck, J. C., Saw, W. T., Rao, S., Eisenberg, R. J., et al. (2013). Regulation of herpes simplex virus gB-induced cell-cell fusion by mutant forms of gH/gL in the absence of gD and cellular receptors. *mBio* 4:e00046-13. doi: 10.1128/mBio.00046-13

Aubert, M., Chen, Z., Lang, R., Dang, C. H., Fowler, C., Sloan, D. D., et al. (2008). The antiapoptotic herpes simplex virus glycoprotein J localizes to multiple cellular organelles and induces reactive oxygen species formation. *J. Virol.* 82, 617–629. doi: 10.1128/JVI.01341-07

Bauerfeind, R., and Huttner, W. B. (1993). Biogenesis of constitutive secretory vesicles, secretory granules and synaptic vesicles. *Curr. Opin. Cell Biol.* 5, 628–635. doi: 10.1016/0955-0674(93)90132-a

Benetti, L., and Roizman, B. (2007). In transduced cells, the US3 protein kinase of herpes simplex virus 1precludes activation and induction of apoptosis by transfected procaspase 3. *J. Virol.* 81, 10242–10248. doi: 10.1128/JVI.00820-07

Bertolotti, A., Zhang, Y., Hendershot, L. M., Harding, H. P., and Ron, D. (2000). Dynamic interaction of BiP and ER stress transducers in the unfolded protein response. *Nat. Cell Biol.* 2, 326–332. doi: 10.1038/35014014

Bhavsar, R. B., Makley, L. N., and Tsonis, P. A. (2010). The other lives of ribosomal proteins. *Hum. Genomics* 4, 327–344. doi: 10.1186/1479-7364-4-5-327

Bonifacino, J. S., and Glick, B. S. (2004). The mechanisms of vesicle budding and fusion. *Cell* 116, 153–166. doi: 10.1016/s0092-8674(03)01079-1

Campadelli, G., Brandimarti, R., Di Lazzaro, C., Ward, P. L., Roizman, B., and Torrisi, M. R. (1993). Fragmentation and dispersal of Golgi proteins and redistributionof glycoproteins and glycolipids processed through the Golgi apparatus after infection with herpes simplex virus 1. *Proc. Natl. Acad. Sci. U.S.A.* 90, 2798–2802. doi: 10.1073/pnas.90.7.2798

Campadelli-Fiume, G., Cocchi, F., Menotti, L., and Lopez, M. (2000). The novel receptors that mediate the entry of herpes simplex viruses and animal alphaherpesviruses into cells. *Rev. Med. Virol.* 10, 305–319. doi: 10.1002/1099-1654(200009/10)

Cao, H., Chen, J., Krueger, E. W., and McNiven, M. A. (2010). Src mediated phosphorylation of dynamin and cortactin regulates the "constitutive" endocytosis of transferrin. *Mol. Cell. Biol.* 30, 781–792. doi: 10.1128/MCB.00330-09

Carpenter, D., Hsiang, C., Brown, D. J., Jin, L., Osorio, N., BenMohamed, L., et al. (2007). Stable cell lines expressing high levels of the herpes simplex virus type 1 LAT are refractory to caspase 3 activation and DNA laddering following cold shock induced apoptosis. *Virology* 369, 12–18. doi: 10.1016/j.virol.2007.07.023

Chen, F. W., and Ioannou, Y. A. (1999). Ribosomal proteins in cell proliferation and apoptosis. *Int. Rev. Immunol.* 18, 429–448. doi: 10.3109/08830189909088492

Chuluunbaatar, U., Roller, R., Feldman, M. E., Brown, S., Shokat, K. M., and Mohr, I. (2010). Constitutive mTORC1 activation by a herpesvirus Akt surrogate stimulates mRNA translation and viral replication. *Genes Dev.* 24, 2627–2639. doi: 10.1101/gad.1978310

Clement, C., Tiwari, V., Scanlan, P. M., Valyi-Nagy, T., Yue, B. Y., and Shukla, D. (2006). A novel role for phagocytosis-like uptake in herpes simplex virus entry. *J. Cell Biol.* 174, 1009–1021. doi: 10.1083/jcb.200509155

Colpitts, C. C., and Schang, L. M. (2014). A small molecule inhibits virion attachment to heparan sulfate- or sialic acid-containing glycans. *J. Virol.* 88, 7806–7817. doi: 10.1128/JVI.00896-14

Connolly, S. A., Jackson, J. O., Jardetzky, T. S., and Longnecker, R. (2011). Fusing structure and function: a structural view of the herpesvirus entry machinery. *Nat. Rev. Microbiol.* 9, 369–381. doi: 10.1038/nrmicro2548

Conti, M. A., and Adelstein, R. S. (2008). Nonmuscle myosin II moves in new directions. *J. Cell Sci.* 121, 11–18. doi: 10.1242/jcs.007112

Credle, J. J., Finer-Moore, J. S., Papa, F. R., Stroud, R. M., and Walter, P. (2005). On the mechanism of sensing unfolded proteins in the endoplasmic reticulum. *Proc. Natl. Acad. Sci. U.S.A.* 102, 18773–18784. doi: 10.1073/pnas.0509487102

Dammermann, A., Desai, A., and Oegema, K. (2003). The minus end in sight. *Curr. Biol.* 13, R614–R624. doi: 10.1016/s0960-9822(03)00530-x

Dauber, B., Saffran, H. A., and Smiley, J. R. (2014). The herpes simplex virus 1 virion host shutoff protein enhances translation of viral late mRNAs by preventing mRNA overload. *J. Virol.* 88, 9624–9632. doi: 10.1128/JVI.01350-14

David, A. T., Baghian, A., Foster, T. P., Chouljenko, V. N., and Kousoulas, K. G. (2008). The HSV type 1 (HSV-1) glycoprotein K(gK) is essential for viral corneal spread and neuroinvasiveness. *Curr. Eye Res.* 33, 455-467. doi: 10.1080/02713680802130362

David, A. T., Saied, A., Charles, A., Subramanian, R., Chouljenko, V. N., and Kousoulas, K. G. (2012). A HSV 1 (McKrae) mutant lacking the glycoprotein K gene is unable to infect via neuronal axons and egress from neuronal cell bodies. *mBio* 3:e00144-12. doi: 10.1128/mBio.00144-12 ,

De Las Heras-Rubio, A., Perucho, L., Paciucci, R., Vilardell, J., and Leonart, M. E. (2014). Ribosomal proteins as novel players in tumorigenesis. *Cancer Metastasis Rev.* 33, 115–141. doi: 10.1007/s10555-013-9460-6

Deng, X., Xiong, F., Li, X., Xiang, B., Zheng, L., Wu, X., et al. (2018). Application of atomic force microscopy in cancer research. *J. Nanobiotechnol.* 16:102. doi: 10.1186/s12951-018-0428-0

Diefenbach, R. J., Miranda-Saksena, M., Douglas, M. W., and Cunningham, A. L. (2008). Transport and egress of herpes simplex virus in neurons. *Rev. Med. Virol.* 18, 35–51. doi: 10.1002/rmv.560

Doepker, R. C., Hsu, W.-L., Saffran, H. A., and Smiley, J. R. (2004). Herpes simplex virus virion host shutoff protein is stimulated by translation initiation factors eIF4B and eIF4H. *J. Virol.* 78, 4684–4699. doi: 10.1128/jvi.78.9.4684-4699.2004

Dohner, K., Nagel, C. H., and Sodeik, B. (2005). Viral stop-and-go along microtubules: taking a ride with dynein and kinesins. *Trends Microbiol.* 13, 320–327. doi: 10.1016/j.tim.2005.05.010

Douglas, M. W., Diefenbach, R. J., Homa, F. L., Miranda-Saxena, M., Rixon, F. J., Vittone, V., et al. (2004). Herpes simplex virus type 1 capsid protein VP26 interacts with dynein light chains RP3 and Tctex1 and plays a role in retrograde cellular transport. *J. Biol. Chem.* 279, 28522–28530. doi: 10.1074/jbc.M311671200

Egger, D., Wolk, B., Gosert, R., Bianchi, L., Blum, H. E., Moradpour, D., et al. (2002). Expression of hepatitis C virus proteins induces distinct membrane alterations including a candidate viral replication complex. *J. Virol.* 76, 5974–5984. doi: 10.1128/JVI.76.12.5974-5984.2002

Elliott, G., Pheasant, K., Ebert-Keel, K., Stylianou, J., Franklyn, A., and Jones, J. (2018). Multiple post-transcriptional strategies to regulate the herpes simplex virus type 1 vhs endoribonuclease. *J. Virol.* 92:e00818-18. doi: 10.1128/JVI.00818-18

English, L., Chemali, M., Duron, J., Rondeau, C., Laplante, A., Gingras, D., et al. (2009). Autophagy enhances the presentation of endogenous viral antigens on MHC class I molecules during HSV-1 infection. *Nat. Immunol.* 10, 480–487. doi: 10.1038/ni.1720

Fan, Q., Longnecker, R., and Connolly, S. A. (2014). Substitution of herpes simplex virus 1 entry glycoproteins with those of saimiriine herpesvirus 1 reveals a gD-gH/gL functional interaction and a region within the gD profusion domain that is critical for fusion. *J. Virol.* 88, 6470–6482. doi: 10.1128/JVI.00465-14

Farnsworth, A., and Johnson, D. C. (2006). HSV gE/gI must accumulate in the trans-Golgi network at early times and then redistribute to cell junctions to promote cell–cell spread. *J. Virol.* 80, 3167–3179. doi: 10.1128/JVI.80.7.3167-3179.2006

Farnsworth, A., Wisner, T. W., Webb, M., Roller, R., Cohen, G., Eisenberg, R., et al. (2007). Herpes simplex virus glycoproteins gB and gH function in fusion between the virion envelope and the outer nuclear membrane. *Proc. Natl. Acad. Sci. U.S.A.* 104, 10187–10192. doi: 10.1073/pnas.0703790104

Fatahzadeh, M., and Schwartz, R. A. (2007). Human HSV infections: epidemiology, pathogenesis, symptomatology, diagnosis, and management. *J. Am. Acad. Dermatol.* 57, 737–763. doi: 10.1016/j.jaad.2007.06.027

Feierbach, B., Piccinotti, S., Bisher, M., Denk, W., and Enquist, L. W. (2006). Alpha-herpesvirus infection induces the formation of nuclear actin filaments. *PLoS Pathog.* 2:e85. doi: 10.1371/journal.ppat.0020103

Fenczik, C. A., Sethi, T., Ramos, J. W., Hughes, P. E., and Ginsberg, M. H. (1997). Complementation of dominant suppression implicates CD98 in integrin activation. *Nature* 390, 81–85. doi: 10.1038/36349

Feng, P., Everly, D. N., and Read, G. S. (2005). mRNA decay during herpes simplex virus (HSV) infections: protein-protein interactions involving the HSV virion host shutoff protein and translation factors eIF4H and eIF4A. *J. Virol.* 79, 9651–9664. doi: 10.1128/JVI.79.15.9651-9664.2005

Feral, C. C., Nishiya, N., Fenczik, C. A., Stuhlmann, H., Slepak, M., and Ginsberg, M. H. (2005). CD98hc (SLC3A2) mediates integrin signaling. *Proc. Natl. Acad. Sci. U.S.A.* 102, 355–360. doi: 10.1073/pnas.0404852102

Fontaine-Rodriguez, E. C., and Knipe, D. M. (2008). Herpes simplex virus ICP27 increases translation of a subset of viral late mRNAs. *J. Virol.* 82, 3538–3545. doi: 10.1128/JVI.02395-07

Fromont-Racine, M., Senger, B., Saveanu, C., and Fasiolo, F. (2003). Ribosome assembly in eukaryotes. *Gene* 313, 17–42. doi: 10.1016/S0378-1119(03)00629-2

Gaglia, M. M., Covarrubias, S., Wong, W., and Glaunsinger, B. A. (2012). A common strategy for host RNA degradation by divergent viruses. *J. Virol.* 86, 9527–9530. doi: 10.1128/JVI.01230-12

Gallagher, J. R., Saw, W. T., Atanasiu, D., Lou, H., Eisenberg, R. J., and Cohen, G. H. (2013). Displacement of the C terminus of herpes simplex virus gD is sufficient to expose the fusion-activating interfaces on gD. *J. Virol.* 87, 12656–12666. doi: 10.1128/JVI.01727-13

Galluzzi, L., Kepp, O., and Kroemer, G. (2012). Mitochondria: master regulators of danger signalling. *Nat. Rev. Mol. Cell Biol.* 13, 780–788. doi: 10.1038/nrm3479

Gao, J., Hay, T. J. M., and Banfield, B. W. (2017). The product of the herpes simplex virus 2 UL16 gene is critical for the egress of capsids from the nuclei of infected cells. *J. Virol.* 91:e00350-17. doi: 10.1128/JVI.00350-17

Gianni, T., Gatta, V., and Campadelli-Fiume, G. (2010). αvβ3-integrin routes herpes simplex virus to an entry pathway dependent on cholesterol-rich lipid rafts and dynamin 2. *Proc. Natl. Acad. Sci. U.S.A.* 107, 22260–22265. doi: 10.1073/pnas.1014923108

Goldberg, M. W., Fiserova, J., Huttenlauch, I., and Stick, R. (2008). A new model for nuclear lamina organization. *Biochem. Soc. Trans.* 36, 1339–1343. doi: 10.1042/BST0361339

Greco, A., Laurent, A. M., and Madjar, J. J. (1997). Repression of beta-actin synthesis and persistence of ribosomal protein synthesis after infection of HeLa cells by herpes simplex virus type 1 infection are under translational control. *Mol. Gen. Genet.* 256, 320–327. doi: 10.1007/s004380050575

Hadigal, S. R., Agelidis, A. M., Karasneh, G. A., Antoine, T. E., Yakoub, A. M., Ramani, V. C., et al. (2015). Heparanase is a host enzyme required for HSV-1 release from cells. *Nat. Commun.* 6:6985. doi: 10.1038/ncomms7985

Harding, H. P., Calfon, M., Urano, F., Novoa, I., and Ron, D. (2002). Transcriptional and translational control in the mammalian unfolded protein response. *Annu. Rev. Cell Dev. Biol.* 18, 575–599. doi: 10.1146/annurev.cellbio.18.011402.160624

Harding, H. P., Zhang, Y., and Ron, D. (1999). Protein translation and folding are coupled by an endoplasmic-reticulum-resident kinase. *Nature* 397, 271–274. doi: 10.1038/16729

Hargett, D., McLean, T., and Bachenheimer, S. L. (2005). Herpes simplex virus ICP27 activation of stress kinases JNK and p38. *J. Virol.* 79, 8348–8360. doi: 10.1128/JVI.79.13.8348-8360.2005

Hargett, D., Rice, S., and Bachenheimer, S. L. (2006). Herpes simplex virus type 1 ICP27-dependent activation of NF-κB. *J. Virol.* 80, 10565–10578. doi: 10.1128/JVI.01119-06

Hauri, H. P., and Schweizer, A. (1992). The endoplasmic reticulum-Golgi intermediate compartment. *Curr. Opin. Cell Biol.* 4, 600–608. doi: 10.1016/0955-0674(92)90078-q

He, B., Gross, M., and Roizman, B. (1997). The γ134.5 protein of herpes simplex virus 1 complexes with protein phosphatase 1 alpha to dephosphorylate the alpha subunit of eukaryotic initiation factor 2 and preclude theshutoff of protein synthesis by double-stranded RNA-activated protein kinase. *Proc. Natl. Acad. Sci. U.S.A.* 94, 843–848. doi: 10.1073/pnas.94.3.843

Heldwein, E. E., and Krummenacher, C. (2008). Entry of herpesviruses into mammalian cells. *Cell. Mol. Life Sci.* 65, 1653–1668. doi: 10.1007/s00018-008-7570-z

Henderson, G., Peng, W., Jin, L., Perng, G.-C., Nesburn, B., Wechsler, S. L., et al. (2002). Regulation of caspase 8-and caspase 9-induced apoptosis by the herpes

simplex virus type 1 latency associated transcript. *J. Neurovirol.* 8, 103–111. doi: 10.1080/13550280290101085

Herpetic Eye Disease Study Group. (1998). Acyclovir for the prevention of recurrent herpes simplex virus eye disease. *N. Engl. J. Med.* 339, 300–306. doi: 10.1056/NEJM199807303390503

Hirohata, Y., Arii, J., Liu, Z., Shindo, K., Oyama, M., Kozuka-Hata, H., et al. (2015). Herpes simplex virus 1 recruits CD98 heavy chain and beta1 integrin to the nuclear membrane for Viral de-envelopment. *J. Virol.* 89, 7799–7812. doi: 10.1128/JVI.00741-15

Hoppe, S., Schelhaas, M., Jaeger, V., Liebig, T., Petermann, P., and Knebel-Mörsdorf, D. (2006). Early herpes simplex virus type 1 infection is dependent on regulated Rac1/Cdc42 signalling in epithelial MDCKII cells. *J. Gen. Virol.* 87, 3483–3494. doi: 10.1099/vir.0.82231-0

Howard, P. W., Howard, T. L., and Johnson, D. C. (2012). HSV membrane proteins gE/gI and US9 act cooperatively to promote transport of capsids and glycoproteins from neuron cell bodies into initial axon segments. *J. Virol.* 87, 403–414. doi: 10.1128/JVI.02465-12

Howard, P. W., Wright, C. C., Howard, T., and Johnson, D. C. (2014). HSV gE/gI Extracellular domains promote axonal transport and spread from neurons to epithelial cells. *J. Virol.* 88, 11178–11186. doi: 10.1128/JVI.01627-14

Ishida, N., Nakamura, Y., Tanabe, K., Li, S. A., and Takei, K. (2011). Dynamin 2 associates with microtubules at mitosis and regulates cell cycle progression. *Cell Struct. Funct.* 36, 145–154. doi: 10.1247/csf.10016

Ito, Y., Komada, H., Kusagawa, S., Tsurudome, M., Matsumura, H., Kawano, M., et al. (1992). Fusion regulation proteins on the cell surface: isolation and characterization of monoclonal antibodies which enhance giant polykaryocyte formation in Newcastle disease virus-infected cell lines of human origin. *J. Virol.* 66, 5999–6007.

Jackson, R. J., Hellen, C. U., and Pestova, T. V. (2010). The mechanism of eukaryotic translation initiation and principles of its regulation. *Nat. Rev. Mol. Cell Biol.* 11, 113–127. doi: 10.1038/nrm2838

Jackson, W. T. (2015). Viruses and the autophagy pathway. *Virology* 47, 450–456. doi: 10.1016/J.VIROL.2015.03.042

Jaishankar, D., Yakoub, A. M., Bogdanov, A., Valyi-Nagy, T., and Shukla, D. (2015). Characterization of a proteolytically stable d-Peptide that suppresses HSV 1 infection: implications for the development of entry-based antiviral therapy. *J. Virol.* 89, 1932–1938. doi: 10.1128/JVI.02979-14

Jaishankar, D., Yakoub, A. M., Bogdanov Jaishankar, D., Yakoub, A. M., Yadavalli, T., Agelidis, A., et al. (2018). An off-target effect of BX795 blocks herpes simplex virus type 1 infection of the eye. *Sci. Transl. Med.* 10:eaan5861. doi: 10.1126/scitranslmed.aan5861

James, S. H., and Prichard, M. N. (2014). Current and future therapies for HSV infections: mechanism of action and drug resistance. *Curr. Opin. Virol.* 8, 54–61. doi: 10.1016/j.coviro.2014.06.003

Jiang, X. (2014). "The intrinsic apoptotic pathway," in *Cell Death*, ed. H. Wu, (New York, NY: Springer), 15–40.

Johnson, D. C., and Baines, J. D. (2011). Herpesviruses remodel host membranes for virus egress. *Nat. Rev. Microbiol.* 9, 382–394. doi: 10.1038/nrmicro2559

Jones, C. (2013). Bovine Herpes Virus 1 (BHV-1) and Herpes Simplex Virus Type 1 (HSV-1) Promote Survival of Latently Infected Sensory Neurons, in Part by Inhibiting Apoptosis. *J. Cell Death* 6, 1–16. doi: 10.4137/JCD.S10803

Jose, G. G., Larsen, I. V., Gauger, J., Carballo, E., Stern, R., Brummel, R., et al. (2013). A cationic peptide, TAT-Cd0, inhibits HSV type 1 ocular infection in vivo. *Invest. Ophthalmol. Vis. Sci.* 54, 1070–1079. doi: 10.1167/iovs.12-10250

Jovasevic, V., Naghavi, M. H., and Walsh, D. (2015). Microtubule plus end-associated CLIP-170 initiates HSV-1 retrograde transport in primary human cells. *J. Cell Biol.* 211, 323–337. doi: 10.1083/jcb.201505123

Karasneh, G. A., and Shukla, D. (2011). Herpes simplex virus infects most cell types in vitro: clues to its success. *Virol. J.* 8:481. doi: 10.1186/1743-422X-8-481

Kennedy, P. G. E., and Steiner, I. (2013). Recent issues in herpes simplex encephalitis. *J. Neurovirol.* 19, 346–350. doi: 10.1007/s13365-013-0178-6

Klumperman, J. (2000). Transport between ER and Golgi. *Curr. Opin. Cell Biol.* 12, 445–449. doi: 10.1016/s0955-0674(00)00115-0

Krummenacher, C., Baribaud, F., Ponce de Leon, M., Baribaud, I., Whitbeck, J. C., Xu, R., et al. (2004). Comparative usage of herpesvirus entry mediator A and nectin-1 by laboratory strains and clinical isolates of HSV. *Virology* 322, 286–299. doi: 10.1016/j.virol.2004.02.005

Latchman, D. S. (1988). Effect of herpes simplex virus type 2 infection on mitochondrial gene expression. *J. Gen. Virol.* 69, 1405–1410. doi: 10.1099/0022-1317-69-6-1405

Le Sage, V., and Banfield, B. W. (2012). Dysregulation of autophagy in murine fibroblasts resistant to HSV-1 infection. *PLoS One* 7:e42636. doi: 10.1371/journal.pone.0042636

Le Sage, V., Jung, M., Alter, J. D., Wills, E. G., Johnston, S. M., Kawaguchi, Y., et al. (2013). The herpes simplex virus 2 UL21 protein is essential for virus propagation. *J. Virol.* 87, 5904–5915. doi: 10.1128/JVI.03489-12

Leach, N., Bjerke, S. L., Christensen, D. K., Bouchard, J. M., Mou, F., Park, R., et al. (2007). Emerin is hyperphosphorylated and redistributed in herpes simplex virus type 1-infected cells in a manner dependent on both UL34 and US3. *J. Virol.* 81, 10792–10803. doi: 10.1128/JVI.00196-07

Leach, N. R., and Roller, R. J. (2010). Significance of host cell kinases in herpes simplex virus type 1 egress and lamin-associated protein disassembly from the nuclear lamina. *Virology* 406, 127–137. doi: 10.1016/j.virol.2010.07.002

Lee, C. P., and Chen, M. R. (2010). Escape of herpesviruses from the nucleus. *Rev. Med. Virol.* 20, 214–230. doi: 10.1002/rmv.643

Lee, G. E., Murray, J. W., Wolkoff, A. W., and Wilson, D. W. (2006). Reconstitution of herpes simplex virus microtubule-dependent trafficking in vitro. *J. Virol.* 80, 4264–4275. doi: 10.1128/JVI.80.9.4264-4275.2006

Leopardi, R., and Roizman, B. (1996). Functional interaction and colocalization of the herpes simplex virus 1major regulatory protein ICP4 with EAP, a nucleolar-ribosomal protein. *Proc. Natl. Acad. Sci. U.S.A.* 93, 4572–4576. doi: 10.1073/pnas.93.10.4572

Leuzinger, H., Ziegler, U., Schraner, E. M., Fraefel, C., Glauser, D. L., Heid, I., et al. (2005). Herpes simplex virus 1 envelopment follows two diverse pathways. *J. Virol.* 79, 13047–13059. doi: 10.1128/JVI.79.20.13047-13059.2005

Levine, B. (2005). Eating oneself and uninvited guests: autophagy-related pathways in cellular defense. *Cell* 120, 159–162. doi: 10.1016/j.cell.2005.01.005

Levine, B., Mizushima, N., and Virgin, H. W. (2011). Autophagy in immunity and inflammation. *Nature* 469, 323–335. doi: 10.1038/nature09782

Li, S. (2019). Regulation of Ribosomal Proteins on Viral Infection. *Cells* 8:E508. doi: 10.3390/cells8050508

Liu, N., Kuang, X., Kim, H. T., Stoica, G., Qiang, W., Scofield, V. L., et al. (2004). Possible involvement of both endoplasmic reticulum- and mitochondria- dependent pathways in MoMuLV-ts1-induced apoptosis in astrocytes. *J. Neurovirol.* 10, 189–198. doi: 10.1080/13550280490448043

Liu, X., and Cohen, J. I. (2015). The role of PI3K/Akt in human herpesvirus infection: from the bench to the bedside. *Virology* 479, 568–577. doi: 10.1016/j.virol.2015.02.040

Liu, Z., Kato, A., Oyama, M., Kozuka-Hata, H., Arii, J., and Kawaguchi, Y. (2015). Role of host cell p32 in herpes simplex virus 1 de-envelopment during viral nuclear egress. *J. Virol.* 89, 8982–8998. doi: 10.1128/JVI.01220-15

Liu, Z., Kato, A., Shindo, K., Noda, T., Sagara, H., Kawaoka, Y., et al. (2014). Herpes simplex virus 1 UL47 interacts with viral nuclear egress factors UL31, UL34, and Us3 and regulates viral nuclear egress. *J. Virol.* 88, 4657–4667. doi: 10.1128/JVI.00137-14

Lund, K., and Ziola, B. (1986). Synthesis of mitochondrial macromolecules in herpes simplex type 1 virus infected Vero cells. *Biochem. Cell Biol.* 64, 1303–1309. doi: 10.1139/o86-171

Lussignol, M., Queval, C., Bernet-Camard, M.-F., Cotte-Laffitte, J., Beau, I., Codogno, P., et al. (2013). The herpes simplex virus 1 Us11 protein inhibits autophagy through its interaction with the protein kinase PKR. *J. Virol.* 87, 859–871. doi: 10.1128/JVI.01158-12

Lyman, M. G., and Enquist, L. W. (2009). Herpesvirus interactions with the host cytoskeleton. *J. Virol.* 83, 2058–2066. doi: 10.1128/JVI.01718-08

Maeda, F., Arii, J., Hirohata, Y., Maruzuru, Y., Koyanagi, N., Kato, A., et al. (2017). Herpes simplex virus 1 UL34 protein regulates the global architecture of the endoplasmic reticulum in infected cells. *J. Virol.* 91:e00271-17. doi: 10.1128/JVI.00271-17

Martin, C., Leyton, L., Hott, M., Arancibia, Y., Spichiger, C., McNiven, M. A., et al. (2017). Herpes Simplex Virus Type 1 Neuronal Infection Perturbs Golgi Apparatus Integrity through Activation of Src Tyrosine Kinase and Dyn-2 GTPase. *Front. Cell. Infect. Microbiol.* 7:371. doi: 10.3389/fcimb.2017.00371

Maruzuru, Y., Shindo, K., Liu, Z., Oyama, M., Kozuka-Hata, H., Arii, J., et al. (2014). Role of herpes simplex virus 1 immediate early protein ICP22 in viral nuclear egress. *J. Virol.* 88, 7445–7454. doi: 10.1128/JVI.01057-14

Mas, V. M., and Melero, J. A. (2013). "Entry of enveloped viruses into host cells: membrane fusion," in *Structure and Physics of Viruses: An Integrated Textbook*, ed. M. G. Mateu, (Dordrecht: Springer), 467–487. doi: 10.1007/978-94-007-6552-8_16

McElwee, M., Beilstein, F., Labetoulle, M., Rixon, F. J., and Pasdeloup, D. (2013). Dystonin/BPAG1 promotes plus-end-directed transport of herpes simplex virus 1 capsids on microtubules during entry. *J. Virol.* 87, 11008–11018. doi: 10.1128/JVI.01633-13

McGeoch, D. J., Rixon, F. J., and Davison, A. J. (2006). Topics in herpesvirus genomics and evolution. *Virus Res.* 117, 90–104. doi: 10.1016/j.virusres.2006.01.002

Mettenleiter, T. C. (2004). Budding events in herpesvirus morphogenesis. *Virus Res.* 106, 167–180. doi: 10.1016/j.virusres.2004.08.013

Mettenleiter, T. C., Muller, F., Granzow, H., and Klupp, B. G. (2013). The way out: What we know and do not know about herpesvirus nuclear egress. *Cell. Microbiol.* 15, 170–178. doi: 10.1111/cmi.12044

Miranda-Saksena, M., Denes, C. E., Diefenbach, R. J., and Cunningham, A. L. (2018). Infection and transport of herpes simplex virus type 1 in neurons: role of the cytoskeleton. *Viruses* 10:E92. doi: 10.3390/v10020092

Mizushima, N., Yoshimori, T., and Ohsumi, Y. (2011). The role of Atg proteins in autophagosome formation. *Annu. Rev. Cell Dev. Biol.* 27, 107–132. doi: 10.1146/annurev-cellbio-092910-15400

Mohr, I. (2006). Phosphorylation and dephosphorylation events that regulate viral mRNA translation. *Virus Res.* 119, 89–99. doi: 10.1016/j.virusres.2005.10.009

Morris, J. B., Hofemeister, H., and O'Hare, P. (2007). Herpes simplex virus infection induces phosphorylation and delocalization of emerin, a key inner nuclear membrane protein. *J. Virol.* 81, 4429–4437. doi: 10.1128/JVI.02354-06

Mou, F., Wills, E., and Baines, J. D. (2009). Phosphorylation of the U(L)31 protein of herpes simplex virus 1 by the U(S)3-encoded kinase regulates localization of the nuclear envelopment complex and egress of nucleocapsids. *J. Virol.* 83, 5181–5191. doi: 10.1128/JVI.00090-09

Mulvey, M., Arias, C., and Mohr, I. (2006). Resistance of mRNA translation to acute endoplasmic reticulum stress-inducing agents in herpes simplex virus type 1-infected cells requires multiple virus-encoded functions. *J. Virol.* 80, 7354–7363. doi: 10.1128/JVI.00479-06

Mulvey, M., Arias, C., and Mohr, I. (2007). Maintenance of endoplasmic reticulum (ER) homeostasis in herpes simplex virus type 1-infected cells through the association of a viral glycoprotein with PERK, a cellular ER stress sensor. *J. Virol.* 81, 3377–3390. doi: 10.1128/JVI.02191-06

Murata, T., Goshima, F., Daikoku, T., Inagaki-Ohara, K., Takakuwa, H., Kato, K., et al. (2000). Mitochondrial distribution and function in herpes simplex virus-infected cells. *J. Gen. Virol.* 81, 401–406. doi: 10.1099/0022-1317-81-2-401

Nakashima, H., Kaufmann, J. K., Wang, P. Y., Nguyen, T., Speranza, M. C., Kasai, K., et al. (2015). Histone deacetylase 6 inhibition enhances oncolytic viral replication in glioma. *J. Clin. Invest.* 125, 4269–4280. doi: 10.1172/JCI80713

Naranatt, P. P., Krishnan, H. H., Smith, M. S., and Chandran, B. (2005). Kaposi's sarcoma-associated herpesvirus modulates microtubule dynamics via RhoA-GTP-diaphanous 2 signaling and utilizes the dynein motors to deliver its DNA to the nucleus. *J. Virol.* 79, 1191–1206. doi: 10.1128/JVI.79.2.1191-1206.2005

Neumann, J., Eis-Hubinger, A. M., and Koch, N. (2003). Herpes simplex virus type 1 targets the MHC class II processing pathway for immune evasion. *J. Immunol.* 171, 3075–3083. doi: 10.4049/jimmunol.171.6.3075

Nicola, A. V., Hou, J., Major, E. O., and Straus, S. E. (2005). Herpes simplex virus type 1 enters human epidermal keratinocytes, but not neurons, via a pH-dependent endocytic pathway. *J. Virol.* 79, 7609–7616. doi: 10.1128/JVI.79

Novoa, I., Zeng, H., Harding, H. P., and Ron, D. (2001). Feedback inhibition of the unfolded protein response by *GADD34*-mediated dephosphorylation of eIF2 alpha. *J. Cell Biol.* 153, 1011–1022. doi: 10.1083/jcb.153.5.1011

Oh, M. J., Akhtar, J., Desai, P., and Shukla, D. (2010). A role for heparan sulfate in viral surfing. *Biochem. Biophys. Res. Commun.* 391, 176–181. doi: 10.1016/j.bbrc.2009.11.027

Ohgimoto, S., Tabata, N., Suga, S., Nishio, M., Ohta, H., Tsurudome, M., et al. (1995). Molecular characterization of fusion regulatory protein-1 (FRP-1) that induces multinucleated giant cell formation of monocytes and HIV gp160-mediated cell fusion. FRP-1 and 4F2/CD98 are identical molecules. *J. Immunol.* 155, 3585–3592.

Okamoto, K., Tsurudome, M., Ohgimoto, S., Kawano, M., Nishio, M., Komada, H., et al. (1997). An anti-fusion regulatory protein-1 monoclonal antibody suppresses human parainfluenza virus type 2-induced cell fusion. *J. Gen. Virol.* 78, 83–89. doi: 10.1099/0022-1317-78-1-83

Orci, L., Montesano, R., and Perrelet, A. (1981). Exocytosis-endocytosis as seen with morphological probes of membrane organization. *Methods Cell Biol.* 23, 283–300.

Orvedahl, A., Alexander, D., Tallóczy, Z., Sun, Q., Wei, Y., Zhang, W., et al. (2007). HSV-1 ICP34.5 confers neurovirulence by targeting the beclin 1 autophagy protein. *Cell Host Microbe* 1, 23–35. doi: 10.1016/j.chom.2006.12.001

Page, H. G., and Read, G. S. (2010). The virion host shutoff endonuclease (UL41) of herpes simplex virus interacts with the cellular cap-binding complex eIF4F. *J. Virol.* 84, 6886–6890. doi: 10.1128/JVI.00166-10

Palade, G. (1975). Intracellular aspects of the process of protein synthesis. *Science* 189, 347–358. doi: 10.1126/science.1096303

Paladino, P., and Mossman, K. L. (2009). Mechanisms employed by herpes simplex virus 1 to inhibit the interferon response. *J. Interferon Cytokine Res.* 29, 599–607. doi: 10.1089/jir.2009.0074

Pasdeloup, D., McElwee, M., Beilstein, F., Labetoulle, M., and Rixon, F. J. (2013). Herpesvirus tegument protein pUL37 interacts with dystonin/BPAG1 to promote capsid transport on microtubules during egress. *J. Virol.* 87, 2857–2867. doi: 10.1128/JVI.02676-12

Paul, P., and Münz, C. (2016). Autophagy and mammalian viruses. *Adv. Virus Res.* 95, 149–195. doi: 10.1016/bs.aivir.2016.02.002

Pellett, P., and Roizman, B. (2013). "Herpesviridae," in *Fields Virology*, 6th Edn, eds D. M. Knipe, and P. M. Howley, (Philadelphia, PA: Lippincott), 1802–1822.

Pheasant, K., Möller-Levet, C. S., Jones, J., Depledge, D., Breuer, J., and Elliott, G. (2018). Nuclear cytoplasmic compartmentalization of the herpes simplex virus 1 infected cell transcriptome is coordinated by the viral endoribonuclease vhs and cofactors to facilitate the translation of late proteins. *PLoS Pathog.* 14:e1007331. doi: 10.1371/journal.ppat.1007331

Pietsch, E. C., Sykes, S. M., McMahon, S. B., and Murphy, M. E. (2008). The p53 family and programmed cell death. *Oncogene* 27, 6507–6521. doi: 10.1038/onc.2008.315

Pilli, M., Arko-Mensah, J., Ponpuak, M., Roberts, E., Master, S., Mandell, M. A., et al. (2012). TBK-1 promotes autophagy-mediated antimicrobial defense by controlling autophagosome maturation. *Immunity* 37, 223–234. doi: 10.1016/j.immuni.2012.04.015

Prager, G. W., Feral, C. C., Kim, C., Han, J., and Ginsberg, M. H. (2007). CD98hc (SLC3A2) interaction with the integrin beta subunit cytoplasmic domain mediates adhesive signaling. *J. Biol. Chem.* 282, 24477–24484. doi: 10.1074/jbc.M702877200

Radtke, K., English, L., Rondeau, C., Leib, D., Lippé, R., and Desjardins, M. (2013). Inhibition of the host translation shutoff response by herpes simplex virus 1 triggers nuclear envelope-derived autophagy. *J. Virol.* 87, 3990–3997. doi: 10.1128/JVI.02974-12

Read, G. S. (2013). Virus-encoded endonucleases: expected and novel functions. *Wiley Interdiscip. Rev. RNA* 4, 693–708. doi: 10.1002/wrna.1188

Reynolds, A. E., Liang, L., and Baines, J. D. (2004). Conformational changes in the nuclear lamina induced by herpes simplex virus type 1 require genes U(L)31 and U(L)34. *J. Virol.* 78, 5564–5575. doi: 10.1128/JVI.78.11.5564-5575.2004

Reynolds, A. E., Ryckman, B. J., Baines, J. D., Zhou, Y., Liang, L., and Roller, R. J. (2001). UL31 and UL34 proteins of herpes simplex virus type 1 form a complex that accumulates at the nuclear rim and is required for envelopment of nucleocapsids. *J. Virol.* 75, 8803–8817. doi: 10.1128/JVI.75.18.8803-8817.2001

Reynolds, A. E., Wills, E. G., Roller, R. J., Ryckman, B. J., and Baines, J. D. (2002). Ultrastructural localization of the herpes simplex virus type 1 UL31, UL34, and US3 proteins suggests specific roles in primary envelopment and egress of nucleocapsids. *J. Virol.* 76, 8939–8952. doi: 10.1128/jvi.76.17.8939-8952.2002

Roizman, B., Knipe, D. M., and Whitley, R. J. (2014). "Herpes simplex viruses," in *Fields Virology*, Vol. 2, eds D. M. Knipe, and P. M. Howley, (Philadelphia, PA: Wolters Kluver), 1823–1897.

Roller, R. J., Zhou, Y., Schnetzer, R., Ferguson, J., and DeSalvo, D. (2000). Herpes simplex virus type 1 U(L)34 gene product is required for viral envelopment. *J. Virol.* 74, 117–129. doi: 10.1128/JVI.74.1.117-129.2000

Romero-Brey, I., and Bartenschlager, R. (2016). Endoplasmic reticulum: the favorite intracellular niche for viral replication and assembly. *Viruses* 8:E160. doi: 10.3390/v8060160

Roskoski, R. (2015). Src protein-tyrosine kinase structure, mechanism, and small molecule Inhibitors. *Pharmacol. Res.* 94, 9–25. doi: 10.1016/j.phrs.2015.01.003

Saffran, H. A., Pare, J. M., Corcoran, J. A., Weller, S. K., and Smiley, J. R. (2007). Herpes simplex virus eliminates host mitochondrial DNA. *EMBO Rep.* 8, 188–193. doi: 10.1038/sj.embor.7400878

Saied, A. A., Chouljenko, V. N., Subramanian, R., and Kousoulas, K. G. (2014). A replication competent HSV-1(McKrae) with a mutation in the amino-terminus of glycoprotein K (gK) is unable to infect mouse trigeminal ganglia after cornea infection. *Curr. Eye Res.* 39, 596–603. doi: 10.3109/02713683.2013.855238

Saraste, J., Dale, H. A., Bazzocco, S., and Marie, M. (2009). Emerging new roles of the pre-Golgi intermediate compartment in biosynthetic-secretory trafficking. *FEBS Lett.* 583, 3804–3810. doi: 10.1016/j.febslet.2009

Shen, W. E., Silva, M. S., Jaber, T., Vitvitskaia, O., Li, S., Henderson, G., et al. (2009). Two small RNAs encoded within the first 1.5 kilobases of the herpes simplex virus type 1 latency-associated transcript can inhibit productive infection and cooperate to inhibit apoptosis. *J. Virol.* 83, 9131–9139. doi: 10.1128/JVI.00871-09

Shiflett, L. A., and Read, G. S. (2013). mRNA decay during herpes simplex virus (HSV) infections: mutations that affect translation of an mRNA influence the sites at which it is cleaved by theHSVvirion host shutoff (Vhs) protein. *J. Virol.* 87, 94–109. doi: 10.1128/JVI.01557-12

Shoji, H., Azuma, K., Nishimura, Y., Fujimoto, H., Sugita, Y., and Eizuru, Y. (2002). Acute viral encephalitis: the recent progress. *Intern. Med.* 41, 420–428. doi: 10.2169/internalmedicine.41.420

Shukla, D., and Spear, P. G. (2001). Herpesviruses and heparan sulfate: an intimate relationship in aid of viral entry. *J. Clin. Invest.* 108, 503–510. doi: 10.1172/JCI13799

Sievers, E., Neumann, J., Raftery, M., Schonrich, G., Eis-Hubinger, A. M., and Koch, N. (2002). Glycoprotein B from strain 17 of herpes simplex virus type I contains an invariant chain homologous sequence that binds to MHC class II molecules. *Immunology* 107, 129–135. doi: 10.1046/j.1365-2567.2002.01472.x

Simonin, D., Diaz, J. J., Massé, T., and Madjar, J. J. (1997). Persistence of ribosomal protein synthesis after infection of HeLa cells by herpes simplex virus type 1. *J. Gen. Virol.* 78, 435–443. doi: 10.1099/0022-1317-78-2-435

Smith, R. W., Graham, S. V., and Gray, N. K. (2008). Regulation of translation initiation by herpesviruses. *Biochem. Soc. Trans.* 36, 701–707. doi: 10.1042/BST0360701

Sparrer, K. M. J., Gableske, S., Zurenski, M. A., Parker, Z. M., Full, F., Baumgart, G. J., et al. (2017). TRIM23 mediates virus-induced autophagy via activation of TBK1. *Nat. Microbiol.* 2, 1543–1557. doi: 10.1038/s41564-017-0017-2

Stewart, C. L., Roux, K. J., and Burke, B. (2007). Blurring the boundary: the nuclear envelope extends its reach. *Science* 318, 1408–1412. doi: 10.1126/science.1142034

Stolz, A., Ernst, A., and Dikic, I. (2014). Cargo recognition and trafficking in selective autophagy. *Nat. Cell Biol.* 16, 495–501. doi: 10.1038/ncb2979

Strunk, U., Ramos, D. G., Saffran, H. A., and Smiley, J. R. (2016). Role of Herpes simplex virus 1 VP11/12 tyrosine-based binding motifs for Src family kinases, p85, Grb2 and Shc in activation of the phosphoinositide 3-kinase-Akt pathway. *Virology* 498, 31–35. doi: 10.1016/j.virol.2016.08.007

Suhy, D. A., Giddings, T. H. Jr., and Kirkegaard, K. (2000). Remodeling the endoplasmic reticulum by poliovirus infection and by individual viral proteins: an autophagy-like origin for virus-induced vesicles. *J. Virol.* 74, 8953–8965. doi: 10.1128/JVI.74.19.8953-8965.2000

Tiwari, V., Clement, C., Xu, D., Valyi-Nagy, T., Yue, B. Y., Liu, J., et al. (2006). Role for 3-O-sulfated heparan sulfate as the receptor for HSV type 1 entry into primary human corneal fibroblasts. *J. Virol.* 80, 8970–8980. doi: 10.1128/JVI.00296-06

Tiwari, V., Liu, J., Valyi-Nagy, T., and Shukla, D. (2011). Anti-heparan sulfate peptides that block HSV infection *in vivo*. *J. Biol. Chem.* 286, 25406–25415. doi: 10.1074/jbc.M110.201103

Tolonen, N., Doglio, L., Schleich, S., Krijnse, and Locker, J. (2001). Vaccinia virus DNA replication occurs in endoplasmic reticulum-enclosed cytoplasmic mini-nuclei. *Mol. Biol. Cell* 12, 2031–2046. doi: 10.1091/mbc.12.7.2031

Trigilio, J., Antoine, T. E., Paulowicz, I., Mishra, Y. K., Adelung, R., and Shukla, D. (2012). Tin oxide nanowires suppress HSV-1 entry and cell-to-cell membrane fusion. *PLoS One* 7:e48147. doi: 10.1371/journal.pone.0048147

Turner, A., Bruun, B., Minson, T., and Browne, H. (1998). Glycoproteins gB, gD, and gHgL of herpes simplex virus type 1 are necessary and sufficient to mediate membrane fusion in a Cos cell transfection system. *J. Virol.* 72, 873–875.

Verma, G., and Datta, M. (2012). The critical role of JNK in the ER-mitochondrial crosstalk during apoptotic cell death. *J. Cell. Physiol.* 227, 1791–1795. doi: 10.1002/jcp.22903

Verrey, F., Closs, E. I., Wagner, C. A., Palacin, M., Endou, H., and Kanai, Y. (2004). CATs and HATs: the SLC7 family of amino acid transporters. *Pflugers Arch.* 447, 532–542. doi: 10.1007/s00424-003-1086-z

Wagner, E. K., Flanagan, W. M., Devi-Rao, G., Zhang, Y. F., Hill, J. M., Anderson, K. P., et al. (1988). The herpes simplex virus latency-associated transcript is spliced during the latent phase of infection. *J. Virol.* 62, 4577–4585.

Walsh, D., and Mohr, I. (2004). Phosphorylation of eIF4E by Mnk-1 enhances HSV-1 translation and replication in quiescent cells. *Genes Dev.* 18, 660–672. doi: 10.1101/gad.1185304

Walsh, D., and Mohr, I. (2006). Assembly of an active translation initiation factor complex by a viral protein. *Genes Dev.* 20, 461–472. doi: 10.1101/gad.1375006

Walsh, D., and Mohr, I. (2011). Viral subversion of the host protein synthesis machinery. *Nat. Rev. Microbiol.* 9, 860–875. doi: 10.1038/nrmicro2655

Wang, M., Zhao, J., Zhang, L., Wei, F., Lian, Y., Wu, Y., et al. (2017). Role of tumor microenvironment in tumorigenesis. *J. Cancer* 8, 761–773. doi: 10.7150/jca.17648

Wang, Y., Cao, H., Chen, J., and McNiven, M. (2011). A direct interaction between the large GTPase dynamin-2 and FAK regulates focal adhesion dynamics in response to active Src. *Mol. Biol. Cell* 22, 1529–1538. doi: 10.1091/mbc.E10-09-0785

Weller, S. G., Capitani, M., Cao, H., Micaroni, M., Luini, A., Sallese, M., et al. (2010). Src kinase regulates the integrity and function of the Golgi apparatus via activation of dynamin 2. *Proc. Natl. Acad. Sci. U.S.A.* 107, 5863–5868. doi: 10.1073/pnas.0915123107

Whitley, R. J., and Roizman, B. (2001). HSV infections. *Lancet* 357, 1513–1518.

Wild, P., Engels, M., Senn, C., Tobler, K., Zeigler, U., Schraner, E. M., et al. (2005). Impairment of nuclear pores in bovine herpesvirus 1-infected MDBK cells. *J. Virol.* 79, 1071–1083. doi: 10.1128/JVI.79.2.1071-1083.2005

Wild, P., Farhan, H., McEwan, D. G., Wagner, S., Rogov, V. V., Brady, N. R., et al. (2011). Phosphorylation of the autophagy receptor optineurin restricts *Salmonella* growth. *Science* 333, 228–233. doi: 10.1126/science.1205405

Wild, P., Kaech, A., Schraner, E. M., Walser, L., and Ackermann, M. (2018). Endoplasmic reticulum-to-Golgi transitions upon herpes virus infection. *F1000Res.* 6:1804. doi: 10.12688/f1000research.12252.2

Wild, P., Leisinger, S., de Oliveira, A. P., Doehner, J., Schraner, E. M., Fraefel, C., et al. (2019). Nuclear envelope impairment is facilitated by the herpes simplex virus 1 Us3 kinase. *F1000Res.* 8:198. doi: 10.12688/f1000research.17802.1

Wild, P., Leisinger, S., de Oliveira, A. P., Schraner, E. M., Kaech, A., Ackermann, M., et al. (2015). Herpes simplex virus 1 Us3 deletion mutant is infective despite impaired capsid translocation to the cytoplasm. *Viruses* 7, 52–71. doi: 10.3390/v7010052

Wilson, D. N., and Doudna Cate, J. H. (2012). The structure and function of the eukaryotic ribosome. *Cold Spring Harb. Perspect. Biol.* 4:a011536. doi: 10.1101/cshperspect.a011536

Wisner, T. W., Wright, C. C., Kato, A., Kawaguchi, Y., Mou, F., Baines, J. D., et al. (2009). Herpesvirus gB-induced fusion between the virion envelope and outer nuclear membrane during virus egress is regulated by the viral US3 kinase. *J. Virol.* 83, 3115–3126. doi: 10.1128/JVI.01462-08

Wittels, M., and Spear, P. G. (1991). Penetration of cells by herpes simplex virus does not require a low pH-dependent endocytic pathway. *Virus Res.* 18, 271–290. doi: 10.1016/0168-1702(91)90024-P

Wnêk, M., Ressel, L., Ricci, E., Rodriguez-Martinez, C., Guerrero, J. C., Ismail, Z., et al. (2016). Herpes simplex encephalitis is linked with selective mitochondrial damage; a post-mortem and in vitro study. *Acta Neuropathol.* 132, 433–451. doi: 10.1007/s00401-016-15972

Wu, Y., Wei, F., Tang, L., Liao, Q., Wang, H., Shi, L., et al. (2019). Herpesvirus acts with the cytoskeleton and promotes cancer progression. *J. Cancer* 10, 2185–2193. doi: 10.7150/jca.30222

Wyllie, A. (1997). Apoptosis: an overview. *Br. Med. Bull.* 53, 451–465. doi: 10.1093/oxfordjournals.bmb.a011623

Xu, X., Xiong, X., and Sun, Y. (2016). The role of ribosomal proteins in the regulation of cell proliferation, tumorigenesis, and genomic integrity. *Sci. China Life Sci.* 59, 656–672. doi: 10.1007/s11427-016-0018-0

Yadavalli, T., Ames, J., Agelidis, A., Suryawanshi, R., Jaishankar, D., Hopkins, J., et al. (2019). Drug-encapsulated carbon (DECON): a novel platform for enhanced drug delivery. *Sci. Adv.* 5:eaax0780. doi: 10.1126/sciadv.aax0780

Yakoub, A. M., and Shukla, D. (2015). Autophagy stimulation abrogates herpes simplex virus-1 infection. *Sci. Rep.* 5:9730. doi: 10.1038/srep09730

Yordy, B., Iijima, N., Huttner, A., Leib, D., and Iwasaki, A. (2012). A neuron-specific role for autophagy in antiviral defense against herpes simplex virus. *Cell Host Microbe* 12, 334–345. doi: 10.1016/j.chom.2012.07.013

Yuan, S., and Akey, C. W. (2013). Apoptosome structure, assembly, and procaspase activation. *Structure* 21, 501–515. doi: 10.1016/j.str.2013.02.024

Yuan, S., Topf, M., Reubold, T. F., Eschenburg, S., and Akey, C. W. (2013). Changes in Apaf-1 conformation that drive apoptosome assembly. *Biochemistry* 52, 2319–2327. doi: 10.1021/bi301721g

Zhang, N., Yan, J., Lu, G., Guo, Z., Fan, Z., Wang, J., et al. (2011). Binding of HSV glycoprotein D to nectin-1 exploits host cell adhesion. *Nat. Commun.* 2:577. doi: 10.1038/ncomms1571

Zheng, Z., Zhou, Y., Xiong, W., Luo, X., Zhang, W., Li, X., et al. (2007). Analysis of gene expression identifies candidate molecular markers in nasopharyngeal carcinoma using microdissection and cDNA microarray. *J. Cancer Res. Clin. Oncol.* 133, 71–81. doi: 10.1007/s00432-006-0136-2

Conflict of Interest: The authors declare that the research was conducted in the absence of any commercial or financial relationships that could be construed as a potential conflict of interest.

frontiers in Microbiology

ORIGINAL RESEARCH
published: 26 June 2020
doi: 10.3389/fmicb.2020.01446

Singapore Grouper Iridovirus (SGIV) Inhibited Autophagy for Efficient Viral Replication

Chen Li[1,2], Liqun Wang[1,2], Jiaxin Liu[1,2], Yepin Yu[1,2], Youhua Huang[1,2], Xiaohong Huang[1,2], Jingguang Wei[1,2] and Qiwei Qin[1,2,3]**

[1] Joint Laboratory of Guangdong Province and Hong Kong Region on Marine Bioresource Conservation and Exploitation, College of Marine Sciences, South China Agricultural University, Guangzhou, China, [2] Guangdong Laboratory for Lingnan Modern Agriculture, Guangzhou, China, [3] Laboratory for Marine Biology and Biotechnology, Qingdao National Laboratory for Marine Science and Technology, Qingdao, China

Autophagy is a conserved catabolic process that occurs at basal levels to maintain cellular homeostasis. Most virus infections can alter the autophagy level, which functions as either a pro-viral or antiviral pathway, depending on the virus and host cells. Singapore grouper iridovirus (SGIV) is a novel fish DNA virus that has caused great economic losses for the marine aquaculture industry. In this study, we found that SGIV inhibited autophagy in grouper spleen (GS) cells which was evidenced by the changes of LC3-II, Beclin1 and p-mTOR levels. Further study showed that SGIV developed at least two strategies to inhibit autophagy: (1) increasing the cytoplasmic p53 level; and (2) encoding viral proteins (VP48, VP122, VP132) that competitively bind autophagy related gene 5 and mediately affect LC3 conversion. Moreover, activation of autophagy by rapamycin or overexpressing LC3 decreased SGIV replication. These results provide an antiviral strategy from the perspective of autophagy.

Keywords: SGIV, grouper, autophagy, LC3, Atg5, p53

OPEN ACCESS

Edited by:
Indranil Banerjee, Indian Institute of Science Education and Research Mohali, India

Reviewed by:
Fabien P. Blanchet, Institut National de la Santé et de la Recherche Médicale (INSERM), France
Roberta Olmo Pinheiro, Oswaldo Cruz Foundation, Brazil

****Correspondence:***
Jingguang Wei
weijg@scau.edu.cn
Qiwei Qin
qinqw@scau.edu.cn

Specialty section:
This article was submitted to Virology, a section of the journal Frontiers in Microbiology

Received: *07 March 2020*
Accepted: *04 June 2020*
Published: *26 June 2020*

Citation:
Li C, Wang L, Liu J, Yu Y, Huang Y, Huang X, Wei J and Qin Q (2020) Singapore Grouper Iridovirus (SGIV) Inhibited Autophagy for Efficient Viral Replication. Front. Microbiol. 11:1446. doi: 10.3389/fmicb.2020.01446

INTRODUCTION

Singapore grouper iridovirus (SGIV) is a novel marine fish virus isolated from diseased groupers (Qin et al., 2001). The clinical symptoms of SGIV-challenged fishes are hemorrhage and enlargement of the spleen. This lethal pathogen has caused considerable economic damage in groupers, with more than 90% mortality (Qin et al., 2003).

To date, the morphogenesis, biochemical pathology, genome, transcriptome, proteomics, and entry mechanisms of SGIV have been systematically studied (Qin et al., 2003; Song et al., 2004; Wang et al., 2014). SGIV is an icosahedral virus with diameter of 154–176 nm, and it belongs to the genus *Ranavirus* and family Iridoviridae (Qin et al., 2001, 2003). The entire SGIV genome is a double-stranded DNA that consists of 140,131 base pairs and codes 162 open reading frames (ORFs) (Song et al., 2004). Among them, the function of some important viral proteins has been explored. For example, ORF136 encodes a lipopolysaccharide-induced tumor necrosis factor (TNF)-α factor (LITAF) homolog, and ORF051 encodes TNF receptor homologs and functions as a critical virulence factor that is involved in apoptosis and virus-mediated immune evasion (Huang et al., 2008; Yu et al., 2017). Study of the unknown viral genes will provide clues to its pathogenic mechanism as well as information about host–pathogen interactions, especially the precise strategy by which viruses escape the host immune response.

Autophagy is a conserved catabolic process that maintains cellular homeostasis by sequestering damaged organelles or misfolded proteins in the autophagosome and fusing with lysosomes for degradation and recycling (Xie and Klionsky, 2007; Klionsky et al., 2011). As a cell steward, autophagy is an essential part of host defense against pathogens (Wong and Sanyal, 2019). So far, approximately 40 autophagy related genes (Atgs) that strictly regulate this membrane trafficking process are known in yeast, and several mammalian homologs of yeast Atgs have been identified (Katherine et al., 2018).

The autophagy pathway involves two ubiquitin-like conjugation systems: Atg5-Atg12-Atg16L1 and LC3 (Atg8)-phosphatidylethanolamine (PE). The conjugation of LC3-I to PE (lipidation of LC3, LC3-II) is required for autophagosome biogenesis and is used as a standard marker of autophagy due to its location on autophagosome membrane (Mizushima et al., 2011). The Atg5-Atg12 conjugate has E3-like activity for LC3 lipidation (Hanada et al., 2007; Mizushima et al., 2011). Autophagy acts as an antiviral defense and inhibits viruses replication when challenged with some virus, such as vesicular stomatitis virus and human parainfluenza virus type 3 (Shelly et al., 2009; Ding et al., 2014; Lin et al., 2019). However, some viruses utilize the autophagy related membrane structures as a factory for replication or a shelter for escaping the host immune response, such as hepatitis B virus and influenza A virus (Zhou et al., 2009; Sir et al., 2010). Additionally, viruses can disrupt autophagy initiation to prevent viral clearance, as is the case for herpes simplex virus type 1 (HSV-1) (Orvedahl et al., 2007).

In recent years, the relationship between some aquatic viruses and autophagy has gradually been revealed, including viral hemorrhagic septicemia virus, spring viremia of carp virus, snakehead fish vesiculovirus, grouper iridovirus, largemouth bass virus, infectious kidney and spleen necrosis virus, and white spot syndrome virus (WSSV) (Garcia-Valtanen et al., 2014; Liu et al., 2015; Chen et al., 2016; Qi et al., 2016; Wang et al., 2016; Li et al., 2017). Based on current studies, the relationship between viruses and autophagy varies according to the type of virus and the host cell line. Most studies to date have focused on describing the phenomenon, information about viral induction of the autophagy signaling pathway and the autophagy–virus interaction is relatively lacking.

In this study, we focused mainly on the interaction between SGIV and autophagy in its target cells (grouper spleen, GS), and we explored the underlying interactional mechanisms.

MATERIALS AND METHODS

Virus Strain, Cell Line, and Reagents

The GS cell line used in this study was established in our laboratory (Huang et al., 2009). GS cells were cultured in Leibovitz's L-15 medium containing 10% fetal bovine serum (FBS, Gibco) at 28°C. The virus stock of SGIV (strain A3/12/98 PPD) was propagated in GS cells and maintained at −80°C (Qin et al., 2001). Rapamycin (Rap, R0395), Wortmannin (WM, S2758) was purchased from Selleckchem.

Virus Infection

Unless otherwise stated, GS cells grown on 24-well culture plates (10^5 cells/well) were infected with SGIV at multiplicity of infection of 2. For the regulating autophagy experiments, cells were pre-treated with 1 μM Rap or 1 μM WM for 2 h and then infected with SGIV according to previous studies (Li et al., 2020). For the transfected cells, SGIV infected at 24 h after transfection. At indicated hours post infection (h p.i.), RNA or protein samples were extracted as described below for further analysis.

Western Blot Analysis

Cells were washed with phosphate buffered saline (PBS) and resuspended in immunoprecipitation (IP) lysis buffer (Invitrogen). Whole cell lysates were separated by SDS-PAGE and transferred onto a PVDF membrane (Millipore). After blocking for 1 h at room temperature in 5% skim milk or 3% bovine serum albumin (BSA) dissolved in PBS, the membrane was incubated with a primary antibody for 2 h at room temperature. The primary antibodies used in the study included anti-LC3 (Abcam, ab 58610), Beclin1 (Proteintech, 11306-1-AP), mTOR (CST, 2983T), p-mTOR (Abcam, ab109268), β-tubulin (Abcam, ab6046), p53 (SAB, 48599), and LaminB1 (Proteintech, 12987-1-AP). After washing with PBS plus 0.1% Tween 20 (PBST), the membrane was incubated with a corresponding horseradish peroxidase-coupled secondary antibody (KPL). After washing with PBST three times, immunoreactive proteins were visualized by chemiluminescence using Thermo Scientific Pierce Western Blot ECL Plus (Thermo).

Flow Cytometry Analysis

Cellular autophagy was detected using flow cytometry according to the manufacturer's recommendations for Cyto-ID (1:1000, Enzo). Briefly, cells were harvested and resuspended in 250 μL of Dulbecco's PBS containing 5% FBS. Then, cells were resuspended in 250 μL of the diluted Cyto-ID Green stain solution and incubated for 30 min at 28°C in the dark. After collection by centrifugation, cells were washed with 1× assay buffer and resuspended in 250 μL of fresh 1× assay buffer. Finally, cells were analyzed using the green (FITC) channel of the flow cytometer (Beckman).

Plasmids and Transfection Assays

The recombinant pEGFP-C1-LC3, pcDNA3.1-3 × HA-LC3, pcDNA3.1-3 × HA-Atg5, and pEGFP-MAVS were available in our laboratory (Huang et al., 2018; Li et al., 2019a, 2020). The genes of SGIV-VP48, SGIV-VP122, and SGIV-VP132 were subcloned into the vector pEGFP-C1 and pcDNA3.1-3 × HA separately. p53 from the orange spotted grouper (*Epinephelus coioides*) was subcloned into the pcDNA3.1-RFP. Lysine at position 289 of wild-type p53 was converted to asparagine by site-directed mutagenesis to create the mutant form lacking the nuclear localization signal (NLS^-). **Table 1** lists the primers used in this analysis. The constructed plasmids were subsequently verified by DNA sequencing.

Cell transfection was carried out using Lipofectamine 2000 reagent (Invitrogen) as described previously (Li et al., 2019b).

TABLE 1 | Primers used in this study.

Name	Sequence (5′–3′)
P53-F	ATGGAAGAGCAAGAGTT
P53-R	TTAGTCGCTGTCGCTCC
RFP-P53-F	GGAATTCATGGAAGAGCAAGAGTT
RFP-P53-R	GGGTACCGTCGCTGTCGCTCC
P53-NLS^{-}-F	ACACCAAAAACCGAAAGAGTGCCCCGGCTGCGGCTC
P53-NLS^{-}-R	CACTCTTTCGGTTTTTGGTGTGTTTGGTGCCGTTCT
VP48-F	ATGTACACTTCAAACTG
VP48-R	CTACTCAAGTTCCATCAA
GFP-VP48-F	GAAGATCTATGTACACTTCAAACTG
GFP-VP48-R	GGGGTACCCTACTCAAGTTCCATCAA
HA-VP48-F	GGGGTACCATGTACACTTCAAACTG
HA-VP48-R	CGGAATTCTCTACTCAAGTTCCATCAA
VP122-F	ATGGCACCGGGAAAAAG
VP122-R	TTATTCCAACCCCCATT
GFP-VP122-F	GAAGATCTATGGCACCGGGAAAAAG
GFP-VP122-R	GGGGTACCTTATTCCAACCCCCATT
HA-VP122-F	GGGGTACCATGGCACCGGGAAAAAG
HA-VP122-R	CGGAATTCTTTATTCCAACCCCCATT
VP132-F	ATGCATAGCGTAAAATCG
VP132-R	TTACTTTTCAAAGTACCGAG
GFP-VP132-F	GAAGATCTATGCATAGCGTAAAATCG
GFP-VP132-R	GGGGTACCTTACTTTTCAAAGTACCGAG
HA-VP132-F	GGGGTACCATGCATAGCGTAAAATCG
HA-VP132-R	CGGAATTCTTTACTTTTCAAAGTACCGAG
β-actin-RT-F	TACGAGCTGCCTGACGGACA
β-actin-RT-R	GGCTGTGATCTCCTTCTGCA
MCP-RT-F	GCACGCTTCTCTCACCTTCA
MCP-RT-R	AACGGCAACGGGAGCACTA
ICP18-RT-F	ATCGGATCTACGTGGTTGG
ICP18-RT-R	CCGTCGTCGGTGTCTATTC
VP19-RT-F	TCCAAGGGAGAAACTGTAAG
VP19-RT-R	GGGGTAAGCGTGAAGACT
LITAF-RT-F	GATGCTGCCGTGTGAACTG
LITAF-RT-R	GCACATCCTTGGTGGTGTTG

For one well of 24-well plate, cells were transfected with the mixture of 800 ng of plasmids and 2 μL of Lipofectamine 2000 diluted in serum-free Opti-MEM (Gibco). After incubation for 6 h, the medium was replaced with fresh normal medium and cells were cultured for further study. To silence endogenous LC3, GS cells were transfected with the specific siRNA (siLC3) or the same volume of the corresponding GC content negative control (NC) as described previously (Li et al., 2020).

Subcellular Localization

To determine the subcellular localization of LC3 and p53, GS cells were seeded into glass-bottom cell culture dishes, and the constructed plasmids were transfected into GS cells as described above. At 24 h post-transfection, cells were fixed with 4% paraformaldehyde and stained with 4,6-diamidino-2-phenylindole (DAPI). LC3 and p53 were observed under a fluorescence microscope (Zeiss).

Nuclear/Cytosol Fractionation Assay

Singapore grouper iridovirus infected cells or non-infected cells were collected and subjected to nuclear and cytosol fractionation using the Nuclear/Cytosol Fractionation Kit (BioVision) following the protocols recommended by the manufacturer. All operations are performed on ice. The separated cytoplasmic protein and nuclear protein were subjected to Western blot analysis.

Co-immunoprecipitation Assays

To verify the interactions, the plasmids of pcDNA3.1-3 × HA-Atg5 or pcDNA3.1-3 × HA-LC3 was co-transfected with pEGFP-C1, pEGFP-MAVS, pEGFP-MAVS-CARD, pEGFP-VP48, pEGFP-VP122, or pEGFP-VP132, respectively. At 36 h after co-transfection, cells were lysed by IP lysis buffer supplemented with a protease inhibitor cocktail, then cell lysates were centrifuged at 12,000 × *g* for 5 min and the supernatant was collected for subsequent Western blot analysis and IP according to the Dynabeads^{TM} Protein G Immunoprecipitation Kit (Invitrogen). Briefly, magnetic beads were prepared and bound with anti-GFP (Abcam, ab290) for 10 min at room temperature, followed by incubation with sample containing the antigen for 30 min. After washing with washing buffer, target antigens were eluted and subjected to Western blot analysis. The primary antibodies specific for GFP and HA (Sigma, H3663) were used to detected the protein expression and interactions.

Mass Spectrometry

Grouper spleen cells were transfected with pEGFP-C1, pEGFP-LC3, pEGFP-Atg5, respectively, in accordance with the above method and then infected with SGIV. The whole cell lysates (WCL) were precipitated with GFP antibody. IP products were detected by reversed phase liquid chromatography-mass spectrum (RPLC-MS), then the raw data was imported into Protein Discoverer 2.1 SP1 (SEQUEST HT) for analysis. The database were human proteins from Uniprot and SGIV genome annotation data set (Song et al., 2004).

RNA Isolation and Real Time Quantitative PCR (qPCR) Analysis

For gene expression analysis, the total RNAs of cells were extracted using the SV Total RNA Isolation Kit (Promega) and reversed to synthesize the first-strand cDNA using the ReverTra Ace kit (Toyobo). Real time PCR analyses were performed using SYBR® Green reagent (Toyobo) according to manufacturer's recommendations in a Quant Studio 5 Real Time Detection System (Applied Biosystems). Primer pairs are listed in **Table 1**. The expression levels of target viral genes (*MCP*, *ICP18*, *VP19*, *LITAF*) were normalized to β-*actin* and calculated using the $2^{-\Delta\Delta CT}$ method. All reactions were performed in triplicate, and the data are presented as relative mRNA expressed as the mean ± standard deviation ($n = 3$). One-way analysis of variance was used to evaluate the variability among treatment groups. Differences were considered statistically significant at $P < 0.05$.

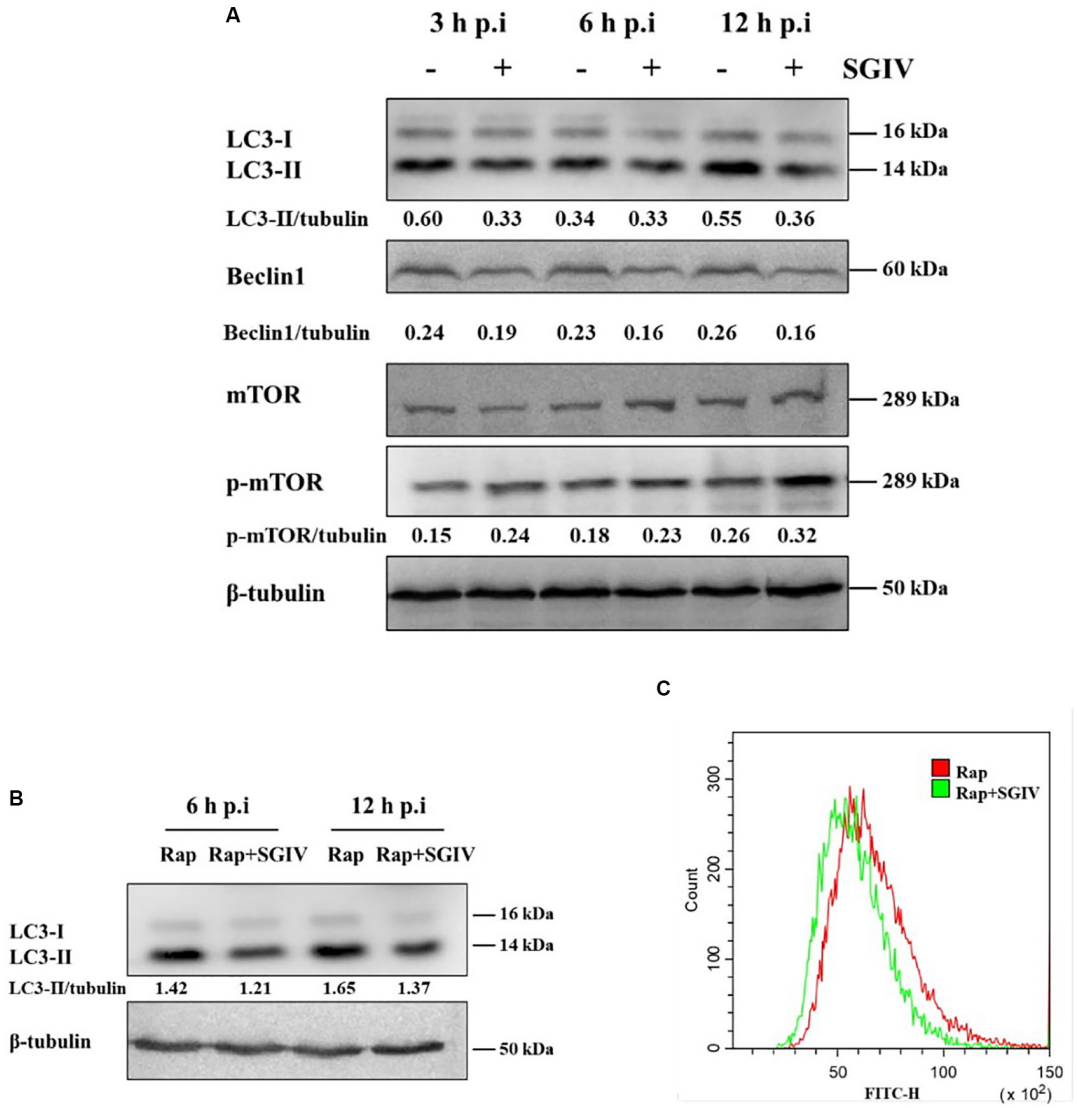

FIGURE 1 | SGIV infection inhibited autophagy in GS cells. **(A)** SGIV infection altered protein levels of LC3, Beclin1, and p-mTOR as determined by Western blot analysis. β-tubulin was used as the internal control. Band intensity was calculated using Quantity-one software, and the ratio of target protein/β-tubulin was shown below the blot. **(B)** The expression of LC3 was detected by Western blot analysis in infected or non-infected SGIV cells after Rap pre-treatment. Band intensity was calculated using Quantity-one software, and the ratio of LC3-II/β-tubulin was shown below the blot. **(C)** Flow cytometry-based profiling of autophagy in infected (12 h p.i.) or non-infected SGIV cells after Rap pre-treatment. Cyto-ID dye was used to stain cells, and 1×10^4 cells were collected for further positive analysis. The data were presented as the means from three independent experiment.

Immunofluorescence Assays

GS cells were seeded in glass-bottom cell culture dishes, then cells were treated with autophagy regulators or transfected with recombinant plasmid or siRNA. At indicated time points, cells were infected with SGIV. At 12 h p.i., cells were fixed in 4% paraformaldehyde for 1 h and permeabilized with 0.2% Triton X-100 for 15 min. After washing three times with PBS, cells were blocked with 2% BSA for 45 min and then incubated with anti-MCP serum (prepared in our laboratory) for 2 h at room temperature. Cells were washed with PBS, followed by incubation with the secondary antibody (fluorescence isothiocyanate-conjugated goat anti-rabbit immunoglobulin G, Pierce) for 1 h at room temperature. Cells then were stained with DAPI and observed under an inverted fluorescence microscope (Zeiss).

RESULTS

SGIV Inhibited Autophagy Initiation in GS Cells

LC3-PE conjugates (LC3-II) are essential for membrane elongation and autophagosome formation (Mizushima et al., 2011). The electrophoresis migration rate of LC3-II in SDS-PAGE

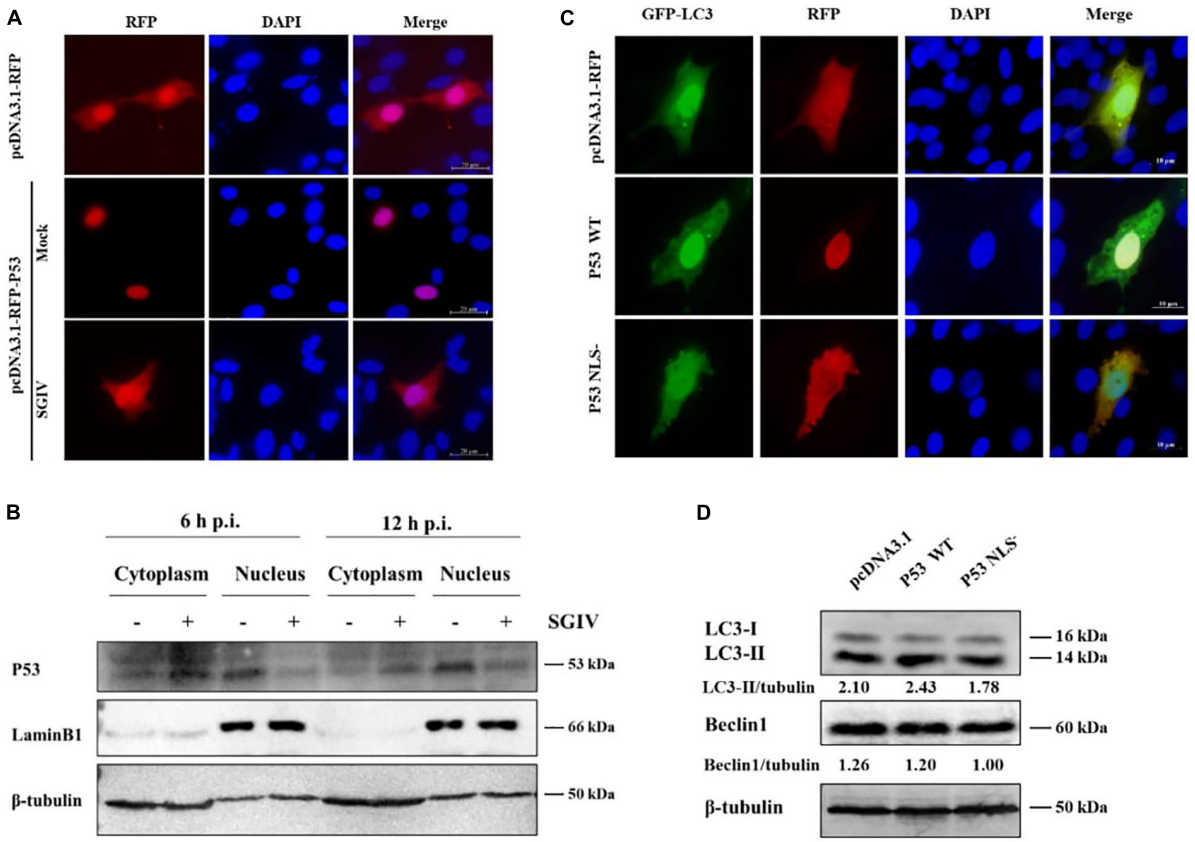

FIGURE 2 | SGIV increased cytoplasmic p53 level to inhibit autophagy. **(A)** SGIV infection altered the subcellular localization of p53. The transfected cells were fixed at 3 h p. i. **(B)** SGIV infection increased cytoplasmic p53 and decreased nuclear p53 levels. β-tubulin and LaminB1 were the internal references for cytoplasmic and nuclear extracts, respectively. **(C)** The cytoplasmic p53 (NLS^-) reduced the clustering of GFP-LC3. pcDNA3.1-RFP, RFP-p53 WT, and RFP-p53 NLS^- were co-transfected with GFP-LC3 plasmid into GS cells for 24 h, and stained with DAPI. **(D)** Subcellular localization of p53 affected the level of autophagy-related proteins. Band intensity was calculated and ratios of target protein/β-tubulin were assessed. The data were presented as the means from three independent experiment.

TABLE 2 | Summary of the proteomic profile of peptides detected following LC3, Atg5 immunoprecipitations in GS cells.

Protein accessions	Protein descriptions	*Q*-value	GFP-C1	GFP-LC3	GFP-Atg5
A0A484BZB5	Autophagy-related protein 3	6.21E-06	Filtered	14972.775	Filtered
Q5YFD3	Uncharacterized protein (ORF132R)	8.16E-06	Filtered	1	26748.252
Q5YFE3	Uncharacterized protein (ORF122L)	5.42E-05	Filtered	4418.675	17621.111

The protein accessions of Candidate molecules in Uniprot database were listed and the detailed information of these proteins can be queried in Uniprot website (https://www.uniprot.org/).

is faster than that of LC3-I. Beclin1(Atg6) plays a central role in initiation of the autophagy pathway by marking membranes to form the first double membrane structure, the phagophore (Kang et al., 2011). In this study, LC3 and Beclin1 protein levels were firstly detected by Western blot at different time points after SGIV infection. As shown as in **Figure 1A**, LC3-II and Beclin1 expression were both decreased in SGIV infected cells compared with the non-infected cells, especially at 3 h p. i. and 12 h p. i.

The mammalian target of Rapamycin (mTOR) is generally considered to be an inhibitor of autophagy, and the levels of mTOR and phosphorylation of mTOR were detected in this study. As shown as in **Figure 1A**, the level of phosphorylated mTOR (p-mTOR, S2448) were increased at 3 h, 6 h, and 12 h p. i., which suggested that SGIV infection might decrease autophagy through unlocking mTOR activity to some extent. To further ascertain the inhibition of SGIV replication on autophagy, we verified the result by means of the positive inducer Rap. In cells which pre-treated by Rap and infected with SGIV, LC3-II level decreased at 6 h p.i. and 12 h p.i. compared with the cells only pre-treated by Rap (**Figure 1B**), indicating that SGIV infection impeded autophagy activity to a certain extent. The measurement of autophagy with Cyto-ID dye also indicated that SGIV infection reduced the number of autophagy positive cells (**Figure 1C**).

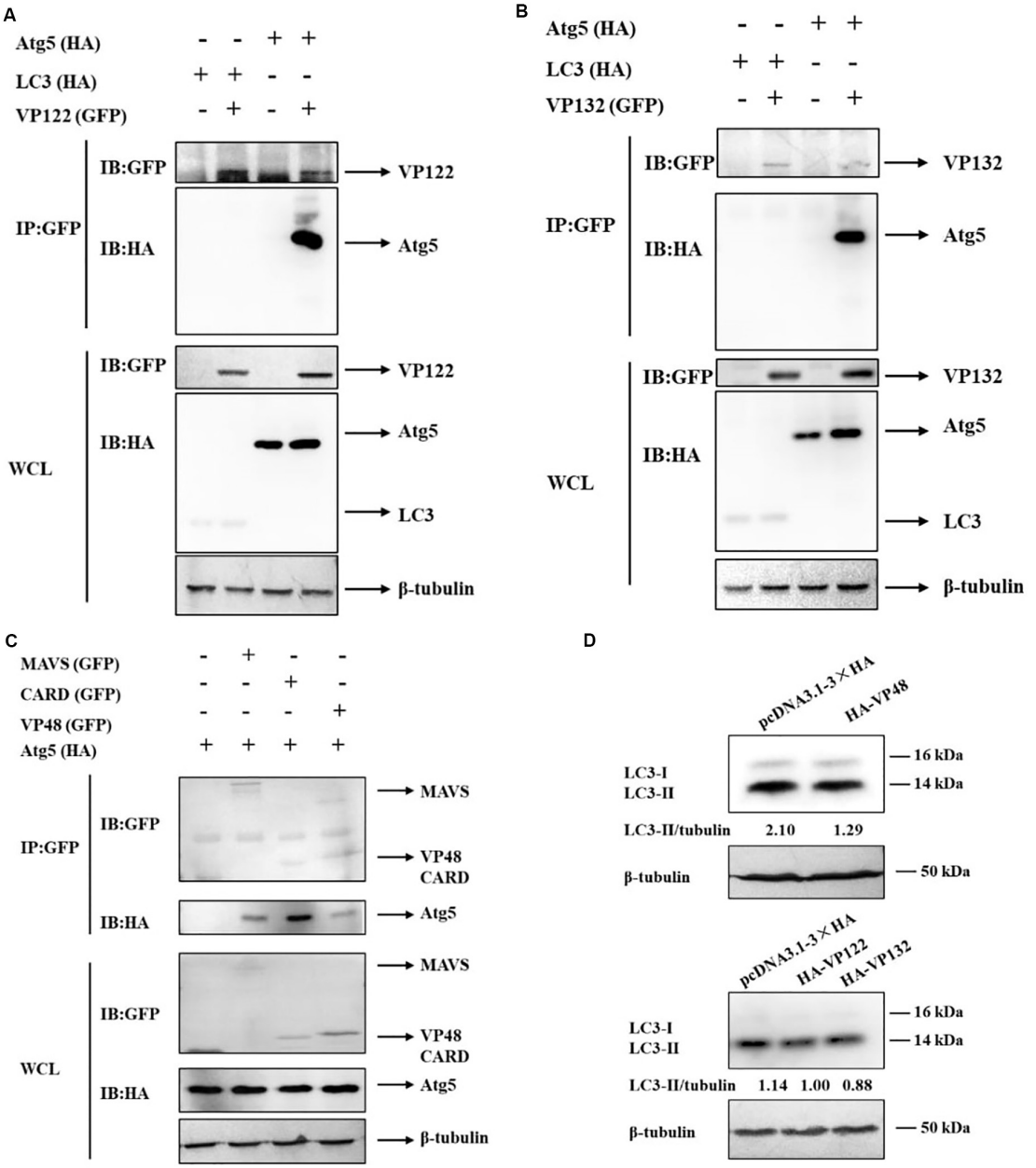

FIGURE 3 | SGIV-VP48, VP122, and VP132 interacted with Atg5 and their ectopic expression decreased the level of LC3-II. **(A)** HA-Atg5 interacted with GFP-VP122. Whole cell lysates (WCL) transfected with GFP-VP122 and HA-Atg5 or HA-LC3 were subjected to immunoprecipitation (IP) and immunoblotting (IB) with indicated antibodies. **(B)** HA-Atg5 interacted with GFP-VP132. WCLs of cells transfected with GFP-VP132 and HA-Atg5 or HA-LC3 were used for IP and IB with indicated antibodies. **(C)** HA-Atg5 interacted with GFP-MAVS, GFP-CARD, and GFP-VP48. WCLs of cells transfected with HA-Atg5 and GFP-MAVS, GFP-CARD, or GFP-VP48 were used for IP and IB with indicated antibodies. **(D)** VP48, VP122, and VP132 decreased the level of LC3-II. Cells transfected with HA-VP48, HA-VP122, or HA-VP132 were collected for Western blot analysis. β-tubulin was used as the internal reference. Band intensity was calculated using Quantity-one software, and ratios of LC3-II/β-tubulin were assessed. The data were presented as the means from three independent experiment.

SGIV Infection Increased Cytoplasmic p53 to Inhibit Autophagy

Research shows p53 affects autophagy activity differently in different locations, which is characterized by cytoplasmic p53 inhibiting autophagy but nuclear p53 promoting autophagy (Tasdemir et al., 2008a). In this study, p53 was distributed mainly in the nucleus in non-infected cells, but it was transferred to the cytoplasm upon SGIV infection (**Figure 2A**). We verified these results by nuclear/cytosol fractionation of p53 at 6 h and 12 h after SGIV infection. In SGIV infected cells, cytoplasmic p53 level was increased and nuclear p53 level was decreased compared with levels in non-infected cells (**Figure 2B**). To ascertain whether

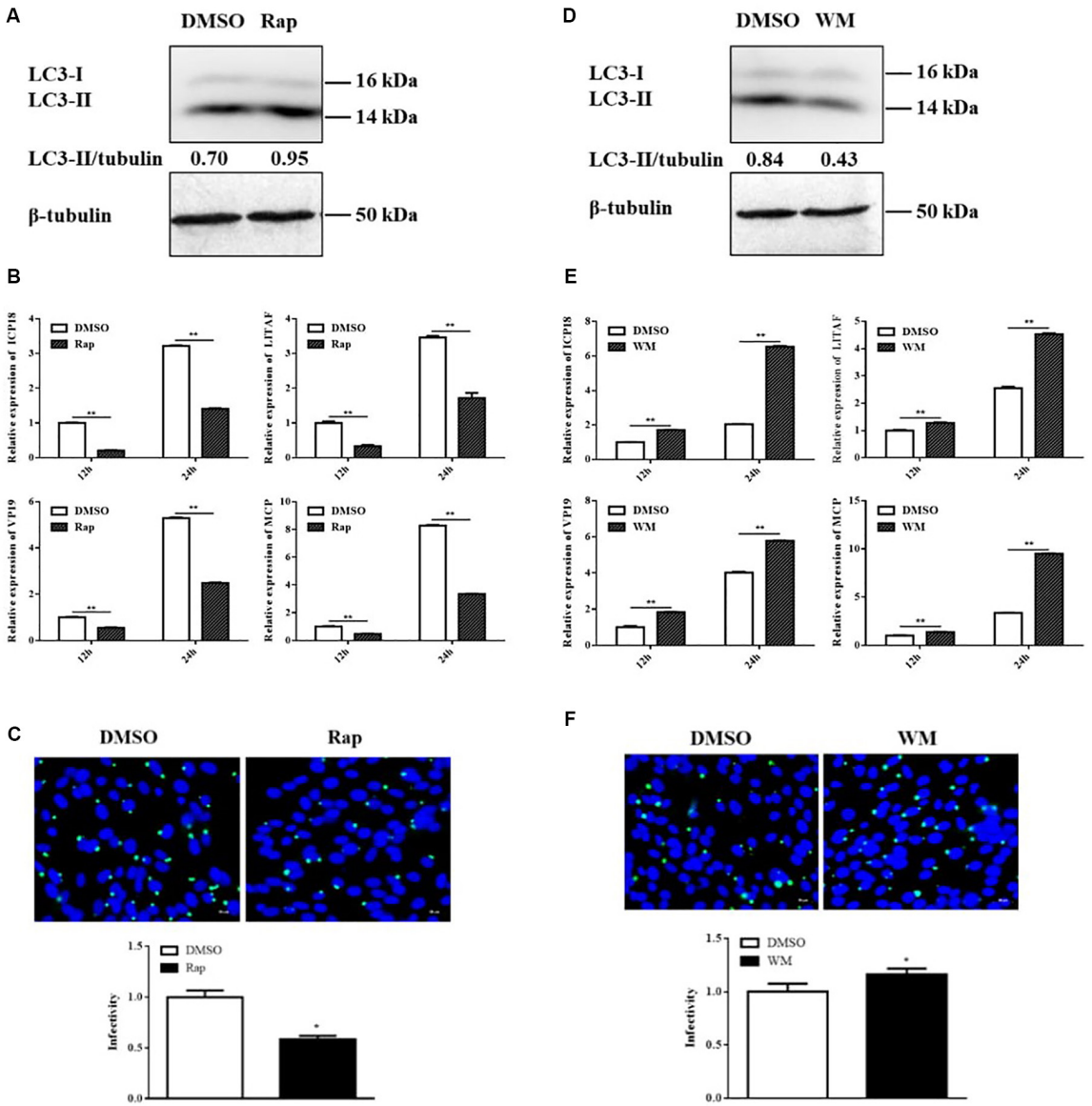

FIGURE 4 | Rap decreased SGIV replication, whereas WM promoted SGIV replication. GS cells were pretreated with Rap or WM or the same dosage of DMSO for 2 h prior to SGIV infection, then the infected cells were collected and analyzed by qPCR and immunofluorescence assay (IFA). **(A,D)** The LC3 expression in Rap or WM pretreated cells. **(B,E)** The relative expression of MCP, ICP18, VP19, and LITAF in SGIV infected cells. The β-actin gene was used as the internal reference for qPCR. **(C,F)** The infected cells were analyzed at 12 h p.i. by IFA using anti-MCP antibody (green). Nuclei were stained by DAPI (blue). The viral infectivity of control (DMSO treated) cells was set as 1. The data were presented as the means from three independent experiment, $^{*}p < 0.05$, $^{**}p < 0.01$.

p53 from grouper has a similar function in autophagy as that in mammals, a p53 mutant with a mutation (NLS^{-}) was generated by converting lysine codons at positions 289 to asparagine using site-directed mutagenesis. The wild type p53 (p53 WT), p53 NLS^{-}, and the empty vector were co-transfected with GFP-LC3 into GS cells. The subcellular localization analysis showed that little LC3 accumulated in the cells transfected with p53 NLS^{-}, indicating that cytoplasmic p53 inhibited autophagy (**Figure 2C**). Meanwhile, we detected the effect of p53 WT and p53 NLS^{-} on autophagy related proteins. As shown in **Figure 2D**, p53 WT increased the level of LC3-II, while cytoplasmic p53 decreased LC3-II and Beclin1, compared with transfected empty vector cells. Above all, SGIV infection leads to the transfer of p53 from the nucleus to the cytoplasm, which might be one of strategies to inhibit autophagy.

SGIV-VP48, VP122, and VP132 Interacted With Atg5 to Inhibit Autophagy Activity

It has been reported that some viral proteins can bind to autophagy-related proteins, such as Atg5 and LC3, to hijack the autophagy process (Guevin et al., 2010). In this study,

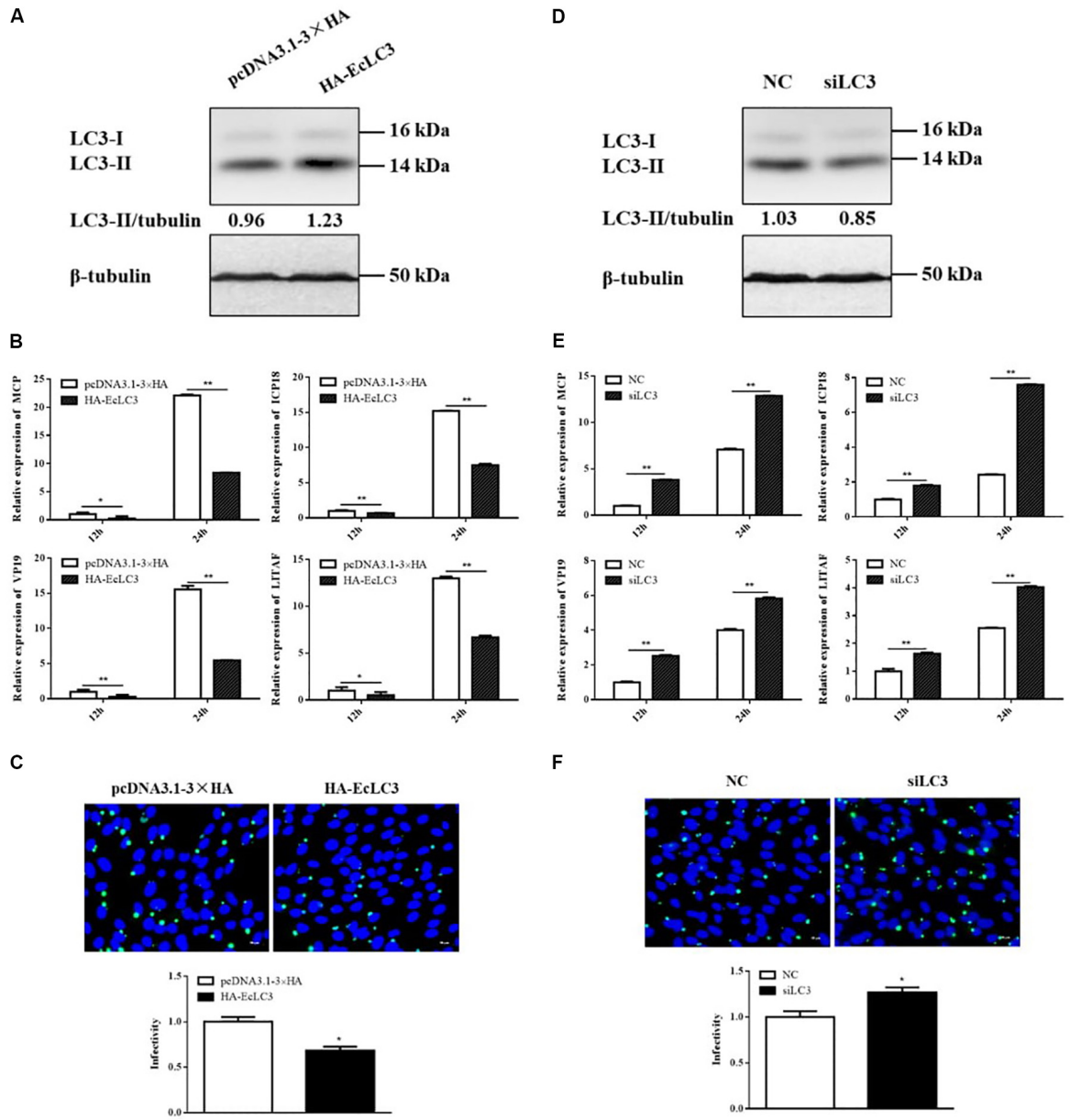

FIGURE 5 | LC3 overexpression decreased SGIV replication, whereas LC3 knockdown promoted SGIV replication. GS cells were transfected with HA-LC3 or the vector, siLC3 or the negative control (NC), and then infected with SGIV. Viral replication was analyzed by qPCR and IFA. **(A,D)** The LC3 expression in transfected cells. **(B,E)** The relative expression of MCP, ICP18, VP19, and LITAF in SGIV infected cells. The β-actin gene was used as the internal reference for qPCR. **(C,F)** The infected cells were analyzed at 12 h p.i. by IFA using anti-MCP antibody (green). Nuclei were stained by DAPI (blue). The viral infectivity of control cells was set as 1. The data were presented as the means from three independent experiment, $^{*}p < 0.05$, $^{**}p < 0.01$.

viral proteins as potential Atg5 or LC3 interactants were analyzed by co-IP and mass spectrometry. ORF122 (VP122) and ORF132 (VP132) of SGIV were identified in the IP products of GFP-Atg5 and GFP-LC3 (**Table 2**). It also has been reported that Atg5 can bind to the CARD domain of mitochondrial antiviral signaling protein (MAVS) and down-regulate innate antiviral immunity (Jounai et al., 2007). Based on the proteins known to be encoded by SGIV, we found that VP48 encodes a CARD domain protein (Song et al., 2004). Herein, we verified the interaction of Atg5 with VP122, VP132, MAVS, the MAVS-CARD domain, and VP48. We also verified the interaction of LC3 with VP122, VP132. By detecting the IP products of GFP-VP122 and GFP-VP132, we found that HA-Atg5 readily interacted with GFP-VP122, GFP-VP132 upon transient overexpression in GS cells (**Figures 3A,B**). The results showed that Atg5 interacted with MAVS and VP48, and more specifically with the CARD domain (**Figure 3C**). However, LC3 did not directly interact with VP122 and VP132.

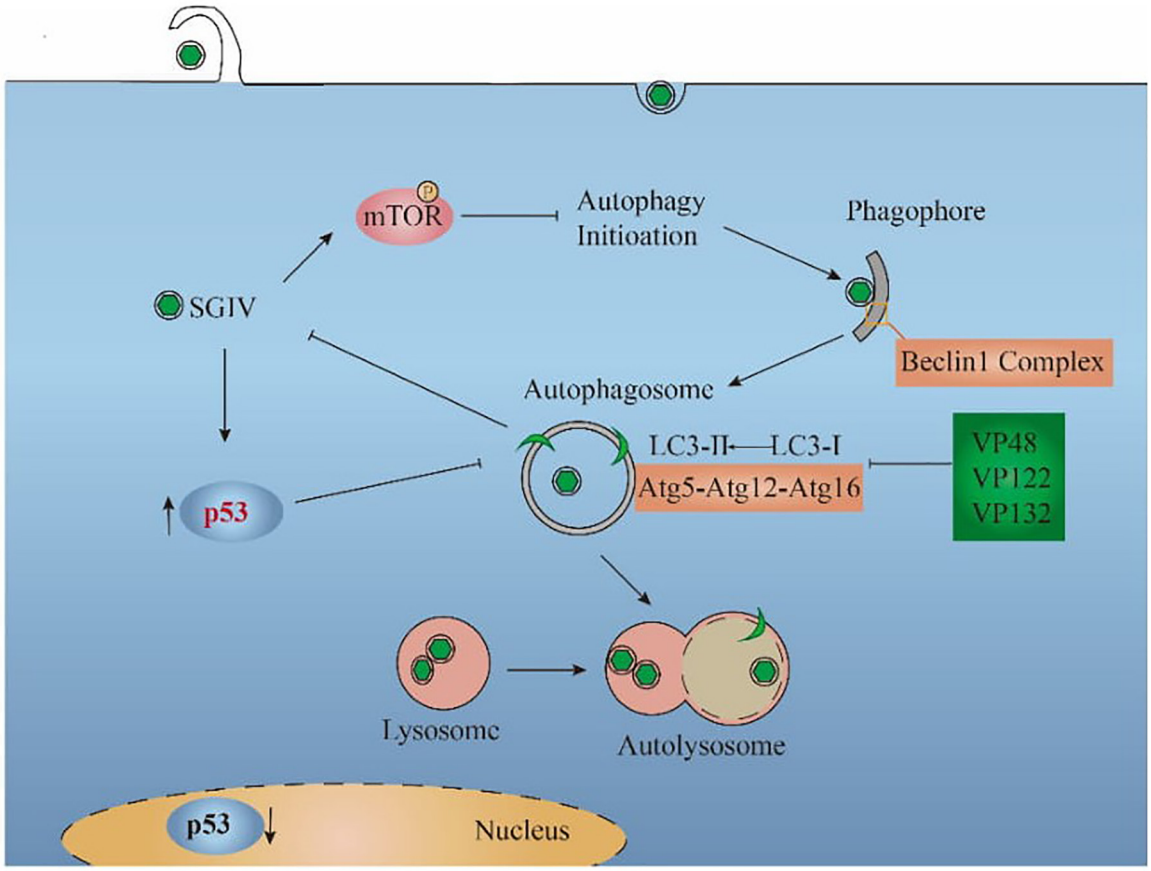

FIGURE 6 | Proposed model for the interaction between SGIV and autophagy. SGIV infection inhibited autophagy initiation, which is mTOR-dependent. The inhibition mechanisms of SGIV include increasing the cytoplasmic p53 level and encoding viral proteins (VP48, VP122, VP132), which bind Atg5 to block the LC3 conversion. From the perspective of the host cell, autophagy pathway decreased SGIV replication.

Atg5 plays an important role in the conversion of LC3-I to LC3-II, we speculated that VP48, VP122, and VP132 might competitively bind with Atg5, thereby blocking of the conversion of LC3-I to LC3-II. In this study, we evaluated the effect of VP48, VP122, and VP132 on the conversion of LC3-I to LC3-II and found that the level of LC3-II was decreased in VP48, VP122, and VP132 overexpressed cells (**Figure 3D**). To sum up, viral proteins can bind to Atg5 and downregulate levels of the autophagosome-associated form of LC3, which might be another strategy that allows SGIV to inhibit autophagy.

Inducing Autophagy by Rap Decreased SGIV Replication, Whereas Inhibiting Autophagy by WM Promoted SGIV Replication

Considering that SGIV inhibited autophagy, we deduced that autophagy might play an antiviral role upon SGIV replication. To verify this supposition, we treated the cells with Rap or WM for 2 h to induce or inhibit autophagy, respectively. The results showed that the LC3-II expression was increased in Rap-treated and decreased in WM-treated cells accordingly (**Figures 4A,D**). The pre-treated cells then were inoculated with SGIV to detect the effect of autophagy on viral replication. In this study, qPCR detection of the expression of viral genes, including *MCP*, *ICP18*, *VP19*, and *LITAF*, showed that they were all significantly decreased in Rap pre-treated cells compared to DMSO treated cells (**Figure 4B**). In addition, the immunofluorescence assay for SGIV major capsid protein (MCP) showed that MCP protein synthesis decreased after Rap treatment (**Figure 4C**). Conversely, the expressions of viral genes and MCP protein synthesis increased in WM pre-treated cells (**Figures 4E,F**). These results indicated that autophagy acts as a defense mechanism upon SGIV replication.

Overexpressing LC3 Decreased SGIV Replication, Whereas Silencing LC3 Promoted SGIV Replication

In addition to chemical regulators, we also explored the effect of autophagy on SGIV replication by overexpressing and silencing LC3. The overexpression and interference effects were reflected by LC3 expression. As shown as in **Figures 5A,D**, overexpressing or silencing LC3 increased or decreased LC3-II level accordingly.

The expressions of viral genes, including *MCP*, *ICP18*, *VP19*, and *LITAF*, were all significantly decreased in cells overexpressing LC3 (**Figure 5B**). The immunofluorescence of MCP showed that MCP protein synthesis also decreased in cells overexpressing LC3 (**Figure 5C**). In contrast, both viral gene expression and protein synthesis increased after silencing LC3 with siRNA (**Figures 5E,F**). These results indicated that LC3 exerted the antiviral role of autophagy against SGIV replication.

DISCUSSION

Autophagy is an essential process required to maintain cellular homeostasis. This process can be induced by various cellular stresses, including nutrient deprivation, oxidative stress, the unfolded protein response, and pathogen invasion (Deretic et al., 2013). A series of studies has demonstrated that some viral infections can alter the autophagy level, which functions as either a pro-viral or antiviral pathway, depending on the virus and its host cells (Lennemann and Coyne, 2015). In this study, we found that SGIV infection inhibited autophagy in GS cells. The strategies by which SGIV inhibited autophagy were demonstrated, which included causing the transfer of p53 from the nucleus to the cytoplasm and encoding some viral proteins that interact with Atg5 to block LC3 lipidation. As a defense mechanism, cellular autophagy and the key protein LC3 play the antiviral role in SGIV replication.

LC3-II is the protein marker that is reliably associated with completed autophagosomes (Klionsky et al., 2008). Beclin1, which forms a complex with Vps34, the class III phosphatidylinositol 3-kinase, is an important protein for autophagy initiation (Shrivastava et al., 2012). In this study, SGIV infection significantly decreased the LC3-II and Beclin1 protein levels. The mammalian target of Rap (mTOR) is generally considered to be an inhibitor of autophagy induction by inhibiting the phosphorylation of ULK1(Atg1) (Sarkar et al., 2009; Wong et al., 2013). Contrary to the trend of LC3-II and Beclin1, the p-mTOR level increased with the extension of infection time. Thus, we preliminarily speculated that SGIV inhibited autophagy and that the pathway was mTOR-dependent. Additional evidence for this inhibition was obtained using an autophagy inducer. In the case of Rap treatment, SGIV also decreased the LC3-II level and the number of autophagy positive cells. These results indicated that SGIV infection inhibited autophagy in GS cells. Similar phenomena have been reported for pseudorabies virus (Sun et al., 2017).

The cytoplasmic and nuclear p53 have different effects on autophagy (Tasdemir et al., 2008a; Morselli et al., 2011). The present study showed that SGIV replication led to the transfer of p53 from the nucleus to the cytoplasm. Moreover, the accumulation of LC3 (LC3-II) was inhibited in the p53 NLS^{-} cells, indicating that grouper p53 has functions similar to those of mammals in regulating autophagy. However, there are various mechanisms by which p53 can suppress autophagy directly or indirectly, independent or dependent on mTOR (Tasdemir et al., 2008b; Morselli et al., 2011; Tang et al., 2015). The specific mechanism by which p53 affects autophagy in SGIV infection needs further study. Interestingly, some viruses manipulate autophagy through interaction with autophagic proteins (Pirooz et al., 2014; Lennemann and Coyne, 2015; O'Connell and Liang, 2016). For example, human immunodeficiency virus-1 (HIV-1) precursor protein Gag interacts with LC3, which augments Gag processing and HIV yields (Kyei et al., 2009). Moreover, HIV-1 accessory protein Nef and HSV-1 ICP34.5 block autophagosome maturation through interaction with Beclin1 (Orvedahl et al., 2007; O'Connell and Liang, 2016). In our study, we demonstrated that SGIV VP48, VP122, and VP132 interacted with Atg5, which impeded the conversion of LC3-I to LC3-II. In addition, our previous studies have shown that Atg5 is a pro-viral factor during SGIV infection (Li et al., 2019a). Therefore, Atg5 is an important target for SGIV to hijack autophagy. Similar results have been reported for hepatitis C virus (Guevin et al., 2010). Whether there are other targets that SGIV utilizes to inhibit autophagy remains to be determined. Recent studies have shown that SGIV is equipped with some viral proteins to regulate apoptosis and escape the host immune and inflammation response (Huang et al., 2008; Yu et al., 2017). Our study showed that some viral proteins are involved in the autophagy pathway, which might be also related to the pathogenesis mechanisms of SGIV.

Previous studies have shown that the effect of autophagy on virus replication is virus and cell-type specific (Mohl et al., 2012; Deretic et al., 2013; Zhang et al., 2014; Sparrer and Gack, 2018). In our study, SGIV replication was inhibited by activation of autophagy by Rap or overexpression of LC3, whereas inhibition of autophagy by WM or silencing LC3 promoted viral replication. These findings indicate that SGIV cannot use autophagy-related membrane structures as viral replication sites. Similarly, GABARAP (a member of the Atg8 family) suppressed WSSV replication in hematopoietic tissue cells (Chen et al., 2016).

In **Figure 6**, the relationship between SGIV and autophagy was summarized based on the results of this study. SGIV infection inhibited autophagy by increasing the cytoplasmic p53 level and encoding VP48, VP122, and VP132, which bind Atg5 to affect the LC3 conversion. As an antiviral defense, autophagy pathway and the autophagic key protein LC3 suppressed SGIV replication. Further discoveries in the area of autophagy-mediated host defenses will help to provide new antiviral strategies.

DATA AVAILABILITY STATEMENT

The datasets generated for this study are available on request to the corresponding author.

AUTHOR CONTRIBUTIONS

QQ and JW designed the experiments. CL performed the majority of the experiments, analyzed data, and wrote the manuscript. LW, JL, and YY contributed to experimental suggestions. YH and XH helped to design the experiments. All authors revised the manuscript.

FUNDING

This work was supported by grants from the National Key R&D Program of China (2018YFD0900501 and 2018YFC0311302), Open Fund of Key Laboratory of Experimental Marine Biology, Chinese Academy of Sciences (No. KF2018NO3), National Natural Science Foundation of China (31772882 and 31572643), China Agriculture Research System (CARS-47-G16), Science and Technology Planning Project of Guangdong Province, China (2015TQ01N118), and National High Technology Development Program of China (863) (2014AA093507).

REFERENCES

Chen, R. Y., Shen, K. L., Chen, Z., Fan, W. W., Xie, X. L., Meng, C., et al. (2016). White spot syndrome virus entry is dependent on multiple endocytic routes and strongly facilitated by Cq-GABARAP in a CME-dependent manner. *Sci. Rep.* 6:28694. doi: 10.1038/srep28694

Deretic, V., Saitoh, T., and Akira, S. (2013). Autophagy in infection, inflammation and immunity. *Nat. Rev. Immunol.* 13, 722–737. doi: 10.1038/nri3532

Ding, B., Zhang, G., Yang, X., Zhang, S., Chen, L., Yan, Q., et al. (2014). Phosphoprotein of human parainfluenza virus type 3 blocks autophagosome-lysosome fusion to increase virus production. *Cell Host Microbe* 15, 564–577. doi: 10.1016/j.chom.2014.04.004

Garcia-Valtanen, P., Ortega-Villaizan Mdel, M., Martinez-Lopez, A., Medina-Gali, R., Perez, L., Mackenzie, S., et al. (2014). Autophagy-inducing peptides from mammalian VSV and fish VHSV rhabdoviral G glycoproteins (G) as models for the development of new therapeutic molecules. *Autophagy* 10, 1666–1680. doi: 10.4161/auto.29557

Guevin, C., Manna, D., Belanger, C., Konan, K. V., Mak, P., and Labonte, P. (2010). Autophagy protein ATG5 interacts transiently with the hepatitis C virus RNA polymerase (NS5B) early during infection. *Virology* 405, 1–7. doi: 10.1016/j.virol.2010.05.032

Hanada, T., Noda, N. N., Satomi, Y., Ichimura, Y., Fujioka, Y., Takao, T., et al. (2007). The Atg12-Atg5 conjugate has a novel E3-like activity for protein lipidation in autophagy. *J. Biol. Chem.* 282, 37298–37302. doi: 10.1074/jbc.C700195200

Huang, X., Huang, Y., Gong, J., Yan, Y., and Qin, Q. (2008). Identification and characterization of a putative lipopolysaccharide-induced TNF-α factor (LITAF) homolog from Singapore grouper iridovirus. *Biochem. Biophys. Res. Commun.* 373, 140–145. doi: 10.1016/j.bbrc.2008.06.003

Huang, X., Huang, Y., Sun, J., Han, X., and Qin, Q. (2009). Characterization of two grouper *Epinephelus akaara* cell lines: application to studies of Singapore grouper iridovirus (SGIV) propagation and virus-host interaction. *Aquaculture* 292, 172–179. doi: 10.1016/j.aquaculture.2009.04.019

Huang, Y., Zhang, J., Ouyang, Z., Liu, J., Zhang, Y., Hu, Y., et al. (2018). Grouper MAVS functions as a crucial antiviral molecule against nervous necrosis virus infection. *Fish Shellfish Immunol.* 72, 14–22. doi: 10.1016/j.fsi.2017.10.035

Jounai, N., Takeshita, F., Kobiyama, K., Sawano, A., Miyawaki, A., Xin, K. Q., et al. (2007). The Atg5 Atg12 conjugate associates with innate antiviral immune responses. *Proc. Natl. Acad. Sci. U.S.A.* 104, 14050–14055. doi: 10.1073/pnas.0704014104

Kang, R., Zeh, H. J., Lotze, M. T., and Tang, D. (2011). The Beclin 1 network regulates autophagy and apoptosis. *Cell Death Differ.* 18, 571–580. doi: 10.1038/cdd.2010.191

Katherine, R., Parzych, A. A., Muriel, M., and Klionsky, D. J. (2018). A newly characterized vacuolar serine carboxypeptidase, Atg42/Ybr139w, is required for normal vacuole function and the terminal steps of autophagy in the yeast\r Saccharomyces cerevisiae. *Mol. Biol. Cell* 29, 1089–1099. doi: 10.1091/mbc.E17-08-0516

Klionsky, D. J., Abeliovich, H., Agostinis, P., Agrawal, D. K., Aliev, G., Askew, B. A., et al. (2008). Guidelines for the use and interpretation of assays for monitoring autophagy in higher eukaryotes. *Autophagy* 4, 151–175. doi: 10.4161/auto.5338

Klionsky, D. J., Baehrecke, E. H., Brumell, J. H., Chu, C. T., Codogno, P., Cuervo, A. M., et al. (2011). A comprehensive glossary of autophagy-related molecules and processes (2nd edition). *Autophagy.* 7, 1273–1294. doi: 10.4161/auto.7.11.17661

Kyei, G. B., Dinkins, C., Davis, A. S., Roberts, E., Singh, S. B., Dong, C., et al. (2009). Autophagy pathway intersects with HIV-1 biosynthesis and regulates viral yields in macrophages. *J. Cell Biol.* 186, 255–268. doi: 10.1083/jcb.200903070

Lennemann, N. J., and Coyne, C. B. (2015). Catch me if you can: the link between autophagy and viruses. *PLoS Pathog.* 11:e1004685. doi: 10.1371/journal.ppat.1004685

Li, C., Fu, X., Lin, Q., Liu, L., Liang, H., Huang, Z., et al. (2017). Autophagy promoted infectious kidney and spleen necrosis virus replication and decreased infectious virus yields in CPB cell line. *Fish Shellfish Immunol.* 60, 25–32. doi: 10.1016/j.fsi.2016.11.037

Li, C., Liu, J., Zhang, X., Wei, S., Huang, X., Huang, Y., et al. (2019a). Fish autophagy protein 5 exerts negative regulation on antiviral immune response against iridovirus and nodavirus. *Front. Immunol.* 10:517. doi: 10.3389/fimmu.2019.00517

Li, C., Liu, J., Zhang, X., Yu, Y., Huang, X., Wei, J., et al. (2020). Red grouper nervous necrosis virus (RGNNV) induces autophagy to promote viral replication. *Fish Shellfish Immunol.* 98, 908–916. doi: 10.1016/j.fsi.2019.11.053

Li, C., Wang, L., Zhang, X., Wei, J., and Qin, Q. (2019b). Molecular cloning, expression and functional analysis of Atg16L1 from orange-spotted grouper (*Epinephelus coioides*). *Fish Shellfish Immunol.* 94, 113–121. doi: 10.1016/j.fsi.2019.09.004

Lin, Y., Wu, C., Wang, X., Liu, S., Zhao, K., Kemper, T., et al. (2019). Glucosamine promotes hepatitis B virus replication through its dual effects in suppressing autophagic degradation and inhibiting MTORC1 signaling. *Autophagy* 16, 548–561. doi: 10.1080/15548627.2019.1632104

Liu, L., Zhu, B., Wu, S., Lin, L., Liu, G., Zhou, Y., et al. (2015). Spring viraemia of carp virus induces autophagy for necessary viral replication. *Cell Microbiol.* 17, 595–605. doi: 10.1111/cmi.12387

Mizushima, N., Yoshimori, T., and Ohsumi, Y. (2011). The role of Atg proteins in autophagosome formation. *Annu. Rev. Cell Dev. Biol.* 27, 107–132. doi: 10.1146/annurev-cellbio-092910-154005

Mohl, B. P., Tedbury, P. R., Griffin, S., and Harris, M. (2012). Hepatitis C virus-induced autophagy is independent of the unfolded protein response. *J. Virol.* 86, 10724–10732. doi: 10.1128/JVI.01667-12

Morselli, E., Shen, S., Ruckenstuhl, C., Bauer, M. A., Marino, G., Galluzzi, L., et al. (2011). p53 inhibits autophagy by interacting with the human ortholog of yeast Atg17, RB1CC1/FIP200. *Cell Cycle* 10, 2763–2769. doi: 10.4161/cc.10.16.16868

O'Connell, D., and Liang, C. (2016). Autophagy interaction with herpes simplex virus type-1 infection. *Autophagy* 12, 451–459. doi: 10.1080/15548627.2016.1139262

Orvedahl, A., Alexander, D., Talloczy, Z., Sun, Q., Wei, Y., Zhang, W., et al. (2007). HSV-1 ICP34.5 confers neurovirulence by targeting the Beclin 1 autophagy protein. *Cell Host Microbe.* 1, 23–35. doi: 10.1016/j.chom.2006.12.001

Pirooz, S., He, S., O'Connell, D., Khalilzadeh, P., Yang, Y., and Liang, C. (2014). Viruses customize autophagy protein for efficient viral entry. *Autophagy.* 10, 1355–1356. doi: 10.4161/auto.29075

Qi, H., Yi, Y., Weng, S., Zou, W., He, J., and Dong, C. (2016). Differential autophagic effects triggered by five different vertebrate iridoviruses in a common, highly permissive mandarinfish fry (MFF-1) cell model. *Fish Shellfish Immunol.* 49, 407–419. doi: 10.1016/j.fsi.2015.12.041

Qin, Q. W., Chang, S. F., Ngoh-Lim, G. H., Gibson-Kueh, S., Shi, C., and Lam, T. J. (2003). Characterization of a novel ranavirus isolated from grouper *Epinephelus tauvina*. *Dis. Aquat. Organ.* 53, 1–9. doi: 10.3354/dao053001

Qin, Q. W., Lam, T. J., Sin, Y. M., Shen, H., Chang, S. F., Ngoh, G. H., et al. (2001). Electron microscopic observations of a marine fish iridovirus isolated from brown-spotted grouper, Epinephelustauina. *J. Virol. Methods.* 98, 17–24. doi: 10.1016/s0166-0934(01)00350-0

Sarkar, S., Ravikumar, B., Floto, R. A., and Rubinsztein, D. C. (2009). Rapamycin and mTOR-independent autophagy inducers ameliorate toxicity of polyglutamine-expanded huntingtin and related proteinopathies. *Cell Death Differ.* 16, 46–56. doi: 10.1038/cdd.2008.110

Shelly, S., Lukinova, N., Bambina, S., Berman, A., and Cherry, S. (2009). Autophagy is an essential component of *Drosophila* immunity against vesicular stomatitis virus. *Immunity*. 30, 588–598. doi: 10.1016/j.immuni.2009.02.009

Shrivastava, S., Bhanja Chowdhury, J., Steele, R., Ray, R., and Ray, R. B. (2012). Hepatitis C virus upregulates Beclin1 for induction of autophagy and activates mTOR signaling. *J. Virol.* 86, 8705–8712. doi: 10.1128/JVI.00616-12

Sir, D., Tian, Y., Chen, W., Ann, D. K., Yen, T.-S. B., and Ou, J.-H. J. (2010). The early autophagic pathway is activated by hepatitis B virus and required for viral DNA replication. *Proc. Natl. Acad. Sci. U.S.A.* 107, 4383–4388. doi: 10.1073/pnas.0911373107

Song, W. J., Qin, Q. W., Qiu, J., Huang, C. H., Wang, F., and Hew, C. L. (2004). Functional genomics analysis of Singapore grouper iridovirus: complete sequence determination and proteomic analysis. *J. Virol.* 78, 12576–12590. doi: 10.1128/JVI.78.22.12576-12590

Sparrer, K. M. J., and Gack, M. U. (2018). TRIM proteins: new players in virus-induced autophagy. *PLoS Pathog.* 14:e1006787. doi: 10.1371/journal.ppat.1006787

Sun, M., Hou, L., Tang, Y. D., Liu, Y., Wang, S., Wang, J., et al. (2017). Pseudorabies virus infection inhibits autophagy in permissive cells in vitro. *Sci. Rep.* 7:39964. doi: 10.1038/srep39964

Tang, J., Di, J., Cao, H., Bai, J., and Zheng, J. (2015). p53-mediated autophagic regulation: a prospective strategy for cancer therapy. *Cancer Lett.* 363, 101–107. doi: 10.1016/j.canlet.2015.04.014

Tasdemir, E., Maiuri, M. C., Galluzzi, L., Vitale, I., Djavaheri-Mergny, M., D'Amelio, M., et al. (2008a). Regulation of autophagy by cytoplasmic p53. *Nat. Cell Biol.* 10, 676–687. doi: 10.1038/ncb1730

Tasdemir, E., Maiuri, M. C., Orhon, I., Kepp, O., Morselli, E., Criollo, A., et al. (2008b). p53 represses autophagy in a cell cycle-dependent fashion. *Cell Cycle* 7, 3006–3011. doi: 10.4161/cc.7.19.6702

Wang, S., Huang, X., Huang, Y., Hao, X., Xu, H., Cai, M., et al. (2014). Entry of a novel marine DNA virus, singapore grouper iridovirus, into host cells occurs via clathrin-mediated endocytosis and macropinocytosis in a pH-dependent manner. *J. Virol.* 88:13047. doi: 10.1128/JVI.01744-14

Wang, Y., Chen, N., Hegazy, A. M., Liu, X., Wu, Z., Liu, X., et al. (2016). Autophagy induced by snakehead fish vesiculovirus inhibited its replication in SSN-1 cell line. *Fish Shellfish Immunol.* 55, 415–422. doi: 10.1016/j.fsi.2016.06.019

Wong, H. H., and Sanyal, S. (2019). Manipulation of autophagy by (+) RNA viruses. *Semin. Cell Dev. Biol.* 101, 3–11. doi: 10.1016/j.semcdb.2019.07.013

Wong, P. M., Puente, C., Ganley, I. G., and Jiang, X. (2013). The ULK1 complex: sensing nutrient signals for autophagy activation. *Autophagy.* 9, 124–137. doi: 10.4161/auto.23323

Xie, Z., and Klionsky, D. J. (2007). Autophagosome formation: core machinery and adaptations. *Nat. Cell Biol.* 9, 1102–1109. doi: 10.1038/ncb1007-1102

Yu, Y., Huang, Y., Ni, S., Zhou, L., Liu, J., Zhang, J., et al. (2017). Singapore grouper iridovirus (SGIV) TNFR homolog VP51 functions as a virulence factor via modulating host inflammation response. *Virology* 511, 280–289. doi: 10.1016/j.virol.2017.06.025

Zhang, Y., Li, Z., Ge, X., Guo, X., and Yang, H. (2014). Autophagy promotes the replication of encephalomyocarditis virus in host cells. *Autophagy* 7, 613–628. doi: 10.4161/auto.7.7.15267

Zhou, Z., Jiang, X., Liu, D., Fan, Z., Hu, X., Yan, J., et al. (2009). Autophagy is involved in influenza A virus replication. *Autophagy* 5, 321–328. doi: 10.4161/auto.5.3.7406

Conflict of Interest: The authors declare that the research was conducted in the absence of any commercial or financial relationships that could be construed as a potential conflict of interest.

frontiers in Microbiology

ORIGINAL RESEARCH
published: 08 July 2020
doi: 10.3389/fmicb.2020.01558

Cellular Organelles Reorganization During Zika Virus Infection of Human Cells

Cybele C. García[1,2], Cecilia A. Vázquez[1,2], Federico Giovannoni[1,2], Constanza A. Russo[1,2], Sandra M. Cordo[1,2], Agustina Alaimo[1,2] and Elsa B. Damonte[1,2]**

[1] Departamento de Química Biológica, Facultad de Ciencias Exactas y Naturales, Universidad de Buenos Aires, Buenos Aires, Argentina, [2] Instituto de Química Biológica de la Facultad de Ciencias Exactas y Naturales (IQUIBICEN), Consejo Nacional de Investigaciones Científicas y Técnicas-Universidad de Buenos Aires, Ciudad Universitaria, Buenos Aires, Argentina

Zika virus (ZIKV) is an enveloped positive stranded RNA virus belonging to the genus *Flavivirus* in the family *Flaviviridae* that emerged in recent decades causing pandemic outbreaks of human infections occasionally associated with severe neurological disorders in adults and newborns. The intracellular steps of flavivirus multiplication are associated to cellular membranes and their bound organelles leading to an extensive host cell reorganization. Importantly, the association of organelle dysfunction with diseases caused by several human viruses has been widely reported in recent studies. With the aim to increase the knowledge about the impact of ZIKV infection on the host cell functions, the present study was focused on the evaluation of the reorganization of three cell components, promyelocytic leukemia nuclear bodies (PML-NBs), mitochondria, and lipid droplets (LDs). Relevant human cell lines including neural progenitor cells (NPCs), hepatic Huh-7, and retinal pigment epithelial (RPE) cells were infected with the Argentina INEVH116141 ZIKV strain and the organelle alterations were studied by using fluorescent cell imaging analysis. Our results have shown that these three organelles are targeted and structurally modified during ZIKV infection. Considering the nuclear reorganization, the analysis by confocal microscopy of infected cells showed a significantly reduced number of PML-NBs in comparison to uninfected cells. Moreover, a mitochondrial morphodynamic perturbation with an increased fragmentation and the loss of mitochondrial membrane potential was observed in ZIKV infected RPE cells. Regarding lipid structures, a decrease in the number and volume of LDs was observed in ZIKV infected cells. Given the involvement of these organelles in host defense processes, the reported perturbations may be related to enhanced virus replication through protection from innate immunity. The understanding of the cellular remodeling will enable the design of new host-targeted antiviral strategies.

Keywords: Zika virus, promyelocytic leukemia nuclear bodies, mitochondria, lipid droplets, flavivirus

OPEN ACCESS

Edited by:
Indranil Banerjee, Indian Institute of Science Education and Research Mohali, India

Reviewed by:
Bo Zhang, Key Laboratory of Special Pathogens and Biosafety (CAS), China
Ana Belen Blazquez, Instituto Nacional de Investigación y Tecnología Agraria y Alimentaria (INIA), Spain

****Correspondence:***
Cybele C. García
cygarcia@qb.fcen.uba.ar, cybele.garcia@gmail.com
Elsa B. Damonte
edamonte@qb.fcen.uba.ar

Specialty section:
This article was submitted to Virology, a section of the journal Frontiers in Microbiology

Received: *13 March 2020*
Accepted: *16 June 2020*
Published: *08 July 2020*

Citation:
García CC, Vázquez CA, Giovannoni F, Russo CA, Cordo SM, Alaimo A and Damonte EB (2020) Cellular Organelles Reorganization During Zika Virus Infection of Human Cells. Front. Microbiol. 11:1558. doi: 10.3389/fmicb.2020.01558

INTRODUCTION

Zika virus (ZIKV) is an enveloped positive stranded RNA virus belonging to the genus *Flavivirus* in the family *Flaviviridae*, which includes other relevant pathogenic arboviruses such as dengue virus (DENV), yellow fever virus (YFV), Japanese encephalitis virus (JEV), and West Nile virus (WNV). ZIKV was initially identified in the Zika forest of Uganda in 1947 from a sentinel rhesus monkey

(Dick et al., 1952). Since its discovery, the infrequent human infections reported in Africa and Asia were asymptomatic or generally associated with very mild clinical manifestations (Gubler et al., 2017). This situation dramatically changed in more recent years when ZIKV spread across Asia first to the Pacific Islands and was then introduced into Brazil in 2014. From Brazil, ZIKV was rapidly disseminated throughout the Americas and other regions, with more than 80 countries currently reporting ZIKV autochthonous transmission. Unlike other flaviviruses, the major outbreaks caused by the Asian lineage of ZIKV, particularly in Brazil, were associated with severe neurological complications such as high frequency of newborns with congenital microcephaly (Calvet et al., 2016; Mlakar et al., 2016) and an increase in the number of adults presenting the Guillain-Barré syndrome (Brasil et al., 2016; doRosário et al., 2016). Other major concerns include meningo-encephalitis, myelitis, and ocular abnormalities (Carteaux et al., 2016; Mecharles et al., 2016; Ventura and Ventura, 2018). Most ZIKV human infections are transmitted by the *Aedes aegypti* and *Aedes albopictus* mosquitoes; however, human to human transmission can also occur through sexual contact, vertically from mother to fetus, and by blood transfusion (Musso et al., 2015; Tabata et al., 2016). In fact, the congenital neurological malformations and the sexual transmission have turned ZIKV unique among flaviviruses and highlighted the wide viral tropism that is determinant of the significant pathogenesis.

At present, no specific antiviral agents are available for ZIKV treatment. Increasing evidence has accumulated in recent years about the efficacy of host-targeted therapeutics to obtain a wide spectrum drug active against several related viruses through the interference with cellular factors required to complete an infective virus replication cycle (Acosta and Bartenschlager, 2016; García et al., 2018; Saiz et al., 2018). Additionally a host-directed compound has lower potential to select for resistant variants. For this antiviral strategy, the basic aspects of the virus-cell interaction must be elucidated. After binding and entry by receptor mediated endocytosis, the ZIKV genome is translated in a single polypeptide that is cleaved by viral and host proteases into three structural proteins (the capsid C, the premembrane prM, and the envelope E) that are assembled with RNA in the virion, and seven non-structural (NS) proteins (NS1, NS2A, NS2B, NS3, NS4A, NS4B, and NS5) that are involved in viral replication, pathogenesis, and host antiviral response (Shi and Gao, 2017). All the intracellular steps of flavivirus multiplication are associated to cellular membranes and their bound organelles, leading to an extensive host cell reorganization. As previously reported for DENV and other mosquito-borne flaviviruses, the endoplasmic reticulum (ER) plays a central role in ZIKV infection. In mosquito C6/36 cells and diverse mammalian cells, including Vero and human hepatoma and neuronal progenitor cells, major rearrangements of the ER after ZIKV infection were demonstrated (Barreto-Vieira et al., 2017; Cortese et al., 2017; Offerdahl et al., 2017; Rossignol et al., 2017). Noted morphological changes include membrane invaginations, with development of structures integral to RNA replication, designed replication factories, which are surrounded by drastically reorganized microtubules and intermediate filaments. Concomitantly, virus assembly and budding takes place at ER regions proximal to the replication sites.

In addition to the ER, other cellular organelles are morphologically remodeled and functionally perturbed by flaviviruses. Very active research is available for the role of such organelles, like mitochondria, peroxisomes, lipid droplets (LDs), nuclear compartments and others, in DENV infection (Samsa et al., 2009; Carvalho et al., 2012; Jordan and Randall, 2017), but very few studies have been performed with ZIKV. The targeting of cellular organelles in ZIKV infection has been proved by studies of intracellular localization of viral proteins through immunocytochemistry and proteomics analysis (Hou et al., 2017; Coyaud et al., 2018). But the current knowledge of alterations in several organelles parameters, like morphology, content, dynamics and, consequently, their function, as result of ZIKV infection is still scarce. Since the involvement of most organelles in innate immunity and host defense is well known, the characterization of the virus-induced intracellular reorganization is a key step in order to understand and counteract the mechanisms of virus infection.

Promyelocytic leukemia nuclear bodies (PML-NBs) are nuclear membraneless organelles which contain several cellular proteins, among them mainly PML protein, involved in intrinsic antiviral responses against a number of viruses (Borden, 2002; Geoffroy and Chelbi-Alix, 2011; Scherer and Stamminger, 2016; Guion and Sapp, 2020). Our previous studies have shown that PML exerts antiviral activity against the four DENV serotypes. Furthermore, microscopic analysis revealed that PML-NBs are disrupted after DENV infection due to the interaction of NS5 protein and PML protein, contributing to the DENV induced suppression of the host antiviral response (Giovannoni et al., 2015, 2019). Considering that the nuclear localization of 3 viral proteins, C, NS1, and NS5, has been described in ZIKV infected Vero cells through immunocytochemistry observations (Hou et al., 2017), here we extend our studies to explore the impact of ZIKV infection on PML-NB structure. Moreover, we also evaluated the effect on the organization of two cytoplasmic organelles also participating in the host defense, mitochondria and LDs, in ZIKV infected human cells.

MATERIALS AND METHODS

Cells and Virus

Human hepatoma Huh-7 and monkey Vero (ATCC, CCL81) cells were grown in Dulbecco's Modified Eagle's medium (DMEM, GIBCO) supplemented with 10 % fetal bovine serum (FBS), 100 IU/ml of penicillin and 100 μg/ml of streptomycin.

Neural progenitor cells (NPCs; ≥90% SOX1+/Nestin+) derived from human pluripotent stem cells (PSCs) under serum-free conditions (Stem Cell Technologies, Catalog # 70901, https://cdn.stemcell.com/media/files/pis/DX21378-PIS_1_1_0.pdf) were grown using neural progenitor medium 2 (Stem Cell Technologies).

Two human retinal pigment epithelial (RPE) cell lines were employed: ARPE-19 (ATCC® CRL-2302™) cell line was kindly

provided by Dr. J.G. Galletti and Dr. M. Guzmán (Instituto de Medicina Experimental IMEX, Buenos Aires, Argentina). The human-Telomerase Reverse Transcriptase immortalized RPE cell line (hTERTRPE-1; ATCC®CRL-4000™) cell line was gently provided by Dr. C.A. Bueno (IQUIBICEN, Buenos Aires, Argentina). ARPE-19 is a spontaneously arising RPE cell line of male origin that maintains normal karyology as well as structural and functional properties of RPE cells *in vivo* (Dunn et al., 1996). hTERTRPE-1 is a near-diploid human cell line of female origin with a modal chromosome number of 46 in 90% of the cells counted (Rambhatla et al., 2002). Cells were cultured in DMEM supplemented with 10% heat- inactivated FBS, 2.0 mM glutamine, 100 units/ml penicillin, 100 μg/ml streptomycin, and 0.25 μg/ml amphotericin.

The C6/36 mosquito cell line (from *Aedes albopictus*, ATCC CRL-1660), adapted to grow at 33°C, was cultured in L-15 medium (Leibovitz; GIBCO) supplemented with 0.3% tryptose phosphate broth, 0.02% glutamine, 1% MEM non-essential amino acids solution and 10% FBS. All cell lines were authenticated and tested for contamination.

The ARG INEVH116141 strain of ZIKV (ZIKV-AR) was provided by the Instituto Nacional de Enfermedades Virales Humanas "Dr. Julio I. Maiztegui," Pergamino, Argentina. Virus stocks were prepared in C6/36 cells and titrated by a standard plaque assay in Vero cells.

All work with infectious agents was performed in biosafety level 2 facilities and approved by the Office of Environmental Health and Safety at the School of Sciences, University of Buenos Aires.

Confocal Immunofluorescence, Imaging and Quantification of PML-NBs and Mitochondria in ZIKV Infected Cells

Immunofluorescence was performed as previously described (Alaimo et al., 2019; Giovannoni et al., 2019). Briefly, NPCs, ARPE-19, and hTERT RPE-1 cells grown on coverslips were infected with ZIKV at a multiplicity of infection (MOI) of 0.1. After 48 h of infection, cells were fixed with paraformaldehyde (PFA) 4%, permeabilized with Triton X-100 0.1% and stained for immunofluorescence. Primary antibodies used were: anti-PML (Santa Cruz Biotechnology, sc-966, 1:300), anti-NS5 (Genetex, GTX133312, 1:300), anti-TOM20 (sc-11415, Santa Cruz Biotechnology, 1:300), and anti-flavivirus E (Abcam, ab155882, 1:300). Secondary antibodies were: Alexa Fluor 488-anti–rabbit/mouse IgG (Thermo Fisher Scientific, Waltham, MA, United States, 1:400) and Alexa Fluor 555-anti–mouse IgG (Thermo Fisher Scientific, 1:400). Finally, coverslips were mounted in Prolong Gold mounting medium with 4', 6-diamidino-2-phenylindole (DAPI; Thermo Fisher Scientific). Samples were examined under epifluorescence and confocal microscope Olympus IX71 and FV300, respectively, (Olympus Optical Co., Tokyo, Japan) employing an Olympus 60× oil-immersion Plan Apo objective. Digital images were optimized for contrast and brightness using Adobe Photoshop 7.0 Software.

Quantification of the average number of PML-NBs per cell nucleus was performed using the Fiji distribution of ImageJ. Each cell to be counted was selected and the Find Maxima tool was used. 3D reconstruction of PML-NBs in ZIKV-infected NPCs were generated using the Volume Viewer plugin in Fiji. 2.5D intensity plots were generated using Zen Blue software (Carl Zeiss).

To quantify the mitochondrial morphologies, 100 cells/sample were scored and classified as cells exhibiting tubular (normal) and fragmented (small and spherical) mitochondria according to (Alaimo et al., 2019; 2020). Confocal images were subjected to 3D reconstructions through Fiji imaging software by applying "3D Volume" plugin [National Institutes of Health (NIH) Bethesda, MD], according to (Chatel-Chaix et al., 2016).

Mitochondrial Membrane Potential Analysis

ARPE-19 cells grown on coverslips were infected with ZIKV (MOI of 0.1). At 48 h post infection (p.i.), supernatant was discarded, cells were washed twice with PBS and incubated with the cell-permeant mitochondria-specific fluorescent reagent MitoTracker Red CMXRos (150 nM in serum-free media, 30 min, 37°C). Accordingly to manufacturer's indications, this probe stains mitochondria in live cells and its accumulation is dependent upon membrane potential. Afterwards, cells were washed twice with PBS and fixed with 4% PFA (20 min at room temperature). Finally, cells were washed with PBS and mounted on glass slides. Samples were examined under a fluorescence microscope Olympus IX71 equipped with objective lens 60X/1.43 oil (λex: 543/20 nm; λem: 593/40 nm). Capture selected images were optimized for contrast and brightness using Adobe Photoshop 7.0 Software.

Lipid Droplet Count and Volume Determinations

Huh-7 cells grown on coverslips were infected with ZIKV at a MOI of 0.1. At 24 h p.i., cells were fixed with PFA 4%, permeabilized with Triton X-100 0.1% and stained for immunofluorescence. Antibodies used were anti-flavivirus E (Abcam, ab155882, 1:300) and Alexa Fluor 488-anti–rabbit IgG (Thermo Fisher Scientific, 1:400). The LDs specific probe used was HCS LipidTOX™ Deep Red Neutral Lipid Stain (H34477, Thermo Fisher, 1:250).

Z-stacks were acquired in a confocal Olympus – FV1000, at 500 nm intervals and analyzed using Fiji software. First, ZIKV infected cells were selected using green channel. This channel was used to select the regions of interest (ROIs) pertaining to individual cells in images of both non-infected and infected cell cultures (**Supplementary Figures 1A,I**). In the case of non-infected cultures, cell autofluorescence signal was enough to detect individual cells (**Supplementary Figure 1A**, see inset). This channel was filtered with a "Gaussian blur" filter with a radius of 40 and binarized using a "Mean" threshold, which sets the threshold as the mean gray level of the stack (**Supplementary Figures 1B,C,J,K**). When needed, the resulting binary mask was refined with "Close," "Fill Holes" or "Watershed" algorithms in order to ensure that the whole cell surface was being selected (**Supplementary Figures 1D,L**).

The final binary mask was analyzed with the "Find Particles" plugin to obtain the ROIs corresponding to each cell in every plane of the *Z*-stack (**Supplementary Figures 1E,M**). Unspecific background was subtracted from LipidTox channel (**Supplementary Figures 1F,N**) and "3D Object Counter" plugin was used to select LDs (**Supplementary Figures 1G,O**). Each LDs was assigned to a cell using "Intensity Measurements 2D/3D in MorphoLibJ" library. Volumes of all LDs in the same cell were added to determine total LDs volume. In order to determine the number of LDs per cell, "Find Maxima" plugin was used, with a prominence <45 (**Supplementary Figures 1H,P**).

Statistical Analysis

Experiments were carried out in triplicate unless otherwise stated. Experimental comparisons between treatments were made by *t*-Student's test with statistical significance set at $p < 0.05$. All analyses were carried out with GraphPad Prism 5 software (San Diego, CA, United States).

RESULTS

ZIKV Infection Promotes PML-NBs Disruption

Promyelocytic leukemia nuclear bodies are highly dynamic nuclear structures that involve the entry of enzymes and substrates to carry out various cellular functions. Without PML-NBs, these processes would be less efficient or not possible at all in the cytoplasm. Importantly, PML-NBs have shown to limit viral replication in several viral models through multiple mechanisms, and in consequence, many viruses encode products that modify the localization or eliminate PML-NBs in cultured cells (Geoffroy and Chelbi-Alix, 2011; Giovannoni et al., 2015; Brown et al., 2016; Schilling et al., 2017). PML is the major structural component of PML-NBs, and their stability depends on PML presence. In this context, any PML role in ZIKV infection is still unknown.

It is well established that ZIKV replicates in NPCs (Qian et al., 2016) provoking alterations of cellular pathways which are thought to promote Zika's congenital syndrome brain abnormalities (Calvet et al., 2016; Mlakar et al., 2016; Yockey et al., 2016; Chavali et al., 2017). Since those studies were performed with different ZIKV strains, we sought to determine the NPCs cultures permissiveness to our viral model. Thus, NPCs were infected with ZIKV-AR and supernatants were collected at 24 and 48 h p.i., for extracellular viral particle quantification. Also, viral antigen detection was performed by IFI. At 24 h p.i. viral yield resulted in 1×10^4 PFU/ml, but no significant viral protein expression was quantified. However, at 48 h p.i. viral titer increased to1.5×10^5 PFU/ml and accordingly, 47% of NPCs were expressing the NS5viral protein (**Figures 1A,B**). In order to explore the PML-NBs distribution in ZIKV infected NPCs, double immunofluorescence studies were performed employing antibodies against the NS5 viral protein, of nuclear localization, and against PML. **Figure 1C** shows representative images from 48 h infected NPCs cultures. 3D reconstruction of high-resolution confocal Z-series images (**Figure 1D**) showing PML (red channel) and NS5 (green channel) and a meticulous analysis using Zen Blue Software (**Figure 1E**) allowed to quantify the number of PML-NBs in the ZIKV infected cell samples (**Figure 1F**). As can be seen in NS5 negative ZIKV cells, the typical punctuated nuclear staining pattern of PML-NBs corresponding to the red channel, with an average number of 5 PML-NBs/cell in these control cells, was found. In contrast, a clear and significant decrease in the number of these structures was found in ZIKV infected cells averaging 2.5 PML-NBs/cell. These data are summarized in **Figure 1F** accounting for a 52 % reduction of PML-NBs in ZIKV infected NPCs cultures in comparison to non-infected ones.

ZIKV Infection Disturbs Mitochondrial Dynamics

Mitochondria are highly dynamic organelles that can fuse and divide during cell life cycle, and these processes are regulated by a tight equilibrium between two antagonistic events: fusion and fission. This balance plays a critical role in preserving functional mitochondria and consequently, in cell physiology (Pernas and Scorrano, 2016; Giacomello et al., 2020), and can get easily disturbed under intracellular or extracellular stresses. The exploration of the interplay between those stressors, the mitochondrial dynamics and the mechanisms that coordinates how cells respond to them is essential for the understanding of the turnover from health to disease (Eisner et al., 2018). Not surprisingly, it has been suggested that viral infections employ mitochondrial dynamics alteration for the maintenance of persistent infection (Khan et al., 2015; Kim et al., 2018).

Ocular abnormalities present in microcephalic infants with presumed ZIKV congenital disease include conjunctivitis, changes in retinal pigmentation, chorioretinal atrophy, optic nerve abnormalities, hemorrhagic retinopathy and abnormal retinal vasculature (Roach and Alcendor, 2017). In addition, ZIKV preferentially infects Müller and RPE cells, impairing their neurotrophic functions, and eliciting retinal inflammatory responses (Zhao et al., 2017). Notably, the RPE localized in the macular area lies in a high oxidative environment, because of its high metabolic demand, reactive oxygen species (ROS) levels, blood flow and mitochondria content (Moine et al., 2018; Dieguez et al., 2019; Alaimo et al., 2020). The permissiveness of the RPE to viral infections makes it a pertinent tissue to explore the host-cell interactions (Simonin et al., 2019).

To gain further insight on this interplay, human ARPE-19, and hTERTRPE-1 cell lines were employed to determine the effect of ZIKV on mitochondrial dynamics. Initially, we evaluated the level of viral infection that could be achieved on these cell systems. RPE cell cultures were infected and supernatants were collected at 24 and 48 h p.i. for viral titers quantification by plaque assay. No extracellular viral particles were detected at 24 h p.i. However, 7.8×10^3 PFU/ml, and 6×10^3 PFU/ml were determined at 48 h p.i. on human ARPE-19 and hTERT RPE-1 infected cell lines, respectively, (**Figure 2A**). In agreement with these results, cytopathic effects were observed under light microscopy only at 48 h p.i. (**Figure 2B**). At this time, 50% of cells expressing viral

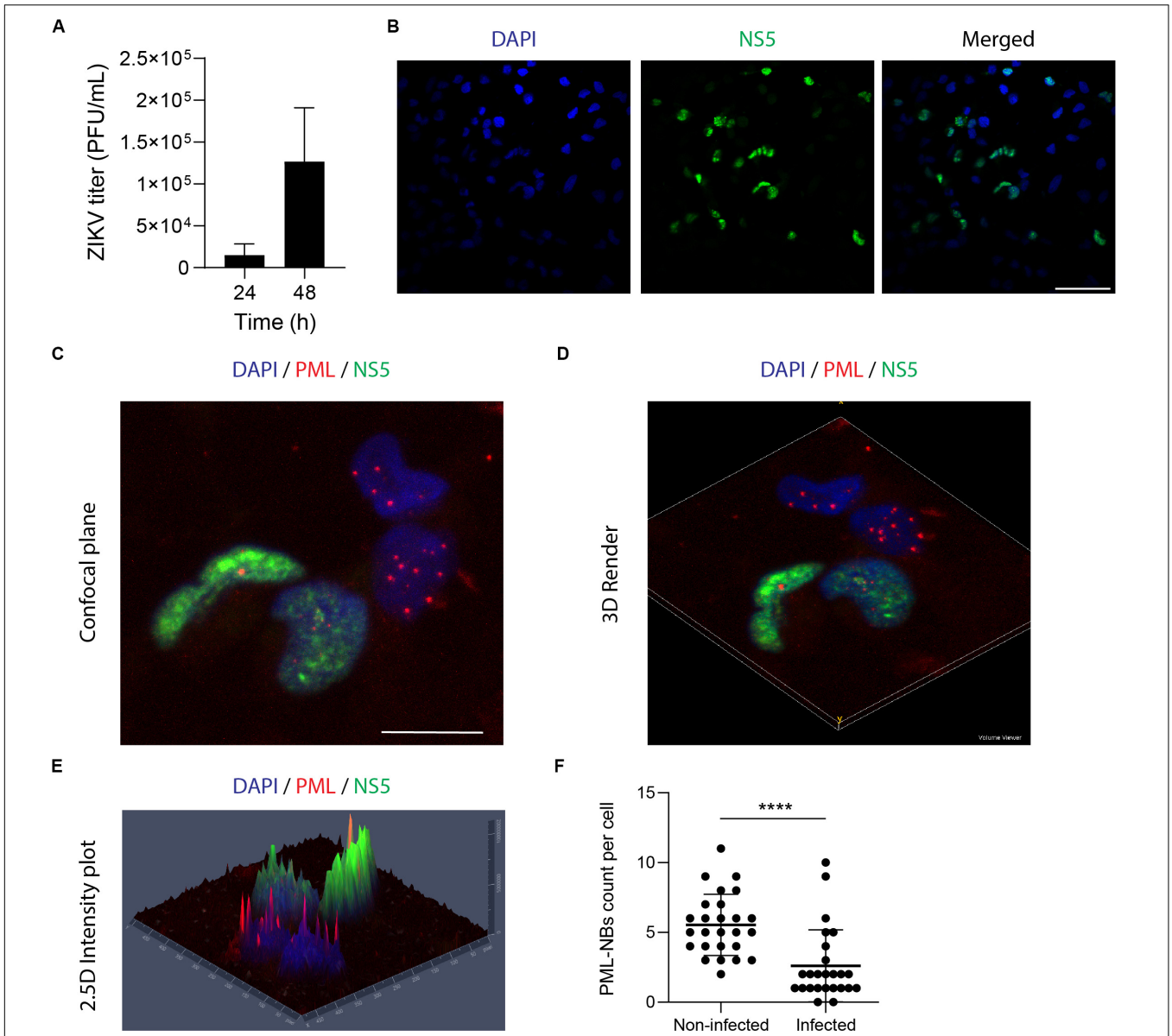

FIGURE 1 | ZIKV infection reduces the number of PML-NBs in NPCs. **(A)** NPCs were infected with ZIKV and supernatants were harvested for plaque assay at 24 h and 48 h p.i. Data represent the mean ± SD (n = 3 independent experiments). **(B)** NPCs were infected with ZIKV for 48 h, fixed, and stained against NS5 (green). Nuclei were counterstained with DAPI. Scale bar: 50 μm. **(C)** NPCs were infected with ZIKV for 48 h, fixed and stained against NS5 (green), and PML (red). Nuclei were counterstained with DAPI. Scale bar: 10 μm. **(D)** 3D reconstruction of PML-NBs in ZIKV-infected NPCs was generated using the Volume Viewer Plugin in Fiji. **(E)** 2.5D intensity plot of PML-NBs in ZIKV-infected NPCs was generated using Zen Blue Software. Individual peaks represent absolute signal intensities of each pixel. **(F)** Quantification of the average number of PML-NBs in ZIKV-infected and non-infected NPCs. Data represent the mean ± SD (n = 25 cells per condition). ****$p < 0.001$ p value was determined by a two-sided Student's t-test.

antigen were determined by immunofluorescence in both RPE cell cultures (**Figure 2C**). Taking together these findings, we decided to perform mitochondrial dynamics studies at this time point of infection.

ARPE-19 (**Figure 3A**) and hTERT RPE-1 (**Figure 3B**) cells were infected with ZIKV and fixed at 48 h p.i.. Immunocytochemical studies of TOM-20 (a central component of TOM, translocase of the outer membrane receptor complex) were performed to analyze mitochondrial morphology. Non-infected ARPE-19 and hTERT RPE-1 cells displayed tubular, filamentous- like mitochondria. On the other hand, ZIKV infection induced a dramatical increase in the population of both RPE cell lines with punctiform fragmented mitochondria (**Figures 3A,B**).

In a complementary way, we generated a 3D image reconstruction and volumetric rendering corresponding to samples visualized with fluorescence microscopy. Tubular

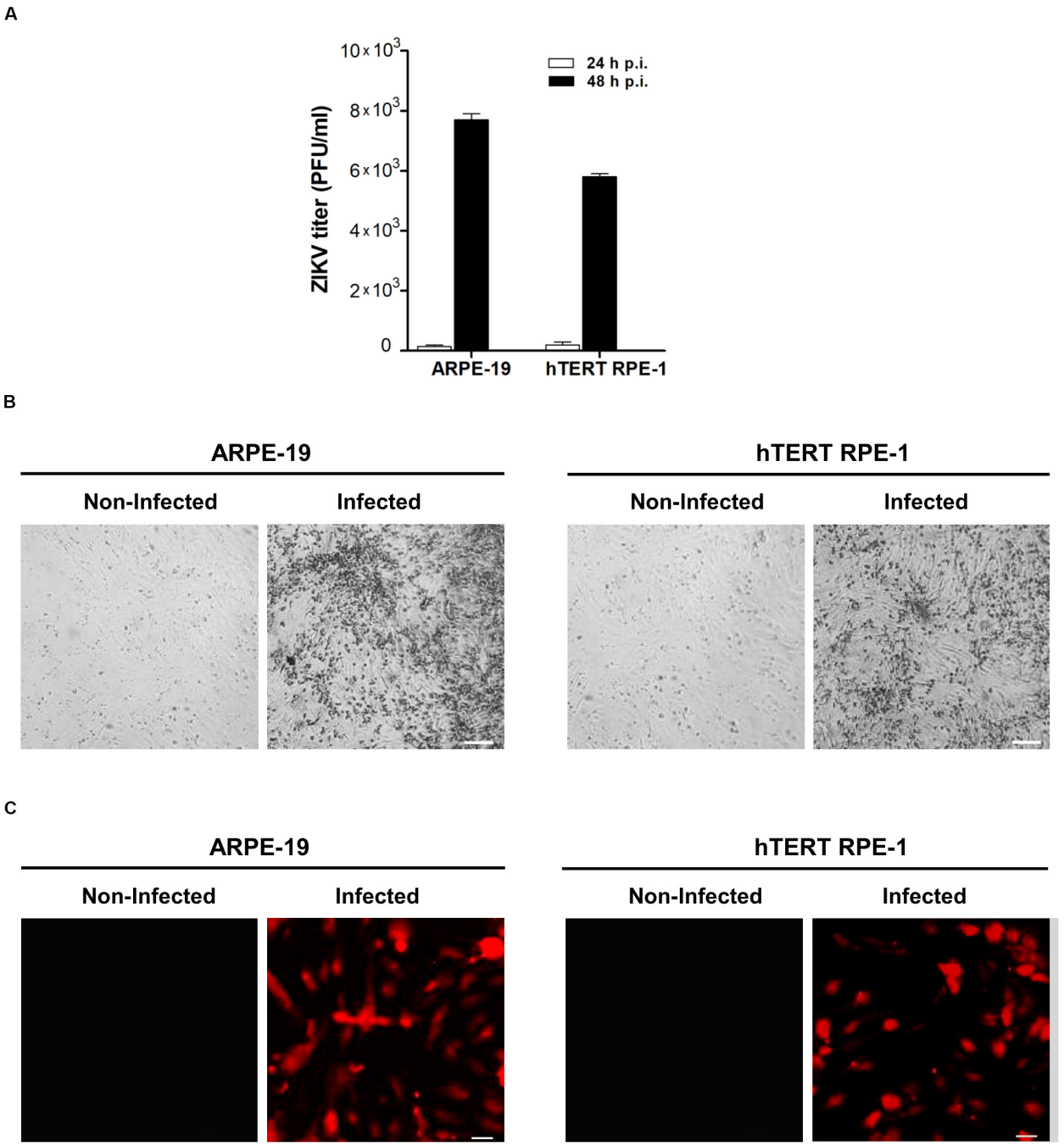

FIGURE 2 | ZIKV infection in human RPE cells. **(A)** ARPE-19 and hTERT RPE-1 cells were infected with ZIKV and infectious virus particles were determined in supernatants at 24 or 48 h p.i., by plaque assay in Vero cells. Data represent the mean ± SD from three independent experiments. **(B)** Morphological signs of cytopathic effects in ZIKV-infected RPE cells at 48 p.i. detected by phase-contrast microscopy. Scale bar: 50 μm. **(C)** ARPE-19 and hTERT RPE-1 cells infected with ZIKV were fixed and stained for flavivirus E protein at 48 h p.i.. Scale bar: 10 μm.

structures that move in and out of the focal plane can be easily mistaken for individual rod or spherical organelles in conventional imaging (Olichon et al., 2003; Alaimo et al., 2014). Consequently, the stacks acquisition of mitochondrial images along the *Z*-axis of the entire cell provided us a more exhaustive visualization and quality of the morphological alterations that occur in mitochondria of infected cells. In addition, *Z*-stacks acquisition allowed us to establish a more exact morphological classification of these organelles (**Figures 4A–C**). By this way, an increased cellular population with fragmented mitochondria were quantified in both ARPE-19 (54.4%, $p < 0.001$), and hTERT RPE-1 (54.5%, $p < 0.001$) cells (**Figures 4D,E**).

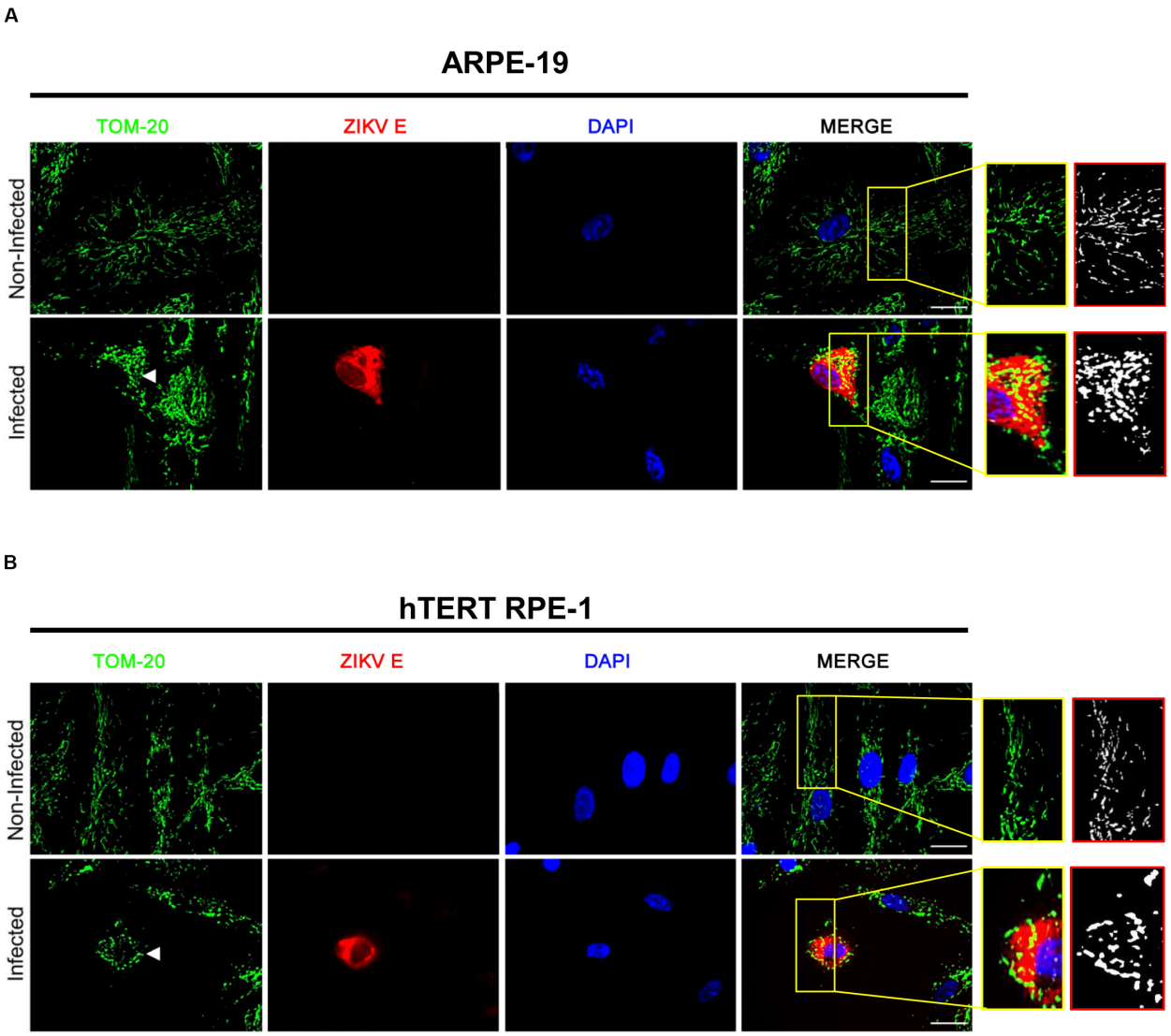

FIGURE 3 | Effect of ZIKV infection on mitochondrial dynamics in RPE cells. ARPE-19 **(A)** and hTERT RPE-1 **(B)** cells were infected with ZIKV at MOI of 0.1 or left uninfected. At 48 h p.i., cells were fixed, permeabilized and mitochondria, viral E glycoprotein and nuclei were stained with anti-TOM-20, 4G2 anti-E mAb, and DAPI, respectively. White arrowhead indicates the branching mitochondrial networks disruption denoted by punctate mitochondria. Insets: for a better visualization of mitochondrial morphology, zoomed areas of grayscale images were pooled to obtain binary images.

Finally, a mitochondrial morphodynamic perturbation with a loss of mitochondrial membrane potential ($\Delta\varphi m$) was observed in ARPE-19 cells infected with ZIKV (**Figures 5A,B**). Overall, these analyses demonstrate that ZIKV infection induces an imbalance in fusion/fission equilibrium in favor to the latter event.

ZIKV Infection Reduces Lipid Droplet Number

Lipid droplets are dynamic intracellular organelles which are required for storing lipids in a cell. They play a major role in energy homeostasis and membrane trafficking (Herker and Ott, 2012). It is very well known that many RNA viruses exploit the LDs energy storing capacity to facilitate their replication (Herker and Ott, 2012). Previous investigations and our data from microarray analysis, which showed the interplay between DENV and lipid pathways, led us to study the LDs pattern changes along the replication of ZIKV (Heaton and Randall, 2011; Martín-Acebes et al., 2016; Vázquez et al., 2019).

In addition to cytosolic LDs that are present in most other cell types, hepatocytes contain at least two more types of LDs in the lumen of the ER where ZIKV replication occurs, representing the most suitable cellular model to study LDs parameters along flavivirus infection. Different reports have shown opposite results on the LDs modulation exerted by flavivirus infection. Both increased (Samsa et al., 2009) and decreased (Heaton and Randall, 2010, 2011) numbers of LDs have been documented

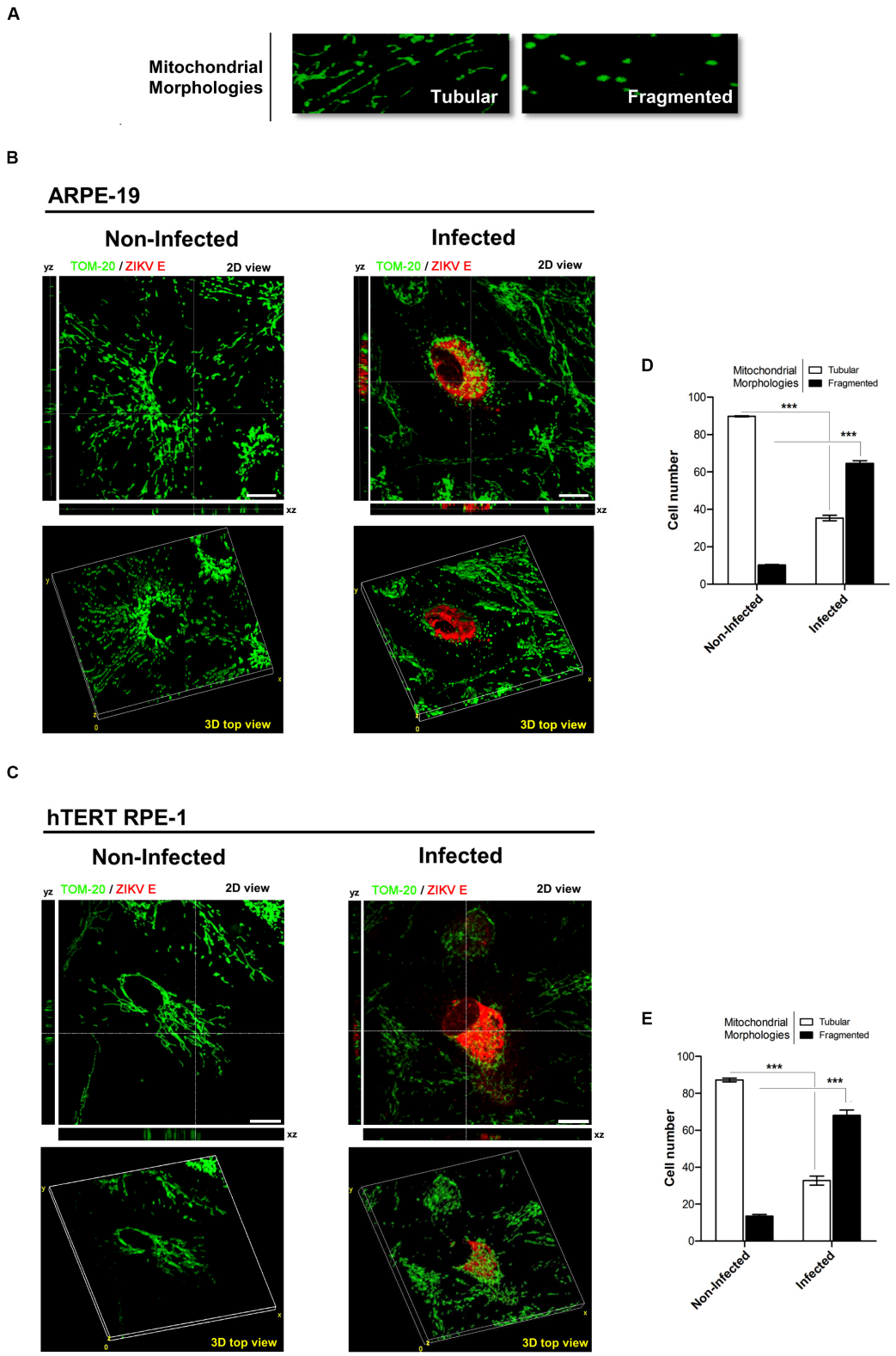

FIGURE 4 | ZIKV infection induces mitochondria fragmentation. **(A)** Mitochondrial morphologies detected: tubular (normal) and fragmented (small and spherical). **(B, C)** Representative confocal *z*-stacks images from non-infected and infected cells used for 3D reconstruction. The crosshairs indicate the positions of the *xz* and *yz* planes. **(B)** ARPE-19, **(C)** hTERT RPE-1. Scale bar: 10 μm. **(D, E)** Quantification of tubular or fragmented mitochondria in infected and non-infected cells; **(D)** ARPE-19, **(E)** hTERTRPE-1. $N = 100$ cells/condition, in quadruplicate. $^{***}p < 0.001$ vs. non-infected cells.

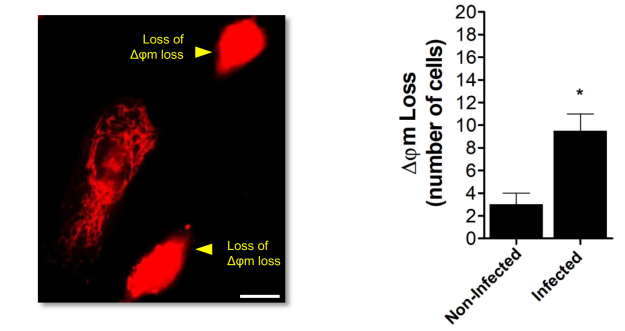

FIGURE 5 | ZIKV-induced mitochondrial dysfunction. **(A)** ARPE-19 cells were infected with ZIKV. At 48 h p.i. cells were stained with MitoTracker Red CMXRos and analyzed by fluorescence microscopy. Cells with loss of mitochondrial transmembrane potential (Δφm, yellow arrowheads) were identified. **(B)** Cells with Δφm loss were scored among 100 cells per condition. Scale bar: 10 μm. Data represent the mean ± SD. *$p < 0.05$ vs. non-infected.

using relevant hepatoma cell lines like (HepG2, Huh-7) and also BHK.21 cells. Interestingly, these studies were performed on monolayers infected at high MOI (i.e., 2 or 10) and times ranging from 24 to 72 h p.i. In our study, Huh-7 cell cultures, which are highly permissive to ZIKV infection, were used to evaluate the interplay between LDs and ZIKV infection. Importantly, in order to ensure that the measured effect occurred upon one cycle of viral replication, we infected samples at MOI = 0.1 and analyzed them at 24 h p.i. Therefore, in our assays we consistently worked with an average of 40–50% of positive cells to study the effect on LDs number and content. Double immunofluorescence *Z*-stacks of non-infected (**Figure 6A**) and infected samples (**Figure 6B**) showing both ZIKV E protein (green channel) and LDs labeled with LipidTox (red channel) were captured with a confocal microscope. LDs quantification was performed from collected images in both positive and negative ZIKV cells. As can be seen in the histogram shown in **Supplementary Figure 1A**'s inset, photographs of the green channel in non-infected cultures carry information of cell's autoflourescence that was enough to detect individual cells. When compared to the histogram shown in **Supplementary Figure 1I**, it should be noted that scales differ and that the gray values detected in infected cultures are higher than the ones acquired for non-infected cultures, confirming the specificity of the signal. From a detailed inspection under the microscope a decreased number of LDs was seen on those ZIKV infected cells. Extensive image processing and analysis proved a significant decline in LDs number in ZIKV infected cells (**Figure 6B**, upper panel) when compared with control non-infected cells (**Figure 6A**, upper panel). A 3D render view of representative fields of both non-infected and infected samples is shown in **Figure 6**, bottom panels. The differences in LDs enumeration (**Figure 6C**) appeared to have a correlate with a trend toward a decrease in total LDs volume in infected cells (**Figure 6D**), suggesting an overall consumption or exhaustion of these organelles.

DISCUSSION

Microscopes have been the primary scientific instrument in biological sciences and their performance and versatility have improved dramatically over the last 20 years. The ground of microscopy has been particularly fruitful in cell biology studies, including organelle characterization. In this paper we made use of confocal microscopy to uncover new details in the subcellular active reorganization of ZIKV infected cells. For instance, applying 3D reconstruction to focal stacks that can be visualized using volume rendering, we could perform volumetric studies in cellular substructures. The results here reported have shown active morphological alterations and remodeling in nuclear and cytoplasmic organelles, like PML-NBs, mitochondria and LDs of human cells infected with ZIKV.

The involvement of the cell nucleus in the infective process of several RNA viruses has been well demonstrated. Among flaviviruses, the localization of DENV and ZIKV proteins, particularly C, and NS5 proteins, in the nucleus/nucleolus was recognized as indicative of a nucleocytoplasmic trafficking central for virus infection (Hou et al., 2017; Tiwari and Cecilia, 2017). It was recently demonstrated that compounds targeted to the nucleolus structure were inhibitors of ZIKV infection, suggesting a critical nuclear function for viral propagation (Tokunaga et al., 2020). The PML-NBs are other subnuclear components which can act as a target for viruses to escape the antiviral signaling response (Geoffroy and Chelbi-Alix, 2011; Scherer and Stamminger, 2016). In previous studies, the role of PML-NBs in DENV infection was reported demonstrating an interaction between the PML isoforms with the viral protein NS5 that lead to PML-NB degradation in the infected cell (Giovannoni et al., 2015, 2019). Here we analyzed the alterations in the PML-NB structure after infection of NPCs with ZIKV. The punctate staining of NS5 was found in the nucleus of infected cells whereas a significant reduction in the number of PML-NBs was determined. PML-NB structures could be interfered through subcellular translocation into the cytoplasm or disturbance of the nuclear structure with dispersion patterns or/and declining expression. Our results show for the first time that ZIKV infection promotes the breakdown and exhaustion of PML-NBs, corroborating the apparent participation of these subnuclear organelles in the flavivirus life cycle.

Mitochondria are organelles found in the cytoplasm that act as a common platform for the execution of a variety of cellular functions in normal or infected cells. In this sense, mitochondria play central roles as a hub of innate immune signaling and energetic metabolism establishing the major causes of viral pathogenesis (Anand and Tikoo, 2013; Pourcelot and Arnoult, 2014; Kim et al., 2018). The viral strategy to avoid the mechanism of antiviral signaling associated with mitochondria is one of the paradigms of virus-mitochondrial interactions. Until now, studies describing the relationship between flavivirus infection and alterations in mitochondrial dynamics are mainly focused on DENV. Notably, while the existing reports all conclude the occurrence of mitochondrial fusion and fission imbalance in infected cells, there are controversies over which process is favored. Yu et al. (2015) demonstrated that the four

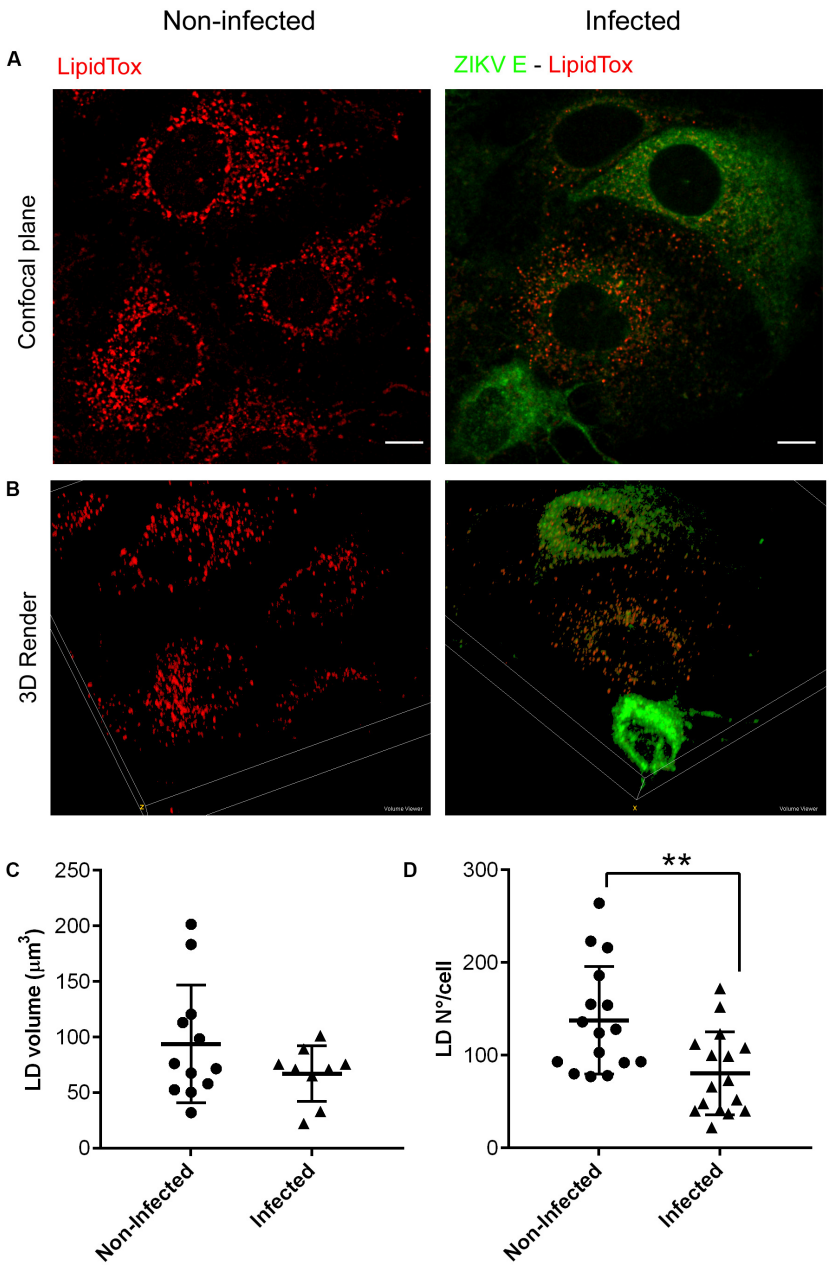

FIGURE 6 | ZIKV infection reduces LDs content. Huh-7 cultures were mock-infected or infected for 24 h. After fixation, LDs were stained with LipidTox (red) and ZIKV infected cells were immunolabeled with anti-E protein (green). Confocal microphotography (upper panel) and 3D render (lower panel) of a non-infected culture **(A)** or a ZIKV infected culture **(B)**. Scale bar: 10 μm. Quantification of LDs number per cell **(C)** and total LDs volume per cell **(D)** in ZIKV-infected and non-infected Huh-7 cultures. Data represent the mean ± SD (n = 16 cells per condition for LDs number, and n = 10 cells per condition for LDs volume). $^{**}p$-value ≤ 0.01 (two-sided Student's t-test).

DENV serotypes blocked mitochondrial fusion to manipulate the outcome of infection in human lung carcinoma A549 cells. In contrast, other authors reported that DENV serotypes 1, 3, and 4 promote mitochondria fusion in the hepatocarcinoma cell line Huh-7, suggesting that the generation of elongated mitochondria would favor viral replication and dampen activation of the interferon response (Chatel-Chaix et al., 2016; Barbier et al., 2017). Notably, as far as we know, only Chatel-Chaix et al. (2016) mentioned that two ZIKV strains, belonging to the Asian and the African lineage, change the mitochondrial dynamics statement by inducing organelle fusion in Huh-7 cells. In the present work, we analyzed the infection of two lines of human retinal cells, according to their relevance due to the ocular abnormalities associated to ZIKV pathology in humans, with a ZIKV strain of the Asian lineage. In these conditions, we demonstrated that ZIKV shifts the balance of mitochondrial dynamics toward

fission in both infected male and female derived-RPE cells in a similar way. At present, all these contrasting results cannot be explained, but it cannot be discarded that both host cell type and the virus source may affect the outcome of the virus-induced alterations in an organelle participating in innate immunity and cell death cascades.

Regarding to cellular structures linked to lipid metabolism, the involvement of LDs in flavivirus infection has been already described for DENV. Some groups have reported an increase in LDs during DENV infection (McLauchlan, 2009; Barletta et al., 2016; Martins et al., 2018), while others have observed that DENV induces a proviral selective autophagy targeting LDs, named lipophagy (Heaton and Randall, 2011). Recently, a role for AUP1, an LDs associated cell protein, has been well described for this process in DENV infection: viral NS4A and NS4B proteins interact with AUP1 to hijack its acyltransferase function, triggering lipophagy to improve the production of infective particles (Zhang et al., 2018). The authors report that this mechanism appears to be also functional in ZIKV and WNV infections, turning it an apparent general phenomenon for infective flavivirus production. Although an explanation for the discrepancy between the published data has not been found yet, it is possible that these differences are the result of a combination of the cellular system and the high virus-to-cell ratio used to infect monolayers (Samsa et al., 2009; Heaton and Randall, 2010, 2011). Moreover, the type of analysis done is not the same in every case, since some authors measure LDs number and total LDs area per cell, while others focus only on LDs number. Given that LDs can vary in size, it is possible that the phenotypes observed correspond to the activation of the same cellular process and that differences arise from the different cell lines and the times of infection used. Also, it cannot be discarded that viruses might induce LDs biogenesis stimulating the initial viral replication, and later on trigger lipophagy decreasing LDs number to release free fatty acids from these lipid structures. Hence, depending on which stage of the viral replication the LDs are measured, different conclusions could be drawn. It is worth to mention that when several viral cycles occur simultaneously on a monolayer, different phenomenon may compete and/or add to the final cell phenotype. Then, we decided to limit our study to 24 h p.i., with few cycles of viral replication, and we found a significantly decreased LDs content in ZIKV infected Huh-7 cells, with reduction in the number of LDs/cell and the LDs volume.

The localization of the capsid C protein of DENV and HCV at LDs organelles has been extensively reported (Shavinskaya et al., 2007; Samsa et al., 2009). Additionally, the localization of the capsid C protein of ZIKV to LDs was documented in HEK 293 (Coyaud et al., 2018), BHK-21 (Shang et al., 2018), and Vero (Hou et al., 2017) infected cells, with LDs representing the main location of C protein in the host cell. Although the mechanism behind the reduced content of LDs in Huh-7 infected cells here reported has not been addressed for ZIKV infection, our results confirm that this virus produces cell phenotypes related to lipid homeostasis comparable to others members of the family.

Collectively, the observations reported here showing a reorganization of three cell components, PML-NBs, mitochondria and LDs, demonstrate the importance of these subcellular structures for proper flavivirus replication, but the *in-vivo* relevance of these results remains unexplored. Several inhibitors targeting host organelles are well characterized. Therefore, a more comprehensive understanding of the molecular biology of viruses and their dependence on host organelles is of utmost priority for development of broad-spectrum and specific anti-flaviviral strategies.

DATA AVAILABILITY STATEMENT

All datasets generated for this study are included in the article/**Supplementary Material**.

AUTHOR CONTRIBUTIONS

CG, SC, AA, and ED contributed conception and design of the study. CV, FG, and CR performed the experiments and analyzed data. All authors contributed to manuscript revision, read, and approved the submitted version.

FUNDING

This work was supportedby Universidad de Buenos Aires (UBA; 200201170100363BA and 20020160100091BA), and Agencia Nacional de Promoción Científica y Tecnológica (PICT 3080 and 1151), Argentina. CG, SC, AA, and ED are members of the Research Career from CONICET, CV, and FG are fellows from the same institution.

ACKNOWLEDGMENTS

We thank all members of the laboratories involved for helpful advice and discussions.

SUPPLEMENTARY MATERIAL

The Supplementary Material for this article can be found online at: https://www.frontiersin.org/articles/10.3389/fmicb.2020.01558/full#supplementary-material

FIGURE S1 | Single-cell image analysis for LDs quantification. Upper panels: Non-infected Huh-7 monolayer. Lower panels: ZIKV- infected Huh-7 monolayer. Augmentation: 60×. **(A, I)** Confocal plane of the green channel (ZIKV-E protein) in non-infected and infected cultures. Inset: Histogram of each image, showing that even though there is no visible image in non-infected cultures, autofluorescence signal from cells can be detected. **(B, J)** After being processed with a Gaussian Blur filter, the pattern present in the microphotographs is smoothed, simplifying whole-cell thresholding. **(C, K)** Automatically selected areas in each photograph by using the mean of gray levels of the stack as the threshold. **(D, L)** Final binary masks obtained after refining the thresholding output, by using the "Fill holes" and "Watershed" algorithms. **(E, M)** ROIs corresponding to individual cells, as obtained after using "Analyze Particles" plugin. **(F, N)** Confocal plane of LipidTox-stained LDs in both, infected and non-infected cultures. **(G, O)** LDs area obtained with "3D Object Counter" plugin. **(H, P)** LDs selected with "Find Maxima" plugin for LDs number quantification.

REFERENCES

Acosta, E. G., and Bartenschlager, R. (2016). The quest for host targets to combat dengue virus infections. *Curr. Opin. Virol.* 20, 47–54. doi: 10.1016/j.coviro.2016.09.003

Alaimo, A., Di Santo, M. C., Domínguez Rubio, A. P., Chaufan, G., GarcíaLiñares, G., Pérez, O. E., et al. (2020). Toxic effects of A2E in human ARPE-19 cells were prevented by resveratrol: a potential nutritional bioactive for age-related macular degeneration treatment. *Arch. Toxicol.* 94, 553–572. doi: 10.1007/s00204-019-02637-w

Alaimo, A., Gorojod, R. M., Beauquis, J., Muñoz, M. J., Saravia, F., and Kotler, M. L. (2014). Deregulation of mitochondria-shaping proteins Opa-1 and Drp-1 in manganese-induced apoptosis. *PLoS One* 9:e91848. doi: 10.1371/journal.pone.0091848

Alaimo, A., Liñares, G. G., Bujjamer, J. M., Gorojod, R. M., Alcon, S. P., Martínez, J. H., et al. (2019). Toxicity of blue led light and A2E is associated to mitochondrial dynamics impairment in ARPE-19 cells: implications for age-related macular degeneration. *Arch. Toxicol.* 93, 1401–1415. doi: 10.1007/s00204-019-02409-6

Anand, S. K., and Tikoo, S. K. (2013). Viruses as modulators of mitochondrial functions. *Adv. Virol.* 2013:738794. doi: 10.1155/2013/738794

Barbier, V., Lang, D., Valois, S., Rothman, A. L., and Medin, C. L. (2017). Dengue virus induces mitochondrial elongation through impairment of Drp1-triggered mitochondrial fission. *Virology* 500, 149–160. doi: 10.1016/j.virol.2016.10.022

Barletta, A. B., Alves, L. R., Silva, M. C., Sim, S., Dimopoulos, G., Liechocki, S., et al. (2016). Emerging role of lipid droplets in Aedesaegypti immune response against bacteria and Dengue virus. *Sci. Rep.* 6:19928. doi: 10.1038/srep19928

Barreto-Vieira, D. F., Jacome, F. C., Nunes da Silva, M. A., Caldas, G. C., Bispo de Filippis, A. M., Carvalho de Sequeira, P., et al. (2017). Structural investigation of C6/36 and Vero cell cultures infected with a Brazilian Zika virus. *PLoS One* 12:e0184397. doi: 10.1371/journal.pone.0184397

Borden, K. L. (2002). Pondering the promyelocyticleukemia protein (PML) puzzle: possible functions for PML nuclear bodies. *Mol. Cell Biol.* 22, 5259–5269. doi: 10.1128/mcb.22.15

Brasil, P., Sequeira, P. C., Freitas, A. D., Zogbi, H. E., Calvet, G. A., de Souza, R. V., et al. (2016). Guillain-Barre syndrome associated with Zika virus infection. *Lancet* 387:1482. doi: 10.1016/S0140-6736(16)30058-7

Brown, J. R., Conn, K. L., Wasson, P., Charman, M., Tong, L., Grant, K., et al. (2016). SUMO ligase protein inhibitor of activated STAT1 (PIAS1) is a constituent promyelocyticleukemia nuclear body protein that contributes to the intrinsic antiviral immune response to Herpes Simplex Virus 1. *J. Virol.* 90, 5939–5952. doi: 10.1128/JVI.00426-16

Calvet, G., Aguiar, R. S., Melo, A. S., Sampaio, S. A., de Filippis, I., Fabri, A., et al. (2016). Detection and sequencing of Zika virus from amniotic fluid of fetuses with microcephaly in Brazil: a case study. *Lancet Infect. Dis.* 16, 653–660. doi: 10.1016/S1473-3099(16)00095-5

Carteaux, G., Maquart, M., Bedet, A., Contou, D., Brugieres, P., Fourati, S., et al. (2016). Zika virus associated withmeningoencephalitis. *N. Engl. J. Med.* 374, 1595–1596. doi: 10.1056/NEJMc1602964

Carvalho, F. A., Carneiro, F. A., Martins, I. C., Assunção-Miranda, I., Faustino, A. F., Pereira, R. M., et al. (2012). Dengue virus capsid protein binding to hepatic lipid droplets (LD) is potassium-dependent and is mediated by LD surface proteins. *J. Virol.* 86, 2096–2108. doi: 10.1128/jvi.06796-11

Chatel-Chaix, L., Cortese, M., Romero-Brey, I., Bender, S., Neufeldt, C. J., Fischl, W., et al. (2016). Dengue virus perturbs mitochondrial morphodynamics to dampeninnate immune responses. *Cell Host Microbe* 20, 342–356. doi: 10.1016/j.chom.2016.07.008

Chavali, P. L., Stojic, L., Meredith, L. W., Joseph, N., Nahorski, M. S., Sanford, T. J., et al. (2017). Neurodevelopmental protein Musashi-1 interacts with the Zika genome and promotes viral replication. *Science* 357, 83–88. doi: 10.1126/science.aam9243

Cortese, M., Goellner, S., Acosta, E. G., Neufeldt, C. J., Oleksiuk, O., Lampe, M., et al. (2017). Ultrastructural characterization of Zika virus replication factories. *Cell Rep.* 18, 2113–2123. doi: 10.1016/j.celrep.2017.02.014

Coyaud, E., Ranadheera, C., Cheng, D., Gonçalves, J., Dyakov, B. J. A., Laurent, E. M. N., et al. (2018). Global interactomics uncovers extensive organellar targeting by Zika virus. *Mol. Cell. Proteomics* 17, 2242–2255. doi: 10.1074/mcp.TIR118.000800

Dick, G. W., Kitchen, S. F., and Haddow, A. J. (1952). Zika virus. I. Isolations and serological specificity. *Trans. R. Soc. Trop. Med. Hyg.* 46, 509–520. doi: 10.1016/0035-9203(52)90042-4

Dieguez, H. H., Romeo, H. E., Alaimo, A., González Fleitas, M. F., Aranda, M. L., Rosenstein, R. E., et al. (2019). Oxidative stress damage circumscribed to the central temporal retinal pigment epithelium in early experimental non-exudative age-related macular degeneration. *Free Radic. Biol. Med.* 131, 72–80. doi: 10.1016/j.freeradbiomed.2018.11.035

doRosário, M. S., de Jesus, P. A. P., Vasilakis, N., Farias, D. S., Novaes, M. A. C., Rodrigues, S. G., et al. (2016). Guillain-Barré syndrome after Zika virus infection in Brazil. *Am. J. Trop. Med. Hyg.* 95, 1157–1160. doi: 10.4269/ajtmh.16-0306

Dunn, K. C., Aotaki-Keen, A. E., Putkey, F. R., and Hjelmeland, L. M. (1996). ARPE-19, a human retinal pigment epithelial cell line with differentiated properties. *Exp. Eye Res.* 62, 155–169. doi: 10.1006/exer.1996.0020

Eisner, V., Picard, M., and Hajnóczky, G. (2018). Mitochondrial dynamics in adaptive and maladaptive cellular stress responses. *Nat. Cell Biol.* 20, 755–765. doi: 10.1038/s41556-018-0133-0

García, C. C., Quintana, V. M., Castilla, V., and Damonte, E. B. (2018). "Towards host-cell targeting therapies to treat dengue virus infections," in *Frontiers in Anti-Infective Drug Discovery*, Vol. 7, eds A. Rahman and M. I. Choudhary (Sharjah, UAE: Bentham Science Publishers), 45–87. doi: 10.2174/9781681085623118070004

Geoffroy, M. C., and Chelbi-Alix, M. K. (2011). Role of promyelocyticleukemia protein in host antiviral defense. *J. Interferon Cytokine Res.* 31, 145–158. doi: 10.1089/jir.2010.0111

Giacomello, M., Pyakurel, A., Glytsou, C., and Scorrano, L. (2020). The cell biology of mitochondrial membrane dynamics. *Nat. Rev. Mol. Cell Biol.* 21, 204–224. doi: 10.1038/s41580-020-0210-7

Giovannoni, F., Damonte, E. B., and García, C. C. (2015). Cellular promyelocytic leukemia protein is an important dengue virus restriction factor. *PLoS One* 10:e0125690. doi: 10.1371/journal.pone.0125690

Giovannoni, F., Ladelfa, M. F., Monte, M., Jans, D. A., Hemmerich, P., and García, C. (2019). Dengue non-structural protein 5 polymerase complexes with promyelocyticleukemia protein (PML) isoforms III and IV to disrupt PML-nuclear bodies in infected cells. *Front. Cell. Infect. Microbiol.* 9:284. doi: 10.3389/fcimb.2019.00284

Gubler, D. J., Vasilakis, N., and Musso, D. (2017). History and emergence of Zika virus. *J. Infect. Dis.* 216, S860–S867. doi: 10.1093/infdis/jix451

Guion, L. G., and Sapp, M. (2020). The role of promyelocytic leukemia nuclear bodies during HPV infection. *Front. Cell. Infect. Microbiol.* 10:35. doi: 10.3389/fcimb.2020.00035

Heaton, N. S., and Randall, G. (2010). Dengue virus-induced autophagy regulates lipid metabolism. *Cell Host Microbe* 8, 422–432. doi: 10.1016/j.chom.2010.10.006

Heaton, N. S., and Randall, G. (2011). Dengue virus and autophagy. *Viruses* 3, 1332–1341. doi: 10.3390/v3081332

Herker, E., and Ott, M. (2012). Emerging role of lipid droplets in host/pathpogenintercations. *J. Biol. Chem.* 287, 2280–2287. doi: 10.1074/jbc.R111.300202

Hou, W., Cruz-Cosme, R., Armstrong, N., Obwolo, L. A., Wen, F., Hu, Q., et al. (2017). Molecular cloning and characterization of the genes encoding the proteins of Zika virus. *Gene* 628, 117–128. doi: 10.1016/j.gene.2017.07.049

Jordan, T. X., and Randall, G. (2017). Dengue virus activates the AMP kinase-mTOR axis to stimulate a provirallipophagy. *J. Virol.* 91:e02020-16. doi: 10.1128/JVI.02020-16

Khan, M., Syed, G. H., Kim, S. J., and Siddiqui, A. (2015). Mitochondrial dynamics and viral infections: a close nexus. *Biochim. Biophys. Acta* 1853, 2822–2833. doi: 10.1016/j.bbamcr.2014.12.040

Kim, S. J., Ahn, D. G., Syed, G. H., and Siddiqui, A. (2018). The essential role of mitochondrial dynamics in antiviral immunity. *Mitochondrion* 41, 21–27. doi: 10.1016/j.mito.2017.11.007

Martín-Acebes, M. A., Vázquez-Calvo, A., and Saiz, J. C. (2016). Lipids and flaviviruses, present and future perspectives for the control of dengue, Zika and West Nile viruses. *Prog. Lipid Res.* 64, 123–137. doi: 10.1016/j.plipres.2016.09.005

Martins, A. S., Martins, I. C., and Santos, N. C. (2018). Methods for lipid droplet biophysical characterization in flaviviridae infections. *Front. Microbiol.* 9:1951. doi: 10.3389/fmicb.2018.01951

McLauchlan, J. (2009). Lipid droplets and hepatitis C virus infection. *Biochim. Biophys. Acta* 1791, 552–559. doi: 10.1016/j.bbalip.2008.12.012

Mecharles, S., Herrmann, C., Poullain, P., Tran, T. H., Deschamps, N., Mathon, G., et al. (2016). Acute myelitis due to Zika virus infection. *Lancet* 387:1481. doi: 10.1016/S0140-6736(16)00644-9

Mlakar, J., Korva, M., Tul, N., Popovic, M., Poljšak-Prijatelj, M., Mraz, J., et al. (2016). Zika virus associated with microcephaly. *N. Engl. J. Med.* 374, 951–958. doi: 10.1056/NEJMoa1600651

Moine, E., Brabet, P., Guillou, L., Durand, T., Vercauteren, J., and Crauste, C. (2018). New lipophenol antioxidants reduce oxidative damage in retina pigment epithelial cells. *Antioxidants* 7:E197. doi: 10.3390/antiox7120197

Musso, D., Roche, C., Robin, E., Nhan, T., Teissier, A., and Cao-Lormeau, V. M. (2015). Potential sexual transmission of Zika virus. *Emerg. Infect. Dis.* 21, 359–361. doi: 10.3201/eid2102.141363

Offerdahl, D. K., Dorward, D. W., Hansen, B. T., and Bloom, M. E. (2017). Cytoarchitecture of Zika virus infection in human neuroblastoma and Aedesalbopictus cell lines. *Virology* 501, 54–62. doi: 10.1016/j.virol.2016.11.002

Olichon, A., Baricault, L., Gas, N., Guillou, E., Valette, A., Belenguer, P., et al. (2003). Loss of OPA1 perturbates the mitochondrial inner membrane structure and integrity, leading to cytochrome c release and apoptosis. *J. Biol. Chem.* 278, 7743–7746. doi: 10.1074/jbc.C200677200

Pernas, L., and Scorrano, L. (2016). Mito-Morphosis: Mitochondrial fusion, fission, and cristae remodeling as key mediators of cellular function. *Annu. Rev. Physiol.* 78, 505–531. doi: 10.1146/annurev-physiol-021115-105011

Pourcelot, M., and Arnoult, D. (2014). Mitochondrial dynamics and the innate antiviral immune response. *FEBS J.* 281, 3791–3802. doi: 10.1111/febs.12940

Qian, X., Nguyen, H. N., Song, M. M., Hadiono, C., Ogden, S. C., Hammack, C., et al. (2016). Brain-region-specific organoids using mini-bioreactors for modeling ZIKV exposure. *Cell* 165, 1238–1254. doi: 10.1016/j.cell.2016.04.032

Rambhatla, L., Chiu, C. P., Glickman, R. D., and Rowe-Rendleman, C. (2002). In vitro differentiation capacity of telomerase immortalized human RPE cells. *Invest. Ophthalmol. Vis. Sci.* 43, 1622–1630.

Roach, T., and Alcendor, D. J. (2017). Zika virus infection of cellular components of the blood-retinal barriers: implications for viral associated congenital ocular disease. *J. Neuroinflamm.* 14:43. doi: 10.1186/s12974-017-0824-7

Rossignol, E. D., Peters, K. N., Connor, J. H., and Bullitt, E. (2017). Zika virus induced cellular remodelling. *Cell Microbiol.* 19:e12740. doi: 10.1111/cmi.12740

Saiz, J. C., Oya, N. J., Blazquez, A. B., Escribano-Romero, E., and Martin-Acebes, M. A. (2018). Host-directed antivirals: a realistic alternative to fight Zika virus. *Viruses* 10:453. doi: 10.3390/v10090453

Samsa, M. M., Mondotte, J. A., Iglesias, N. G., Assuncao-Miranda, I., Barbosa-Lima, G., Da Poian, A. T., et al. (2009). Dengue virus capsid protein usurps lipid droplets for viral particle formation. *PLoS Pathog.* 5:e1000632. doi: 10.1371/journal.ppat.1000632

Scherer, M., and Stamminger, T. (2016). Emerging role of PML nuclear bodies in innate immune signaling. *J. Virol.* 90, 5850–5854. doi: 10.1128/JVI.01979-15

Schilling, E. M., Scherer, M., Reuter, N., Schweininger, J., Muller, Y. A., Stamminger, T., et al. (2017). The human cytomegalovirus IE1 protein antagonizes PML nuclear body-mediated intrinsic immunity via the inhibition of PML de novo SUMOylation. *J. Virol.* 91:e02049-16. doi: 10.1128/JVI.02049-16

Shang, Z., Song, H., Shi, Y., Qi, J., and Gao, G. F. (2018). Crystal structure of the capsid protein from Zika Virus. *J. Mol. Biol.* 430, 948–962. doi: 10.1016/j.jmb.2018.02.006

Shavinskaya, A., Boulant, S., Penin, F., McLauchlan, J., and Bartenschlager, R. (2007). The lipid droplet binding domain of hepatitis C virus core protein is a major determinant for efficient virus assembly. *J. Biol. Chem.* 282, 37158–37169. doi: 10.1074/jbc.M707329200

Shi, Y., and Gao, G. F. (2017). Structural biology of the Zika virus. *Trends Biochem. Sci.* 42, 443–456. doi: 10.1016/j.tibs.2017.02.009

Simonin, Y., Erkilic, N., Damodar, K., Clé, M., Desmetz, C., Bolloré, K., et al. (2019). Zika virus induces strong inflammatory responses and impairs homeostasis and function of the human retinal pigment epithelium. *EBioMedicine* 39, 315–331. doi: 10.1016/j.ebiom.2018.12.010

Tabata, T., Petitt, M., Puerta-Guardo, H., Michlmayr, D., Wang, C., Fang-Hoover, J., et al. (2016). Zika virus targets different primary human placental cells, suggesting two routes for vertical transmission. *Cell Host Microbe* 20, 155–166. doi: 10.1016/j.chom.2016.07.002

Tiwari, A. K., and Cecilia, D. (2017). Kinetics of the association of dengue virus capsid protein with the granular component of nucleolus. *Virology* 502, 48–55. doi: 10.1016/j.virol.2016.12.013

Tokunaga, M., Miyamoto, Y., Suzuki, T., Otani, M., Inukic, S., and Esakid, T. (2020). Novel anti-flavivirus drugs targeting the nucleolar distribution of core protein. *Virology* 541, 41–51. doi: 10.1016/j.virol.2019.11.015

Vázquez, C. A., Giovannoni, F., Bosch, I., de Oliveira Mota, M. T., Lacerda Nogueira, M., Cordo, S. M., et al. (2019). "Lipid droplets as potential antiviral targets for flaviviruses," in *Biochemistry Research Trends. Lipid Droplets*, ed. A. Catalá (New York, NY: NOVA Science Publishers), 1–17.

Ventura, C. V., and Ventura, L. O. (2018). Ophthalmologic manifestations associated with Zika virus infection. *Pediatrics* 141, S161–S166. doi: 10.1542/peds.2017-2038E

Yockey, L. J., Varela, L., Rakib, T., Khoury-Hanold, W., Fink, S. L., Stutz, B., et al. (2016). Vaginal exposure to Zika virus during pregnancy leads to fetal brain infection. *Cell* 166, 1247–1256. doi: 10.1016/j.cell.2016.08.004

Yu, C.-Y., Liang, J. J., Li, J.-K., Lee, Y.-L., Chang, B.-L., Su, C.-I., et al. (2015). Dengue virus impairs mitochondrial fusion by cleaving mitofusins. *PLoS Pathog.* 11:e1005350. doi: 10.1371/journal.ppat.1005350

Zhang, J., Lan, Y., Li, M. Y., Lamers, M. M., Fusade-Boyer, M., Klemm, E., et al. (2018). Flaviviruses exploit the lipid droplet protein AUP1 to trigger lipophagy and drive virus production. *Cell Host Microbe* 23, 819–831. doi: 10.1016/j.chom.2018.05.005

Zhao, Z., Yang, M., Azar, S. R., Soong, L., Weaver, S. C., Sun, J., et al. (2017). Viral retinopathy in experimental models of zika infection. *Invest. Ophthalmol. Vis. Sci.* 58, 4075–4085. doi: 10.1167/iovs.17-22016

Conflict of Interest: The authors declare that the research was conducted in the absence of any commercial or financial relationships that could be construed as a potential conflict of interest.

frontiers in Microbiology

MINI REVIEW
published: 31 August 2020
doi: 10.3389/fmicb.2020.01990

Picking up a Fight: Fine Tuning Mitochondrial Innate Immune Defenses Against RNA Viruses

*Sourav Dutta, Nilanjana Das and Piyali Mukherjee**

School of Biotechnology, Presidency University, Kolkata, India

As the world faces the challenge of the COVID-19 pandemic, it has become an urgent need of the hour to understand how our immune system sense and respond to RNA viruses that are often life-threatening. While most vaccine strategies for these viruses are developed around a programmed antibody response, relatively less attention is paid to our innate immune defenses that can determine the outcome of a viral infection *via* the production of antiviral cytokines like Type I Interferons. However, it is becoming increasingly evident that the "cytokine storm" induced by aberrant activation of the innate immune response against a viral pathogen may sometimes offer replicative advantage to the virus thus promoting disease pathogenesis. Thus, it is important to fine tune the responses of the innate immune network that can be achieved *via* a deeper insight into the candidate molecules involved. Several pattern recognition receptors (PRRs) like the Toll like receptors (TLRs), NOD-like receptors (NLRs), and the retinoic acid inducible gene-I (RIG-I) like receptors (RLRs) recognize cytosolic RNA viruses and mount an antiviral immune response. RLRs recognize invasive viral RNA produced during infection and mediate the induction of Type I Interferons *via* the mitochondrial antiviral signaling (MAVS) molecule. It is an intriguing fact that the mitochondrion, one of the cell's most vital organelle, has evolved to be a central hub in this antiviral defense. However, cytokine responses and interferon signaling *via* MAVS signalosome at the mitochondria must be tightly regulated to prevent overactivation of the immune responses. This review focuses on our current understanding of the innate immune sensing of the host mitochondria by the RLR-MAVS signalosome and its specificity against some of the emerging/re-emerging RNA viruses like Ebola, Zika, Influenza A virus (IAV), and severe acute respiratory syndrome-coronavirus (SARS-CoV) that may expand our understanding for novel pharmaceutical development.

Keywords: mitochondria, innate immunity, mitochondrial antiviral signaling, retinoic acid inducible gene-I, RNA virus, cytokine storm

OPEN ACCESS

Edited by:
Miguel A. Martín-Acebes, National Institute for Agricultural and Food Research and Technology (INIA), Spain

Reviewed by:
Maria Teresa Sanchez-Aparicio, Icahn School of Medicine at Mount Sinai, United States
Mitsutoshi Yoneyama, Chiba University, Japan

***Correspondence:**
Piyali Mukherjee
piyali.dbs@presiuniv.ac.in

Specialty section:
This article was submitted to Virology, a section of the journal Frontiers in Microbiology

Received: *17 April 2020*
Accepted: *28 July 2020*
Published: *31 August 2020*

Citation:
Dutta S, Das N and Mukherjee P (2020) Picking up a Fight: Fine Tuning Mitochondrial Innate Immune Defenses Against RNA Viruses. Front. Microbiol. 11:1990. doi: 10.3389/fmicb.2020.01990

INTRODUCTION

Mitochondrion, also known as the "powerhouse" of the cell, is critically involved in cellular respiration and ATP synthesis. Apart from its canonical role in cellular energetics, it orchestrates cell fate through the process of apoptosis and mitophagy, thus maintaining cellular homeostasis (Tsujimoto and Shimizu, 2007; Murphy, 2009; Friedman and Nunnari, 2014; Mishra and Chan, 2014; Khan et al., 2015; Sliter et al., 2018). In recent years, several studies have pinpointed the crucial role of mitochondria in stimulating innate immune responses, as well as modulating parts of the adaptive immune response (Walker et al., 2014; Weinberg et al., 2015; Mills et al., 2017). The evolutionary

conserved pattern recognition receptors (PRRs), expressed by most immune effector cells recognize conserved sequence within the pathogen and aids in their early detection and containment (Green et al., 2016). The Toll like receptors (TLRs) are a class of PRRs that recognize either dsRNA (TLR3) or ssRNA (TLR7/8) virus (Lester and Li, 2014; Hartmann, 2017; Miyake et al., 2018). The NOD-like receptor (NLR) family of PRRs is cytoplasmic receptors that form a multiprotein complex called "inflammasome" involved in the production of the pro-inflammatory cytokines IL1β and IL18 (He et al., 2016; Hughes and O'Neill, 2018). Another class of PRRs, the RIG-I like receptor (RLR) family involving retinoic acid inducible gene-I (RIG-I), melanoma differentiation-associated protein-5 (MDA-5), and laboratory of genetics and physiology 2 (LGP2) are cytoplasmic sensors of non-self and viral RNA (Vazquez and Horner, 2015; Sadler, 2017; Chow et al., 2018). A few of these receptors have been shown to augment mitochondria mediated antiviral innate immune responses *via* stimulation of Type I Interferon. Evolutionary conserved signaling intermediate in Toll (ECSIT) pathway, a component of the mitochondrial complex I, has been shown to enhance TLR7 responses *via* the mitochondrial adaptor protein tumor necrosis factor receptor (TNFR) associated factor 6 (TRAF6; Carneiro et al., 2018). NLRP3 has been shown to form the active inflammasome complex at the mitochondria by associating with the adaptor protein mitochondrial antiviral signaling protein (MAVS; Dorn, 2012; Haneklaus and O'Neill, 2015; Yabal et al., 2019). However, of special interest is the first identified RLR, RIG-I, which recognizes viral RNA that has a triphosphate moiety at its 5' end and has been shown to be targeted by some of the deadliest form of the RNA viruses (Kell and Gale, 2015; Dai et al., 2018). Following viral recognition, RIG-I binds to MAVS located on the outer surface of healthy intact mitochondria leading to interferon production and activation of the NFκB pathway (Kawai and Akira, 2007; Okamoto et al., 2018). This review speculates whether subversion of early viral sensing *via* the RIG-I/MAVS pathway could determine viral persistence within the host. Further, aberrant activation of the MAVS signalosome by the RLRs could cause hyperstimulation of the inflammatory responses and hence this arm of the innate immune defense could serve as a potential therapeutic target to combat highly communicable infectious RNA viruses.

The "Flu pandemic" over the last century has drawn particular attention to enveloped RNA viruses, a characteristic feature that empowers the virus with greater adaptability and high mutagenic potential, a key strategy in the evasion of host immune response and increased survivability within the host. Here, we systematically review our current understanding of the conserved host RIG-I/MAVS pathway and its regulation in some of the emerging/re-emerging RNA virus infections that include Ebola virus (EBOV) belonging to Filoviridae family, Zika virus (ZIKV) belonging to Flaviviridae family, Influenza A virus (IAV) belonging to Orthomyxoviridae family, and severe acute respiratory syndrome-coronavirus (SARS-CoV) belonging to Coronaviridae family. These viruses have been known to cause deadly outbreaks across the world and it is important to analyze whether key sensors of RNA viruses like the RIG-I/MAVS pathway are important targets of these viruses either to suppress of hyper-activate the immune responses.

MAVS SIGNALOSOME IN ENVELOPED RNA VIRUS

Mitochondria play an important role in antiviral immunity by eliciting and maintaining the RLR/MAVS signaling cascade. RLRs are soluble RNA helicase type receptors containing N-terminal tandem of caspase activation and recruitment domains (CARDs) and a DECH-helicase domain required for RNA binding and ATP hydrolysis (Kao et al., 2015; Brisse and Ly, 2019). All the three known RLRs (i.e., RIG-I, MDA-5, and LGP-2) are very efficient in distinguishing between cellular RNAs from those produced by RNA viruses (Züst et al., 2011). Upon recognition of viral RNA, one of the widely studied RLRs, RIG-I, binds to the downstream adaptor protein MAVS (also known as IPS-1, VISA, Cardif) at the mitochondria *via* CARD-CARD interaction (Liu et al., 2017). MAVS is an integral protein of the mitochondrial outer membrane that binds to the mitochondrial membrane *via* its C-terminal domain and acts as a key determinant of the antiviral signaling cascade (Xu et al., 2014). Following its interaction with RIG-I, MAVS bind with several kinases and other signaling molecules including TRAF3 and 6, TNFR associated death domain (TRADD), and TRAF associated NF-κB activator (TANK1) to form a large multimeric complex called the "MAVS signalosome" (Biacchesi et al., 2009; Vazquez and Horner, 2015). This structure ultimately leads to the activation of the interferon regulatory factor 3 (IRF3) and phosphorylation of IKKε to stimulate the NF-κB pathway leading to transcriptional activation of Type I Interferons and other inflammatory cytokines (Pothlichet et al., 2013; Refolo et al., 2020). Interferons in turn stimulate a plethora of interferon stimulated genes (ISGs) that aid in the containment of the viruses as well crosstalk with the adaptive immune response. Thus mitochondrial targeting *via* the MAVS signalosome by the viral proteins upon their entry appears to be a central executioner of antiviral responses as summarized in **Table 1**. In a continuous war with the host, viruses have evolved strategies to avoid MAVS mediated innate immune activation. For example, MAVS is expressed only on the surface of intact mitochondria and several studies suggest that RNA viruses alter mitochondrial metabolism and homeostasis that ultimately lead to mitochondrial damage and blocking interferon response *via* MAVS (Lei et al., 2009; Zhao et al., 2012; Wang et al., 2013; Choi et al., 2017; He et al., 2019). Over centuries, it has been found that enveloped RNA virus causes persistent human infections like the current COVID-19 pandemic (Schoeman and Fielding, 2019). Whether the viral envelope provides additional arsenal to the RNA viruses in the suppression of the protective interferon response *via* the MAVS signalosome is not known yet.

FINE TUNING INTERFERON RESPONSES AT THE MITOCHONDRIA

Following viral infection, our cellular defense machinery systematically induces a number of cytokines (both pro- and anti-inflammatory) that, in certain instances, may lead to hyperstimulation of the immune response in a positive feedback loop (Geoghegan et al., 2016; Shrivastava et al., 2016; Orzalli and Kagan, 2017). This leads to

TABLE 1 | Summary of viral proteins and their targets in mitochondria mediated antiviral response.

Virus	Viral proteins	Targets in mitochondrial functioning	References
Ebola virus	VP24	Inhibits RIGI pathway: binds karyopherin α1 and prevents localization of p-STAT in nucleus	(Reid et al., 2006; He et al., 2017)
	VP35	Inhibits RLR/MAVS signaling: binds PACT, binds dsRNA and prevents recognition by RIGI, inhibits IKKε/TBK1 complex, inhibits TNFα mediated activation of PKR, causes SUMOylation of IRF7	(Cárdenas et al., 2006; Feng et al., 2007; Chang et al., 2009; Prins et al., 2009; Luthra et al., 2013)
Zika virus	NS4B	Induces mitochondrial elongation: inhibits activation of DRP1; disrupts MAVS signaling: inhibits phosphorylation of TBK1	(Keystone Symposia, n.d.; Wu et al., 2017)
	NS4A	Inhibits MAVS signaling: binds CARD domain of MAVS	(Ma et al., 2018)
	NS5	Restricts MAVS signaling: inhibits phosphorylation of IRF3 by binding TBK1, binds and degrades STAT2	(Grant et al., 2016; Lin et al., 2019)
	NS3	Binds and degrades MAVS	(Li et al., 2019)
Influenza A virus	PB2	Binds and inhibits MAVS	(Graef et al., 2010)
	PB1-F2	Binds and inhibits MAVS; induces mitophagy: interacts with TUFM and MAP1 LC3B/LC3B; disrupts MMP and induces apoptosis: binds VDAC1 and ANT	(Zamarin et al., 2005; Varga et al., 2012; Wang et al., 2020b)
	NS1	Inhibits RIG1 activation: degrades deubiquitylase OTUB1, binds TRIM25, binds CARD of RIG1	(Gack et al., 2009; Jahan et al., 2019; Jureka et al., 2020)
SARS-CoV	ORF3b	Translocates to mitochondria and inhibits RIG1/MAVS signaling; inhibits phosphorylation of IRF3	(Kopecky-Bromberg et al., 2007; Freundt et al., 2009)
	Nsp10	Induces ROS production: binds NADH 4 L subunit and cytochrome oxidase II; depolarizes inner mitochondrial membrane	(Li et al., 2005)

a catastrophic damage to the surrounding cells and the side effects of this manifests itself in some of the symptoms like fever, fatigue, nausea along with multiple organ failure (Chen et al., 2020; Hackbart et al., 2020). This has been observed not only in COVID-19 patients but also in case of other strains of the Flu virus, the MERS-CoV, and SARS-CoV1 leading to severe respiratory distress and increased mortality rates (DeDiego et al., 2014; Nieto-Torres et al., 2015; Liang et al., 2020). Hence, the question automatically arises is whether mitochondria can fine tune this response to prevent such overreaction of the immune cells.

Since mitochondria provide the first line of defense against viral infection, signals converging at the mitochondria need to be tightly regulated to prevent bystander tissue damage within the host. One such checkpoint is provided by the NLR, NLRX1 which prevents overactivation of the immune response by its direct competition with RIG-I at its MAVS binding site and antagonizing Type I Interferon responses (Allen et al., 2012; Qin et al., 2017). Further, ubiquitination plays an important immunomodulatory role in the MAVS-signalosome (Gack et al., 2007, 2009). The ubiquitin ligase, tripartite motif containing-25 (TRIM-25), mediates Lys63 polyubiquitination of RIG-I thus, enabling its binding with MAVS for antiviral signaling. It has been shown that TRIM-25 also ubiquitinates MAVS at Lys7 and Lys10 inducing its proteolysis and dissociating it from RIG-I to halt the antiviral signaling cascade (Castanier et al., 2012). Mitophagy induction by reactive oxygen species is another strategy for MAVS degradation at the damaged mitochondria which is sometime adopted by certain viruses to dampen the host immune response (Zhang et al., 2018; He et al., 2019). These observations suggest that stimulators of the MAVS signalosome must work in concert with the negative regulators to strike a balance between activation and deactivation in a timely manner and have been summarized in **Figure 1**. However, extensive studies are required to find candidate molecules that may act to dampen the overzealous immune activation following an initial protective response *via* mitochondrial sensing (D'Elia et al., 2013; Cusabio, 2020).

INSIGHT INTO REGULATION OF MAVS SIGNALOSOME BY RNA VIRUSES

Ebola Virus

The EBOV that causes Ebola Virus Disease (EVD) is an emerging pathogen and has an almost 90% mortality rate. Although it is mostly endemic to West Africa with the Democratic Republic of Congo (DRC) being the hardest hit region over the past decade (2013–2019), it remains a major health concern worldwide due to its high potential to infect other species and the unavailability of a viable therapy till date (Kaner and Schaack, 2016; Chowell et al., 2019; Ebola virus disease, n.d.). EBOV is a non-segmented enveloped (−) single-stranded RNA virus that initially infects the innate immune cells such as macrophages (Structure of Ebola Virus, n.d.). However, the virus has the remarkable ability to infect a wide variety of cells that enables its rapid spread to different tissues. EBOV infection is characterized by hemorrhagic fever accompanied by massive cytokine storm, cytolytic damage, vascular leakage in liver, lungs, and kidneys, and ultimately death (Yu et al., 2012; Falasca et al., 2015).

The role of the viral sensor RIG-I and the subsequent activation of the MAVS pathway in determining the outcome of EBOV infection has not been thoroughly investigated. A study on mouse adapted EBOV (MA-EBOV) infection demonstrated that IFN-dependent and independent MAVS signaling takes place in an organ specific manner, where activation of monocytes and subsequent trafficking to the spleen occurs in a MAVS-dependent manner (Green et al., 2016; Dutta et al., 2017). EBOV mitigates the host immune response by using two viral IFN-antagonists, VP24 and VP35. VP35 has been shown to suppress the IFN-pathway by antagonizing the function of interferon regulatory factor (IRF) activating kinases IKKε and TANK binding kinase-1 (TBK-1; Messaoudi et al., 2015).

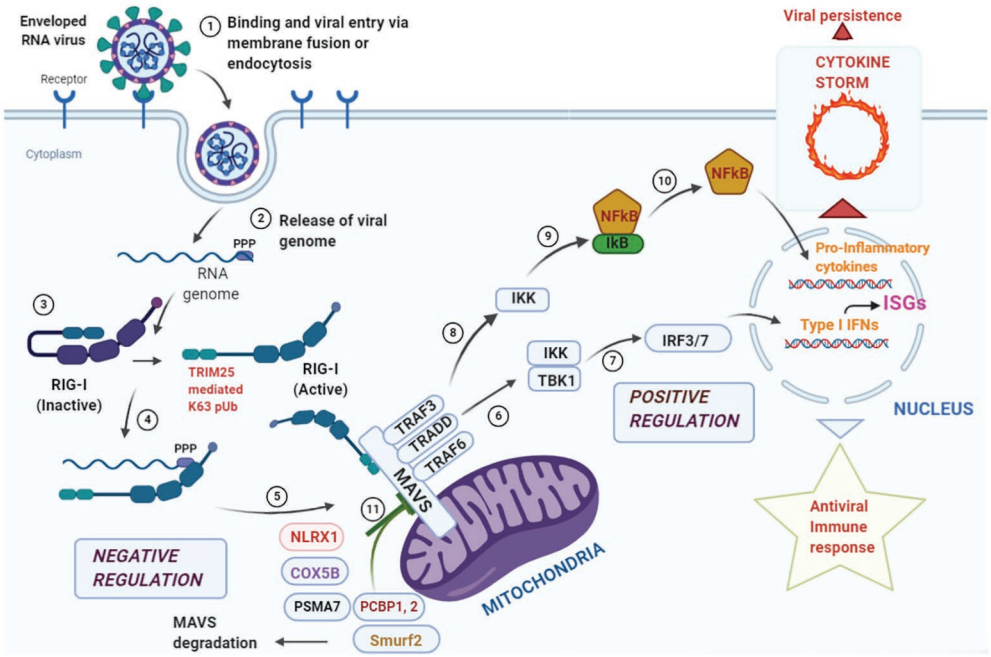

FIGURE 1 | Overview of antiviral response at the mitochondrial antiviral signaling (MAVS) signalosome. Enveloped RNA virus can enter the cell *via* membrane fusion or endocytosis (Step 1). Following entry, the "ppp" group at the 5' end of the viral genome is recognized by the core domain of the retinoic acid inducible gene-I (RIG-I) like receptor (RLR) helicase RIG-I (Steps 2, 3, and 4). The activated RIG-I molecule binds to MAVS *via* caspase activation and recruitment domain (CARD)-CARD interaction at the N-terminal domain of MAVS leading to the formation of the "MAVS Signalosome" (Step 5). Two different signals can emanate from this signalosome, the first one leads to the activation of interferon regulatory factor 3/7 (IRF3/7), transcriptional activation of Type I Interferons and stimulation of interferon stimulated genes (ISGs; Steps 6 and 7) leading to a protective antiviral immunity. The second signal phosphorylates IκB *via* IKK and releases NFκB that translocates to the nucleus and results in the transcriptional activation of pro-inflammatory cytokines (Steps 8, 9, and 10). Events at this step needs to be finely tuned as hyperstimulation of the responses may lead to a "cytokine storm" that aids in viral persistence within the infected cells. To fine tune the hyperstimualtion of the MAVS-signalosome NLRX1 antagonizes IFN signaling by binding to MAVS that may act as a brake on the hyperactive immune response. COX 5B suppress ROS production *via* suppressing MAVS aggregation and the proteasomal subunit PSMA-7 inhibits MAVS by enhancing its proteasomal degradation. Further, PCBP1, 2 and Smurf2 similarly degrade MAVS *via* K48 linked polyubiquitination and inhibit Type I Interferon production (Step 11).

Further, VP35 has been shown to inhibit RIG-activation *via* binding to transiently produced dsRNA during EBOV infection, thus preventing viral sensing and also by binding to the RIG-I ATPase activator PACT (Luthra et al., 2013). In an *in vitro* study, VP24 has been shown to prevent IFN-gene expression by targeting the RIG-I/MAVS pathway. It works downstream of the RIG-I/MAVS pathway by binding karyopherin α1 and inhibiting p-STAT translocation (Reid et al., 2006). Further studies are required to understand how EBOV suppress early innate immune sensing to develop antiviral strategies.

Zika Virus

Zika virus (ZIKV) is a re-emerging mosquito borne pathogen belonging to the genus *Flavivirus*. However, apart from mosquito-transmission, several other modes of ZIKV infection have been reported and the most striking is the mother to fetus transmission *via* the transplacental route (Plourde and Bloch, 2016). Although the first document of human infection by ZIKV occurred in 1954 and was associated with mild flu-like symptoms, a recent epidemic in French Polynesia during 2013–2014 that subsequently spread to South and Central America caught the world's attention with rising symptoms of microcephaly in newborns (Song et al., 2017; Haby et al., 2018). The re-emergence and the rising cases of ZIKV infection with higher infectivity are poorly understood and no clinically approved drug or vaccine is available till date.

ZIKV is a non-segmented enveloped (+) single stranded RNA virus that has shown to co-evolve with the host and strongly antagonizes the host antiviral IFN-responses. Several non-structural proteins of ZIKV like NS1, NS2B/3, NS4A, NS4B, and NS5 have been shown to antagonize IFN-responses (Wu et al., 2017; Ding et al., 2018; Zheng et al., 2018; Lundberg et al., 2019; Zhao et al., 2019). Studies have shown a direct interaction of the ZIKV NS4 with the N-terminal CARD domain of MAVS at the mitochondria (Ma et al., 2018). This prevents binding of RIG-I to MAVS and downstream activation of the interferon responses. It has been further shown that ZIKV NS4 specifically inhibits RIG-I mediated interferon responses and not that mediated by TLRs (Ma et al., 2018; Hu et al., 2019; Schilling et al., 2020). It is also known to disrupt mitochondrial dynamics which aids in infection (Keystone Symposia, n.d.). Further, the non-structural protein NS3 have been shown to target MAVs to proteasomal degradation *via* K48 linked polyubiquitination and subsequent downregulation of IFNβ pathway (Li et al., 2019). Further, these responses vary among the different ZIKV strains isolated from different

geographical locations. ZIKV strains from Brazil and Uganda showed delayed activation of the innate immune responses mediated by RIG-I as compared to the milder Cambodia strain that correlates with their pathological outcomes (Esser-Nobis et al., 2019). Studies using these different strains in lung A549 cells revealed the important role of RIG-I sensing in early innate immune response and induction of Type I Interferon responses (Strottmann et al., 2019). However, the role of this pathway in the host tropism of different isolates of ZIKV is yet to be fully uncovered that may provide a deeper insight into the importance of early viral sensing and productive IFN-response *via* the MAVS signalosome in ZIKV clearance.

Influenza A Virus

Influenza A virus (IAV) is one of the four types of influenza virus and the only influenza virus sub-type that has been known to cause global pandemic. Based on the presence of two surface proteins, hemagglutinin (HA) and neuraminidase (N), IAV can be sub-categorized into different strains (Bouvier and Palese, 2008). The 1918 Spanish Flu and the pandemic of 2009 were associated with the H1N1 subtype of IAV. H1N1 mostly affect children and young and middle-aged adult contrary to other flu where it affects mostly the older people.

The Influenza virus contains eight segmented (−) single stranded RNA and affects the upper respiratory tract epithelial cells causing the "seasonal" flu or fatal pulmonary disorder in extreme conditions (Shao et al., 2017). The polymeric basic 2 (PB2) subunit of the RNA polymerase complex is a major pathogenic determinant of seasonal IAV (Liu et al., 2019). Further, an intact mitochondrial membrane potential (MMP) is required for MAVS-mediated interferon production and PB2 might indirectly affect MAVS function by altering MMP (Varga et al., 2012). PB2 protein of pdm/09 variant of IAV carrying T5881 mutation has been shown to suppress MAVS-mediated interferon signaling more robustly that could potentially contribute to its increased pathogenicity. It has been demonstrated that PB2 is imported into the mitochondrial matrix and associates with MAVS at the mitochondria that correlates with reduced IFNβ production *in vitro* (Graef et al., 2010; Long and Fodor, 2016). Besides PB2, other proteins of IAV like the non-structural protein 1 (NS1) can block the RIG-I mediated induction of IFNβ by inhibiting TRIM25 (Gack et al., 2009). Inflammasome formation, a complex of NLRP3/ASC/Caspase-1, that is required for the production the inflammatory cytokine IL1β, is triggered by IFNβ in a positive feedback loop in primary lung epithelial cells and was shown to be mediated by RIG-I *via* its interaction with MAVS/TRIM2/Riplet (Mibayashi et al., 2007; Pothlichet et al., 2013). TRIM25 and Riplet positively regulates the antiviral responses mediated by RIG-I and the NS1 protein of highly pathogenic 1918 virus binds to RIG-I and TRIM25 to antagonize IFNβ activation (Gack et al., 2009; Koliopoulos et al., 2018). This correlated with the reduced induction of both Type I Interferon, as well as IL1β production by NS1 in IAV infected ferrets. Further RNAse L, a ubiquitous endonuclease for single stranded RNA, enhances NLRP3 activation and complex formation with the DExD/H-box helicase, DHX33, and MAVS in bone marrow derived dendritic cells and THP-1 derived macrophages (Chakrabarti et al., 2015). However, this antiviral response appears to be a double-edged sword as heightened inflammation and production of pro-inflammatory cytokines is often associated with increased morbidity following IAV infection. One of the NLRs, NLRX1 was shown to inhibit the production of antiviral cytokines and reduce lung pathology in IAV virus infected mice *via* its direct interaction with the RIG-I/MAVS pathway (Allen et al., 2011). Thus, NLRX1 at the mitochondria could provide a brake on the cytokine storm induced by IAV that has often been associated with the higher mortality rates during influenza virus pandemic.

SARS-Coronavirus

Coronavirus is emerging pathogens that has serious life-threatening impact on human health. Severe acute respiratory syndrome-related coronavirus (SARS-CoV1) caused a major outbreak of respiratory disease in 2002–2004 (SARS | Home | Severe Acute Respiratory Syndrome | SARS-CoV Disease | CDC, n.d.). The current pandemic which has bypassed the death rate of all previous pandemic of the last century is caused by a novel subtype of SARS-CoV and has been named SARS-CoV2 causing corona virus disease 19 (COVID-19). Coming from zoonotic reservoir, SARS-CoV shows extreme adaptivity through species jump and is a major health concern worldwide with the probability of new strains with heightened pathogenic potential emerging every year. SARS-CoV is an enveloped (+) single stranded RNA virus and in human host, it mainly infects the ciliated epithelium and alveolar type II pneumocytes (de Wit et al., 2016). Being mostly asymptomatic in the early stages of infection with flu like symptoms, it can quickly escalate to acute respiratory distress syndrome (ARDS) and multiorgan failure (Cameron et al., 2008; Yin and Wunderink, 2018). A similar manifestation has also been observed in COVID-19 patients, where cytokine storm has been shown to result in ARDS-like symptoms. SARS-CoV-2 can efficiently alter the cytokine profile by promoting the production of pro-inflammatory genes and blocking the stimulation of interferon genes based on their mode of infectivity (i.e., severe or non-severe form of SARS; Mahmudpour et al., 2020; Ratajczak and Kucia, 2020; Wang et al., 2020a; Yap et al., 2020). An arsenal of viral proteins is dedicated for this process and the host mitochondria play a pivotal role in the early response to infection (Maier et al., 2015). SARS-CoV-1 proteins, ORF-3b and nsp-10, show direct mitochondrial association where ORF-3b co-localizes with mitochondria specific markers and nsp-10 specifically interacts with NADH 4 L subunit and cytochrome c oxidase that affects mitochondrial function (Li et al., 2005; Yuan et al., 2006). It can also inhibit the MAVS downstream signaling by directly binding to STAT1 and inhibiting the TBK1/IKKε signaling. Further, the SARS-CoV-1 envelope protein has been shown to activate inflammasome formation and stimulate the production of pro-inflammatory cytokines like IL6 and TNF which makes it an attractive target for future studies (Nieto-Torres et al., 2014). Hence, studies on SARS-CoV-1 points toward the relevance of mitochondria mediated innate immune signaling pathway that may be further extrapolated to SARS-CoV-2 infection (Singh et al., 2020).

No study has reported the role of the mitochondrial innate immune sensing in COVID-19 pathogenesis that may provide effective strategies to limit viral replication within the host and the generation of a protective adaptive immune response.

CONCLUSION

RNA viruses have become important etiological agents of emerging pathogens in humans constituting a major percentage of all human emerging diseases including those induced by bacteria or parasites. The past decade has seen several cases of pandemics arising due to RNA viruses originating from wild life reservoirs like the Ebola, H1N1 influenza, SARS, and MERS and the recent COVID-19 pandemic. The RNA polymerases of these viruses often lack proofreading activity increasing their mutation rates during the replicative stage of the virus. This comes as a severe challenge in developing vaccine strategies and it is important to understand conserved host immune responses which may help combat a wide range of these RNA viruses.

The innate immune response, which provides the first line of defense against these RNA viruses *via* the production of Type I Interferon, is often targeted by the viruses for the successful establishment of an infection. However, priming of IFN-responses prior to an infection can be a double edged sword as cytokine storm following hyper-stimulation of the immune responses and the over production of pro-inflammatory cytokines have been shown to be associated with diseases like Ebola, Influenza, and COVID-19 (D'Elia et al., 2013; Infection-cusabio and Topics, 2020) and the mitochondria may act as a central hub in modulating these responses. MAVS dependent pathway at the mitochondria act as a critical factor for limiting virus infection and a detailed understanding of its regulation can help fine tune the host immune responses toward a productive antiviral strategy. Several molecules like NLRX1 and DUBs regulate RIG-I binding to MAVS at the mitochondria or directly target MAVS for degradation, thus acting as a counterbalance to prevent overproduction of Type I Interferons during a persistent viral infection. Further, development of agonists for the RIG-I/MAVS pathways can be used synergistically with antiviral compounds to restrict the replication of viruses at the initial stage and offer prophylactic solution to prevent such deadly outbreaks and rapid spread of RNA-virus induced infection.

AUTHOR CONTRIBUTIONS

PM conceived the work. SD, ND, and PM wrote the manuscript. PM prepared the figures and revised the entire manuscript. All authors contributed to the article and approved the submitted version.

FUNDING

The work was funded by the extramural funding from Dept. of Biotechnology, India (#BT/PR10983/BRB/10/1282/2014) to PM. SD is a recipient of CSIR-NET Fellowship, Govt. of India (File No: 08/155(0085)/2020-EMR-I).

ACKNOWLEDGMENTS

The authors thank Dr. Amit Sarkar and members of the lab for their insightful comments during the preparation of the manuscript.

REFERENCES

Allen, I. C., Moore, C. B., Schneider, M., Lei, Y., Davis, B. K., Scull, M. A., et al. (2011). NLRX1 protein attenuates inflammatory responses to infection by interfering with the RIG-I-MAVS and TRAF6-NF-κB signaling pathways. *Immunity* 34, 854–865. doi: 10.1016/j.immuni.2011.03.026

Allen, I. C., Moore, C. B., Schneider, M., Lei, Y., Davis, B. K., Scull, A., et al. (2012). NLRX1 protein attenuates inflammatory responses to virus infection by interfering with the RIG-I-MAVS signaling pathway and TRAF6 ubiquitin ligase. *Immunity* 34, 854–865. doi: 10.1016/j.immuni.2011.03.026.NLRX1

Biacchesi, S., LeBerre, M., Lamoureux, A., Louise, Y., Lauret, E., Boudinot, P., et al. (2009). Mitochondrial antiviral signaling protein plays a major role in induction of the fish innate immune response against RNA and DNA viruses. *J. Virol.* 83, 7815–7827. doi: 10.1128/JVI.00404-09

Bouvier, N. M., and Palese, P. (2008). The biology of influenza viruses. *Vaccine* 26, D49–D53. doi: 10.1016/j.vaccine.2008.07.039

Brisse, M., and Ly, H. (2019). Comparative structure and function analysis of the RIG-I-like receptors: RIG-I and MDA5. *Front. Immunol.* 10:1586. doi: 10.3389/fimmu.2019.01586

Cameron, M. J., Bermejo-Martin, J. F., Danesh, A., Muller, M. P., and Kelvin, D. J. (2008). Human immunopathogenesis of severe acute respiratory syndrome (SARS). *Virus Res.* 133, 13–19. doi: 10.1016/j.virusres.2007.02.014

Cárdenas, W. B., Loo, Y. -M., Gale, M., Hartman, A. L., Kimberlin, C. R., Martínez-Sobrido, L., et al. (2006). Ebola virus VP35 protein binds double-stranded RNA and inhibits alpha/beta interferon production induced by RIG-I signaling. *J. Virol.* 80, 5168–5178. doi: 10.1128/JVI.02199-05

Carneiro, F. R. G., Lepelley, A., Seeley, J. J., Hayden, M. S., and Ghosh, S. (2018). An essential role for ECSIT in mitochondrial complex I assembly and mitophagy in macrophages. *Cell Rep.* 22, 2654–2666. doi: 10.1016/j.celrep.2018.02.051

Castanier, C., Zemirli, N., Portier, A., Garcin, D., Bidère, N., Vazquez, A., et al. (2012). MAVS ubiquitination by the E3 ligase TRIM25 and degradation by the proteasome is involved in type I interferon production after activation of the antiviral RIG-I-like receptors. *BMC Biol.* 10:44. doi: 10.1186/1741-7007-10-44

Chakrabarti, A., Banerjee, S., Franchi, L., Loo, Y. M., Gale, M., Núñez, G., et al. (2015). RNase L activates the NLRP3 inflammasome during viral infections. *Cell Host Microbe* 17, 466–477. doi: 10.1016/j.chom.2015.02.010

Chang, T. H., Kubota, T., Matsuoka, M., Jones, S., Bradfute, S. B., Bray, M., et al. (2009). Ebola Zaire virus blocks type I interferon production by exploiting the host SUMO modification machinery. *PLoS Pathog.* 5:e1000493. doi: 10.1371/journal.ppat.1000493

Chen, G., Wu, D., Guo, W., Cao, Y., Huang, D., Wang, H., et al. (2020). Clinical and immunological features of severe and moderate coronavirus disease 2019. *J. Clin. Invest.* 130, 2620–2629. doi: 10.1172/JCI137244

Choi, Y. B., Shembade, N., Parvatiyar, K., Balachandran, S., and Harhaj, E. W. (2017). TAX1BP1 restrains virus-induced apoptosis by facilitating itch-mediated degradation of the mitochondrial adaptor MAVS. *Mol. Cell. Biol.* 37, e00422–e00416. doi: 10.1128/mcb.00422-16

Chow, K. T., Gale, M., and Loo, Y. -M. (2018). RIG-I and other RNA sensors in antiviral immunity. *Annu. Rev. Immunol.* 36, 667–694. doi: 10.1146/annurev-immunol-042617-053309

Chowell, G., Tariq, A., and Kiskowski, M. (2019). Vaccination strategies to control Ebola epidemics in the context of variable household inaccessibility levels. *PLoS Negl. Trop. Dis.* 13:e0007814. doi: 10.1371/journal.pntd.0007814

Cusabio (2020). What You Have to Know about Cytokine Storm and Virus Infection. 1–8.

Dai, T., Wu, L., Wang, S., Wang, J., Xie, F., Zhang, Z., et al. (2018). FAF1 regulates antiviral immunity by inhibiting MAVS but is antagonized by phosphorylation upon viral infection. *Cell Host Microbe* 24, 776.e5–790.e5. doi: 10.1016/j.chom.2018.10.006

de Wit, E., Van Doremalen, N., Falzarano, D., and Munster, V. J. (2016). SARS and MERS: recent insights into emerging coronaviruses. *Nat. Rev. Microbiol.* 14, 523–534. doi: 10.1038/nrmicro.2016.81

DeDiego, M. L., Nieto-Torres, J. L., Regla-Nava, J. A., Jimenez-Guardeno, J. M., Fernandez-Delgado, R., Fett, C., et al. (2014). Inhibition of NF-κB-mediated inflammation in severe acute respiratory syndrome coronavirus-infected mice increases survival. *J. Virol.* 88, 913–924. doi: 10.1128/jvi.02576-13

D'Elia, R. V., Harrison, K., Oyston, P. C., Lukaszewski, R. A., and Clark, G. C. (2013). Targeting the "Cytokine Storm" for therapeutic benefit. *Clin. Vaccine Immunol.* 20, 319–327. doi: 10.1128/CVI.00636-12

Ding, Q., Gaska, J. M., Douam, F., Wei, L., Kim, D., Balev, M., et al. (2018). Species-specific disruption of STING-dependent antiviral cellular defenses by the Zika virus NS2B3 protease. *Proc. Natl. Acad. Sci. U. S. A.* 115, E6310–E6318. doi: 10.1073/pnas.1803406115

Dorn, G. W. (2012). Inflame on!: mitochondrial escape provokes cytokine storms that doom the heart. *Circ. Res.* 111, 271–273. doi: 10.1161/CIRCRESAHA.112.275867

Dutta, M., Robertson, S. J., Okumura, A., Scott, D. P., Chang, J., Weiss, J. M., et al. (2017). A systems approach reveals MAVS signaling in myeloid cells as critical for resistance to Ebola virus in murine models of infection. *Cell Rep.* 18, 816–829. doi: 10.1016/j.celrep.2016.12.069

Ebola virus disease (n.d.). Available at: https://www.who.int/health-topics/ebola/#tab=tab_1 (Accessed April 17, 2020).

Esser-Nobis, K., Aarreberg, L. D., Roby, J. A., Fairgrieve, M. R., Green, R., and Gale, M. (2019). Comparative analysis of African and Asian lineage-derived Zika virus strains reveals differences in activation of and sensitivity to antiviral innate immunity. *J. Virol.* 93, e00640–e00619. doi: 10.1128/JVI.00640-19

Falasca, L., Agrati, C., Petrosillo, N., Di Caro, A., Capobianchi, M. R., Ippolito, G., et al. (2015). Molecular mechanisms of Ebola virus pathogenesis: focus on cell death. *Cell Death Differ.* 22, 1250–1259. doi: 10.1038/cdd.2015.67

Feng, Z., Cerveny, M., Yan, Z., and He, B. (2007). The VP35 protein of Ebola virus inhibits the antiviral effect mediated by double-stranded RNA-dependent protein kinase PKR. *J. Virol.* 81, 182–192. doi: 10.1128/JVI.01006-06

Freundt, E. C., Yu, L., Park, E., Lenardo, M. J., and Xu, X. -N. (2009). Molecular determinants for subcellular localization of the severe acute respiratory syndrome coronavirus open reading frame 3b protein. *J. Virol.* 83, 6631–6640. doi: 10.1128/JVI.00367-09

Friedman, J. R., and Nunnari, J. (2014). Mitochondrial form and function. *Nature* 505, 335–343. doi: 10.1038/nature12985

Gack, M. U., Albrecht, R. A., Urano, T., Inn, K. S., Huang, I. C., Carnero, E., et al. (2009). Influenza A virus NS1 targets the ubiquitin ligase TRIM25 to evade recognition by the host viral RNA sensor RIG-I. *Cell Host Microbe* 5, 439–449. doi: 10.1016/j.chom.2009.04.006

Gack, M. U., Shin, Y. C., Joo, C. H., Urano, T., Liang, C., Sun, L., et al. (2007). TRIM25 RING-finger E3 ubiquitin ligase is essential for RIG-I-mediated antiviral activity. *Nature* 446, 916–920. doi: 10.1038/nature05732

Geoghegan, J. L., Senior, A. M., Di Giallonardo, F., and Holmes, E. C. (2016). Virological factors that increase the transmissibility of emerging human viruses. *Proc. Natl. Acad. Sci. U. S. A.* 113, 4170–4175. doi: 10.1073/pnas.1521582113

Graef, K. M., Vreede, F. T., Lau, Y. -F., McCall, A. W., Carr, S. M., Subbarao, K., et al. (2010). The PB2 subunit of the influenza virus RNA polymerase affects virulence by interacting with the mitochondrial antiviral signaling protein and inhibiting expression of beta interferon. *J. Virol.* 84, 8433–8445. doi: 10.1128/JVI.00879-10

Grant, A., Ponia, S. S., Tripathi, S., Balasubramaniam, V., Miorin, L., Sourisseau, M., et al. (2016). Zika virus targets human STAT2 to inhibit type I interferon signaling. *Cell Host Microbe* 19, 882–890. doi: 10.1016/j.chom.2016.05.009

Green, R. R., Wilkins, C., Pattabhi, S., Dong, R., Loo, Y., and Gale, M. (2016). Transcriptional analysis of antiviral small molecule therapeutics as agonists of the RLR pathway. *Genom. Data* 7, 290–292. doi: 10.1016/j.gdata.2016.01.020

Haby, M. M., Pinart, M., Elias, V., and Reveiz, L. (2018). Prevalence of asymptomatic Zika virus infection: a systematic review. *Bull. World Health Organ.* 96, 402D–413D. doi: 10.2471/BLT.17.201541

Hackbart, M., Deng, X., and Baker, S. C. (2020). Coronavirus endoribonuclease targets viral polyuridine sequences to evade activating host sensors. *Proc. Natl. Acad. Sci. U. S. A.* 117, 8094–8103. doi: 10.1073/pnas.1921485117

Haneklaus, M., and O'Neill, L. A. J. (2015). NLRP3 at the interface of metabolism and inflammation. *Immunol. Rev.* 265, 53–62. doi: 10.1111/imr.12285

Hartmann, G. (2017). Nucleic acid immunity. *Adv. Immunol.* 133, 121–169. doi: 10.1016/bs.ai.2016.11.001

He, Y., Hara, H., and Núñez, G. (2016). Mechanism and regulation of NLRP3 inflammasome activation. *Trends Biochem. Sci.* 41, 1012–1021. doi: 10.1016/j.tibs.2016.09.002

He, F., Melén, K., Maljanen, S., Lundberg, R., Jiang, M., Österlund, P., et al. (2017). Ebolavirus protein VP24 interferes with innate immune responses by inhibiting interferon-λ1 gene expression. *Virology* 509, 23–34. doi: 10.1016/j.virol.2017.06.002

He, X., Zhu, Y., Zhang, Y., Geng, Y., Gong, J., Geng, J., et al. (2019). RNF 34 functions in immunity and selective mitophagy by targeting MAVS for autophagic degradation. *EMBO J.* 38:e100978. doi: 10.15252/embj.2018100978

Hu, Y., Dong, X., He, Z., Wu, Y., Zhang, S., Lin, J., et al. (2019). Zika virus antagonizes interferon response in patients and disrupts RIG-I-MAVS interaction through its CARD-TM domains. *Cell Biosci.* 9, 1–15. doi: 10.1186/s13578-019-0308-9

Hughes, M. M., and O'Neill, L. A. J. (2018). Metabolic regulation of NLRP3. *Immunol. Rev.* 281, 88–98. doi: 10.1111/imr.12608

Infection-cusabio, V., and Topics, O. P. (2020). What you have to know about cytokine storm and virus infection. 1–8.

Jahan, A. S., Biquand, E., Muñoz-Moreno, R., Le Quang, A., Mok, C. K. -P., Wong, H. H., et al. (2019). OTUB1 is a key regulator of RIG-I dependent immune signalling and is targeted for proteasomal degradation by influenza A NS1. *Cell Rep.* 30, 1570.e6–1584.e6. doi: 10.1016/j.celrep.2020.01.015

Jureka, A. S., Kleinpeter, A. B., Tipper, J. L., Harrod, K. S., and Petit, C. M. (2020). The influenza NS1 protein modulates RIG-I activation via a strain-specific direct interaction with the second CARD of RIG-I. *J. Biol. Chem.* 295, 1153–1164. doi: 10.1074/jbc.RA119.011410

Kaner, J., and Schaack, S. (2016). Understanding Ebola: the 2014 epidemic. *Glob. Health* 12:53. doi: 10.1186/s12992-016-0194-4

Kao, W. P., Yang, C. Y., Su, T. W., Wang, Y. T., Lo, Y. C., and Lin, S. C. (2015). The versatile roles of CARDs in regulating apoptosis, inflammation, and NF-κB signaling. *Apoptosis* 20, 174–195. doi: 10.1007/s10495-014-1062-4

Kawai, T., and Akira, S. (2007). Antiviral signaling through pattern recognition receptors. *J. Biochem.* 141, 137–145. doi: 10.1093/jb/mvm032

Kell, A. M., and Gale, M. (2015). RIG-I in RNA virus recognition. *Virology* 479–480, 110–121. doi: 10.1016/j.virol.2015.02.017

Keystone Symposia (n.d.). Available at: https://virtual.keystonesymposia.org/ks/articles/3460/view (Accessed May 17, 2020).

Khan, M., Syed, G. H., Kim, S. J., and Siddiqui, A. (2015). Mitochondrial dynamics and viral infections: a close nexus. *Biochim. Biophys. Acta* 1853, 2822–2833. doi: 10.1016/j.bbamcr.2014.12.040

Koliopoulos, M. G., Lethier, M., van Der Veen, A. G., Haubrich, K., Hennig, J., Kowalinski, E., et al. (2018). Molecular mechanism of influenza A NS1-mediated TRIM25 recognition and inhibition. *Nat. Commun.* 9:1820. doi: 10.1038/s41467-018-04214-8

Kopecky-Bromberg, S. A., Martínez-Sobrido, L., Frieman, M., Baric, R. A., and Palese, P. (2007). Severe acute respiratory syndrome coronavirus open reading frame (ORF) 3b, ORF 6, and nucleocapsid proteins function as interferon antagonists. *J. Virol.* 81, 548–557. doi: 10.1128/JVI.01782-06

Lei, Y., Moore, C. B., Liesman, R. M., O'Connor, B. P., Bergstralh, D. T., Chen, Z. J., et al. (2009). MAVS-mediated apoptosis and its inhibition by viral proteins. *PLoS One* 4:e5466. doi: 10.1371/journal.pone.0005466

Lester, S. N., and Li, K. (2014). Toll-like receptors in antiviral innate immunity. *J. Mol. Biol.* 426, 1246–1264. doi: 10.1016/j.jmb.2013.11.024

Li, W., Li, N., Dai, S., Hou, G., Guo, K., Chen, X., et al. (2019). Zika virus circumvents host innate immunity by targeting the adaptor proteins MAVS and MITA. *FASEB J.* 33, 9929–9944. doi: 10.1096/fj.201900260R

Li, Q., Wang, L., Dong, C., Che, Y., Jiang, L., Liu, L., et al. (2005). The interaction of the SARS coronavirus non-structural protein 10 with the

cellular oxido-reductase system causes an extensive cytopathic effect. *J. Clin. Virol.* 34, 133–139. doi: 10.1016/j.jcv.2004.12.019

Liang, Y., Wang, M. L., Chien, C. S., Yarmishyn, A. A., Yang, Y. P., Lai, W. Y., et al. (2020). Highlight of immune pathogenic response and hematopathologic effect in SARS-CoV, MERS-CoV, and SARS-Cov-2 infection. *Front. Immunol.* 11:1022. doi: 10.3389/fimmu.2020.01022

Lin, S., Yang, S., He, J., Guest, J. D., Ma, Z., Yang, L., et al. (2019). Zika virus NS5 protein antagonizes type I interferon production via blocking TBK1 activation. *Virology* 527, 180–187. doi: 10.1016/j.virol.2018.11.009

Liu, Y., Olagnier, D., and Lin, R. (2017). Host and viral modulation of RIG-I-mediated antiviral immunity. *Front. Immunol.* 7:662. doi: 10.3389/fimmu.2016.00662

Liu, X., Yang, C., Sun, X., Lin, X., Zhao, L., Chen, H., et al. (2019). Evidence for a novel mechanism of influenza A virus host adaptation modulated by PB2-627. *FEBS J.* 286, 3389–3400. doi: 10.1111/febs.14867

Long, J. C. D., and Fodor, E. (2016). The PB2 subunit of the Influenza A virus RNA polymerase is imported into the mitochondrial matrix. *J. Virol.* 90, 8729–8738. doi: 10.1128/JVI.01384-16

Lundberg, R., Melén, K., Westenius, V., Jiang, M., Österlund, P., Khan, H., et al. (2019). Zika virus non-structural protein NS5 inhibits the RIG-I pathway and interferon lambda 1 promoter activation by targeting IKK epsilon. *Viruses* 11:1024. doi: 10.3390/v11111024

Luthra, P., Ramanan, P., Mire, C. E., Weisend, C., Tsuda, Y., Yen, B., et al. (2013). Mutual antagonism between the ebola virus VP35 protein and the RIG-I activator PACT determines infection outcome. *Cell Host Microbe* 14, 74–84. doi: 10.1016/j.chom.2013.06.010

Ma, J., Ketkar, H., Geng, T., Lo, E., Wang, L., Xi, J., et al. (2018). Zika virus non-structural protein 4A blocks the RLR-MAVS signaling. *Front. Microbiol.* 9:1350. doi: 10.3389/fmicb.2018.01350

Mahmudpour, M., Roozbeh, J., Keshavarz, M., Farrokhi, S., and Nabipour, I. (2020). COVID-19 cytokine storm: the anger of inflammation. *Cytokine* 133:155151. doi: 10.1016/j.cyto.2020.155151

Maier, H. J., Bickerton, E., and Britton, P. (2015). *Coronaviruses: Methods and protocols*. *Vol. 1282*. 1–282.

Messaoudi, I., Amarasinghe, G. K., and Basler, C. F. (2015). Filovirus pathogenesis and immune evasion: insights from Ebola virus and Marburg virus. *Nat. Rev. Microbiol.* 13, 663–676. doi: 10.1038/nrmicro3524

Mibayashi, M., Martinez-Sobrido, L., Loo, Y. -M., Cardenas, W. B., Gale, M., and Garcia-Sastre, A. (2007). Inhibition of retinoic acid-inducible gene I-mediated induction of beta interferon by the NS1 protein of Influenza A virus. *J. Virol.* 81, 514–524. doi: 10.1128/JVI.01265-06

Mills, E. L., Kelly, B., and O'Neill, L. A. J. (2017). Mitochondria are the powerhouses of immunity. *Nat. Immunol.* 18, 488–498. doi: 10.1038/ni.3704

Mishra, P., and Chan, D. C. (2014). Mitochondrial dynamics and inheritance during cell division, development and disease. *Nat. Rev. Mol. Cell Biol.* 15, 634–646. doi: 10.1038/nrm3877

Miyake, K., Shibata, T., Ohto, U., Shimizu, T., Saitoh, S. -I., Fukui, R., et al. (2018). Mechanisms controlling nucleic acid-sensing Toll-like receptors. *Int. Immunol.* 30, 43–51. doi: 10.1093/intimm/dxy016

Murphy, M. P. (2009). How mitochondria produce reactive oxygen species. *Biochem. J.* 417, 1–13. doi: 10.1042/BJ20081386

Nieto-Torres, J. L., DeDiego, M. L., Verdiá-Báguena, C., Jimenez-Guardeño, J. M., Regla-Nava, J. A., Fernandez-Delgado, R., et al. (2014). Severe acute respiratory syndrome coronavirus envelope protein ion channel activity promotes virus fitness and pathogenesis. *PLoS Pathog.* 10:e1004077. doi: 10.1371/journal.ppat.1004077

Nieto-Torres, J. L., Verdiá-Báguena, C., Jimenez-Guardeño, J. M., Regla-Nava, J. A., Castaño-Rodriguez, C., Fernandez-Delgado, R., et al. (2015). Severe acute respiratory syndrome coronavirus E protein transports calcium ions and activates the NLRP3 inflammasome. *Virology* 485, 330–339. doi: 10.1016/j.virol.2015.08.010

Okamoto, M., Kouwaki, T., Fukushima, Y., and Oshiumi, H. (2018). Regulation of RIG-I activation by K63-linked polyubiquitination. *Front. Immunol.* 8:1942. doi: 10.3389/fimmu.2017.01942

Orzalli, M. H., and Kagan, J. C. (2017). Apoptosis and necroptosis as host defense strategies to prevent viral infection. *Trends Cell Biol.* 27, 800–809. doi: 10.1016/j.tcb.2017.05.007

Plourde, A. R., and Bloch, E. M. (2016). A literature review of Zika virus. *Emerg. Infect. Dis.* 22, 1185–1192. doi: 10.3201/eid2207.151990

Pothlichet, J., Meunier, I., Davis, B. K., Ting, J. P. Y., Skamene, E., von Messling, V., et al. (2013). Type I IFN triggers RIG-I/TLR3/NLRP3-dependent inflammasome activation in Influenza A virus infected cells. *PLoS Pathog.* 9:e1003256. doi: 10.1371/journal.ppat.1003256

Prins, K. C., Cardenas, W. B., and Basler, C. F. (2009). Ebola virus protein VP35 impairs the function of interferon regulatory factor-activating kinases IKK and TBK-1. *J. Virol.* 83, 3069–3077. doi: 10.1128/JVI.01875-08

Qin, Y., Xue, B., Liu, C., Wang, X., Tian, R., Xie, Q., et al. (2017). NLRX1 mediates MAVS degradation to attenuate the hepatitis C virus-induced innate immune response through PCBP2. *J. Virol.* 91, e01264–e01217. doi: 10.1128/jvi.01264-17

Ratajczak, M. Z., and Kucia, M. (2020). SARS-CoV-2 infection and overactivation of Nlrp3 inflammasome as a trigger of cytokine "storm" and risk factor for damage of hematopoietic stem cells. *Leukemia* 34, 1726–1729. doi: 10.1038/s41375-020-0887-9

Refolo, G., Vescovo, T., Piacentini, M., Fimia, G. M., and Ciccosanti, F. (2020). Mitochondrial interactome: a focus on antiviral signaling pathways. *Front. Cell Dev. Biol.* 8:8. doi: 10.3389/fcell.2020.00008

Reid, S. P., Leung, L. W., Hartman, A. L., Martinez, O., Shaw, M. L., Carbonnelle, C., et al. (2006). Ebola virus VP24 binds karyopherin α1 and blocks STAT1 nuclear accumulation. *J. Virol.* 80, 5156–5167. doi: 10.1128/JVI.02349-05

Sadler, A. J. (2017). The role of MDA5 in the development of autoimmune disease. *J. Leukoc. Biol.* 103, 185–192. doi: 10.1189/jlb.4mr0617-223r

SARS | Home | Severe Acute Respiratory Syndrome | SARS-CoV Disease | CDC (n.d.). Available at: https://www.cdc.gov/sars/index.html (Accessed April 17, 2020).

Schilling, M., Bridgeman, A., Gray, N., Hertzog, J., Hublitz, P., Kohl, A., et al. (2020). RIG-I plays a dominant role in the induction of transcriptional changes in Zika virus-infected cells, which protect from virus-induced cell death. *Cells* 9:1476. doi: 10.3390/cells9061476

Schoeman, D., and Fielding, B. C. (2019). Coronavirus envelope protein: current knowledge. *Virol. J.* 16, 1–22. doi: 10.1186/s12985-019-1182-0

Shao, W., Li, X., Goraya, M. U., Wang, S., and Chen, J. L. (2017). Evolution of influenza a virus by mutation and re-assortment. *Int. J. Mol. Sci.* 18:1650. doi: 10.3390/ijms18081650

Shrivastava, G., León-Juárez, M., García-Cordero, J., Meza-Sánchez, D. E., and Cedillo-Barrón, L. (2016). Inflammasomes and its importance in viral infections. *Immunol. Res.* 64, 1101–1117. doi: 10.1007/s12026-016-8873-z

Singh, K. K., Chaubey, G., Chen, J. Y., and Suravajhala, P. (2020). Decoding SARS-CoV-2 hijacking of host mitochondria in pathogenesis of COVID-19. *Am. J. Physiol. Cell Physiol.* 319, C258–C267. doi: 10.1152/ajpcell.00224.2020

Sliter, D. A., Martinez, J., Hao, L., Chen, X., Sun, N., Fischer, T. D., et al. (2018). Parkin and PINK1 mitigate STING-induced inflammation. *Nature* 561, 258–262. doi: 10.1038/s41586-018-0448-9

Song, B. H., Yun, S. I., Woolley, M., and Lee, Y. M. (2017). Zika virus: history, epidemiology, transmission, and clinical presentation. *J. Neuroimmunol.* 308, 50–64. doi: 10.1016/j.jneuroim.2017.03.001

Strottmann, D. M., Zanluca, C., Mosimann, A. L. P., Koishi, A. C., Auwerter, N. C., Faoro, H., et al. (2019). Genetic and biological characterization of Zika virus isolates from different Brazilian regions. *Mem. Inst. Oswaldo Cruz* 114:e190150. doi: 10.1590/0074-02760190150

Structure of Ebola Virus (n.d.). Available at: https://microbiologyinfo.com/structure-of-ebola-virus/ (Accessed April 17, 2020).

Tsujimoto, Y., and Shimizu, S. (2007). Role of the mitochondrial membrane permeability transition in cell death. *Apoptosis* 12, 835–840. doi: 10.1007/s10495-006-0525-7

Varga, Z. T., Grant, A., Manicassamy, B., and Palese, P. (2012). Influenza virus protein PB1-F2 inhibits the induction of type I interferon by binding to MAVS and decreasing mitochondrial membrane potential. *J. Virol.* 86, 8359–8366. doi: 10.1128/JVI.01122-12

Vazquez, C., and Horner, S. M. (2015). MAVS coordination of antiviral innate immunity. *J. Virol.* 89, 6974–6977. doi: 10.1128/JVI.01918-14

Walker, M. A., Volpi, S., Sims, K. B., Walter, J. E., and Traggiai, E. (2014). Powering the immune system: mitochondria in immune function and deficiency. *J. Immunol. Res.* 2014:164309. doi: 10.1155/2014/164309

Wang, J., Jiang, M., Chen, X., and Montaner, L. J. (2020a). Cytokine storm and leukocyte changes in mild versus severe SARS-CoV-2 infection: review of 3939 COVID-19 patients in China and emerging pathogenesis and therapy concepts. *J. Leukoc. Biol.* 108, 17–41. doi: 10.1002/JLB.3COVR0520-272R

Wang, P., Yang, L., Cheng, G., Yang, G., Xu, Z., You, F., et al. (2013). UBXN1 interferes with Rig-I-like receptor-mediated antiviral immune response by targeting MAVS. *Cell Rep.* 3, 1057–1070. doi: 10.1016/j.celrep.2013.02.027

Wang, R., Zhu, Y., Ren, C., Yang, S., Tian, S., Chen, H., et al. (2020b). Influenza A virus protein PB1-F2 impairs innate immunity by inducing mitophagy. *Autophagy* 1–16. doi: 10.1080/15548627.2020.1725375 [Epub ahead of print]

Weinberg, S. E., Sena, L. A., and Chandel, N. S. (2015). Mitochondria in the regulation of innate and adaptive immunity. *Immunity* 42, 406–417. doi: 10.1016/j.immuni.2015.02.002

Wu, Y., Liu, Q., Zhou, J., Xie, W., Chen, C., Wang, Z., et al. (2017). Zika virus evades interferon-mediated antiviral response through the co-operation of multiple nonstructural proteins in vitro. *Cell Discov.* 3, 1–14. doi: 10.1038/celldisc.2017.6

Xu, H., He, X., Zheng, H., Huang, L. J., Hou, F., Yu, Z., et al. (2014). Structural basis for the prion-like MAVS filaments in antiviral innate immunity. *Elife* 3:e01489. doi: 10.7554/elife.01489

Yabal, M., Calleja, D. J., Simpson, D. S., and Lawlor, K. E. (2019). Stressing out the mitochondria: mechanistic insights into NLRP3 inflammasome activation. *J. Leukoc. Biol.* 105, 377–399. doi: 10.1002/JLB.MR0318-124R

Yap, J. K. Y., Moriyama, M., and Iwasaki, A. (2020). Inflammasomes and pyroptosis as therapeutic targets for COVID-19. *J. Immunol.* 205, 307–312. doi: 10.4049/jimmunol.2000513

Yin, Y., and Wunderink, R. G. (2018). MERS, SARS and other coronaviruses as causes of pneumonia. *Respirology* 23, 130–137. doi: 10.1111/resp.13196

Yu, C., Chen, R., Li, J. J., Li, J. J., Drahansky, M., Paridah, M., et al. (2012). We are IntechOpen, the world's leading publisher of Open Access books built by scientists, for scientists TOP 1%. Intech, 13.

Yuan, X., Shan, Y., Yao, Z., Li, J., Zhao, Z., Chen, J., et al. (2006). Mitochondrial location of severe acute respiratory syndrome coronavirus 3b protein. *Mol. Cells* 21, 186–191.

Zamarin, D., García-Sastre, A., Xiao, X., Wang, R., and Palese, P. (2005). Influenza virus PB1-F2 protein induces cell death through mitochondrial ANT3 and VDAC1. *PLoS Pathog.* 1:e4. doi: 10.1371/journal.ppat.0010004

Zhang, L., Qin, Y., and Chen, M. (2018). Viral strategies for triggering and manipulating mitophagy. *Autophagy* 14, 1665–1673. doi: 10.1080/15548627.2018.1466014

Zhao, Y., Sun, X., Nie, X., Sun, L., Tang, T. S., and Chen, D., et al. (2012). COX5B regulates MAVS-mediated antiviral signaling through interaction with ATG5 and repressing ROS production. *PLoS Pathog.* 8:e1003086. doi: 10.1371/journal.ppat.1003086

Zhao, Z., Tao, M., Han, W., Fan, Z., Imran, M., Cao, S., et al. (2019). Nuclear localization of Zika virus NS5 contributes to suppression of type I interferon production and response. *J. Gen. Virol.* doi: 10.1099/jgv.0.001376 [Epub ahead of print]

Zheng, Y., Liu, Q., Wu, Y., Ma, L., Zhang, Z., Liu, T., et al. (2018). Zika virus elicits inflammation to evade antiviral response by cleaving cGAS via NS 1-caspase-1 axis. *EMBO J.* 37:e99347. doi: 10.15252/embj.201899347

Züst, R., Cervantes-Barragan, L., Habjan, M., Maier, R., Neuman, B. W., Ziebuhr, J., et al. (2011). Ribose 2'-O-methylation provides a molecular signature for the distinction of self and non-self mRNA dependent on the RNA sensor Mda5. *Nat. Immunol.* 12, 137–143. doi: 10.1038/ni.1979

Conflict of Interest: The authors declare that the research was conducted in the absence of any commercial or financial relationships that could be construed as a potential conflict of interest.

frontiers in Microbiology

REVIEW
published: 04 December 2020
doi: 10.3389/fmicb.2020.559792

From Entry to Egress: Strategic Exploitation of the Cellular Processes by HIV-1

*Pavitra Ramdas†, Amit Kumar Sahu†, Tarun Mishra, Vipin Bhardwaj and Ajit Chande**

Molecular Virology Laboratory, Indian Institute of Science Education and Research (IISER) Bhopal, Bhopal, India

HIV-1 employs a rich arsenal of viral factors throughout its life cycle and co-opts intracellular trafficking pathways. This exquisitely coordinated process requires precise manipulation of the host microenvironment, most often within defined subcellular compartments. The virus capitalizes on the host by modulating cell-surface proteins and cleverly exploiting nuclear import pathways for post entry events, among other key processes. Successful virus–cell interactions are indeed crucial in determining the extent of infection. By evolving defenses against host restriction factors, while simultaneously exploiting host dependency factors, the life cycle of HIV-1 presents a fascinating montage of an ongoing host–virus arms race. Herein, we provide an overview of how HIV-1 exploits native functions of the host cell and discuss recent findings that fundamentally change our understanding of the post-entry replication events.

Keywords: HIV-1 infection, cell organelles, capsid uncoating, restriction factors, host-virus interactions

OPEN ACCESS

Edited by:
Parikshit Bagchi,
University of Michigan, United States

Reviewed by:
Ramón A. Gonzalez,
Universidad Autónoma del Estado de Morelos, Mexico
Smita Kulkarni,
National AIDS Research Institute, India

***Correspondence:**
Ajit Chande
ajitg@iiserb.ac.in

†These authors have contributed equally to this work

Specialty section:
This article was submitted to Virology, a section of the journal Frontiers in Microbiology

Received: *07 May 2020*
Accepted: *05 November 2020*
Published: *04 December 2020*

Citation:
Ramdas P, Sahu AK, Mishra T, Bhardwaj V and Chande A (2020) From Entry to Egress: Strategic Exploitation of the Cellular Processes by HIV-1. Front. Microbiol. 11:559792. doi: 10.3389/fmicb.2020.559792

INTRODUCTION

Human immunodeficiency virus (HIV)-1 is a complex retrovirus known to infect humans and diminish the immune system leading to acquired immunodeficiency syndrome (AIDS). The virus measures about 100 nm with viral envelope glycoproteins (gp120 and gp41) trimers embedded in the host cell-derived lipid membrane. This envelope encases a conical capsid that contains two copies of an RNA genome (∼9.2 kb) in addition to the retroviral enzymes. The HIV-1 genome encodes accessory proteins (Vif, Vpr, Vpu, and Nef) and regulatory proteins, Tat and Rev, apart from the canonical proteins (Gag, Pol, and Env) that other retroviruses encode. The gag gene translates into a polyprotein comprised of matrix (MA), capsid (CA), and nucleocapsid (NC). The pol gene encodes for the enzymes protease (PR), reverse transcriptase (RT), and integrase (IN). The env gene encodes for the viral surface glycoprotein comprising of surface (SU), gp120 and transmembrane (TM), gp41. In addition to the structural and accessory proteins encoding regions, the genome is flanked by long terminal repeats (LTRs). Since HIV-1 encodes a few functional genes, host cell machinery plays a rather significant role in completing the virus life cycle. Thus, this review provides a conceptual advance on how HIV-1 exploits intracellular processes most required during its journey in and out of the host cell. Providing with an updated model of the viral life-cycle, we also highlight the latest findings that fundamentally change our understanding of post-entry steps.

PLASMA MEMBRANE: THE SITE OF VIRION FUSION AND ENTRY

During HIV-1 transmission, the virus utilizes the envelope glycoprotein and the chemokine co-receptors CXCR4 or CCR5, depending on the viral tropism, to gain an entry into the $CD4^+$ T

cells. The envelope glycoprotein gp120 establishes contact with the surface-expressed CD4, leading to conformational changes (Berger et al., 1999) that subsequently facilitate binding to co-receptors, a critical event for initiating a fusion apparatus (**Figure 1**, step 1). Binding of the co-receptor later results in conformational changes that enable the gp41 subunit to insert its hydrophobic fusion peptide into the host lipid membrane to drive the fusion process (**Figure 1**, step 2) (Doms and Moore, 2000; Waheed and Freed, 2009). The molecular mechanism of HIV-1 entry and viral membrane fusion are reviewed extensively elsewhere (Harrison, 2008, 2015; Kielian, 2014; Chen, 2019). The virus interplays with a myriad of host plasma membrane proteins. The host factors P-selectin glycoprotein ligand-1 (PSGL-1) and CD43 modulate HIV attachment to the plasma membrane by being incorporated into virions (Fu et al., 2020). HIV-1 encoded Vpu along with co-clustered Gag at the membrane downregulates PSGL-1 to exclude it from the virions to ensure efficient attachment to the target cell membrane. Interferon (IFN)-induced transmembrane proteins (IFITMs) constitute another IFN-inducible gene that has also been shown to interfere with the entry of HIV-1 by modulating fusion with the host membrane (Compton et al., 2014; Zhao et al., 2019). Retroviral envelope glycoproteins have the ability to alter the sensitivity of the virus from restriction by host factors that target early steps of the infection cycle like IFITMs and SERINC5 (Foster et al., 2016; Beitari et al., 2017; Firrito et al., 2018). The binding of HIV-1 to its receptor and co-receptors alone has shown to induce and alter a plethora of signaling pathways (**Figure 2**). For instance, pattern recognition receptor like NLRP3 inhibits F-actin remodeling and regulates the susceptibility to HIV-1 infection. Once the virus binds to its receptors, P2Y2 signaling is activated to mediate the degradation of NLRP3. In the absence of NLRP3, protein tyrosine kinase, PYK2, undergoes phosphorylation and activation, leading to a cytoskeletal rearrangement favorable for viral entry (**Figure 2A**; Paoletti et al., 2019). Moreover, the interaction of viral protein Nef and host-derived p21-activated kinase2 (PAK2) was found to play a role in activating NFAT and NF-κB transcription factors required for T-cell activation (**Figure 2B**) (Fenard et al., 2005). On the other hand, the binding of HIV-1 to its receptor and co-receptors myristoylates Lck at p56 and activates the PLC-γ (**Figure 2C**). This facilitates the breakdown of PIP3 into DAG and IP3. The DAG activates the MAP kinase pathway, whereas IP3 triggers the opening of Ca^{2+} channels in the ER. In addition, the virally encoded Vpr induces Ca^{2+} influx and promotes the nuclear import of NFAT. The NFAT and ERK activated by MAPK signaling then promote the transcription of genes for cytokine production and T-cell proliferation and activation (Höhne et al., 2016). Besides relaying cell signaling and host immune evasion, multiple reports emphasize the nature of HIV-1 that induces apoptosis by increasing the expression of membrane-bound Fas in T-cells and FasL in monocytes, macrophages, and NK cells during infection (**Figure 2D**) (Kottilil et al., 2007; Li et al., 2009). It was shown *in vitro* that these enhanced expression levels led to faster apoptosis via caspase 8 than the uninfected cells (Badley et al., 1996). Further, the virally derived Tat and Nef in the host cytosol increase the FasL level in the plasma membrane and directly activate caspase 3 and caspase 8 to promote apoptosis (**Figure 2E**) (Bartz and Emerman, 1999; Jacob et al., 2017). Altogether, just the binding and fusion of the virus with the host cell triggers a wider variety of pathways to trick the cell into creating a facile environment for HIV-1 replication.

CYTOPLASM: THE SITE OF COMMENCEMENT OF UNCOATING AND REVERSE TRANSCRIPTION

Successful binding and fusion with the plasma membrane result in the release of viral content into the cytoplasm of the host cell. In the cytoplasm, critical events of HIV-1 replication occurs, such as core delivery, reverse transcription, and translation **(Figure 1, steps 3–4** and **step** 8). In this section, we attempt to give an insight into how HIV-1 adopts mechanisms to use or deceive the function of host cellular factors in core delivery and reverse transcription initiation.

Initiation of Uncoating

Prevailing models suggested that for completing the reverse transcription of viral RNA, partial disassembly of CA protein is indispensable and that the uncoating event precedes the reverse transcription, though, until recently, the precise mechanism, timing, and location of uncoating remained contentious (Arhel, 2010; Ambrose and Aiken, 2014). Post-entry, in the cytoplasm, the HIV-1 core engages the host cytoskeleton for the commencement of uncoating and cytoplasm-nuclear trafficking (McDonald et al., 2002; Lukic et al., 2014; Delaney et al., 2017). In a yeast two-hybrid screening, the Arhel lab found two microtubule-associated proteins MAP1A and MAP1S, to bind to the CA of HIV-1 and to tether the virus to the microtubule network *en route* to the nucleus (Fernandez et al., 2015). Later, the same group identified that cellular β-karyopherin Transportin-1 (TRN-1) binding to the CA is necessary and sufficient for uncoating and efficient nuclear import (Fernandez et al., 2019). In addition, the host kinesin-1 adaptor protein, FEZ1, and dynein adapter protein, BICD2, interact with the CA and promote the uncoating of the core by pulling in opposite directions, as in "tug-of-war" (Lukic et al., 2014; Campbell and Hope, 2015; Malikov et al., 2015; Dharan et al., 2017; Carnes et al., 2018). Besides, two other cellular factors, Dia1 and Dia2, known to stabilize microtubules, interact with the CA and promote uncoating and DNA synthesis (Delaney et al., 2017). The completion of uncoating as a nuclear phenomenon will be discussed in detail with newer insights in later sections.

Numerous cellular factors are known to restrict retroviral infection (Malim and Bieniasz, 2012; Colomer-Lluch et al., 2018), one of which is a tripartite motif protein, TRIM5α, known to interfere with the uncoating and reverse transcription by interacting with the viral CA (Stremlau et al., 2004, 2006). The TRIM5α, in non-human primates, was shown not to hamper

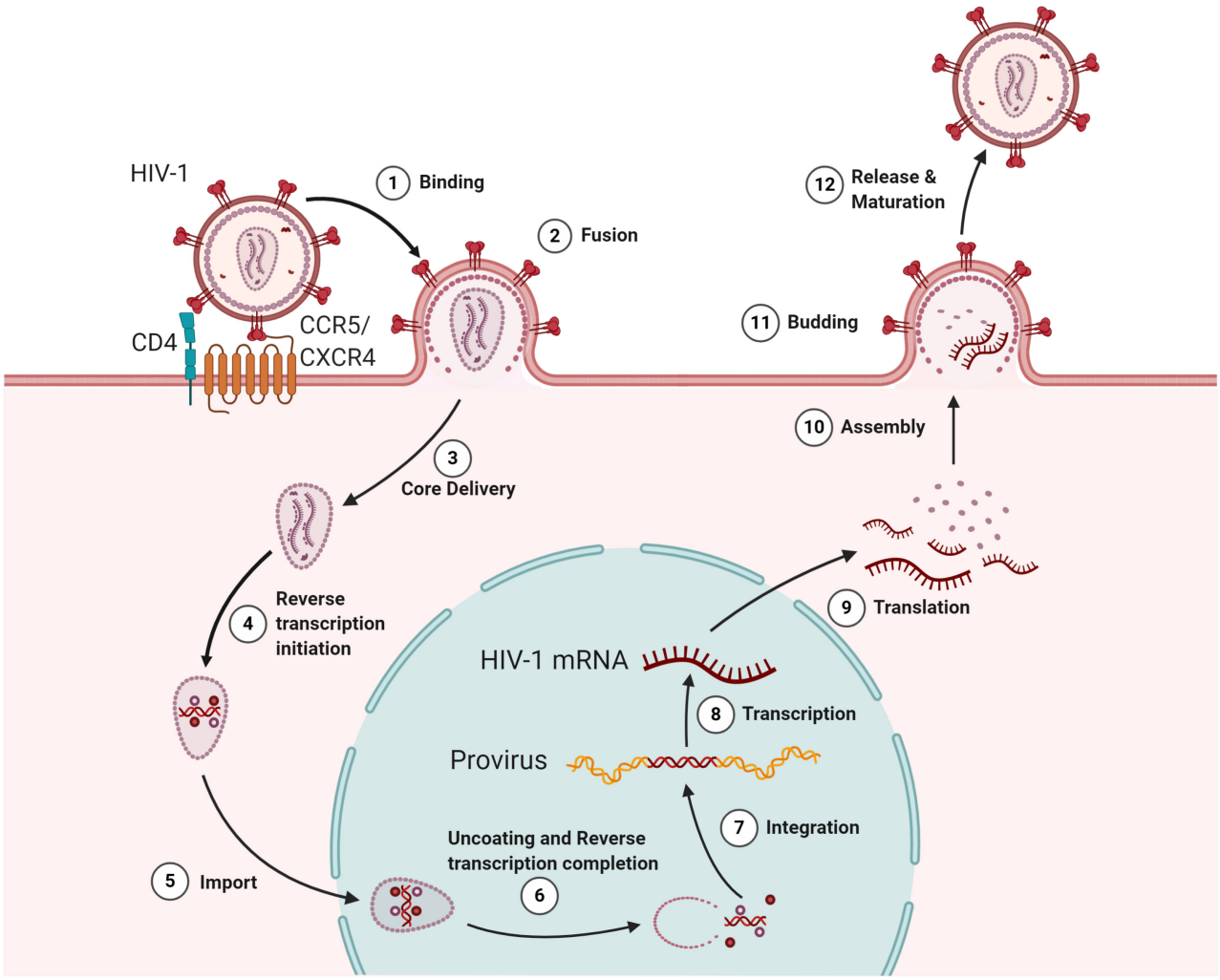

FIGURE 1 | The HIV lifecycle. The infection begins when the envelope glycoprotein attaches to the receptor CD4 and the membrane-spanning co-receptors (CXCR4/CCR5) (step 1), facilitating the entry and fusion of the viral particle into the target cell (step 2). Following core delivery (step 3), reverse transcription begins in the cytoplasm (step 4), and the core is imported into the nucleus (step 5). Following the nuclear import, uncoating and reverse transcription completes (step 6) and viral integrase facilitate viral genome integration into the host chromosome (step 7). Proviral transcription (step 8) yields viral RNAs that are exported to the cytoplasm for viral protein production (step 9). Genome-length viral RNA and viral proteins are assembled to package into virions for budding (steps 10 and 11). Ensuing budding, the virus progeny releases and matures to become an infectious virion (step 12).

HIV-1 infection; however, the replacement of the PRYSPRY domain of TRIM5α by cyclophilin A (CypA) binding domain in New World owl monkeys restrict the HIV-1 infection strongly (Sayah et al., 2004; Stremlau et al., 2005; Balakrishna and Kondapi, 2016; Colomer-Lluch et al., 2018). Contrastingly, a recent discovery using primary human blood cells suggested that the interaction between CypA and CA is necessary to evade the restriction by TRIM5α. The absence of this interaction, however, decreases the viral infectivity in human cells (Kim et al., 2019; Selyutina et al., 2020b). The CypA is a peptidylprolyl isomerase that catalyzes the *cis*/*trans*-isomerization of the peptide bond between Gly89 and Pro90 of the CA domain of Gag and is known to prevent premature uncoating (Luban et al., 1993; Bosco et al., 2002). Such tricks played by HIV-1 against host cellular factors in different models suggest HIV as one of the clever viruses to alter the host cellular factors for its benefit.

Commencement of Reverse Transcription

Following partial uncoating, reverse transcription begins (**Figure 1**, step 4) in an intricately organized manner forming an RT complex (RTC) in the host cytoplasm and completes in the nucleus just before successful uncoating (**Figure 1**, step 6) (Fassati and Goff, 2001; Burdick et al., 2020; Selyutina et al., 2020a). The RTC consists of viral RNA, host-derived $tRNA^{Lys3}$ primer, eukaryotic translational elongation factor 1A (eEF1A), synthesized DNA, several viral factors, and host factors (Isel et al., 1996; Fassati and Goff, 2001; Balakrishna and Kondapi, 2016).

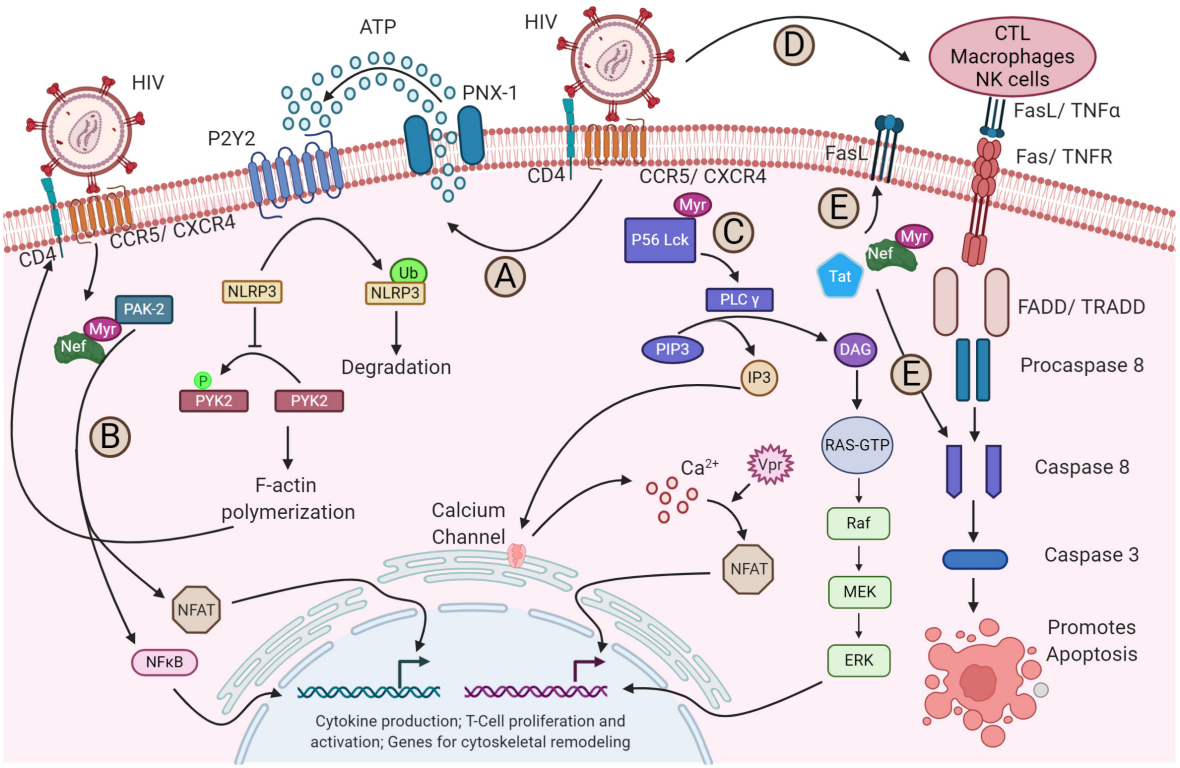

FIGURE 2 | Alteration of host signaling pathways by HIV-1. **(A)** The binding of HIV-1 to its receptor and co-receptor triggers the activation of P2Y2 by releasing ATP from host cytosol through pannexin-1 (PNX-1). The activated P2Y2 promotes the ubiquitin-mediated degradation of NLRP3, facilitating the phosphorylation and activation of PYK-2, which subsequently enables the F-actin polymerization required for the fusion and entry of HIV-1 into the host cell (not shown). **(B)** Nef activates NFAT and NF-κB via PAK2, which triggers the expression of cytoskeletal remodeling genes. **(C)** Binding of the virus also activates the lipid-associated Lck protein by myristoylation at p56. Lck activates the PLC-γ that breaks PIP3 into IP3 and DAG. IP3 triggers the opening of calcium channels in the ER and increases the concentration of Ca^{2+} in the cytosol. Increased Ca^{2+} activates the NFAT signaling. The virally encoded Vpr can also trigger the NFAT signaling through Ca^{2+} efflux and interferes with cGSK3β kinase for NFAT export (not shown). On the other hand, DAG via PKC activates the MAPK pathway. The NFAT and MAPK then promote the transcription of genes required for cytokine production and T-cell proliferation and activation. **(D)** The gp120-CD4 and CXCR4/CCR5 interaction upregulates the apoptotic receptor and ligand, Fas/FasL expression, which in turn activates the caspase 8 and caspase 3 for apoptosis of the infected cell via FADD/TRADD. **(E)** Additionally, the released viral Tat and Nef in the cytoplasm can also upregulate the Fas expression in the plasma membrane and can directly act on the caspase 8, promoting apoptosis.

The $tRNA^{Lys3}$ works as a primer by binding to the 5′ primer binding site (PBS) in the vRNA and initiates the reverse transcription process with the help of several cellular factors such as integrase interactor 1 (INI1 and hSNF5), survival motor neuron (SMN)-interacting protein 2 (Gemin2), histone deacetylase 1 (HDAC1), and sin3A-associated protein (SAP18) (Isel et al., 1996; Balakrishna and Kondapi, 2016). Recently, David Harrich's group reported the interaction between positively charged host eEF1A and the surface-exposed acidic E300 residue in the thumb domain of RT to play an essential role in viral uncoating, reverse transcription, replication, and infectivity (Rawle et al., 2018; Li D. et al., 2019). They also showed that E300R mutation or oxazole-benzenesulfonamide treatment reduces the RT interaction with eEF1A and thus delays the uncoating and reduces the viral reverse transcription and replication (Rawle et al., 2018, 2019). Once the minus-strand DNA is synthesized at the 5′ end, it is transferred to the 3′ end of the genome based on LTR's repeated (R) region complementarity, where the minus-strand DNA synthesis is completed. During this synthesis process, the RNaseH activity of RT cleaves the RNA molecules except at central PPT (cPPT). The cPPT serve as the template for the synthesis of a dsDNA fragment. Following second-strand transfer, the plus-strand DNA synthesis continues till the central termination sequence (CTS), displacing almost 100 nucleotides of previously made DNA, generating a central DNA flap. Thus, the final product of the reverse transcription process in HIV-1 generates a dsDNA molecule with a flap in the center (Arhel, 2010).

Like TRIM5α, APOBEC3G and SAMHD1 acts as post entry restriction factors against HIV-1. APOBEC3G is encapsidated into the budding virions and is present in the RTC, inducing G-to-A hypermutation and fragmented cDNA production in a deaminase-dependent pathway. Besides, a deep sequencing strategy further revealed the role of APOBEC3G in a sequence- and site-independent interference with cDNA synthesis by direct interaction with the RT. Concomitant defective viral protein synthesis thus inhibits HIV-1 replication and assembly strongly

(Sheehy et al., 2002; Pollpeter et al., 2018). While APOBEC3G-induced changes result in dysfunctional proteins, SAMHD1 depletes the cytoplasmic dNTP pool to hinder the reverse transcription process (Hrecka et al., 2011). To counteract these restriction factors, HIV1/2 encode accessory proteins like Vif and Vpx, which degrades APOBEC3G and SAMHD1, respectively, by employing Cullin E3 ubiquitin ligase complex (Sheehy et al., 2002; Hrecka et al., 2011). Further details on how HIV acts against other such restriction factors are described in the reviews of Malim and Bieniasz (2012) and Colomer-Lluch et al. (2018). Although the HIV-1 RNA is encapsidated within a core, several innate immune sensors are known to be activated upon capsid disruption. For instance, a member of the PYHIN family, IFI16 detects and binds to the incomplete HIV-1 cDNA and triggers the STING-TBK1-IRF3 signaling axis to promote the transcription of antiviral genes in myeloid cells. However, considering recent understanding of the completion of reverse transcription within the nucleus, the IFI16 sensing mechanism may have to be reconsidered. IFI16, in addition, triggers IL-1β production and promotes $CD4^+$ T cell death via ASC and caspase-1 in lymphoid cells (Jakobsen et al., 2013). Another cytosolic DNA sensor, cyclic GMP-AMP synthase (cGAS), is widely known for its antiviral immunity in the context of HIV-1 infection. cGAS preferentially detects abruptly formed HIV-1 reverse-transcribed DNAs in monocyte-derived dendritic cells (DCs) via polyglutamine binding protein-1 (PQBP1) and triggers the IFN response against HIV-1 through the STING-TBK1-IRF3 signaling pathway. However, HIV-1 suppresses the cGAS-STING activation by exploiting the NOD-like receptors family, NLRC3, an ATPase that promotes the sequestration and attenuation of STING activation and thus inhibits the transcription of IFN (Barouch et al., 2016). Moreover, recently, it was found that even though SAMHD1 acts as a restriction factor, it promotes the degradation of nascent incomplete HIV-1 DNA, and prevents the activation of cGAS-STING-mediated IFN production. Similarly, a ubiquitously expressed three prime repair exonuclease 1 (TREX-1) acts on incomplete reverse transcription products and prevents the cGAS-STING activation (Kumar et al., 2018; Chen et al., 2019). Further, the integrity and stability of CA along with the host cleavage and polyadenylation specificity factor 6 (CPSF6) and cyclophilins physically protect the viral reverse transcripts in the cytoplasm from cGAS and thus inhibits the production of type I IFNs (Rasaiyaah et al., 2013; Sumner et al., 2020). To understand the various stratagem employed by HIV-1 against cellular immunity, readers are encouraged to follow the recent review by Yin et al. (2020).

NUCLEAR INTERACTIONS

Cytoplasm to Nuclear Import and the Process of Uncoating and Reverse Transcription Completion

To integrate viral genomic DNA into the host chromosome, prior CA uncoating becomes indispensable. The exact location of uncoating and the precise timing of reverse transcription are incompletely understood. Based on earlier findings, different uncoating models were proposed and are explicated in the reviews of Arhel (2010), Ambrose and Aiken (2014), and Campbell and Hope (2015). One of the prevailing models of uncoating suggests that the viral core is trafficked to the cytoplasmic side of the nuclear envelope by the host microtubules and host factors such as FEZ1 and BICD2, where the uncoating occurs at the nuclear pore complex (NPC). The capsid is disassembled after uncoating, leaving the viral genetic material complexed with the host and viral proteins. This nucleoprotein complex is known as PIC and is protected from nuclease degradation and innate sensing in the host cell (Khiytani and Dimmock, 2002; Arhel, 2010; Malikov et al., 2015; Dharan et al., 2017). The uncoating process and docking at NPC are in agreement with earlier work from the Melikyan laboratory, where authors showed the importance of CA in these events. They also reported the proteasomal degradation of HIV-1 complexes if uncoating happens in the cytoplasm (Francis and Melikyan, 2018). The uncoating at NPC and trafficking to the nucleus are mediated by the interaction of viral CA with nucleoporin, NUP-153, and the coordinated facilitation between NUP-358 and kinesin-1 family, KIF5B (Brass et al., 2008; König et al., 2008; Dharan et al., 2016; Burdick et al., 2017). Besides, TRN-1, a β-karyopherin, was identified to bind to the CA, promoting uncoating and subsequent nuclear import (Fernandez et al., 2019). Similarly, another TRN, TNPO3 (also known as TRN-SR2), now known to play a role during integration, also associates with the CA and promotes uncoating and nuclear trafficking by regulating the localization of cellular protein CPSF6 (Brass et al., 2008; König et al., 2008; Price et al., 2012; De Iaco et al., 2013; Chin et al., 2015). For further details into the older understanding of uncoated core trafficking into the nucleus, the readers are encouraged to refer to Ambrose and Aiken (2014), Campbell and Hope (2015), and Novikova et al. (2019).

However, the latest findings of Burdick et al. and Selyutina et al. revealed that the intact viral core (or nearly intact) is trafficked into the nucleus with the assistance from the CPSF6 (**Figure 1**, step 5) and uncoats < 1.5 h prior to integration at the proximity of 1.5 μm from the sites of integration (**Figure 1**, step 6). Their findings also stress the fact that the process of reverse transcription completes within the nucleus at SC35 nuclear speckles before the completion of uncoating (Lahaye et al., 2018; Burdick et al., 2020; Selyutina et al., 2020a). Preceding this study, using primary human macrophages, Bejarano et al. showed that CPSF6 is excluded from the cytoplasmic RTC/PIC; however, they are present in the nuclear replication complexes. Moreover, the reduction in CPSF6 leads to the accumulation of HIV-1 particles at the nuclear envelope. They also established that CPSF6 directly interacts with the CA and induces the nuclear import of the viral complex (Bejarano et al., 2019). This interaction also decides the integration site of the proviral DNA in the host euchromatin. The disruption of CA–CPSF6 interaction led to integrating viral DNA in the heterochromatin region of the host chromosome (Burdick et al., 2020). Further, independently, other researchers have claims supporting the observations that nuclear import precedes the reverse transcription and uncoating process (Dharan et al., 2020; Selyutina et al., 2020a). Collectively, all these

new findings change our understanding of HIV-1 infection and post-entry events.

Similar to every other step, the host thwarts the HIV-1 life cycle at the nucleus as well. Myxovirus resistance 2 (MX2/MXB), an IFN-induced post-entry inhibitor of HIV-1, was found to act as an antiviral host factor by blocking the nuclear import of viral cDNAs. This MXB sensitivity was found to be dependent on the conformation of HIV-1 CA, but how exactly HIV-1 overcomes this hurdle is yet to be elucidated in detail (Goujon et al., 2013; Kane et al., 2013; Dicks et al., 2018; Miles et al., 2020). In addition, the TRIM5 interacts with the CA and activates protein kinase enzyme TAK1, which in turn activates the activator protein 1 (AP-1) and NF-κB innate immune signaling pathway (Sultana et al., 2019; Yin et al., 2020). Further, Lahaye et al. (2018) found the binding of host NONO with the HIV-1 and HIV-2 nuclear monomeric CA, HIV-1 DNA, and cGAS to trigger the production of IFN inside the nucleus. These findings support the previously mentioned nuclear model of uncoating and reverse transcription (Lahaye et al., 2018). Crossing these obstacles to gain an entry into the nucleus and successful uncoating, the HIV-1 integrates its genome into the host chromosome to complete the process of transcription, one of the major events in the HIV-1 life cycle. Thus, in the following subsections, we attempt to review the current knowledge about how integration, transcription, latency, and latency reactivation occurs inside the nucleus.

Integration of Viral DNA Into the Host Chromosome

Once inside the nucleus, the HIV-1 modulates the nuclear environment for viral cDNA integration into the host chromosome as a provirus (**Figure 1**, step 7), specifically at the AT-rich euchromatin region and other active transcriptional units (Craigie and Bushman, 2012; Balakrishna and Kondapi, 2016; Ciuffi, 2016). The viral protein IN mediates the process of integration, and the IN is destabilized by cellular E3 RING ligase TRIM33, preventing the formation of provirus (Ali et al., 2019). In addition, the host polypyrimidine tract binding protein and associated splicing factor (PSF) binds to the HIV-1 IN-cDNA complex and destabilizes the complex, suppressing the integration event (Yadav et al., 2019). On the other hand, the host lens epithelium-derived growth factor (LEDGF/p75) binds to the IN and directs the integration of viral cDNA at transcriptionally active sites by interacting simultaneously with the host chromatin (Llano et al., 2006; Ciuffi, 2016). The component of SWI/SNF chromatin remodeler, INI1, then interacts with the IN domain of Gag-Pol protein and promotes the DNA joining activity of IN (Turelli et al., 2001; Yung et al., 2004). In LEDGF/p75 depleted cells, HIV-1 utilizes hepatoma-derived growth factor-related protein 2 (HRP-2) for successful integration; however, this process's efficiency is significantly less (Schrijvers et al., 2012a,b). In addition to LEDGF/p75, HIV-1 also influences other host factors such as high-mobility group protein A1 (HMGA1), HMG I(Y), barrier-to-auto-integration factor (BAF), SUV39H1, EED, and HP1γ for the integration process (Farnet and Bushman, 1997; Lin and Engelman, 2003; Du Chéné et al., 2007). Further, as described above, fresh observations regarding the role of CPSF6 in integration also determine the fate of integrated proviral DNA (Bejarano et al., 2019; Burdick et al., 2020). It has been hypothesized that CA–CPSF6 interaction facilitates the HIV-1 to the gene-rich regions, whereas IN-LEDFG/p75 explains the preference for integration in the gene bodies. Of note, it is not always that PIC in the nucleus is favored for the process of integration. Sometimes, the PIC dissociates, leaving the two ends of the viral cDNA to get ligated by the host non-homologous DNA end-joining mechanism (NHEJ), forming a 2-long LTR circles. These 2-LTR circles represent the dead ends for the virus and are overcome by host LEDGF/p75 (Farnet and Haseltine, 1991; Li et al., 2001). The molecular mechanisms of integration are reviewed in detail elsewhere (Kvaratskhelia et al., 2014; Ciuffi, 2016; Poletti and Mavilio, 2018). Taking this into consideration, like in the other steps of the viral life cycle, the host tries to prevent provirus formation. However, the virus influences the host factors, especially chromatin-binding proteins, to integrate its genome into the host chromosome successfully. Downstream to integration, another crucial event in the viral life cycle is described below, where the provirus is transcribed into RNAs for making several progenies of its own.

Transcription and Latency

Following successful integration, the virus has two possibilities: it either goes for active transcription and production of virions, or undergoes latency and remains silent if inefficient transcription occurs. The viral transcription (**Figure 1**, step 8) is a crucial step that recapitulates the host transcription in many aspects, especially by manipulating most of the host transcriptional machinery. The process commences by recruiting host RNA polymerase (pol) II at 5′-LTR and several other transcriptional regulators such as NF-κB, NFAT, AP-1, and SP-1 at their respective binding sites upstream to the LTR promoter. These regulators work synergistically to ensure the viral gene expression while minimizing the host's antiviral gene activity (reviewed in Ruelas and Greene, 2013; Van Lint et al., 2013; Röling et al., 2016). Blocking any of the ways by which transcription is favored, such as by adding repressive chromatin marks, epigenetic silencing, limiting positive transcription factors, or excessively supplying negative transcriptional regulators, leads to the inhibition of viral DNA transcription resulting in latency. The post-integrated latent virus has since then been a bottleneck for using antiretroviral therapies (ARTs) for achieving a complete cure. This priority research area, the mechanism of latency, and approaches to treat the latently infected cells are well rationalized in Coiras et al. (2009), Liu et al. (2014), Cary et al. (2016), Mbonye and Karn (2017), Lindqvist et al. (2020), and Shukla et al. (2020). The latency at any later time point does relive and can reactivate the integrated HIV-1 for transmission.

In both fresh and reactivated transcription processes, the pol II at 5′-LTR transcribes the stem loop of transactivating response (TAR) element and halts due to secondary structures, generating abortive transcripts. This halting is vanquished by recruiting positive transcription elongation factor b (P-TEFb) by Tat at the TAR element. The P-TEFb is a heterodimer of cyclin-dependent kinase 9 (CDK9) and cyclin T1 (CycT1) that phosphorylates the c-terminal domain (CTD) of RNA pol II and thus favors

the elongation process producing full-length HIV-1 transcripts (Jones and Peterlin, 1994; Jones, 1997; Garber et al., 1998; Bieniasz et al., 1999; Zhou et al., 2000). Since P-TEFb is required for both viral and cellular gene expression, its tight control in the cell is indispensable. In most of the cells, P-TEFb is in an inactive state and is sequestered in a kinase-inactive complex that contains hexamethylene bis-acetamide inducible 1 (HEXIM1), and this P-TEFb–HEXIM1 interaction is mediated by 7SK small nuclear RNA as a molecular scaffold. Besides, the kinase-inactivated complex also contains Lupus antigen (La)-related protein 7 (LARP7), a methyl phosphate capping enzyme called MePCE, AF9, AFF1, AFF4, ENL, ELL1, and ELL2. Together, this entire complex is known as super elongation complex (SEC) (Nguyen et al., 2001; Yik et al., 2004; He et al., 2010; Liu et al., 2014). In an infected cell, the P-TEFb dissociates from the SEC and forms an association with the bromodomain-containing protein 4 (Brd4). Brd4 then facilitates the recruitment of P-TEFb at the promoter site for Tat-independent transcription stimulation (Yang et al., 2005). However, it is compelling to note that in the presence of Tat, Brd4 plays a negative role in the transcriptional process by competing with the Tat (Yang et al., 2005; Bisgrove et al., 2007). A decade ago, work led by the D'Orso group revolutionized the understanding of how and when Tat and P-TEFb are recruited to the HIV promoter. Their studies showed that even before TAR element formation, Tat, in association with P-TEFb, is mobilized to the 5′-LTR promoter in a specificity protein 1 (SP1)-dependent manner facilitating the transcription process (D'Orso and Frankel, 2010; D'Orso et al., 2012; McNamara et al., 2013).

Initially, it was reported that TRIM22 has a broad antiviral activity, inhibits SP1, and thus represses the transcription (Turrini et al., 2015). More recently, it was revealed that IFI16 sequesters the SP1 transcription factor concurrently, inhibiting the viral gene expression (Hotter et al., 2019; Bosso et al., 2020). Besides, a short isoform of Per-1 was identified to suppress the transcription process in resting $CD4^+$ T cells. However, this suppression is overcome by the activity of Tat (Zhao et al., 2018). Taura et al. (2019), in a recent finding, showed an unexpected role of APOBEC3A in inducing latency. The APOBEC3A interacts with the proviral 5′-LTR and adds repressive histone marks by recruiting HP1 and KAP1. In addition, a member of the heterogeneous nuclear ribonucleoproteins (hnRNPs) family, X-linked RNA-binding motif protein (RBMX), was found to bind to the LTR downstream region and to block the recruitment of RNA pol II at the promoter by maintaining repressive trimethylation of histone H3 lysine 9 (H3K9me3) (Ma et al., 2020). Further, a recent CRISPR-based knockout screen by Rathore et al. (2020) revealed the role of several host deubiquitinases such as UCH37, USP14, OTULIN, and USP5 in HIV-1 latency. In the lymph node, where oxygen availability is less, Zhuang et al. (2020) showed that hypoxia-inducible factor 2α (HIF2α) binds to LTR, suppresses the transcription, and promotes latency. These studies further await independent confirmations on the factors identified to regulate the latency. On the contrary, several other findings suggested the novel mechanism of reactivation of latent HIV-1. For instance, ELL2 being the part of SEC, however, stimulates the transcriptional elongation, but the freshly synthesized ELL2 is prone to degradation by Siah1. This inhibitory activity of Siah1 is antagonized by host cell factor 1 and 2 (HCF1 and HCF2), thus favoring the transcriptional activation (Wu et al., 2020). Additionally, the same group also suggested that the levels of ELL2 and ELL2-SEC can be elevated by downregulating/inhibiting the proteasomes favoring Tat transactivation (Li Z. et al., 2019). Interestingly, another finding suggests that YY1 is known to inhibit HIV-1 expression and to promote latent infection, which, when over-expressed, leads to transcriptional upregulation with the synergistic effect of viral Tat protein (Yu et al., 2020). Another viral accessory protein, Vpr, was found to reactivate HIV-1 by targeting the chromatin-modifying enzyme CTIP2 (Forouzanfar et al., 2019). Taken together, the consequent HIV-1 transcription being either active or silenced depends mostly on host cellular factors, epigenetic factors, and viral factors in addition to the chromatin status at the integration site.

Splicing and Export of Viral Transcripts to Cytoplasm

Upon completion of transcription, a full-length mRNA transcript (∼9.2 kb) is produced containing eight open reading frames (ORFs). The transcript then undergoes alternative splicing to form Rev, Tat, and Nef mRNA (∼1.8 kb) by a mechanism similar to that of the host (Chen and Manley, 2009; Kutluay et al., 2014; Sertznig et al., 2018). The Rev mRNA is transported out of the nucleus through the NPC and is translated into Rev proteins in the cytoplasm (Köhler and Hurt, 2007). The Rev protein-containing NLS is imported back to the nucleus by binding to the nuclear import receptor, importin β (Henderson and Percipalle, 1997).

In the late phase of infection, when the concentration of Rev protein in the nucleus is above a certain threshold, it binds to the Rev response element (RRE) in the second intron of unspliced and incompletely spliced transcripts (Pollard and Malim, 1998). The Rev also contains a nucleus export signal (NES) through which it binds to the karyopherin family member exportin 1 [also known as chromosome maintenance region 1 (CRM1)] and transport the transcripts from the nucleus to the cytoplasm (Fischer et al., 1995; Arnold et al., 2006). Of note, Rev multimerizes and masks the NES, which thus can be retained in the nucleus (Behrens et al., 2017). It was later discovered that RRE–Rev interaction also recruits hypermethylation enzyme PIMT, which modifies the 7-methylguanosine (m7G) cap of mRNA to a trimethylguanosine (TMG) cap. The acquisition of TMG caps allows the HIV-1 RNA to get recognized by CRM1 and targets for CRM1-dependent nuclear export (Yedavalli and Jeang, 2010). In addition to several host factors (such as DDX1, DDX3, DDX5, DDX21, Matrin-3, CBP80, Sam68, and MOV10) found to interact with Rev–RRE, Wang et al. (2019) found two proteins, ANP32A and ANP32B, which directly interact with RRE–Rev–CRM1 and facilitate the viral RNA nuclear export. The HIV-1 Nef-associated factor 1 (Naf-1, a cellular protein) was also found to interact with CRM-1 and promote the export of HIV-1 gag mRNA (Ren et al., 2016). Exported HIV transcripts then undergo translation and encode viral structural proteins (Gag

and Pol from unspliced RNA) and accessory proteins from singly spliced transcripts (Env, Vif, and Vpr). These viral proteins are then trafficked via different cellular compartments to the virion assembly site at the plasma membrane.

CYTOPLASM: THE SITE OF VIRAL PROTEIN TRANSLATION AND INTERACTION WITH OTHER ORGANELLES

Translation

Besides using the cytoplasmic environment for initiating reverse transcription and traversing the core toward the nucleus, HIV-1 also utilizes cytoplasm for viral translation and assembly (**Figure 1**, steps 9–10), after the successful production of viral RNA and their export to the cytoplasm. Prior to translation initiation, HIV-1 encounters several hurdles elicited by the host cellular environment as a result of the innate sensing of virion components. To limit viral production, the host induces the production of IFN-stimulated gene products. Following cellular stress, protein activator of PKR (PACT) activates an IFN-activated protein kinase (PKR) and mounts antiviral immunity (Burugu et al., 2014; Guerrero et al., 2015). However, a few years back, Chukwurah et al. (2017) showed that HIV employs a strategy to subdue this antiviral response by interacting viral Tat protein, host ADAR1, and PACT, inhibiting the PKR activation and thus enhancing own protein synthesis. Earlier, we have discussed the role of IFITMs in the inhibition of viral entry, but Lee et al. recently unveiled the translational inhibition role for IFITMs. The IFITM excludes the viral mRNA from incorporation into the polysomes and thus inhibits the protein synthesis. Furthermore, as a countermeasure, Lee et al. (2018) found that HIV Nef overcomes this inhibitory effect by IFITM by a mechanism not known yet.

For translation initiation and protein production, HIV-1 misappropriates the eukaryotic translational machinery by recruiting 40S ribosomes to its 5′ UTR region of RNA, which is capped (secondary structure) like host RNAs. This region is known as the TAR element required for translation initiation. However, similar to eukaryotic translation, the presence of highly stable RNA structures in the viral TAR RNA region has raised several questions about the recruitment of the 43S pre-initiation complex (PIC). In eukaryotes, the 43S PIC containing 40S ribosome, initiator tRNA, eIF1, eIF1A, eIF2-GTP, and eIF3, is recruited to the 5′ Cap by eIF4F multi-subunit complex and facilitates the scanning of mRNA for initiator codon from 5′ to 3′ direction. Interestingly, HIV-1 masters itself by recruiting a cellular RNA helicase DDX3 (DEAD/H box family) and facilitates PIC assembly in an ATP-dependent manner (Ricci et al., 2008; Guerrero et al., 2015). HIV-1 also recruits host TAR RNA-binding protein (TRBP—known to be involved in RNA silencing) at TAR elements and resolve the secondary structure for translation initiation. This year, Komori et al. (2020) showed that TRBP interacts with the DICER and mediates TAR miRNA degradation, reliving the hurdle. Apart from canonical translation initiation, eukaryotes and many viruses, including HIV-1, employ a cap-independent translation mechanism. In this process, the 43S initiation complex is recruited at the internal ribosome entry site (IRES) containing mRNA stem loops to initiate the translation in a cap-independent manner. The HIV-1 virus, in the first 24–48 h of viral replication, uses cap-dependent translation process, whereas after 48 h, it opts for the IRES-dependent translation process to produce viral particles (Amorim et al., 2014; Ohlmann et al., 2014). For further understanding of the molecular mechanism of translation initiation, elongation, and completion, readers are encouraged to follow the articles by Ohlmann et al. (2014) and Guerrero et al. (2015).

Altogether, these studies show that apart from using host cellular factors and plasma membrane for viral entry and budding, the virus tricks the host machinery and makes the host environment favorable for viral replication. Post translation, the viral proteins are targeted to several cellular organelles for protein modifications. These modified proteins are then transported to the plasma membrane for assembly and virion production. In the upcoming section, we attempt to describe various tricks played by HIV-1 within these organelles for its benefit.

The Interactions With the Endoplasmic Reticulum, Mitochondria, and Peroxisome

Preparatory to the assembly of virions, HIV-1 proteins are synthesized on the endoplasmic reticulum (ER) and are targeted to various cellular compartments for protein modification, maturation, and alteration of immune pathways. For instance, the HIV-1 uses the host ribosome machinery bound to the ER to produce gp160, an Env polyprotein precursor. The gp160 is then glycosylated in the ER, concomitant with translation, and multimerizes for trafficking to the TGN. In Golgi, the precursor proteins undergo oligosaccharide modification and are processed to yield transmembrane glycoprotein, gp41, and surface glycoprotein, gp120 (Checkley et al., 2011). To prevent premature interaction of gp120 with newly synthesized CD4 on ER, HIV-1 employs Vpu to manipulate the β-TrCP/proteasome-mediated degradation pathway to downregulate CD4 (Margottin et al., 1998; Magadán et al., 2010). Of note, CD4 receptors in the cell surface are downregulated by viral Nef protein by hijacking adaptor protein complex 2 (AP2)- and clathrin-dependent endocytosis (Kwon et al., 2020).

It is interesting to note that, although HIV-1 seizes ER for protein synthesis, glycosylation, and CD4 downregulation via ERAD machinery, the ERAD acts as a double-edged sword that traps gp160 at its birthplace. Besides, in the ER, the guanylate-binding protein, GBP2/5, decreases the activity of furin convertase required for conversion of precursor gp160 into mature gp41 and gp120 (Braun et al., 2019). An ER protein, known as ERManI, modulates the glycosylation of Env protein vis-à-vis regulating TSPO, a mitochondrial translocator protein that alters the folding process and diminishes Env expression by ERAD (Zhou et al., 2014, 2015). This suggests that mitochondrial involvement in regulating the Env protein folding process. Currently, we do not know how exactly HIV-1 responds to this,

but recent findings by Zhang et al. (2016) showed that HIV-1 accessory protein Vpr augments proper Env folding in the ER that, in turn, shields Env from lysosomal degradation in the ERAD pathway. Another study showed that HIV-1 hijacks PERK, ATF6, and IRE1 ER stress sensors and modulates their activity to increase BiP expression and subsequent increased protein folding capacity of ER (Borsa et al., 2015).

In addition to this, HIV-1 was also found to manipulate the ERAD pathway and other innate immune triggering pathways to antagonize the immune responses as described in Byun et al. (2014) and Yin et al. (2020). In myeloid cells, the adaptor protein mitochondrial antiviral-signaling protein (MAVS) transduces signals from cytosolic RIG-I upon sensing viral RNAs that induce IRF3 and IκB activation. This leads to the activation of mitochondrial MAVS-mediated innate immunity (**Figure 3A**). The MAVS triggers the type I IFN signaling by another viral RNA sensor, DDX3, which interacts with the abortive HIV-1 RNA upon infection. However, HIV-1 utilizes the viral protease to diminish RIG-I from the cytosol, thus subverting RIG-I-MAVS initial signaling cascades. Additionally, HIV-1 sensing by host DC-SIGN activates a mitotic kinase PLK1 that lessens the downstream cascade signaling of MAVS, thereby escaping innate immune activation during HIV-1 infection. PLK1-mediated viral subversion strategy prevents DDX3-MAVS signaling, thereby promoting HIV-1 replication during infection (Gringhuis et al., 2016).

Intriguingly, MAVS signaling not only is limited to the mitochondrial membrane but also indulges in peroxisome membranes. Upon HIV-1 RNA sensing, peroxisomal MAVS triggers the rapid induction of type III IFNs and ISGs that acts as antiviral factors (Hopfensperger and Sautera, 2020). To antagonize the peroxisomal MAVS-mediated immunity, HIV-1 directly modulates the biogenesis of peroxisome factors. The viral accessory protein Vpu sequesters β-TRcP and stabilizes the β-catenin, required for activation of TCF4 TF to transcribe miRNAs (miR-34c-3p, miR-93-3p, miR-500a-5p, and miR-381-3p). These miRNAs are found to regulate the expression of factors required for peroxisome biogenesis and, thus, expropriates the peroxisome function (**Figure 3B**) (Xu et al., 2017, 2020; Hopfensperger and Sautera, 2020). However, whether the suppression of peroxisome biogenesis by Vpu inhibits the peroxisomal MAVS signaling and activation of IFN-stimulated genes (ISGs) and type III IFN is yet to be determined. Being an enveloped virus, HIV-1 may rewire peroxisome features to enhance lipid synthesis for new viral assembly.

Apart from antagonizing MAVS-dependent signaling, the HIV-1 employs accessory protein Vpr, Tat, and envelope glycoprotein gp120 to induce host cell death by altering the mitochondrial dynamics, membrane potential, and oxygen consumption. The Vpr reduces the expression of mitofusin 2 (Mfn2) post-transcriptionally, thus weakening and increasing the permeability of mitochondrial outer membrane (MOM). This leads to increased mitochondrial deformation and a reduction in mitochondrial membrane potential (MMP). Vpr also decreases the cytoplasmic level of fission protein, dynamin-related protein 1 (DRP1), and increases the bulging in membranes of mitochondria associated with mitochondria, MAMs. This suggests that Vpr-mediated cellular damage is modulated by DRP1 and MFN2 on an alternative protein transport pathway from the ER to mitochondria via mitochondria-associated membranes (MAMs) (Huang et al., 2012). Like Vpr, Tat and gp120 were found to alter the mtDNA content, mitochondrial dynamics, function, distribution, and trafficking. Tat and gp120 were also shown to induce the expression of mitophagy signaling proteins (DNM1L, PRKN, and PINK1) and autophagosome-related proteins (MAP1LC3B-II and BECN1). However, the increase in Parkin/SQSTM suggests the blockade in mitophagy flux and thus the accumulation of mitophagosomes in neurons (Avdoshina et al., 2016; Rozzi et al., 2018; Teodorof-Diedrich and Spector, 2018; Thangaraj et al., 2018). Additionally, HIV-1 promotes mitochondrial dysfunction for infection-mediated apoptosis by downregulation of mitochondrial complex I subunit NDUFA6 and the complex I enzyme activity (Ladha et al., 2005). HIV-1 protease has also been shown to play a role in apoptosis by localizing to the mitochondria and decreasing the MMP, following which it activates caspase 9, PARP cleavage, and DNA fragmentation (Rumlová et al., 2014). Furthermore, the HIV-1 gp120 induces the caspase-9/caspase-3-mediated programmed cell death by JNK, IRE1α, and AP-1 pathway by upregulating CHOP and BiP production (Shah et al., 2016). Altogether, emerging evidence suggests that HIV-1 exploits cytoplasm and nucleus, targets other subcellular compartments, and alters canonical cellular pathways for the completion of its life cycle.

PLASMA MEMBRANE: THE SITE OF VIRION ASSEMBLY AND BUDDING

Assembly

In the later stages of the HIV-1 life cycle, post-translation and protein modification, the virus utilizes the inner leaflets of the host plasma membrane for assembly of HIV-1 (**Figure 1**, step 10). The gag protein of a virus consisting of MA, CA, and NC protein is essential for virion assembly. The Gag is translated from the viral RNA by programmed ribosome-1 frameshifting via two regimes established by Korniy et al. (2019). This frameshifting event is required for maintaining a constant Gag to Gag-Pol ratio for proper structural organization and infectivity of the virions. Besides, the cellular polyanion, inositol hexakisphosphate (IP6), interacts and enhances the assembly of Gag proteins into the immature viral particles (Dick et al., 2018; Mallery et al., 2019). During assembly, the viral RNA is recognized by the NC domain of uncleaved Gag protein via two zinc finger motifs and several basic amino acids and is selectively incorporated in the virions. Although HIV-1 RNA serves as a viral genome and template for translation, at a given time, a single RNA molecule carries out only one function (Bell et al., 2012; Kutluay et al., 2014; Chen et al., 2020). Recent studies indicate that viral RNA also interacts with the MA, leading to a reduction in the non-specific binding of Gag to the plasma membrane (Meng and Lever, 2013). Immediately after translation, Gag protein forms complexes with the two RNA granule proteins ABCE1 (ATP-binding cassette family of protein subfamily E1) and DDX6 (DEAD-box RNA helicase) present in the cytoplasm

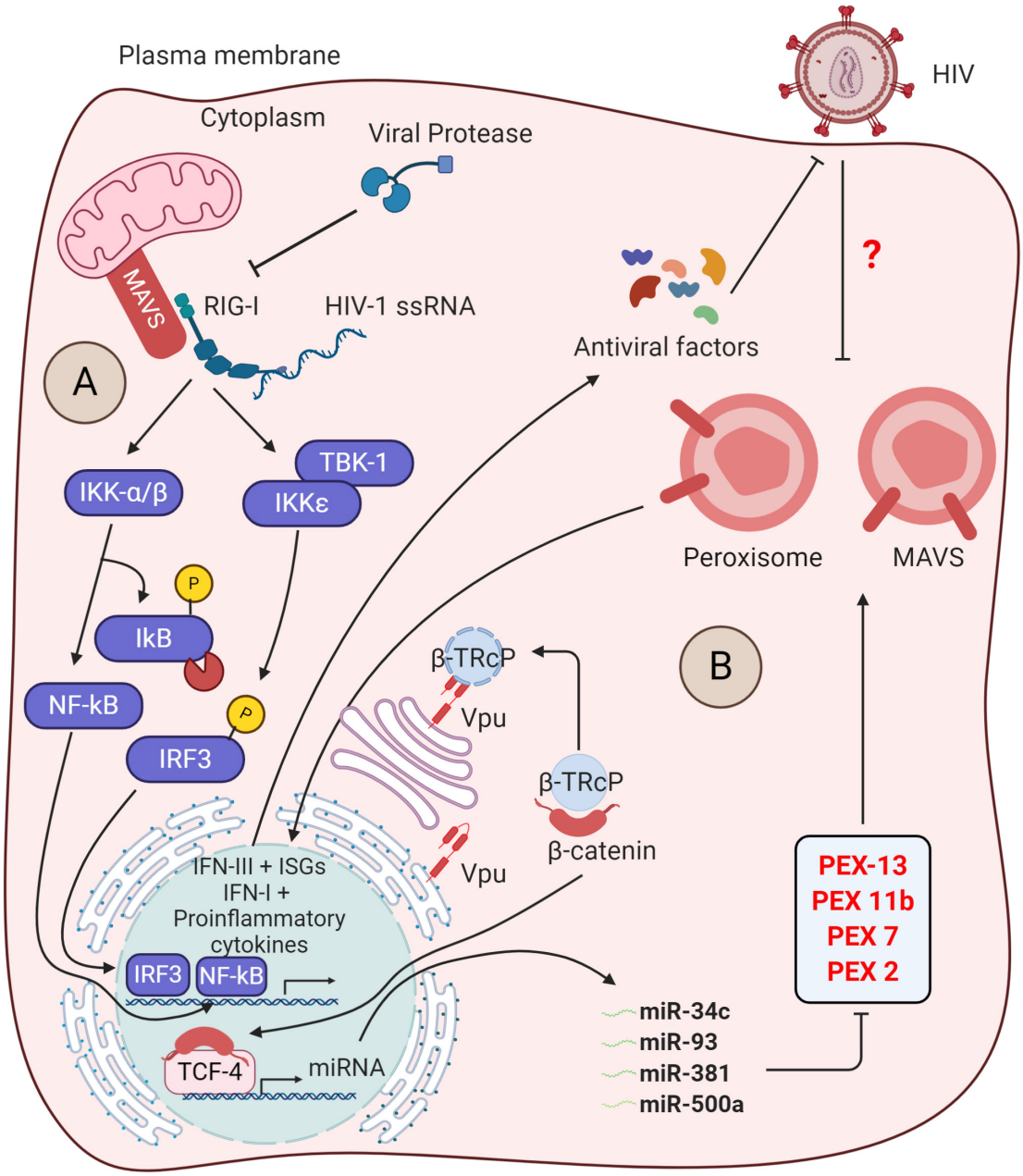

FIGURE 3 | Insights into the counteraction of host defense by viral protease and Vpu. **(A)** Inhibition of antiviral signaling by viral protease: The host RIG-I senses viral ssRNA to promote the antiviral signaling through MAVS and activates the IκB kinases (IKKs). The IKKε phosphorylates IRF3, which then translocates into the nucleus to trigger the IFN-I production. On the other hand, IKK-α/β phosphorylates and degrades IκB, reliving NF-κB to go into the nucleus for transcription of proinflammatory cytokine genes. The viral protease (PR) promotes the degradtaion of RIG-I in the cytosol. **(B)** Suppression of peroxisome biogenesis by Vpu: in the absence of HIV-1 infection, the adapter protein βTrCP binds to β-catenin and promotes its degradation via ubiquitin-mediated proteasomal pathway. Upon HIV-1 infection, the Vpu stabilizes the β-catenin by sequestering βTrCP. Subsequently, β-catenin enters into the nucleus and activates the transcription factor TCF-4, which is required to drive the expression of indicated microRNAs. These microRNAs were found to regulate the expression of peroxisome biogenesis factors for peroxisome synthesis. However, the peroxisomal MAVS triggers the rapid induction of type III IFNs downstream ISGs that acts as antiviral factors. The direct/indirect counteraction of peroxisomal MAVS signaling by HIV-1 remains to be elucidated.

of infected cells. ABCE1 is a cellular ATPase and binds Gag independent of viral RNA, and its association with Gag protein during assembly indicated the energy-dependent polymerization of Gag monomers (Abrahamyan et al., 2008; Meng and Lever, 2013). The role of DDX6 during HIV-1 assembly still needs to be further studied. Another protein, Staufen1, is an RNA binding protein that indirectly binds to viral gag RNA and helps in gag oligomerization (Cochrane et al., 2006; Abrahamyan et al., 2008).

Inhibition, as well as overexpression of Staufen1 protein, inhibits virus infectivity. Further, Staufen1, along with ABCE1 and DDX6, helps in Gag multimerization. Interestingly, these proteins only help during the assembly of HIV-1 but are not packaged in the budded virions (Abrahamyan et al., 2008; Meng and Lever, 2013; Lingappa et al., 2014).

Swindling Cellular Factors During Virion Egress

Apart from entry into the target cell and harnessing the plasma membrane for assembly, HIV-1 also exploits the plasma membrane during budding from the producer cells (**Figure 1**, step 11). The budding process ensues the release of viral progeny from the infected cell, which will further help the virus disseminate the infection to new target cells. During egress, the PTAP motif in L-domain of HIV-1 gag p6 interacts with host tumor susceptibility gene 101 (TSG101), apoptosis-linked gene 2-interacting protein X (AIP1/ALIX), and endosomal sorting complexes required for transport (ESCRT) machinery, promoting the budding event (Garrus et al., 2001; Strack et al., 2003; Martin-Serrano and Neil, 2011). The budding requires all ESCRT-1 complex components, which consist of TSG101 VPS28, VPS37, and MVB12; and the latest member to this is the ubiquitin associated protein-1 (UBAP-1) (Ahmed et al., 2019). Recent studies revealed that mutation in NC leads to the delocalization of TSG101 but not ALIX1, suggesting that the distribution and interaction of TSG101 are Gag dependent (El Meshri et al., 2018). HIV-1 recruits the charged multivesicular body protein 4 (CHMP4) fission factor, an ESCRT III protein via ESCRT-1 at PTAP late domain. Besides, HIV-1 recruits two small subunits of ESCRT-III, CHMP2a, and CHMP2b. The recruitment of ESCRT-III is facilitated by the interaction of the C-terminal domain of CHMP4 with ALIX1 at the membrane, which further enables the formation of ESCRT-III filaments (Martin-Serrano and Neil, 2011). The ESCRT-III of ESCRT machinery acts as the key scissor to cut the filament, which then separates the nascent virion from the host plasma membrane. The vacuolar protein sorting associated protein 4 (VPS4) then continuously removes the ESCRT-III molecules from the excision site until membrane fission and virion release (**Figure 1**, step 12) is completed for another round of the budding event. For further insight into the event of budding, the readers are encouraged to have a look into the articles by Pincetic and Leis (2009), Martin-Serrano and Neil (2011), Weiss and Göttlinger (2011), and Lee et al. (2015). Recently, Popov et al. (2018) demonstrated that independent of the ESCRT-mediated budding process, the p6 region also recruits host PACSIN2, an actin cytoskeleton, and cellular membrane remodeler, via ubiquitin to promote cell-to-cell virion spreading, and this p6 domain ubiquitination was found to be facilitated by NEDD4 family ubiquitin ligase ITCH. Although being the predominant mode of transmission, the mechanism is yet to be understood in detail and thus opens up several questions in the biology of HIV-1 budding. At this stage, while the virions are ready to excise and leave the infected cells, this egress is challenged by the cellular protein tetherin (Neil et al., 2008; Van Damme et al., 2008). Tetherin is an IFN (IFN)-induced host protein, encoded by the BST-2 gene, known to sense the viral particles by transducing signals to activate proinflammatory signaling (Skasko et al., 2011; Galão et al., 2012). Tetherin cross-links the enveloped viruses during budding from the infected cell and thus inhibits the process. HIV-1 accessory protein Vpu counteracts this block at the plasma membrane by downregulating tetherin from the cell surface and promoting its degradation by recruitment of β-TrCP2 (Douglas et al., 2009).

Similar to Vpu, HIV-1 accessory protein, Nef has been extensively studied for its ability to alter cell surface protein composition. The primary function of Nef is known for trafficking a myriad of proteins from the cell surface to the trans-Golgi network or lysosome by hijacking the vesicular endocytic machinery. One such crucial function is the downregulation of the CD4 receptor by expropriating the endocytosis process, upon which the susceptibility of gp120 epitopes to host antibodies diminishes, thereby preventing antibody-dependent cellular cytotoxicity (ADCC) (Wyatt et al., 1995; Ferrari et al., 2011; Pham et al., 2014; Veillette et al., 2014; Kwon et al., 2020). Furthermore, by an uncharacterized mechanism, Nef was also shown to enhance virion's infectivity by showing its effect in the HIV-1 producer cells rather than in the viral progeny itself (Chowers et al., 1994; Basmaciogullari and Pizzato, 2014). In 2015, host restriction factors SERINC3 and SERINC5 were identified. These multipass proteins dramatically inhibited Nef defective HIV-1 infectivity in target cells by being incorporated into the virus particle. In the presence of Nef, these cell-surface proteins are downregulated to late Rab-7 positive endosomal compartments and prevent the incorporation of these proteins into the budding virions. While infectivity defect is inherited during the egress from the producer-cell plasma membrane, the effect on virus inhibition is seen in the target cells (Rosa et al., 2015; Usami et al., 2015; Firrito et al., 2018). Nef and Vpu are also known to downregulate several tetraspanins such as CD81, CD63, and CD53, which are involved in the formation of tetraspanin-enriched microdomains (TEMs) (Haller et al., 2014). Nef further downregulates a plethora of cell surface receptors such as NKG2D-L required for NK cell activation. *In vitro*, it was shown that the decrease in levels of NKG2D-L that binds to NKG2D on NK cells reduced the cytolytic activity of co-cultured NK cells (Cerboni et al., 2007; Alsahafi et al., 2017). Apart from this, an essential aspect of Nef is that it also reduces the levels of MHC-I from the cell surface by using AP-1 to direct the MHCs to endosomes and lysosomes as a tactic of evading the immune response (Schwartz et al., 1996; Collins et al., 1998; Lubben et al., 2007). Thus HIV-1 accessory proteins, during binding, fusion, and budding, extensively remodel the plasma membrane and manipulate the host intracellular environment for productive infection and immune evasion.

SUMMARY

From entry to egress, at each step, HIV-1 depends on the host. This dependency also portrays the interaction with diverse cellular organelles that are otherwise essential for normal

homeostasis. The plasma membrane is cleverly taken advantage of throughout the virus life cycle. Upon binding to HIV-1 gp120, various chemokine-dependent signal transduction pathways are rewired, many of which are crucial for immune effector functions. Further, the plasma membrane is the sight of HIV-1 budding, which is considerably reorganized to release newly formed virions. In addition to this, the cell surface protein composition is altered by accessory proteins like Nef and Vpu to counteract major host restriction factors, SERINC5 and Tetherin, respectively. The success of HIV-1 as a pathogen is perhaps imputed to these accessory proteins' ability to hijack the host endocytic machinery and the trans-Golgi network efficiently to downregulate a vast number of cell surface proteins. Not only the interaction with endocytic machinery but Nef also utilizes the ER-associated protein degradation (ERAD) pathway for this purpose. After the efficient exploitation of the cell membrane, the viral core enters the cytoplasm where HIV-1 can interact with the cytoplasmic proteins and rearrange the cytoskeleton to sanction its retrograde transport toward the nucleus. Besides this, the viral CA can coherently interact with multiple host proteins to protect from premature uncoating and risking the viral genome being sensed by cytoplasmic immune sensors, and now we know that an intact capsid enters the nucleus. Apart from this, another viral accessory protein, Vif, can recruit the proteasomal machinery to degrade the host restriction factor APOBEC3G that induces mutations in the proviral DNA during reverse transcription resulting in truncated viral proteins or premature stop codons. After reaching the nuclear envelope, the viral core recruits host proteins like CPSF6 to employ nuclear importins, thus seizing the nuclear import machinery to transport into the nucleus. Within the nucleus, the virus becomes crucially dependent on nuclear proteins for uncoating and effective integration into actively transcribed regions of the host chromosome. Furthermore, the transcription of the integrated proviral DNA depends on the host RNA polymerase (RNA pol II). Although HIV-1 Tat considerably augments the transcription rate, it does so by interacting with host transcription factors like P-TEFB to utilize RNA pol II efficiently. After the generation of alternatively spliced and unspliced transcripts of HIV-1, they are transported to the cytoplasm for translation. The export of these viral transcripts is enabled by the viral protein Rev, which again depends on the host CRM1-dependent nuclear traffic. Once again, in the cytoplasm, HIV-1 employs the cellular protein translation machinery to produce viral proteins. Following this, the virus further takes advantage of host intracellular trafficking machinery for assembly of progeny near the plasma membrane, after which the virus buds off by altering the plasma membrane and recruiting the ESCRT machinery. Thus, the virus effortlessly exploits the machinery that is utilized by the host for its own survival and persistence.

CONCLUDING REMARKS

The involvement of various subcellular entities in HIV-1 infection and their contribution to pathogenesis is becoming increasingly apparent. Thus, this review attempts to comprehend previously known and recently discovered compartmentalized cellular and molecular interactions during HIV-1 infection. With an increased understanding of host–virus cross talk, a future goal may be to utilize cutting-edge technologies, preferentially in relevant models, to identify candidates that could target organelle-specific host mechanisms. For instance, identifying how HIV-1 can evade innate sensors by preventing early uncoating, essentially to pathogenic effect, will have a profound impact on future drug developments. Consequently, a combination of therapeutic strategies in a fashion to abrogate compartmentalized interactions could prove to accentuate better adjunct treatment options.

AUTHOR CONTRIBUTIONS

PR, AKS, VB, and TM did literature review, generated figures using BioRender, and draft writing. AC conceived, reviewed, and edited the manuscript. All authors approved the final version.

FUNDING

Research in the lab was supported by grants from the DBT/Wellcome-Trust India Alliance (grant no. IA/I/18/2/504006 awarded to AC) and the Department of Biotechnology (DBT), Government of India.

ACKNOWLEDGMENTS

VB and AKS acknowledge fellowships from the CSIR and DST-INSPIRE, respectively. PR and TM thank MHRD for fellowship support. AC is a recipient of the Innovative Young Biotechnologist Award from the DBT. Apologies to many authors whose papers are not cited adequately due to space limitations or simply our ignorance.

REFERENCES

Abrahamyan, L. G., Chatel-chaix, L., Ajamian, L., Milev, M. P., Monette, A., Clément, J., et al. (2008). Novel Staufen1 ribonucleoproteins prevent formation of stress granules but favour encapsidation of HIV-1 genomic RNA. *J. Cell Sci.* 123(Pt 3), 369–383. doi: 10.1242/jcs.055897

Ahmed, I., Akram, Z., Iqbal, H. M. N., and Munn, A. L. (2019). The regulation of endosomal sorting complex required for transport and accessory proteins in multivesicular body sorting and enveloped viral budding – an overview. *Int. J. Biol. Macromol.* 127, 1–11. doi: 10.1016/j.ijbiomac.2019.01.015

Ali, H., Mano, M., Braga, L., Naseem, A., Marini, B., Vu, D. M., et al. (2019). Cellular TRIM33 restrains HIV-1 infection by targeting viral integrase for proteasomal degradation. *Nat. Commun.* 10:926. doi: 10.1038/s41467-019-08810-0

Alsahafi, N., Richard, J., Prévost, J., Coutu, M., Brassard, N., Parsons, M. S., et al. (2017). Impaired downregulation of NKG2D ligands by Nef proteins from

elite controllers sensitizes HIV-1-infected cells to antibody-dependent cellular cytotoxicity. *J. Virol.* 91:e00109-17. doi: 10.1128/JVI.00109-17

Ambrose, Z., and Aiken, C. (2014). *HIV-1 Uncoating: Connection to Nuclear Entry and Regulation by Host Proteins*. New York, NY: Academic Press. , doi: 10.1016/j.virol.2014.02.004

Amorim, R., Costa, S. M., Cavaleiro, N. P., da Silva, E. E., and da Costa, L. J. (2014). HIV-1 transcripts use IRES-initiation under conditions where cap-dependent translation is restricted by poliovirus 2A protease. *PLoS One* 9:e88619. doi: 10.1371/journal.pone.0088619

Arhel, N. (2010). Revisiting HIV-1 uncoating. *Retrovirology* 7:96. doi: 10.1186/1742-4690-7-96

Arnold, M., Nath, A., Hauber, J., and Kehlenbach, R. H. (2006). Multiple importins function as nuclear transport receptors for the rev protein of human immunodeficiency virus type 1. *J. Biol. Chem.* 281, 20883–20890. doi: 10.1074/jbc.M602189200

Avdoshina, V., Fields, J. A., Castellano, P., Dedoni, S., Palchik, G., Trejo, M., et al. (2016). The HIV protein gp120 alters mitochondrial dynamics in neurons. *Neurotox Res.* 29, 583–593. doi: 10.1007/s12640-016-9608-6

Badley, A. D., McElhinny, J. A., Leibson, P. J., Lynch, D. H., Alderson, M. R., and Paya, C. V. (1996). Upregulation of Fas ligand expression by human immunodeficiency virus in human macrophages mediates apoptosis of uninfected T lymphocytes. *J. Virol.* 70, 199–206. doi: 10.1128/jvi.70.1.199-206.1996

Balakrishna, L. S., and Kondapi, A. K. (2016). Role of host proteins in HIV-1 early replication. *Adv. Mol. Retrovirology* 21,

Barouch, D. H., Ghneim, K., Bosche, W. J., Li, Y., Berkemeier, B., Hull, M., et al. (2016). Rapid inflammasome activation following mucosal SIV infection of rhesus monkeys. *Cell* 165, 656–667. doi: 10.1016/j.cell.2016.03.021

Bartz, S. R., and Emerman, M. (1999). Human immunodeficiency virus type 1 Tat induces apoptosis and increases sensitivity to apoptotic signals by up-regulating FLICE/Caspase-8. *J. Virol.* 73, 1956–1963. doi: 10.1128/JVI.73.3.1956-1963.1999

Basmaciogullari, S., and Pizzato, M. (2014). The activity of Nef on HIV-1 infectivity. *Front. Microbiol.* 5:232. doi: 10.3389/fmicb.2014.00232

Behrens, R. T., Aligeti, M., Pocock, G. M., Higgins, C. A., and Sherer, N. M. (2017). Nuclear export signal masking regulates HIV-1 rev trafficking and viral RNA nuclear export. *J. Virol.* 91:e02107-16. doi: 10.1128/JVI.02107-16

Beitari, S., Ding, S., Pan, Q., Finzi, A., and Liang, C. (2017). Effect of HIV-1 Env on SERINC5 Antagonism. *J. Virol.* 91:e02214-16. doi: 10.1128/JVI.02214-16

Bejarano, D. A., Peng, K., Laketa, V., Börner, K., Jost, K. L., Lucic, B., et al. (2019). HIV-1 nuclear import in macrophages is regulated by CPSF6-capsid interactions at the nuclear pore complex. *eLife* 8:e41800. doi: 10.7554/eLife.41800

Bell, N. M., Kenyon, J. C., Balasubramanian, S., and Lever, A. M. L. (2012). Comparative structural effects of HIV-1 gag and nucleocapsid proteins in binding to and unwinding of the viral RNA packaging signal. *Biochemistry* 51, 3162–3169. doi: 10.1021/bi2017969

Berger, E. A., Murphy, P. M., and Farber, J. M. (1999). Chemokine receptors as HIV-1 coreceptors: roles in viral entry, tropism, and disease. *Annu. Rev. Immunol.* 17, 657–700. doi: 10.1146/annurev.immunol.17.1.657

Bieniasz, P. D., Grdina, T. A., Bogerd, H. P., and Cullen, B. R. (1999). Recruitment of cyclin T1/P-TEFb to an HIV type 1 long terminal repeat promoter proximal RNA target is both necessary and sufficient for full activation of transcription. *Proc. Natl. Acad. Sci. U.S.A.* 96, 7791–7796. doi: 10.1073/pnas.96.14.7791

Bisgrove, D. A., Mahmoudi, T., Henklein, P., and Verdin, E. (2007). Conserved P-TEFb-interacting domain of BRD4 inhibits HIV transcription. *Proc. Natl. Acad. Sci. U.S.A.* 104, 13690–13695. doi: 10.1073/pnas.0705053104

Borsa, M., Ferreira, P. L. C., Petry, A., Ferreira, L. G. E., Camargo, M. M., Bou-Habib, D. C., et al. (2015). HIV infection and antiretroviral therapy lead to unfolded protein response activation. *Virol. J.* 12:77. doi: 10.1186/s12985-015-0298-0

Bosco, D. A., Eisenmesser, E. Z., Pochapsky, S., Sundquist, W. I., and Kern, D. (2002). Catalysis of cis/trans isomerization in native HIV-1 capsid by human cyclophilin A. *Proc. Natl. Acad. Sci. U.S.A.* 99, 5247–5252. doi: 10.1073/pnas.082100499

Bosso, M., Prelli Bozzo, C., Hotter, D., Volcic, M., Stürzel, C. M., Rammelt, A., et al. (2020). Nuclear PYHIN proteins target the host transcription factor Sp1 thereby restricting HIV-1 in human macrophages and CD4+ T cells. *PLoS Pathog.* 16:e1008752. doi: 10.1371/journal.ppat.1008752

Brass, A. L., Dykxhoorn, D. M., Benita, Y., Yan, N., Engelman, A., Xavier, R. J., et al. (2008). Identification of host proteins required for HIV infection through a functional genomic screen. *Science* 319, 921–926. doi: 10.1126/science.1152725

Braun, E., Hotter, D., Koepke, L., Zech, F., Groß, R., Sparrer, K. M. J., et al. (2019). Guanylate-binding proteins 2 and 5 exert broad antiviral activity by inhibiting furin-mediated processing of viral envelope proteins. *Cell Rep.* 27, 2092–2104.e10. doi: 10.1016/j.celrep.2019.04.063

Burdick, R. C., Delviks-Frankenberry, K. A., Chen, J., Janaka, S. K., Sastri, J., Hu, W.-S., et al. (2017). Dynamics and regulation of nuclear import and nuclear movements of HIV-1 complexes. *PLoS Pathog.* 13:e1006570. doi: 10.1371/journal.ppat.1006570

Burdick, R. C., Li, C., Munshi, M., Rawson, J. M. O., Nagashima, K., Hu, W.-S., et al. (2020). HIV-1 uncoats in the nucleus near sites of integration. *Proc. Natl. Acad. Sci. U.S.A.* 117, 5486–5493. doi: 10.1073/pnas.1920631117

Burugu, S., Daher, A., Meurs, E. F., and Gatignol, A. (2014). HIV-1 translation and its regulation by cellular factors PKR and PACT. *Virus Res.* 193, 65–77. doi: 10.1016/j.virusres.2014.07.014

Byun, H., Gou, Y., Zook, A., Lozano, M. M., and Dudley, J. P. (2014). ERAD and how viruses exploit it. *Front. Microbiol.* 5:330. doi: 10.3389/fmicb.2014.00330

Campbell, E. M., and Hope, T. J. (2015). HIV-1 capsid: the multifaceted key player in HIV-1 infection. *Nat. Rev. Microbiol.* 13, 471–483. doi: 10.1038/nrmicro3503

Carnes, S. K., Zhou, J., and Aiken, C. (2018). HIV-1 engages a dynein-dynactin-BICD2 complex for infection and transport to the nucleus. *J. Virol.* 92:e00358-18. doi: 10.1128/JVI.00358-18

Cary, D. C., Fujinaga, K., and Peterlin, B. M. (2016). Molecular mechanisms of HIV latency. *J. Clin. Invest.* 126, 448–454. doi: 10.1172/JCI80565

Cerboni, C., Neri, F., Casartelli, N., Zingoni, A., Cosman, D., Rossi, P., et al. (2007). Human immunodeficiency virus 1 Nef protein downmodulates the ligands of the activating receptor NKG2D and inhibits natural killer cell-mediated cytotoxicity. *J. Gen. Virol.* 88, 242–250. doi: 10.1099/vir.0.82125-0

Checkley, M. A., Luttge, B. G., and Freed, E. O. (2011). HIV-1 envelope glycoprotein biosynthesis, trafficking, and incorporation. *J. Mol. Biol.* 410, 582–608. doi: 10.1016/j.jmb.2011.04.042

Chen, B. (2019). Molecular mechanism of HIV-1 entry. *Trends Microbiol.* 27, 878–891. doi: 10.1016/j.tim.2019.06.002

Chen, J., Liu, Y., Wu, B., Nikolaitchik, O. A., Mohan, P. R., Chen, J., et al. (2020). Visualizing the translation and packaging of HIV-1 full-length RNA. *Proc. Natl. Acad. Sci. U.S.A.* 117, 6145–6155. doi: 10.1073/pnas.1917590117

Chen, M., and Manley, J. L. (2009). Mechanisms of alternative splicing regulation: insights from molecular and genomics approaches. *Nat. Rev. Mol. Cell Biol.* 10, 741–754. doi: 10.1038/nrm2777

Chen, S., Bonifati, S., Qin, Z., St Gelais, C., and Wu, L. (2019). SAMHD1 suppression of antiviral immune responses. *Trends Microbiol.* 27, 254–267. doi: 10.1016/j.tim.2018.09.009

Chin, C. R., Perreira, J. M., Savidis, G., Portmann, J. M., Aker, A. M., Feeley, E. M., et al. (2015). Direct visualization of HIV-1 replication intermediates shows that capsid and CPSF6 modulate HIV-1 intra-nuclear invasion and integration. *Cell Rep.* 13, 1717–1731. doi: 10.1016/j.celrep.2015.10.036

Chowers, M. Y., Spina, C. A., Kwoh, T. J., Fitch, N. J. S., Richman, D. D., Guatellii, J. C., et al. (1994). Optimal infectivity in vitro of human immunodeficiency virus type 1 requires an intact nef gene. *J. Virol.* 68, 2906–2914. doi: 10.1128/jvi.68.5.2906-2914.1994

Chukwurah, E., Handy, I., and Patel, R. C. (2017). ADAR1 and PACT contribute to efficient translation of transcripts containing HIV-1 trans-activating response (TAR) element. *Biochem. J.* 474, 1241–1257. doi: 10.1042/bcj20160964

Ciuffi, A. (2016). The benefits of integration. *Clin. Microbiol. Infect.* 22, 324–332. doi: 10.1016/j.cmi.2016.02.013

Cochrane, A. W., McNally, M. T., and Mouland, A. J. (2006). The retrovirus RNA trafficking granule: from birth to maturity. *Retrovirology* 3, 1–17. doi: 10.1186/1742-4690-3-18

Coiras, M., López-Huertas, M. R., Pérez-Olmeda, M., and Alcamí, J. (2009). Understanding HIV-1 latency provides clues for the eradication of long-term reservoirs. *Nat. Rev. Microbiol.* 7, 798–812. doi: 10.1038/nrmicro2223

Collins, K. L., Chen, B. K., Kalams, S. A., Walker, B. D., and Baltimore, D. (1998). HIV-1 Nef protein protects infected primary cells against killing by cytotoxic T lymphocytes. *Nature* 391, 397–401. doi: 10.1038/34929

Colomer-Lluch, M., Ruiz, A., Moris, A., and Prado, J. G. (2018). Restriction factors: from intrinsic viral restriction to shaping cellular immunity against HIV-1. *Front. Immunol.* 9:2876. doi: 10.3389/fimmu.2018.02876

Compton, A. A., Bruel, T., Porrot, F., Mallet, A., Sachse, M., Euvrard, M., et al. (2014). IFITM proteins incorporated into HIV-1 virions impair viral fusion and spread. *Cell Host Microbe* 16, 736–747. doi: 10.1016/j.chom.2014.11.001

Craigie, R., and Bushman, F. D. (2012). HIV DNA integration. *Cold Spring Harb. Perspect. Med.* 2:a006890. doi: 10.1101/cshperspect.a006890

De Iaco, A., Santoni, F., Vannier, A., Guipponi, M., Antonarakis, S., and Luban, J. (2013). TNPO3 protects HIV-1 replication from CPSF6-mediated capsid stabilization in the host cell cytoplasm. *Retrovirology* 10:20. doi: 10.1186/1742-4690-10-20

Delaney, M. K., Malikov, V., Chai, Q., Zhao, G., and Naghavi, M. H. (2017). Distinct functions of diaphanous-related formins regulate HIV-1 uncoating and transport. *Proc. Natl. Acad. Sci. U.S.A.* 114, E6932–E6941.

Dharan, A., Bachmann, N., Talley, S., Zwikelmaier, V., and Campbell, E. M. (2020). Nuclear pore blockade reveals that HIV-1 completes reverse transcription and uncoating in the nucleus. *Nat. Microbiol.* 5, 1088–1095. doi: 10.1038/s41564-020-0735-8

Dharan, A., Opp, S., Abdel-Rahim, O., Keceli, S. K., Imam, S., Diaz-Griffero, F., et al. (2017). Bicaudal D2 facilitates the cytoplasmic trafficking and nuclear import of HIV-1 genomes during infection. *Proc. Natl. Acad. Sci. U.S.A.* 114, E10707–E10716. doi: 10.1073/pnas.1712033114

Dharan, A., Talley, S., Tripathi, A., Mamede, J. I., Majetschak, M., Hope, T. J., et al. (2016). KIF5B and Nup358 cooperatively mediate the nuclear import of HIV-1 during infection. *PLoS Pathog.* 12:e1005700. doi: 10.1371/journal.ppat.1005700

Dick, R. A., Zadrozny, K. K., Xu, C., Schur, F. K. M., Lyddon, T. D., Ricana, C. L., et al. (2018). Inositol phosphates are assembly co-factors for HIV-1. *Nature* 560, 509–512. doi: 10.1038/s41586-018-0396-4

Dicks, M. D. J., Betancor, G., Jimenez-Guardeño, J. M., Pessel-Vivares, L., Apolonia, L., Goujon, C., et al. (2018). Multiple components of the nuclear pore complex interact with the amino-terminus of MX2 to facilitate HIV-1 restriction. *PLoS Pathog.* 14:e1007408. doi: 10.1371/journal.ppat.1007408

Doms, R. W., and Moore, J. P. (2000). HIV-1 membrane fusion. *J. Cell Biol.* 151, F9–F14. doi: 10.1083/jcb.151.2.f9

D'Orso, I., and Frankel, A. D. (2010). RNA-mediated displacement of an inhibitory snRNP complex activates transcription elongation. *Nat. Struct. Mol. Biol.* 17, 815–821. doi: 10.1038/nsmb.1827

D'Orso, I., Jang, G. M., Pastuszak, A. W., Faust, T. B., Quezada, E., Booth, D. S., et al. (2012). Transition step during assembly of HIV Tat:P-TEFb transcription complexes and transfer to TAR RNA. *Mol. Cell. Biol.* 32, 4780–4793. doi: 10.1128/MCB.00206-12

Douglas, J. L., Viswanathan, K., McCarroll, M. N., Gustin, J. K., Fruh, K., and Moses, A. V. (2009). Vpu directs the degradation of the HIV restriction factor BST-2/tetherin via a {beta}TrCP-dependent mechanism. *J. Virol.* 83, 7931–7947. doi: 10.1128/jvi.00242-09

Du Chéné, I., Basyuk, E., Lin, Y. L., Triboulet, R., Knezevich, A., Chable-Bessia, C., et al. (2007). Suv39H1 and HP1γ are responsible for chromatin-mediated HIV-1 transcriptional silencing and post-integration latency. *EMBO J.* 26, 424–435. doi: 10.1038/sj.emboj.7601517

El Meshri, S. E., Boutant, E., Mouhand, A., Thomas, A., Larue, V., Richert, L., et al. (2018). The NC domain of HIV-1 Gag contributes to the interaction of Gag with TSG101. *Biochim. Biophys. Acta* 1862, 1421–1431. doi: 10.1016/j.bbagen.2018.03.020

Farnet, C. M., and Bushman, F. D. (1997). HIV-1 cDNA integration: requirement of HMG I(Y) protein for function of preintegration complexes in vitro. *Cell* 88, 483–492. doi: 10.1016/s0092-8674(00)81888-7

Farnet, C. M., and Haseltine, W. A. (1991). Circularization of human immunodeficiency virus type 1 DNA in vitro. *J. Virol.* 65, 6942–6952. doi: 10.1128/jvi.65.12.6942-6952.1991

Fassati, A., and Goff, S. P. (2001). Characterization of intracellular reverse transcription complexes of human immunodeficiency virus type 1. *J. Virol.* 75, 3626–3635. doi: 10.1128/JVI.75.8.3626-3635.2001

Fenard, D., Yonemoto, W., de Noronha, C., Cavrois, M., Williams, S. A., and Greene, W. C. (2005). Nef is physically recruited into the immunological synapse and potentiates T cell activation early after TCR engagement. *J. Immunol.* 175, 6050–6057. doi: 10.4049/jimmunol.175.9.6050

Fernandez, J., Machado, A. K., Lyonnais, S., Chamontin, C., Gärtner, K., Léger, T., et al. (2019). Transportin-1 binds to the HIV-1 capsid via a nuclear localization signal and triggers uncoating. *Nat. Microbiol.* 4, 1840–1850. doi: 10.1038/s41564-019-0575-6

Fernandez, J., Portilho, D. M., Danckaert, A., Munier, S., Becker, A., Roux, P., et al. (2015). Microtubule-associated proteins 1 (MAP1) promote human immunodeficiency virus type I (HIV-1) intracytoplasmic routing to the nucleus. *J. Biol. Chem.* 290, 4631–4646. doi: 10.1074/jbc.m114.613133

Ferrari, G., Pollara, J., Kozink, D., Harms, T., Drinker, M., Freel, S., et al. (2011). An HIV-1 gp120 envelope human monoclonal antibody that recognizes a C1 conformational epitope mediates potent antibody-dependent cellular cytotoxicity (ADCC) activity and defines a common ADCC epitope in human HIV-1 serum. *J. Virol.* 85, 7029–7036. doi: 10.1128/JVI.00171-11

Firrito, C., Bertelli, C., Vanzo, T., Chande, A., and Pizzato, M. (2018). SERINC5 as a new restriction factor for human immunodeficiency virus and murine leukemia virus. *Annu. Rev. Virol.* 5, 323–340. doi: 10.1146/annurev-virology-092917-043308

Fischer, U., Huber, J., Boelens, W. C., Mattaj, I. W., and Lührmann, R. (1995). The HIV-1 Rev activation domain is a nuclear export signal that accesses an export pathway used by specific cellular RNAs. *Cell* 82, 475–483. doi: 10.1016/0092-8674(95)90436-0

Forouzanfar, F., Ali, S., Wallet, C., De Rovere, M., Ducloy, C., El Mekdad, H., et al. (2019). HIV-1 Vpr mediates the depletion of the cellular repressor CTIP2 to counteract viral gene silencing. *Sci. Rep.* 9:13154. doi: 10.1038/s41598-019-48689-x

Foster, T. L., Wilson, H., Iyer, S. S., Coss, K., Doores, K., Smith, S., et al. (2016). Resistance of transmitted founder HIV-1 to IFITM-mediated restriction. *Cell Host Microbe* 20, 429–442. doi: 10.1016/j.chom.2016.08.006

Francis, A. C., and Melikyan, G. B. (2018). Single HIV-1 imaging reveals progression of infection through CA-dependent steps of docking at the nuclear pore, uncoating, and nuclear transport. *Cell Host Microbe* 23, 536–548e6.

Fu, Y., He, S., Waheed, A. A., Dabbagh, D., Zhou, Z., Trinité, B., et al. (2020). PSGL-1 restricts HIV-1 infectivity by blocking virus particle attachment to target cells. *Proc. Natl. Acad. Sci. U.S.A.* 117, 9537–9545. doi: 10.1073/pnas.1916054117

Galão, R. P., Le Tortorec, A., Pickering, S., Kueck, T., and Neil, S. J. D. (2012). Innate sensing of HIV-1 assembly by tetherin induces NFκB-dependent proinflammatory responses. *Cell Host Microbe* 12, 633–644. doi: 10.1016/j.chom.2012.10.007

Garber, M. E., Wei, P., and Jones, K. A. (1998). HIV-1 Tat interacts with cyclin T1 to direct the P-TEFb CTD kinase complex to TAR RNA. *Cold Spring Harb. Symp. Quant. Biol.* 63, 371–380. doi: 10.1101/sqb.1998.63.371

Garrus, J. E., Von Schwedler, U. K., Pornillos, O. W., Morham, S. G., Zavitz, K. H., Wang, H. E., et al. (2001). Tsg101 and the vacuolar protein sorting pathway are essential for HIV-1 budding. *Cell* 107, 55–65. doi: 10.1016/S0092-8674(01)00506-2

Goujon, C., Moncorgé, O., Bauby, H., Doyle, T., Ward, C. C., Schaller, T., et al. (2013). Human MX2 is an interferon-induced post-entry inhibitor of HIV-1 infection. *Nature* 502, 559–562. doi: 10.1038/nature12542

Gringhuis, S. I., Hertoghs, N., Kaptein, T. M., Zijlstra-Willems, E. M., Sarrami-Forooshani, R., Sprokholt, J. K., et al. (2016). HIV-1 blocks the signaling adaptor MAVS to evade antiviral host defense after sensing of abortive HIV-1 RNA by the host helicase DDX3. *Nat. Immunol.* 18, 225–235. doi: 10.1038/ni.3647

Guerrero, S., Batisse, J., Libre, C., Bernacchi, S., Marquet, R., and Paillart, J.-C. (2015). HIV-1 replication and the cellular eukaryotic translation apparatus. *Viruses* 7, 199–218. doi: 10.3390/v7010199

Haller, C., Müller, B., Fritz, J. V., Lamas-Murua, M., Stolp, B., Pujol, F. M., et al. (2014). HIV-1 Nef and Vpu are functionally redundant broad-spectrum modulators of cell surface receptors, including tetraspanins. *J. Virol.* 88, 14241–14257. doi: 10.1128/JVI.02333-14

Harrison, S. C. (2008). Viral membrane fusion. *Nat. Struct. Mol. Biol.* 15, 690–698.

Harrison, S. C. (2015). Viral membrane fusion. *Virology* 479, 498–507. doi: 10.1016/j.virol.2015.03.043

He, N., Liu, M., Hsu, J., Xue, Y., Chou, S., Burlingame, A., et al. (2010). HIV-1 Tat and host AFF4 recruit two transcription elongation factors into a bifunctional complex for coordinated activation of HIV-1 transcription. *Mol. Cell* 38, 428–438. doi: 10.1016/j.molcel.2010.04.013

Henderson, B. R., and Percipalle, P. (1997). Interactions between HIV Rev and nuclear import and export factors: the Rev nuclear localisation signal mediates specific binding to human importin-β. *J. Mol. Biol.* 274, 693–707. doi: 10.1006/jmbi.1997.1420

Höhne, K., Businger, R., van Nuffel, A., Bolduan, S., Koppensteiner, H., Baeyens, A., et al. (2016). Virion encapsidated HIV-1 Vpr induces NFAT to prime non-activated T cells for productive infection. *Open Biol.* 6:160046. doi: 10.1098/rsob.160046

Hopfensperger, K., and Sautera, D. (2020). Decreased, deformed, defective-how HIV-1 vpu targets peroxisomes. *mBio* 11:e00367-20. doi: 10.1128/mBio.00967-20

Hotter, D., Bosso, M., Jønsson, K. L., Krapp, C., Stürzel, C. M., Das, A., et al. (2019). IFI16 targets the transcription factor Sp1 to suppress HIV-1 transcription and latency reactivation. *Cell Host Microbe* 25, 858–872e13. doi: 10.1016/j.chom.2019.05.002

Hrecka, K., Hao, C., Gierszewska, M., Swanson, S. K., Kesik-Brodacka, M., Srivastava, S., et al. (2011). Vpx relieves inhibition of HIV-1 infection of macrophages mediated by the SAMHD1 protein. *Nature* 474, 658–661. doi: 10.1038/nature10195

Huang, C.-Y., Chiang, S.-F., Lin, T.-Y., Chiou, S.-H., and Chow, K.-C. (2012). HIV-1 Vpr triggers mitochondrial destruction by impairing Mfn2-mediated ER-mitochondria interaction. *PLoS One* 7:e33657. doi: 10.1371/journal.pone.0033657

Isel, C., Lanchy, J. M., Le Grice, S. F., Ehresmann, C., Ehresmann, B., and Marquet, R. (1996). Specific initiation and switch to elongation of human immunodeficiency virus type 1 reverse transcription require the post-transcriptional modifications of primer tRNA3Lys. *EMBO J.* 15, 917–924. doi: 10.1002/j.1460-2075.1996.tb00426.x

Jacob, R. A., Johnson, A. L., Pawlak, E. N., Dirk, B. S., Van Nynatten, L. R., Haeryfar, S. M. M., et al. (2017). The interaction between HIV-1 Nef and adaptor protein-2 reduces Nef-mediated CD4+ T cell apoptosis. *Virology* 509, 1–10. doi: 10.1016/j.virol.2017.05.018

Jakobsen, M. R., Bak, R. O., Andersen, A., Berg, R. K., Jensen, S. B., Tengchuan, J., et al. (2013). IFI16 senses DNA forms of the lentiviral replication cycle and controls HIV-1 replication. *Proc. Natl. Acad. Sci. U.S.A.* 110, E4571–E4580. doi: 10.1073/pnas.1311669110

Jones, K. A. (1997). Taking a new TAK on TAT transactivation. *Genes Dev.* 11, 2593–2599. doi: 10.1101/gad.11.20.2593

Jones, K. A., and Peterlin, M. B. (1994). Control of RNA initiation and elongation at the HIV-1 promoter. *Annu. Rev. Biochem.* 63, 717–743. doi: 10.1146/annurev.bi.63.070194.003441

Kane, M., Yadav, S. S., Bitzegeio, J., Kutluay, S. B., Zang, T., Wilson, S. J., et al. (2013). MX2 is an interferon-induced inhibitor of HIV-1 infection. *Nature* 502, 563–566. doi: 10.1038/nature12653

Khiytani, D. K., and Dimmock, N. J. (2002). Characterization of a human immunodeficiency virus type 1 pre-integration complex in which the majority of the cDNA is resistant to DNase I digestion. *J. Gen. Virol.* 83, 2523–2532. doi: 10.1099/0022-1317-83-10-2523

Kielian, M. (2014). Mechanisms of virus membrane fusion proteins. *Annu. Rev. Virol.* 1, 171–189. doi: 10.1146/annurev-virology-031413-085521

Kim, K., Dauphin, A., Komurlu, S., McCauley, S. M., Yurkovetskiy, L., Carbone, C., et al. (2019). Cyclophilin A protects HIV-1 from restriction by human TRIM5α. *Nat. Microbiol.* 4, 2044–2051. doi: 10.1038/s41564-019-0592-5

Köhler, A., and Hurt, E. (2007). Exporting RNA from the nucleus to the cytoplasm. *Nat. Rev. Mol. Cell Biol.* 8, 761–773. doi: 10.1038/nrm2255

Komori, C., Takahashi, T., Nakano, Y., and Ui-Tei, K. (2020). TRBP–Dicer interaction may enhance HIV-1 TAR RNA translation via TAR RNA processing, repressing host-cell apoptosis. *Biol. Open* 9:bio050435. doi: 10.1242/bio.050435

König, R., Zhou, Y., Elleder, D., Diamond, T. L., Bonamy, G. M. C., Irelan, J. T., et al. (2008). Global analysis of host-pathogen interactions that regulate early-stage HIV-1 replication. *Cell* 135, 49–60. doi: 10.1016/j.cell.2008.07.032

Korniy, N., Goyal, A., Hoffmann, M., Samatova, E., Peske, F., Pöhlmann, S., et al. (2019). Modulation of HIV-1 Gag/Gag-Pol frameshifting by tRNA abundance. *Nucleic Acids Res.* 47, 5210–5222. doi: 10.1093/nar/gkz202

Kottilil, S., Jackson, J. O., Reitano, K. N., O'Shea, M. A., Roby, G., Lloyd, M., et al. (2007). Innate immunity in HIV infection. *JAIDS J. Acquir. Immune Defic. Syndr.* 46, 151–159. doi: 10.1097/qai.0b013e3180dc9909

Kumar, S., Morrison, J. H., Dingli, D., and Poeschla, E. (2018). HIV-1 activation of innate immunity depends strongly on the intracellular level of TREX1 and sensing of incomplete reverse transcription products. *J. Virol.* 92:e00001-18. doi: 10.1128/JVI.00001-18

Kutluay, S. B., Zang, T., Blanco-Melo, D., Powell, C., Jannain, D., Errando, M., et al. (2014). Global changes in the RNA binding specificity of HIV-1 Gag regulate virion genesis. *Cell* 159, 1096–1109. doi: 10.1016/j.cell.2014.09.057

Kvaratskhelia, M., Sharma, A., Larue, R. C., Serrao, E., and Engelman, A. (2014). Molecular mechanisms of retroviral integration site selection. *Nucleic Acids Res.* 42, 10209–10225. doi: 10.1093/nar/gku769

Kwon, Y., Kaake, R. M., Echeverria, I., Suarez, M., Karimian Shamsabadi, M., Stoneham, C., et al. (2020). Structural basis of CD4 downregulation by HIV-1 Nef. *Nat. Struct. Mol. Biol.* 27, 822–828. doi: 10.1038/s41594-020-0463-z

Ladha, J. S., Tripathy, M. K., and Mitra, D. (2005). Mitochondrial complex I activity is impaired during HIV-1-induced T-cell apoptosis. *Cell Death Differ.* 12, 1417–1428. doi: 10.1038/sj.cdd.4401668

Lahaye, X., Gentili, M., Silvin, A., Conrad, C., Picard, L., Jouve, M., et al. (2018). NONO detects the nuclear HIV capsid to promote cGAS-mediated innate immune activation. *Cell* 175, 488–501.e22. doi: 10.1016/j.cell.2018.08.062

Lee, I. H., Kai, H., Carlson, L. A., Groves, J. T., and Hurley, J. H. (2015). Negative membrane curvature catalyzes nucleation of endosomal sorting complex required for transport (ESCRT)-III assembly. *Proc. Natl. Acad. Sci. U.S.A.* 112, 15892–15897. doi: 10.1073/pnas.1518765113

Lee, W.-Y. J., Fu, R. M., Liang, C., and Sloan, R. D. (2018). IFITM proteins inhibit HIV-1 protein synthesis. *Sci. Rep.* 8:14551. doi: 10.1038/s41598-018-32785-5

Li, D., Rawle, D. J., Wu, Z., Jin, H., Lin, M.-H., Lor, M., et al. (2019). eEF1A demonstrates paralog specific effects on HIV-1 reverse transcription efficiency. *Virology* 530, 65–74. doi: 10.1016/j.virol.2019.01.023

Li, L., Olvera, J. M., Yoder, K. E., Mitchell, R. S., Butler, S. L., Lieber, M., et al. (2001). Role of the non-homologous DNA end joining pathway in the early steps of retroviral infection. *EMBO J.* 20, 3272–3281. doi: 10.1093/emboj/20.12.3272

Li, Q., Smith, A. J., Schacker, T. W., Carlis, J. V., Duan, L., Reilly, C. S., et al. (2009). Microarray analysis of lymphatic tissue reveals stage-specific, gene expression signatures in HIV-1 infection. *J. Immunol.* 183, 1975–1982. doi: 10.4049/jimmunol.0803222

Li, Z., Wu, J., Chavez, L., Hoh, R., Deeks, S. G., Pillai, S. K., et al. (2019). Reiterative enrichment and authentication of CRISPRi targets (REACT) identifies the proteasome as a key contributor to HIV-1 latency. *PLoS Pathog.* 15:e1007498. doi: 10.1371/journal.ppat.1007498

Lin, C.-W., and Engelman, A. (2003). The barrier-to-autointegration factor is a component of functional human immunodeficiency virus type 1 preintegration complexes. *J. Virol.* 77, 5030–5036. doi: 10.1128/jvi.77.8.5030-5036.2003

Lindqvist, B., Akusjärvi, S. S., Sönnerborg, A., Dimitriou, M., and Svensson, J. P. (2020). Chromatin maturation of the HIV-1 provirus in primary resting CD4+ T cells. *PLoS Pathog.* 16:e1008264. doi: 10.1371/journal.ppat.1008264

Lingappa, J. R., Reed, J. C., Tanaka, M., Chutiraka, K., and Robinson, B. A. (2014). How HIV-1 Gag assembles in cells: putting together pieces of the puzzle. *Virus Res.* 193, 89–107. doi: 10.1016/j.virusres.2014.07.001

Liu, R., Wu, J., Shao, R., and Xue, Y. (2014). Mechanism and factors that control HIV-1 transcription and latency activation. *J. Zhejiang Univ. Sci. B* 15, 455–465. doi: 10.1631/jzus.B1400059

Llano, M., Saenz, D. T., Meehan, A., Wongthida, P., Peretz, M., Walker, W. H., et al. (2006). An essential role for LEDGF/p75 in HIV integration. *Science* 314, 461–464. doi: 10.1126/science.1132319

Luban, J., Bossolt, K. L., Franke, E. K., Kalpana, G. V., and Goff, S. P. (1993). Human immunodeficiency virus type 1 Gag protein binds to cyclophilins A and B. *Cell* 73, 1067–1078. doi: 10.1016/0092-8674(93)90637-6

Lubben, N. B., Sahlender, D. A., Motley, A. M., Lehner, P. J., Benaroch, P., and Robinson, M. S. (2007). HIV-1 Nef-induced down-regulation of MHC class I requires AP-1 and Clathrin but not PACS-1 and is impeded by AP-2. *Mol. Biol. Cell* 18, 3351–3365. doi: 10.1091/mbc.E07-03-0218

Lukic, Z., Dharan, A., Fricke, T., Diaz-Griffero, F., and Campbell, E. M. (2014). HIV-1 uncoating is facilitated by dynein and kinesin 1. *J. Virol.* 88, 13613–13625. doi: 10.1128/jvi.02219-14

Ma, L., Jiang, Q.-A., Sun, L., Yang, X., Huang, H., Jin, X., et al. (2020). X-linked RNA-binding motif protein modulates HIV-1 infection of CD4+ T cells by maintaining the trimethylation of histone H3 lysine 9 at the downstream region

of the 5′ long terminal repeat of HIV proviral DNA. *mBio* 11:e03424-19. doi: 10.1128/mBio.03424-19

Magadán, J. G., Pérez-Victoria, F. J., Sougrat, R., Ye, Y., Strebel, K., and Bonifacino, J. S. (2010). Multilayered mechanism of CD4 downregulation by HIV-1 Vpu involving distinct ER retention and ERAD targeting steps. *PLoS Pathog.* 6:e1000869. doi: 10.1371/journal.ppat.1000869

Malikov, V., Da Silva, E. S., Jovasevic, V., Bennett, G., De Souza Aranha Vieira, D. A., Schulte, B., et al. (2015). HIV-1 capsids bind and exploit the kinesin-1 adaptor FEZ1 for inward movement to the nucleus. *Nat. Commun.* 6:6660. doi: 10.1038/ncomms7660

Malim, M. H., and Bieniasz, P. D. (2012). HIV restriction factors and mechanisms of evasion. *Cold Spring Harb. Perspect. Med.* 2:a006940. doi: 10.1101/cshperspect.a006940

Mallery, D. L., Faysal, K. M. R., Kleinpeter, A., Wilson, M. S. C., Vaysburd, M., Fletcher, A. J., et al. (2019). Cellular IP6 levels limit HIV production while viruses that cannot efficiently package IP6 are attenuated for infection and replication. *Cell Rep.* 29, 3983–3996.e4. doi: 10.1016/j.celrep.2019.11.050

Margottin, F., Bour, S. P., Durand, H., Selig, L., Benichou, S., Richard, V., et al. (1998). A novel human WD protein, h-beta TrCp, that interacts with HIV-1 Vpu connects CD4 to the ER degradation pathway through an F-box motif. *Mol. Cell* 1, 565–574. doi: 10.1016/s1097-2765(00)80056-8

Martin-Serrano, J., and Neil, S. J. D. (2011). Host factors involved in retroviral budding and release. *Nat. Rev. Microbiol.* 9, 519–531. doi: 10.1038/nrmicro2596

Mbonye, U., and Karn, J. (2017). The molecular basis for human immunodeficiency virus latency. *Annu. Rev. Virol.* 4, 261–285. doi: 10.1146/annurev-virology-101416-041646

McDonald, D., Vodicka, M. A., Lucero, G., Svitkina, T. M., Borisy, G. G., Emerman, M., et al. (2002). Visualization of the intracellular behavior of HIV in living cells. *J. Cell Biol.* 159, 441–452. doi: 10.1083/jcb.200203150

McNamara, R. P., McCann, J. L., Gudipaty, S. A., and D'Orso, I. (2013). Transcription factors mediate the enzymatic disassembly of promoter-bound 7SK snRNP to locally recruit P-TEFb for transcription elongation. *Cell Rep.* 5, 1256–1268. doi: 10.1016/j.celrep.2013.11.003

Meng, B., and Lever, A. M. L. (2013). Wrapping up the bad news – HIV assembly and release. *Retrovirology* 10:5. doi: 10.1186/1742-4690-10-5

Miles, R. J., Kerridge, C., Hilditch, L., Monit, C., Jacques, D. A., and Towers, G. J. (2020). MxB sensitivity of HIV-1 is determined by a highly variable and dynamic capsid surface. *eLife* 9:e56910. doi: 10.7554/eLife.56910

Neil, S. J. D., Zang, T., and Bieniasz, P. D. (2008). Tetherin inhibits retrovirus release and is antagonized by HIV-1 Vpu. *Nature* 451, 425–430. doi: 10.1038/nature06553

Nguyen, V. T., Kiss, T., Michels, A. A., and Bensaude, O. (2001). 7SK small nuclear RNA binds to and inhibits the activity of CDK9/cyclin T complexes. *Nature* 414, 322–325. doi: 10.1038/35104581

Novikova, M., Zhang, Y., Freed, E. O., and Peng, K. (2019). Multiple roles of HIV-1 capsid during the virus replication cycle. *Virol. Sin.* 34, 119–134. doi: 10.1007/s12250-019-00095-3

Ohlmann, T., Mengardi, C., and López-Lastra, M. (2014). Translation initiation of the HIV-1 mRNA. *Translation* 2:e960242. doi: 10.4161/2169074x.2014.960242

Paoletti, A., Allouch, A., Caillet, M., Saidi, H., Subra, F., Nardacci, R., et al. (2019). HIV-1 envelope overcomes NLRP3-mediated inhibition of F-actin polymerization for viral entry. *Cell reports* 28, 3381–3394.e7.

Pham, T. N. Q., Lukhele, S., Hajjar, F., Routy, J. P., and Cohen, ÉA. (2014). HIV Nef and Vpu protect HIV-infected CD4+ T cells from antibody-mediated cell lysis through down-modulation of CD4 and BST2. *Retrovirology* 11:15. doi: 10.1186/1742-4690-11-15

Pincetic, A., and Leis, J. (2009). The mechanism of budding of retroviruses from cell membranes. *Adv. Virol.* 2009, 6239691–6239699. doi: 10.1155/2009/623969

Poletti, V., and Mavilio, F. (2018). Interactions between retroviruses and the host cell genome. *Mol. Ther. Methods Clin. Dev.* 8, 31–41. doi: 10.1016/j.omtm.2017.10.001

Pollard, V. W., and Malim, M. H. (1998). The HIV-1 rev protein. *Annu. Rev. Microbiol.* 52, 491–532. doi: 10.1146/annurev.micro.52.1.491

Pollpeter, D., Parsons, M., Sobala, A. E., Coxhead, S., Lang, R. D., Bruns, A. M., et al. (2018). Deep sequencing of HIV-1 reverse transcripts reveals the multifaceted anti-viral functions of APOBEC3G. *Nat. Microbiol.* 3, 220–233. doi: 10.1038/s41564-017-0063-9

Popov, S., Popova, E., Inoue, M., Wu, Y., and Göttlinger, H. (2018). HIV-1 gag recruits PACSIN2 to promote virus spreading. *Proc. Natl. Acad. Sci. U.S.A.* 115, 7093–7098. doi: 10.1073/pnas.1801849115

Price, A. J., Fletcher, A. J., Schaller, T., Elliott, T., Lee, K., KewalRamani, V. N., et al. (2012). CPSF6 defines a conserved capsid interface that modulates HIV-1 replication. *PLoS Pathog.* 8:e1002896. doi: 10.1371/journal.ppat.1002896

Rasaiyaah, J., Tan, C. P., Fletcher, A. J., Price, A. J., Blondeau, C., Hilditch, L., et al. (2013). HIV-1 evades innate immune recognition through specific co-factor recruitment. *Nature* 503, 402–405. doi: 10.1038/nature12769

Rathore, A., Iketani, S., Wang, P., Jia, M., Sahi, V., and Ho, D. D. (2020). CRISPR-based gene knockout screens reveal deubiquitinases involved in HIV-1 latency in two Jurkat cell models. *Sci. Rep.* 10, 1–14. doi: 10.1038/s41598-020-62375-3

Rawle, D. J., Li, D., Swedberg, J. E., Wang, L., Soares, D. C., and Harrich, D. (2018). HIV-1 uncoating and reverse transcription require eEF1A binding to surface-exposed acidic residues of the reverse transcriptase thumb domain. *mBio* 9:e00316-18. doi: 10.1128/mBio.00316-18

Rawle, D. J., Li, D., Wu, Z., Wang, L., Choong, M., Lor, M., et al. (2019). Oxazole-benzenesulfonamide derivatives inhibit HIV-1 reverse transcriptase interaction with cellular eEF1A and reduce viral replication. *J. Virol.* 93, e239–e219. doi: 10.1128/JVI.00239-19

Ren, X.-X., Wang, H.-B., Li, C., Jiang, J.-F., Xiong, S.-D., Jin, X., et al. (2016). HIV-1 Nef-associated Factor 1 enhances viral production by interacting with CRM1 to promote nuclear export of unspliced HIV-1 gag mRNA. *J. Biol. Chem.* 291, 4580–4588. doi: 10.1074/jbc.M115.706135

Ricci, E. P., Rifo, R. S., Herbreteau, C. H., Decimo, D., and Ohlmann, T. (2008). Lentiviral RNAs can use different mechanisms for translation initiation. *Biochem. Soc. Trans.* 36, 690–693. doi: 10.1042/BST0360690

Röling, M. D., Stoszko, M., and Mahmoudi, T. (2016). "Molecular mechanisms controlling HIV transcription and latency – implications for therapeutic viral reactivation," in *Advances in Molecular Retrovirology*, ed. S. K. Saxena (London: InTech Open), 45–106. doi: 10.5772/61948

Rosa, A., Chande, A., Ziglio, S., De Sanctis, V., Bertorelli, R., Goh, S. L., et al. (2015). HIV-1 Nef promotes infection by excluding SERINC5 from virion incorporation. *Nature* 526, 212–217. doi: 10.1038/nature15399

Rozzi, S. J., Avdoshina, V., Fields, J. A., and Mocchetti, I. (2018). Human immunodeficiency virus Tat impairs mitochondrial fission in neurons. *Cell Death Discov.* 4, 1–12. doi: 10.1038/s41420-017-0013-6

Ruelas, D. S., and Greene, W. C. (2013). An integrated overview of HIV-1 latency. *Cell* 155, 519–529. doi: 10.1016/j.cell.2013.09.044

Rumlová, M., Køížová, I., Keprová, A., Hadravová, R., Doležal, M., Strohalmová, K., et al. (2014). HIV-1 protease-induced apoptosis. *Retrovirology* 11:37. doi: 10.1186/1742-4690-11-37

Sayah, D. M., Sokolskaja, E., Berthoux, L., and Luban, J. (2004). Cyclophilin A retrotransposition into TRIM5 explains owl monkey resistance to HIV-1. *Nature* 430, 569–573. doi: 10.1038/nature02777

Schrijvers, R., De Rijck, J., Demeulemeester, J., Adachi, N., Vets, S., Ronen, K., et al. (2012a). LEDGF/p75-independent HIV-1 replication demonstrates a role for HRP-2 and remains sensitive to inhibition by LEDGINs. *PLoS Pathog.* 8:e1002558. doi: 10.1371/journal.ppat.1002558

Schrijvers, R., Vets, S., De Rijck, J., Malani, N., Bushman, F. D., Debyser, Z., et al. (2012b). HRP-2 determines HIV-1 integration site selection in LEDGF/p75 depleted cells. *Retrovirology* 9:84. doi: 10.1186/1742-4690-9-84

Schwartz, O., Maréchal, V., Le Gall, S., Lemonnier, F., and Heard, J. M. (1996). Endocytosis of major histocompatibility complex class I molecules is induced by the HIV-1 Nef protein. *Nat. Med.* 2, 338–342. doi: 10.1038/nm0396-338

Selyutina, A., Persaud, M., Lee, K., KewalRamani, V., and Diaz-Griffero, F. (2020a). Nuclear import of the HIV-1 core precedes reverse transcription and uncoating. *Cell Rep.* 32:108201. doi: 10.1016/j.celrep.2020.108201

Selyutina, A., Persaud, M., Simons, L. M., Bulnes-Ramos, A., Buffone, C., Martinez-Lopez, A., et al. (2020b). Cyclophilin A prevents HIV-1 restriction in lymphocytes by blocking human TRIM5α binding to the viral core. *Cell Rep* 30:e6. doi: 10.1016/j.celrep.2020.02.100

Sertznig, H., Hillebrand, F., Erkelenz, S., Schaal, H., and Widera, M. (2018). Behind the scenes of HIV-1 replication: Alternative splicing as the dependency factor on the quiet. *Virology* 516, 176–188. doi: 10.1016/j.virol.2018.01.011

Shah, A., Vaidya, N. K., Bhat, H. K., and Kumar, A. (2016). HIV-1 gp120 induces type-1 programmed cell death through ER stress employing IRE1α, JNK and AP-1 pathway. *Sci. Rep.* 6:18929. doi: 10.1038/srep18929

Sheehy, A. M., Gaddis, N. C., Choi, J. D., and Malim, M. H. (2002). Isolation of a human gene that inhibits HIV-1 infection and is suppressed by the viral Vif protein. *Nature* 418, 646–650. doi: 10.1038/nature00939

Shukla, A., Ramirez, N.-G. P., and D'Orso, I. (2020). HIV-1 Proviral Transcription and Latency in the New Era. *Viruses* 12, 555. doi: 10.3390/v12050555

Skasko, M., Tokarev, A., Chen, C. C., Fischer, W. B., Pillai, S. K., and Guatelli, J. (2011). BST-2 is rapidly down-regulated from the cell surface by the HIV-1 protein Vpu: evidence for a post-ER mechanism of Vpu-action. *Virology* 411, 65–77. doi: 10.1016/j.virol.2010.12.038

Strack, B., Calistri, A., Craig, S., Popova, E., and Göttlinger, H. G. (2003). AIP1/ALIX is a binding partner for HIV-1 p6 and EIAV p9 functioning in virus budding. *Cell* 114, 689–699. doi: 10.1016/S0092-8674(03)00653-6

Stremlau, M., Owens, C. M., Perron, M. J., Kiessling, M., Autissier, P., and Sodroski, J. (2004). The cytoplasmic body component TRIM5α restricts HIV-1 infection in Old World monkeys. *Nature* 427, 848–853. doi: 10.1038/nature02343

Stremlau, M., Perron, M., Lee, M., Li, Y., Song, B., Javanbakht, H., et al. (2006). Specific recognition and accelerated uncoating of retroviral capsids by the TRIM5alpha restriction factor. *Proc. Natl. Acad. Sci. U.S.A.* 103, 5514–5519. doi: 10.1073/pnas.0509996103

Stremlau, M., Perron, M., Welikala, S., and Sodroski, J. (2005). Species-specific variation in the B30.2(SPRY) domain of TRIM5α determines the potency of human immunodeficiency virus restriction. *J. Virol.* 79, 3139–3145. doi: 10.1128/JVI.79.5.3139-3145.2005

Sultana, T., Mamede, J. I., Saito, A., Ode, H., Nohata, K., Cohen, R., et al. (2019). Multiple pathways to avoid beta interferon sensitivity of HIV-1 by mutations in capsid. *J Virol* 93, e00986. doi: 10.1128/JVI.00986-19

Sumner, R. P., Harrison, L., Touizer, E., Peacock, T. P., Spencer, M., Zuliani-Alvarez, L., et al. (2020). Disrupting HIV-1 capsid formation causes cGAS sensing of viral DNA. *EMBO J.* 39:e103958. doi: 10.15252/embj.2019103958

Taura, M., Song, E., Ho, Y.-C., and Iwasaki, A. (2019). Apobec3A maintains HIV-1 latency through recruitment of epigenetic silencing machinery to the long terminal repeat. *Proc. Natl. Acad. Sci. U.S.A.* 116, 2282–2289. doi: 10.1073/pnas.1819386116

Teodorof-Diedrich, C., and Spector, S. A. (2018). Human immunodeficiency virus type 1 gp120 and Tat induce mitochondrial fragmentation and incomplete mitophagy in human neurons. *J. Virol.* 92, e993–e918. doi: 10.1128/JVI.00993-18

Thangaraj, A., Periyasamy, P., Liao, K., Bendi, V. S., Callen, S., Pendyala, G., et al. (2018). HIV-1 TAT-mediated microglial activation: role of mitochondrial dysfunction and defective mitophagy. *Autophagy* 14, 1596–1619. doi: 10.1080/15548627.2018.1476810

Turelli, P., Doucas, V., Craig, E., Mangeat, B., Klages, N., Evans, R., et al. (2001). Cytoplasmic recruitment of INI1 and PML on incoming HIV preintegration complexes: interference with early steps of viral replication. *Mol. Cell* 7, 1245–1254. doi: 10.1016/s1097-2765(01)00255-6

Turrini, F., Marelli, S., Kajaste-Rudnitski, A., Lusic, M., Van Lint, C., Das, A. T., et al. (2015). HIV-1 transcriptional silencing caused by TRIM22 inhibition of Sp1 binding to the viral promoter. *Retrovirology* 12:104. doi: 10.1186/s12977-015-0230-0

Usami, Y., Wu, Y., and Göttlinger, H. G. (2015). SERINC3 and SERINC5 restrict HIV-1 infectivity and are counteracted by Nef. *Nature* 526, 218–223. doi: 10.1038/nature15400

Van Damme, N., Goff, D., Katsura, C., Jorgenson, R. L., Mitchell, R., Johnson, M. C., et al. (2008). The interferon-induced protein BST-2 restricts HIV-1 release and is downregulated from the cell surface by the viral Vpu protein. *Cell Host Microbe* 3, 245–252. doi: 10.1016/j.chom.2008.03.001

Van Lint, C., Bouchat, S., and Marcello, A. (2013). HIV-1 transcription and latency: an update. *Retrovirology* 10:67. doi: 10.1186/1742-4690-10-67

Veillette, M., Désormeaux, A., Medjahed, H., Gharsallah, N.-E., Coutu, M., Baalwa, J., et al. (2014). Interaction with cellular CD4 exposes HIV-1 envelope epitopes targeted by antibody-dependent cell-mediated cytotoxicity. *J. Virol.* 88, 2633–2644. doi: 10.1128/JVI.03230-13

Waheed, A. A., and Freed, E. O. (2009). Lipids and membrane microdomains in HIV-1 replication. *Virus Res.* 143, 162–176. doi: 10.1016/j.virusres.2009.04.007

Wang, Y., Zhang, H., Na, L., Du, C., Zhang, Z., Zheng, Y.-H., et al. (2019). ANP32A and ANP32B are key factors in the Rev-dependent CRM1 pathway for nuclear export of HIV-1 unspliced mRNA. *J. Biol. Chem.* 294, 15346–15357. doi: 10.1074/jbc.ra119.008450

Weiss, E. R., and Göttlinger, H. (2011). The role of cellular factors in promoting HIV budding. *J. Mol. Biol.* 410, 525–533. doi: 10.1016/j.jmb.2011.04.055

Wu, J., Xue, Y., Gao, X., and Zhou, Q. (2020). Host cell factors stimulate HIV-1 transcription by antagonizing substrate-binding function of Siah1 ubiquitin ligase to stabilize transcription elongation factor ELL2. *Nucleic Acids Res.* 48, 7321–7332. doi: 10.1093/nar/gkaa461

Wyatt, R., Moore, J., Accola, M., Desjardin, E., Robinson, J., and Sodroski, J. (1995). Involvement of the V1/V2 variable loop structure in the exposure of human immunodeficiency virus type 1 gp120 epitopes induced by receptor binding. *J. Virol.* 69, 5723–5733. doi: 10.1128/jvi.69.9.5723-5733.1995

Xu, Z., Asahchop, E. L., Branton, W. G., Gelman, B. B., Power, C., and Hobman, T. C. (2017). MicroRNAs upregulated during HIV infection target peroxisome biogenesis factors: Implications for virus biology, disease mechanisms and neuropathology. *PLoS Pathog.* 13:e1006360. doi: 10.1371/journal.ppat.1006360

Xu, Z., Lodge, R., Power, C., Cohen, E. A., and Hobman, T. C. (2020). The HIV-1 accessory protein vpu downregulates peroxisome biogenesis. *mBio* 11:e03395-19. doi: 10.1128/mBio.03395-19

Yadav, P., Sur, S., Desai, D., Kulkarni, S., Sharma, V., and Tandon, V. (2019). Interaction of HIV-1 integrase with polypyrimidine tract binding protein and associated splicing factor (PSF) and its impact on HIV-1 replication. *Retrovirology* 16:12. doi: 10.1186/s12977-019-0474-1

Yang, Z., Yik, J. H. N., Chen, R., He, N., Moon, K. J., Ozato, K., et al. (2005). Recruitment of P-TEFb for stimulation of transcriptional elongation by the bromodomain protein Brd4. *Mol. Cell* 19, 535–545. doi: 10.1016/j.molcel.2005.06.029

Yedavalli, V. S., and Jeang, K.-T. (2010). Trimethylguanosine capping selectively promotes expression of Rev-dependent HIV-1 RNAs. *Proc. Natl. Acad. Sci. U.S.A.* 107, 14787–14792. doi: 10.1073/pnas.1009490107

Yik, J. H. N., Chen, R., Pezda, A. C., Samford, C. S., and Zhou, Q. (2004). A human immunodeficiency virus type 1 Tat-like arginine-rich RNA-binding domain is essential for HEXIM1 to inhibit RNA polymerase II transcription through 7SK snRNA-mediated inactivation of P-TEFb. *Mol. Cell. Biol.* 24, 5094–5105. doi: 10.1128/MCB.24.12.5094-5105.2004

Yin, X., Langer, S., Zhang, Z., Herbert, K. M., Yoh, S., König, R., et al. (2020). Sensor sensibility—HIV-1 and the innate immune response. *Cells* 9:254. doi: 10.3390/cells9010254

Yu, K. L., Jung, Y. M., Park, S. H., Lee, S. D., and You, J. C. (2020). Human transcription factor YY1 could upregulate the HIV-1 gene expression. *BMB Rep.* 53:248. doi: 10.5483/bmbrep.2020.53.5.222

Yung, E., Sorin, M., Wang, E.-J., Perumal, S., Ott, D., and Kalpana, G. V. (2004). Specificity of interaction of INI1/hSNF5 with retroviral integrases and its functional significance. *J. Virol.* 78, 2222–2231. doi: 10.1128/jvi.78.5.2222-2231.2004

Zhang, X., Zhou, T., Frabutt, D. A., and Zheng, Y. H. (2016). HIV-1 Vpr increases Env expression by preventing Env from endoplasmic reticulum-associated protein degradation (ERAD). *Virology* 496, 194–202. doi: 10.1016/j.virol.2016.06.002

Zhao, L., Liu, M., Ouyang, J., Zhu, Z., Geng, W., Dong, J., et al. (2018). The Per-1 short isoform inhibits de novo HIV-1 transcription in resting Cd4+ T-cells. *Curr. HIV Res.* 16, 384–395. doi: 10.2174/1570162x16666190218145048

Zhao, X., Li, J., Winkler, C. A., An, P., and Guo, J. T. (2019). IFITM genes, variants, and their roles in the control and pathogenesis of viral infections. *Front. Microbiol.* 9:3228. doi: 10.3389/fmicb.2018.03228

Zhou, M., Halanski, M. A., Radonovich, M. F., Kashanchi, F., Peng, J., Price, D. H., et al. (2000). Tat modifies the activity of CDK9 to phosphorylate serine 5 of the RNA polymerase II carboxyl-terminal domain during human immunodeficiency virus type 1 transcription. *Mol. Cell. Biol.* 20, 5077–5086. doi: 10.1128/mcb.20.14.5077-5086.2000

Zhou, T., Dang, Y., and Zheng, Y.-H. (2014). The mitochondrial translocator protein, TSPO, inhibits HIV-1 envelope glycoprotein biosynthesis via the

endoplasmic reticulum-associated protein degradation pathway. *J. Virol.* 88, 3474–3484. doi: 10.1128/JVI.03286-13

Zhou, T., Frabutt, D. A., Moremen, K. W., and Zheng, Y.-H. (2015). ERManI (Endoplasmic Reticulum Class I α-Mannosidase) is required for HIV-1 envelope glycoprotein degradation via endoplasmic reticulum-associated protein degradation pathway. *J. Biol. Chem.* 290, 22184–22192. doi: 10.1074/jbc.M115.675207

Zhuang, X., Pedroza-Pacheco, I., Nawroth, I., Kliszczak, A. E., Magri, A., Paes, W., et al. (2020). Hypoxic microenvironment shapes HIV-1 replication and latency. *Commun. Biol.* 3, 1–13. doi: 10.1038/s42003-020-1103-1

Conflict of Interest: The authors declare that the research was conducted in the absence of any commercial or financial relationships that could be construed as a potential conflict of interest.

Advantages of publishing in Frontiers

OPEN ACCESS
Articles are free to read for greatest visibility and readership

FAST PUBLICATION
Around 90 days from submission to decision

HIGH QUALITY PEER-REVIEW
Rigorous, collaborative, and constructive peer-review

TRANSPARENT PEER-REVIEW
Editors and reviewers acknowledged by name on published articles

Frontiers
Avenue du Tribunal-Fédéral 34
1005 Lausanne | Switzerland

Visit us: www.frontiersin.org
Contact us: frontiersin.org/about/contact

REPRODUCIBILITY OF RESEARCH
Support open data and methods to enhance research reproducibility

DIGITAL PUBLISHING
Articles designed for optimal readership across devices

FOLLOW US
@frontiersin

IMPACT METRICS
Advanced article metrics track visibility across digital media

EXTENSIVE PROMOTION
Marketing and promotion of impactful research

LOOP RESEARCH NETWORK
Our network increases your article's readership